# THE MINOR PLANET BULLETIN

BULLETIN OF THE MINOR PLANETS SECTION OF THE ASSOCIATION OF LUNAR AND PLANETARY OBSERVERS

VOLUME 47, NUMBER 3, A.D. 2020 JULY-SEPTEMBER 163.

## ASTEROID PHOTOMETRY FROM THE PRESTON GOTT OBSERVATORY

Dr. Maurice Clark
Department of Physics and Chemistry
Troy University
Troy AL 36801
maclark@troy.edu

(Received: 2020 April 15)

Asteroid lightcurve period and amplitude results obtained at the Preston Gott Observatory during July 2019 are presented. Also presented are results for asteroids observed in previous years but not reported.

During the first week of July 2019, I was able to spend several nights using the Preston Gott Observatory of the Texas Tech University. Located about 20km north of Lubbock, the main instrument is a 20" f/6.8 Dall-Kirkam Cassegrain. An SBIG STL-1001E CCD, was used with this telescope. Also used were several 12" Schmidt-Cassegrain telescopes, with SBIG ST9XE CCD's. All images were unfiltered and were reduced with dark frames and twilight sky flats.

Image analysis was accomplished using differential aperture photometry with MPO Canopus. Period analysis was also done in Canopus. Differential magnitudes were calculated using reference stars from the UCAC4 catalog.

Considerable cloudiness severely interfered with the observations; however, some useful results were obtained. These results are summarized in the table below, and the lightcurve plots are presented at the end of the paper. The data and curves are presented without additional comment except were circumstances warrant.

7778 Markrobinson. The period presented in this paper is in very close agreement with that derived by Warner (7.23h) (Warner, 2009a) and Behrend (7.234h) (Behrend, 2008).

9564 Jeffwynn. The period presented in this paper is uncertain due to the scatter in the data. It is hoped that this result will prove useful for future observations of this asteroid.

(9799) 1996 RJ. With a derived period, close to 12 hours, this Jupiter Trojan would be a good candidate for international collaboration at a future opposition.

(10422) 1999 AN22. Clouds severely limited observations of this asteroid and so no meaningful results could be obtained. Observations by Brincat et al. during May 2019, indicated a period of 35.156h. (Brincat, 2020). With a period, close to 1.5 days, this is another asteroid that could be a target for international collaboration.

(23692) 1997 KA. This asteroid was previously observed by the author in 2015 and a period of 10.430h was derived, but there was a large scatter in the data (Clark, 2016). Although observations from the opposition were limited, they cannot be harmonized with that result. Combining the 2 sets of data yields a period of 9.2801h, but still with considerable scatter. More observations are required to confirm or eliminate this result.

Acknowledgments

I would like to thank Dr Robert Moorhead for allowing the use of the Preston Gott Observatory for this work, and Brian Warner for all of his work with the program *MPO Canopus* and for his efforts in maintaining the "CALL" website.

| Number | Name | 2019 mm/dd | Phase | $L_{PAB}$ | $B_{PAB}$ | Period(h) | P.E. | Amp | A.E. | Grp |
|---|---|---|---|---|---|---|---|---|---|---|
| 3761 | Romanskaya | 07/25-08/01 | 13.5,14.6 | 292 | 22.3 | 9.456 | 0.003 | 0.17 | 0.05 | MBA |
| 7778 | Markrobinson | 07/24-08/01 | 30.7,33.1 | 262 | 22.7 | 7.2339 | 0.0007 | 0.84 | 0.02 | M-C |
| 9186 | Fumikotsukimoto | 08/01-08/05 | 19.6,18.1 | 335 | 20.3 | 3.9128 | 0.0006 | 0.54 | 0.02 | MBA |
| 9564 | Jeffwynn | 07/25-08/02 | 31.6,32.8 | 279 | 34.5 | 4.3105 | 0.0024 | 0.13 | 0.05 | MBA |
| 9799 | 1996 RJ | 07/31-08/05 | 6.6,6.3 | 319 | 29.6 | 12.1 | 0.02 | 0.3 | 0.1 | J-Tr |
| 10422 | 1999 AN22 | 05/13-05/14 | 5.3 | 227 | 8.5 | --- | --- | 0.25 | 0.05 | MBA |
| 23692 | 1997 KA | 08/01-08/05 | 21.1,20.1 | 349 | 16.5 | 9.315 | 0.006 | 0.35 | 0.05 | MBA |
| 43815 | 1991 VD4 | 07/25-07/31 | 18.6,18.1 | 348 | 18.4 | 4.4423 | 0.0003 | 0.62 | 0.02 | MBA |
| 302111 | 2001 MM3 | 08/02-08/05 | 33.3,33.9 | 289 | 43.2 | 3.284 | 0.002 | 0.41 | 0.1 | MBA |

Table I. Observing circumstances and results. The phase angle is given for the first and last date. $L_{PAB}$ and $B_{PAB}$ are the approximate phase angle bisector longitude and latitude at mid-date range (see Harris *et al.*, 1984). Grp is the asteroid family/group (Warner *et al.*, 2009b).

References

Behrend, R. (2008). *Observatoire de Geneve web site. http://obswww.unige.ch/~behrend/page_cou.html*

Brincat S.; Hills, K.; Galdies, C. (2015). "Photometric Observations of Main-Belt Asteroid (10422) 1999 AN22." *Minor Planet Bull.* **47**, 12-13.

Clark, M.L. (2016). "Asteroid Photometry from the Preston Gott Observatory." *Minor Planet Bull.* **43-2**, 132-135.

Harris, A.W.; Young, J.W.; Scaltriti, F.; Zappala, V. (1984). "Lightcurves and phase relations of the asteroids 82 Alkmene and 444 Gyptis." *Icarus* **57**, 251-258.

Warner, B. (2009a). "Asteroid Lightcurve Analysis at the Palmer Divide Observatory: 2008 May – September." *Minor Planet Bull.* **36**, 7-13.

Warner, B.D.; Harris, A.W.; Pravec, P. (2009b). "The Asteroid Lightcurve Database." *Icarus* **202**, 134-146. Updated 2020 February. *http://www.minorplanet.info/lightcurvedatabase.html*

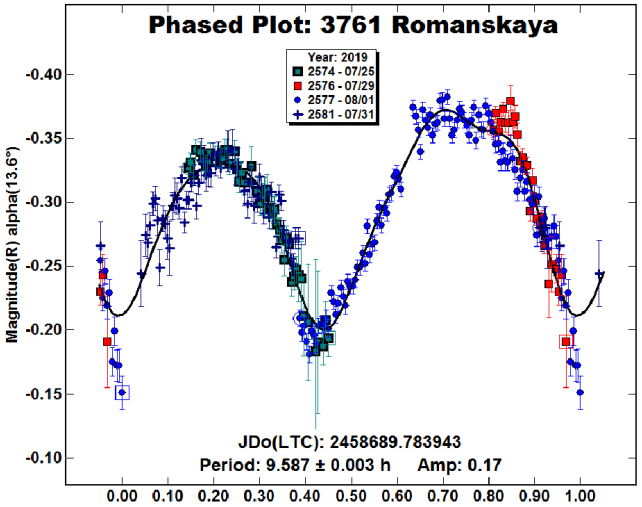


Figure 1. Lightcurve for 3761 Romanskaya.

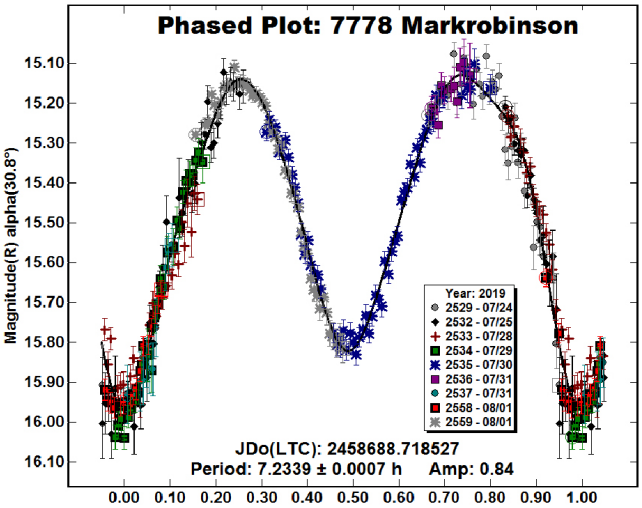


Figure 2. Lightcurve for 7778 Markrobinson.

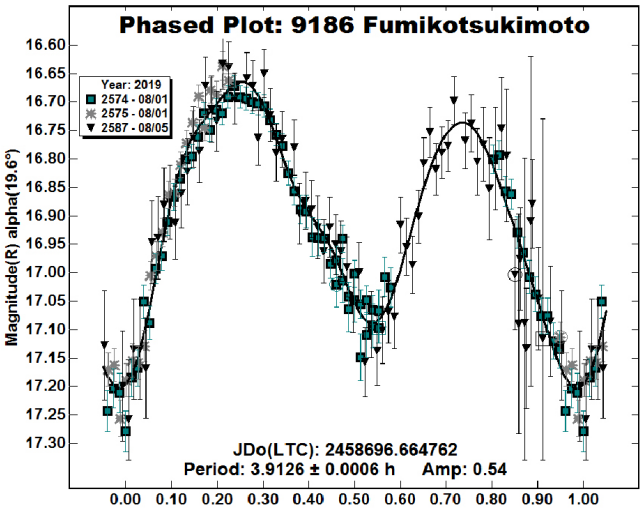


Figure 3. Lightcurve for 9186 Fumikotsukimoto.

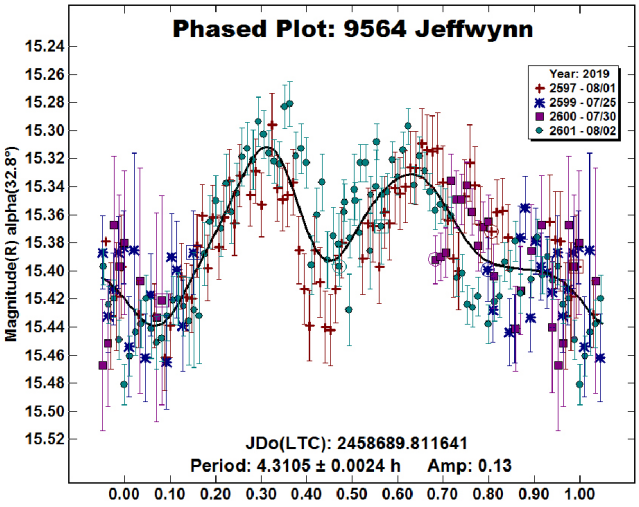


Figure 4. Lightcurve for 9564 Jeffwynn.

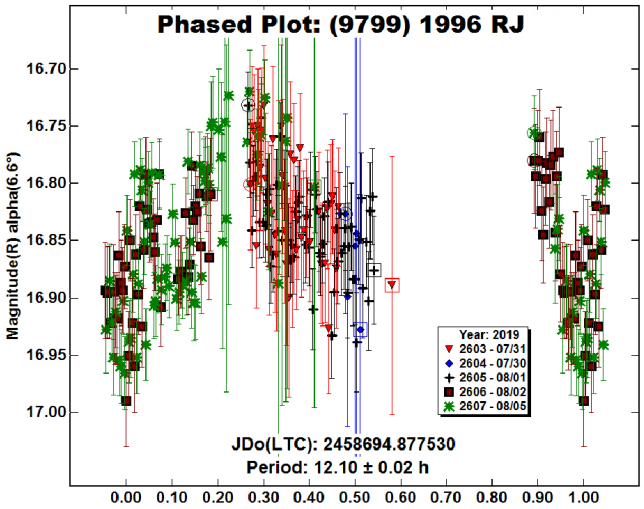


Figure 5. Lightcurve for (9799) 1996 RJ1.

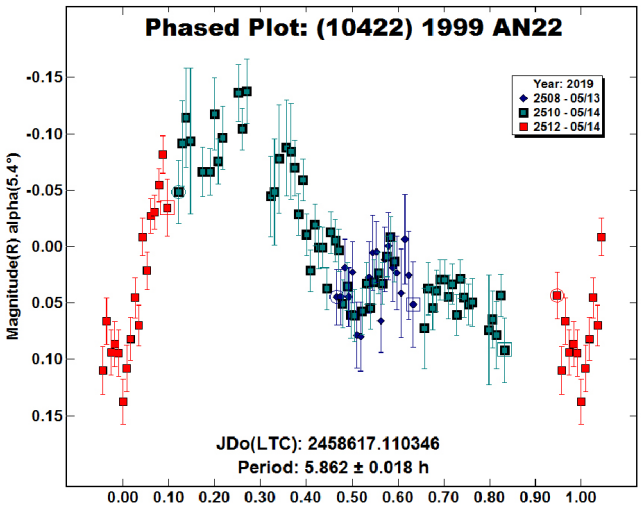


Figure 6. Lightcurve for (10422) 1999 AN22.

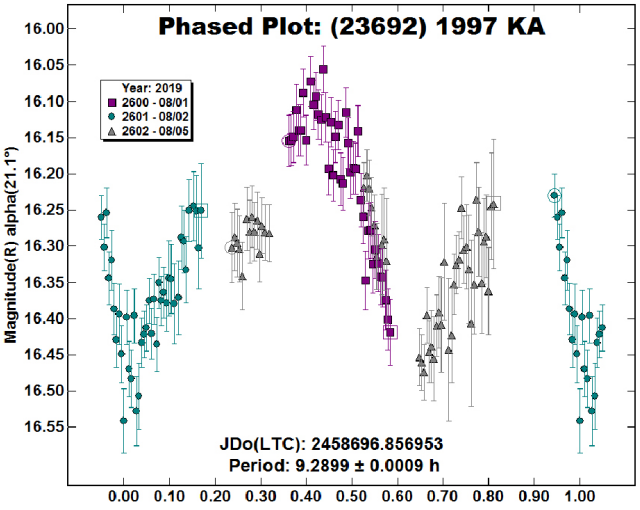


Figure 7. 2019 Lightcurve for (23692) 1997 KA.

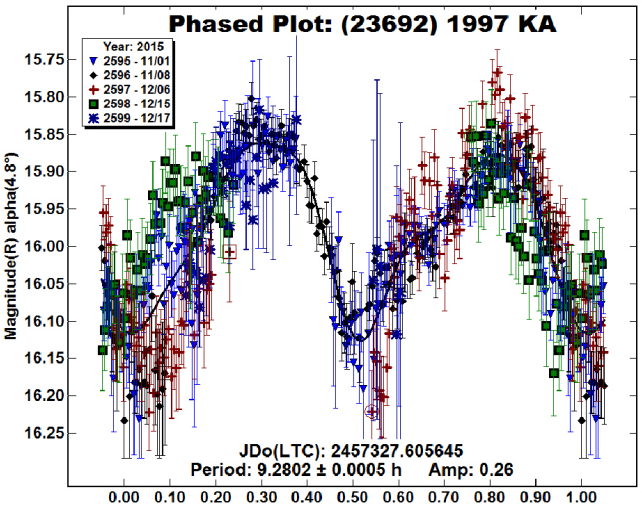


Figure 8. 2015 Lightcurve for (23692) 1997 KA.

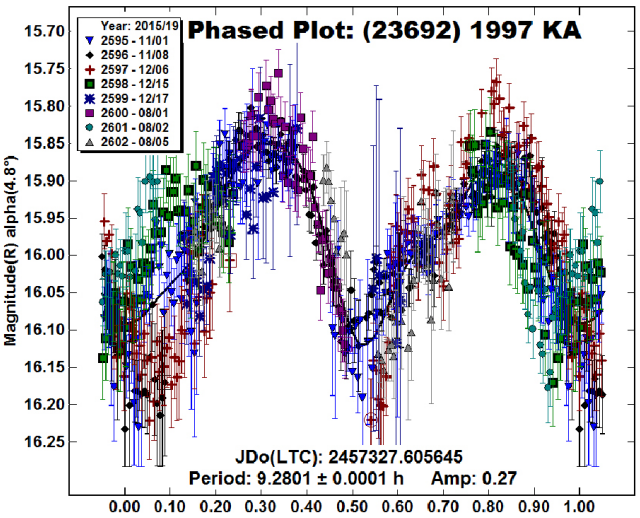


Figure 9. Combined Lightcurve for (23692) 1997 KA.

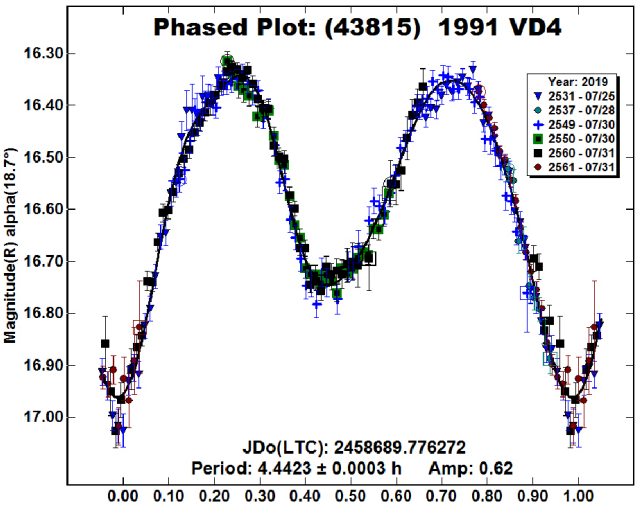


Figure 10. Lightcurve for (43815) 1991 VD4.

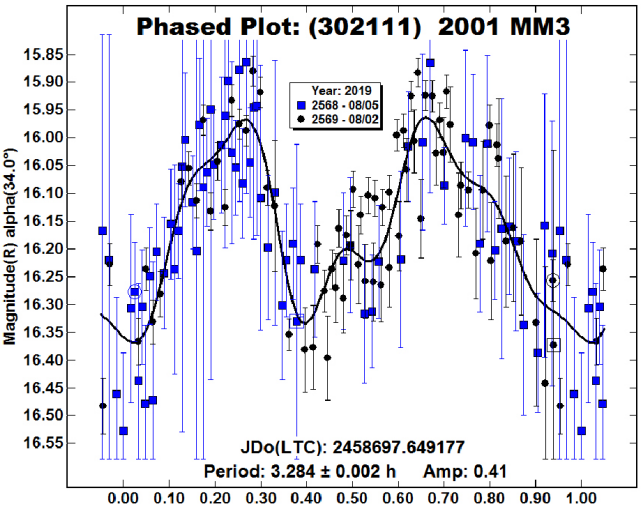


Figure 11. Lightcurve for (302111) 2001 MM3.

# LIGHTCURVES AND ROTATIONAL PERIODS OF FOUR MAIN BELT ASTERIODS

Allan Teer
Kent Montgomery
Texas A&M University–Commerce
P.O. Box 3011
Commerce, TX 75429-3011
Kent.Montgomery@tamuc.edu

(Received: 2020 Feb 20 Revised: 2020 Mar 20)

Lightcurves and rotational periods were determined for the following four asteroids: 1120 Cannonia: 3.810 ± 0.003 h; 6801 Strekov: 6.171 ± 0.016 h; (28885) 2000 KH56: 3.326 ± 0.001 h; and 87312 Akirasuzuki: 3.0439 ± 0.0007 h.

## Introduction

The purpose of this research was to determine the rotational period of four main belt asteroids; 1120 Cannonia, 6801 Strekov, (28885) 2000 KH56 and 87312 Akirasuzuki. The method used lightcurves created from photometric data taken over several nights. The lightcurves were then analyzed to determine the rotational periods.

Asteroid 1120 Cannonia was discovered by Shajn, P. at Simeis in 1928. It has an orbital eccentricity of 0.156 and a semi-major axis of 2.215 AU (JPL). Asteroid 6801 Strekov was discovered in 1995 by Moravec, Z. at Klet. This asteroid has an orbital eccentricity of 0.130 and a semi-major axis of 2.207 AU (JPL). Asteroid (28885) 2000 KH56 was discovered in 2000 by Lincoln Near-Eath Asteroid Research (LINEAR) at Socorro, New Mexico. It has an orbital eccentricity of 0.161 and a semi-major axis of 2.775 AU (JPL). Asteroid 87312 Akirasuzuki was discovered in 2000 by the Bisei Asteroid Tracking Telescope for Rapid Surveys (BATTeRS) at the Bisei Spaceguard Center in Okayama, Japan. It has an orbital eccentricity of 0.146 and a semi-major axis of 2.585 AU (JPL).

## Method

Two separate telescopes were used for this research. One of the telescopes is part of the Southeastern Association for Research in Astronomy (SARA) consortium. The telescope at SARA-North is a 0.9-m telescope located at the Kitt Peak National Observatory (KPNO) in Arizona. It is equipped with a CCD camera manufactured by Astronomical Research Camera, Inc. (ARC). The second is a 0.7-m telescope with an Andor Technologies camera at Texas A&M University-Commerce (TAMUC) in Commerce, Texas. Both cameras used CCDs that were cooled to around -60ºC to reduce background noise in the images.

In order to reduce the images, flats, bias, and dark calibration images were taken each night. The flat field images were taken against the twilight sky. The darks were exposed for the same time as the respective light images, three minutes for both telescopes. The SARA-North telescope used an IR-blocking filter and on the TAMUC telescope a Luminance filter was used. Both filters transmit the visible portion of the spectrum but block the infrared.

The software *MaxIm DL* was used to reduce and align the images. Afterward, the program *MPO Canopus v10.4.0.8* (Warner, 2011) was used to perform differential photometry on the reduced data. For each data set, five stars within the image were used for brightness comparison to the asteroid. Aperture photometry was used to determine the brightness of these comparison stars and the asteroid. The average of the difference in mag. between the stars and the asteroid was found for each image and then plotted in a phased plot, mag. versus time, to create a lightcurve. A Fourier transform was then applied to the lightcurve to determine the rotational period and error in the period.

## Results

1120 Cannonia. The asteroid 1120 Cannonia was imaged 95 times on 2019 April 8 and 93 times on 2019 April 14. Both nights used the TAMUC telescope. A rotation period of 3.810 ± 0.003 h with an amplitude variance of 0.21 mag was found. A previous study found a similar rotation period of 3.8096 ± 0.00033 h with an amplitude variance of 0.15 mag. (Valeau et al., 2017).

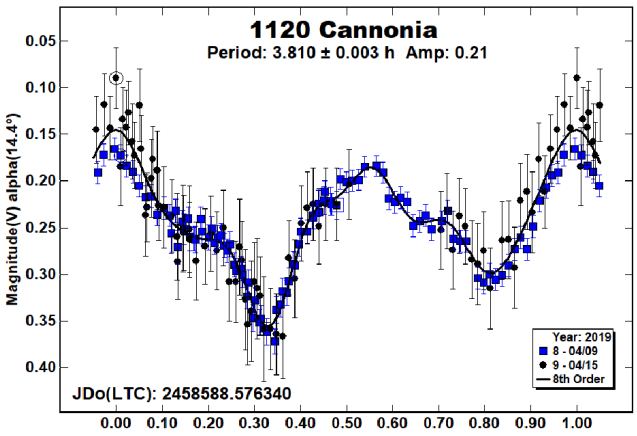


6801 Strekov. The asteroid 6801 Strekov was observed over three nights. It was imaged 117, 75, and 77 times on 2018 November 27, 28, as well as 2019 December 4, respectively. The images were taken with the TAMUC telescope and the resulting lightcurve produced a rotational period of 6.171 ± 0.016 h with an amplitude variance of 0.43 mag. A previous study found a similar rotation period of 6.173 ± 0.008 h with an amplitude variance of 0.17 mag. (Carbo et al., 2009).

| Number | Name | yyyy mm/dd | Phase | $L_{PAB}$ | $B_{PAB}$ | Period(h) | P.E. | Amp | A.E. |
|---|---|---|---|---|---|---|---|---|---|
| 1120 | Cannonia | 2019 04/08-04/14 | 14.0, 16.0 | 167.3 | +1.4 | 3.810 | 0.003 | 0.21 | .02 |
| 6801 | Strekov | 2018 11/27-12/04 | 15.4, 18.6 | 41.0 | +0.7 | 6.171 | 0.016 | 0.43 | .03 |
| 28885 | 2000 KH56 | 2019 08/20-08/27 | 6.3, 7.8 | 323.9 | +11.1 | 3.326 | 0.001 | 0.59 | .01 |
| 87312 | Akirasuzuki | 2019 03/09-03/27 | 14.9, 20.6 | 140.7 | +5.6 | 3.0439 | 0.0007 | 0.16 | .02 |

Table I. Observing circumstances and results. The phase angle is given for the first and last date. If preceded by an asterisk, the phase angle reached an extrema during the period. $L_{PAB}$ and $B_{PAB}$ are the approximate phase angle bisector longitude/latitude at mid-date range (see Harris et al., 1984).

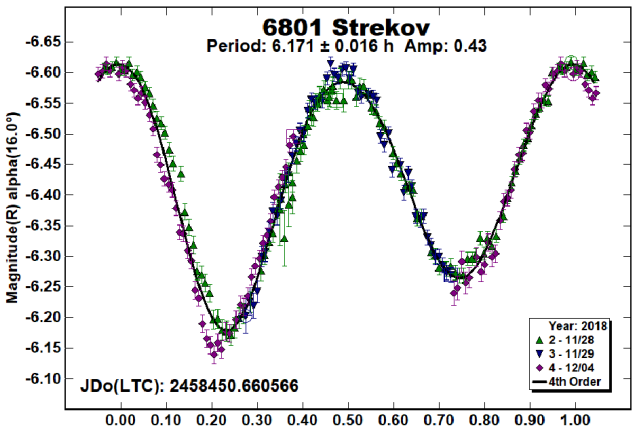


(28885) 2000 KH56. The asteroid (28885) 2000 KH56 was imaged 105 times on 2019 August 20 and 76 times on 2019 August 27, both nights on the TAMUC telescope. The resulting lightcurve produced a rotational period of 3.326 ± 0.001 h with an amplitude variance of 0.59 mag. A previous study found the same rotational period of 3.325 ± 0.0004 h with an amplitude variance of 0.58 mag. (Waszcak et al., 2015).

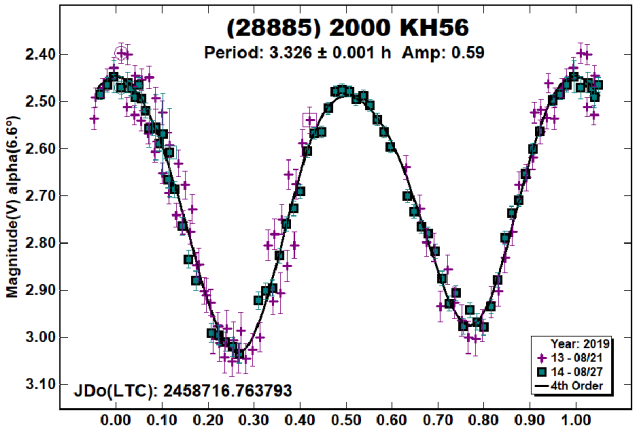


87312 Akirasuzuki. Asteroid 87312 Akirasuzuki was observed over three nights. It was imaged 116 times on 2019 March 9 using the SARA-North telescope. On March 15 2019 70 images were taken, and 66 images were taken on 2019 March 27 using the TAMUC telescope. These observations resulted in a rotational period of 3.0439 ± 0.0007 h and an amplitude variation of .16 mag. Another study produced a rotational period of 3.25 ± 0.025 h and an amplitude variation of 0.14 mag. (Chang et al., 2016)

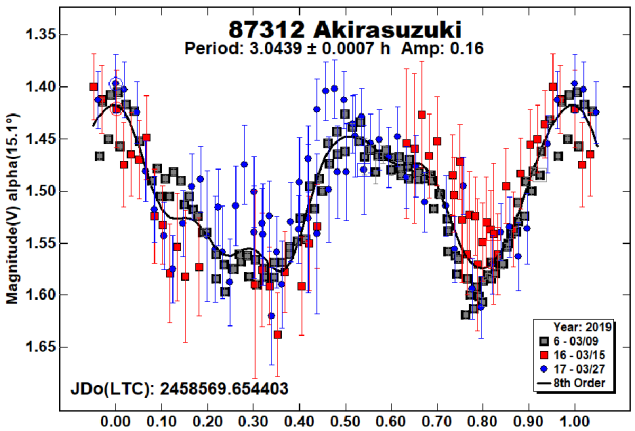


Acknowledgements

This work is supported in part by the Physics and Astronomy Scholarship for Success (PASS) project at Texas A&M University-Commerce funded by the NSF under grant No. 1643567. Based on observations obtained with the SARA Observatory 0.9 m telescope at Kitt Peak, which is owned and operated by the Southeastern Association for Research in Astronomy (*saraobservatory.org*).

References

Carbo, L.; Kragh, K.; Krotz, J.; Meiers, A.; Shaffer, N.; Torno, S.; Sauppe, J.; Ditteon, R. (2009). "Asteroid Lightcurve Analysis at the Oakley Southern Sky Observatory and Oakley Observatory: 2008 September and October." *Minor Planet Bull.* **36**, 91-94.

Chang, C.; Lin, H.; Ip, W.; Prince, T.; Kulkarni, S.; Levitan, D.; Laher, R.; Surace, J.; Cheng, Y.; Ip, W.; Kinoshita, D.; Helou, G.; Prince, T.; Kulkarmi, S. (2016). "Large super-fast rotator hunting using the intermediate palomar transient factory." *The Astrophysical Journal Supp. Series.* **227(2)**, 13.

Harris, A.W.; Young, J.W.; Scaltriti, F.; Zappala, V. (1984). "Lightcurves and phase relations of the asteroids 82 Alkmene and 444 Gyptis." *Icarus* **57**, 251-258.

JPL Small-Body Database Browser.
*http://ssd.jpl.nasa.gov/sbdb.cgi#top*

Diffraction Limited MaxIm DL.
*http://diffractionlimited.com/product/maxim-dl/*

Valeau, P.; Manach, A.; Helas, J.-F.; Pellier, C.; Monachino, G.; Mer, E.; Schmitt, H.; Behrend, R.; Alas, J.-F. (2017). Obsertaoire de Geneve. *http://obswww.unige.ch/~behrend/page_cou.html*

Warner, B.D. (2011). MPO Canopus software Version 10.2.1.0. Bdw Publishing. *http://www.minorplanetobserver.com/*

Waszcak, A.; Chang, C.-K; Ofeck, E.O.; Laher, F.; et al. (2015). "Asteroid light curves from the palomar transient factory survey: rotation periods and phase functions from sparse photometry." *The Astrophysical Journal* **150(3)**, 35.

# MEASURED LIGHTCURVES AND ROTATIONAL PERIODS OF (16579) 1992 GO, (25660) 2000 AO88, AND (37652) 1994 JS1

Natasha S. Abrams, Sebastian Gomez, and Allyson Bieryla
Center for Astrophysics | Harvard & Smithsonian
60 Garden St.
Cambridge, MA 02138
nsabrams@college.harvard.edu

(Received: 2020 March 19)

We determined the rotational periods of (16579) 1992 GO, (25660) 2000 AO88 and (37652) 1994 JS1, with the 1.2 m telescope at the Fred L. Whipple Observatory. We found the rotational periods to be 10.9887 ± 0.0004 h, 2.63705 ± 0.00004 h, and 17.4433 ± 0.0007 h, respectively. The former two were previously undetermined periods. The period that we determined for 1994 JS1 agrees well with the previously measured periods of 17.4501 ± 0.0014 (Noschese et al., 2019) and 17.459 ± 0.002 h (Marchini et al., 2019).

KeplerCam is a 23×23 arcmin CCD mounted on the 1.2-meter telescope at the Fred L. Whipple Observatory in Arizona. We made photometric observations of (16579) 1992 GO, (25660) 2000 AO88 and (37652) 1994 JS1 in the Sloan i-band.

The three asteroids were selected by searching *Minorplanet.info* for the brightest asteroids with (at the time) unknown rotational periods that would still be relatively bright and observable for multiple months.

Following the same procedure as Abrams et al. (2020), we first reduced the data using standard *IDL* procedures and produced a lightcurve using the *AstroImageJ* multi-aperture photometry software (Collins et al., 2017). The python package, *gatspy*, was used to calculate the Lomb-Scargle periodogram and determine the rotational period (VanderPlas and Ivezić, 2015). We measured uncertainties in the rotational periods by finding the maximum and minimum rotational period at which the phased lightcurve no longer had a clear modulation. Amplitudes were determined by the absolute magnitude of -2.5log(max flux/min flux).

1992 GO was discovered 1992 April 3 by Ueda, S. and Kaneda, H. at the Kushiro Observatory in Hokkaido, Japan. It was observed for four nights in June and July 2019, and there are gaps in the data due to crowded fields and weather. The images in which the asteroid passed over bright objects were removed from the analysis. We determined the period to be 10.9887 ± 0.0004 h and the amplitude to be 0.38 ± 0.01.

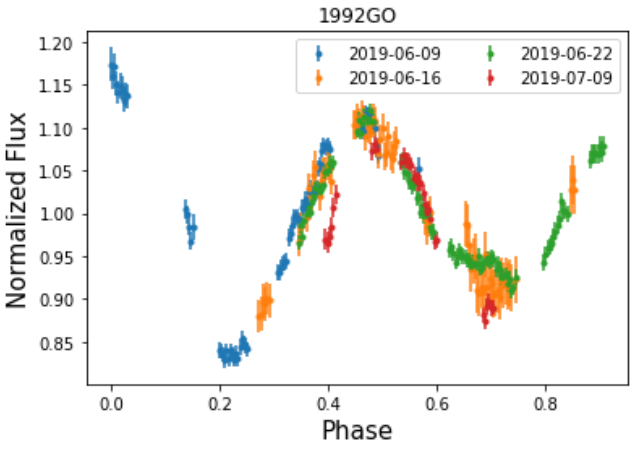


2000 AO88 was discovered 2000 January 5 in Socorro, New Mexico as part of the Lincoln Near-Earth Asteroid Research (LINEAR) project. It was observed with KeplerCam for five nights between 2019 May 02-27. We determined the period to be 2.63705 ± 0.00004 h and amplitude to be 0.36 ± 0.08.

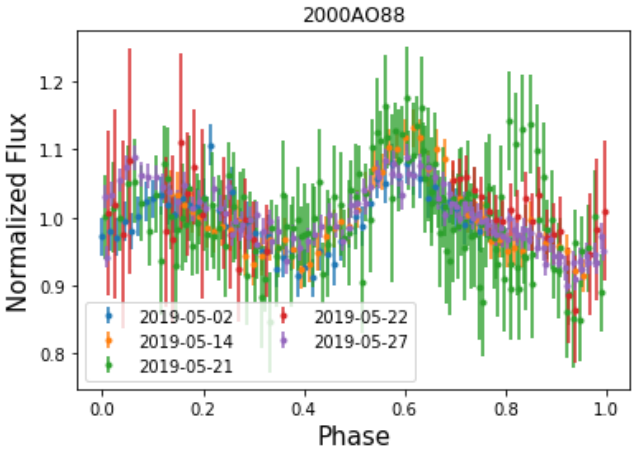


1994 JS1 was discovered 1994 May 4 at Catalina Station Observatory on Mount Bigelow to the northeast of Tucson, Arizona by Hergenrother, C.W. and Spahr, T.B.. We observed the asteroid for ten nights between February and June 2019, though one night had high scatter due to poor weather conditions and was therefore excluded from the datasets. We found the rotational period to be 17.4433 ± 0.0007 h, which agrees reasonably well with the previously determined rotational periods of 17.4501 ± 0.0014 (Noschese et al., 2019) and 17.459 ± 0.002 h (Marchini et al., 2019).

| Number | Name | 20yy/mm/dd | Phase | $L_{PAB}$ | $B_{PAB}$ | Period (h) | P.E. | Amp | A.E. | Grp |
|---|---|---|---|---|---|---|---|---|---|---|
| 16579 | 1992 GO | 19/06/09-07/09 | 12.0,11.6 | 247.4 | 13.9 | 10.9887 | 0.0004 | 0.38 | 0.01 | EUN |
| 25660 | 2000 AO88 | 19/05/02-05/27 | 16.3, 6.5 | 256.9 | 5.8 | 2.63705 | 0.00004 | 0.36 | 0.08 | |
| 37652 | 1994 JS1 | 19/02/18-06/08 | 14.8,34.9 | 220.2 | 19.6 | 17.4433 | 0.0007 | 0.56 | 0.06 | |

Table I. Observing circumstances and results. The phase angle is given for the first and last date. $L_{PAB}$ and $B_{PAB}$ are the approximate phase angle bisector longitude and latitude at mid-date range (see Harris et al., 1984). Grp is the asteroid family/group (Warner et al., 2009).

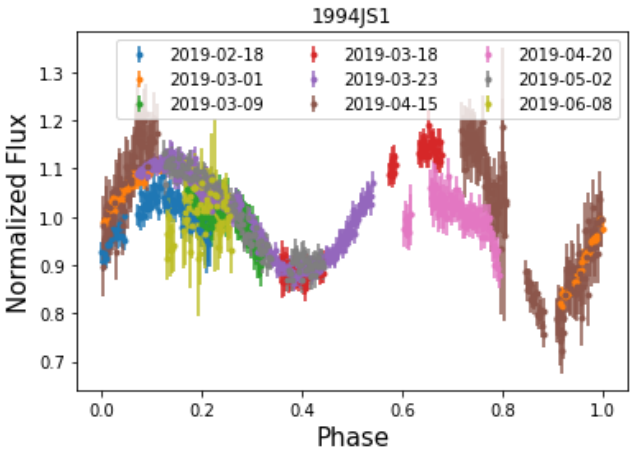


References

Abrams, N.S.; Bieryla, A.; Gomez, S.; Huang, J.; Lewis, J.A.; Garrison, L.H.; Carmichael, T. (2020). "Measured Lightcurves and Rotational Periods of 3122 Florence, 3830 Trelleborg, and (131077) 2000 YH105." *The Minor Planet Bulletin* **47-1**, 3-4.

Collins K.A.; Kielkopf, J.F.; Stassun, K.G.; Hessman, F.V. (2017). "AstroImageJ: Image Processing and Photometric Extraction for Ultra-Precise Astronomical Light Curves." *Astron. J.* **153**, A77.

Harris, A.W.; Young, J.W.; Scaltriti, F.; Zappala, V. (1984). "Lightcurves and phase relations of the asteroids 82 Alkmene and 444 Gyptis." *Icarus* **57**, 251-258.

Marchini, A.; Papini, R.; Banfi, M.; Salvaggio, F.; Franco, L. (2019). "Rotation period determination for the asteroids 3329 Golay and (37652) 1994 JS1." *The Minor Planet Bulletin* **46-3**, 338-339.

Noschese, A.; Vecchione, A.; Catapano, A. (2019). "Lightcurve Analysis and Rotation Period for (37652) 1994 JS1." *The Minor Planet Bulletin* **46-3**, 331.

VanderPlas, J.T.; Ivezić, Ž. (2015). "Periodograms for Multiband Astronomical Time Series." *Ap. J.* **812,** A18.

Warner, B.D.; Harris, A.W.; Pravec, P. (2009). "The Asteroid Lightcurve Database." *Icarus* **202**, 134-146. Updated 2017 Nov. *http://www.minorplanet.info/lightcurvedatabase.html*

## SPIN-SHAPE MODEL FOR 118 PEITHO

Lorenzo Franco
Balzaretto Observatory (A81), Rome, ITALY
lor_franco@libero.it

Frederick Pilcher
4438 Organ Mesa Loop
Organ Mesa Observatory (G50)
Las Cruces, NM 88011 USA

Brian D. Warner
Center for Solar System Studies (CS3) / MoreData!
Eaton, CO 80615 USA

Alessandro Marchini, Leonella-Filippa Saya
Astronomical Observatory, DSFTA - University of Siena (K54)
Siena, ITALY

Audejean Maurice
Observatoire de Chinon (B92)
Mairie de Chinon, Chinon, FRANCE

(Received: 2020 April 6)

We present a shape and spin axis model for main-belt asteroid 118 Peitho. The model was achieved with the lightcurve inversion process, using combined dense photometric data acquired from five apparitions between 1977-2020 and sparse data from USNO Flagstaff. Analysis of the resulting data found a sidereal period P = 7.806397 ± 0.000009 hours and two mirrored pole solutions at (λ = 179°, β = 60°) and (λ = 345°, β = 39°) with an uncertainty of ± 10 degrees.

The minor planet 118 Peitho has been observed at past oppositions and most recently (2020 opposition) by Pilcher at Organ Mesa Observatory (Pilcher, 2020) and by Marchini and Saya at Astronomical Observatory of the University of Siena. Dense photometric data were downloaded from Asteroid Photometric Catalogue (APC, 1993) and from ALCDEF (ALCDEF, 2019). Moreover, in order to improve the coverage at various aspect angles, we also used sparse data from USNO Flagstaff Station (MPC Code 689), taken from the Asteroids Dynamic Site (AstDyS-2, 2020).

The observational details of the dense data used are reported in Table I with the mid date, number of the lightcurves used for the inversion process, longitude and latitude of phase angle bisector ($L_{PAB}$, $B_{PAB}$).

| Reference | Mid date | # LC | $L_{PAB}$° | $B_{PAB}$° |
|---|---|---|---|---|
| Stanzel, Schober (1980) | 1977-12-05 | 1 | 76 | 5 |
| Warner (2009) | 2009-05-13 | 3 | 177 | 6 |
| Audejean (2013) Web | 2013-04-16 | 2 | 196 | 5 |
| Pilcher (2017) | 2017-05-18 | 3 | 216 | 1 |
| Pilcher (2020) | 2020-01-11 | 2 | 103 | 9 |
| Franco et al. (2020) | 2020-01-22 | 1 | 104 | 10 |

Table I. Observational details for the data used in the lightcurve inversion process for 118 Peitho.

Lightcurve inversion was performed using *MPO LCInvert* v.11.8.2.0 (BDW Publishing, 2016). For a description of the modeling process see *LCInvert Operating Instructions Manual* (Durech et al., 2010; and references therein).

Figure 1 shows the PAB longitude/latitude distribution for dense/sparse data used in the lightcurve inversion process. Figure 2 (top panel) shows the sparse photometric data distribution (intensities vs JD) and (bottom panel) the corresponding phase curve (reduced magnitudes vs phase angle).

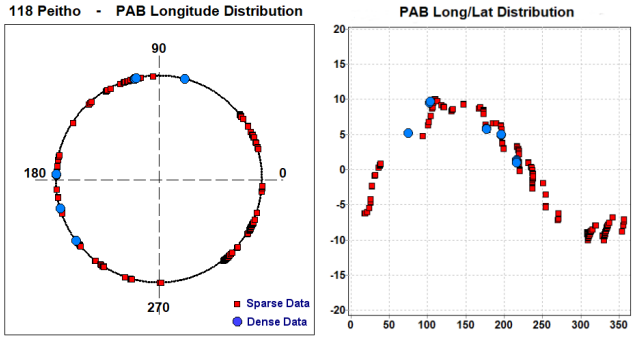


Figure 1. PAB longitude and latitude distribution of the data used for the lightcurve inversion model.

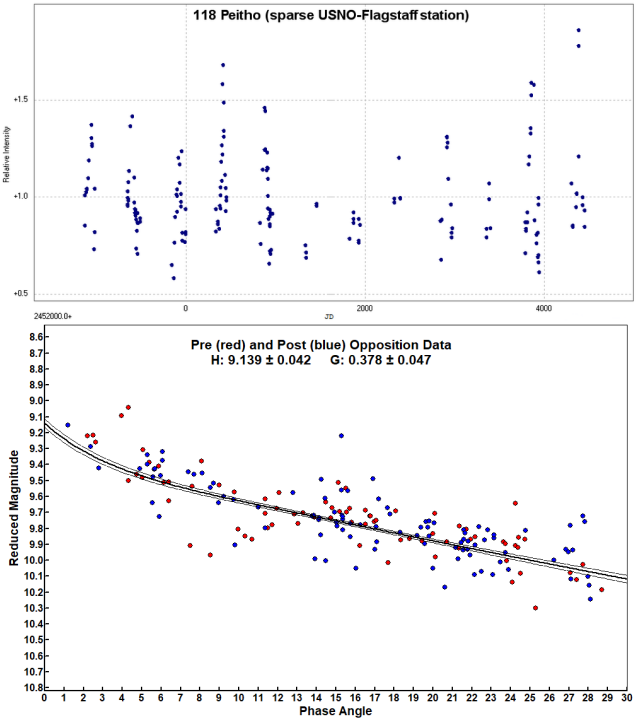


Figure 2. Top: sparse photometric data point distribution from (689) USNO Flagstaff station (relative intensity of the asteroid's brightness vs Julian Day). Bottom: phase curve obtained from sparse data (reduced magnitude vs phase angle).

In the analysis the processing weighting factor was set to 1.0 for dense data and to 0.3 for sparse data. The "dark facet" weighting factor was set to 0.5 to keep the dark facet area below 1% of total area and the number of iterations was set to 50.

The sidereal period search was started around the average of the synodic periods found in the asteroid lightcurve database (LCDB; Warner et al., 2009). We found one isolated sidereal period with a Chi-Sq value within 10% of the lowest Chi-Sq (Figure 3).

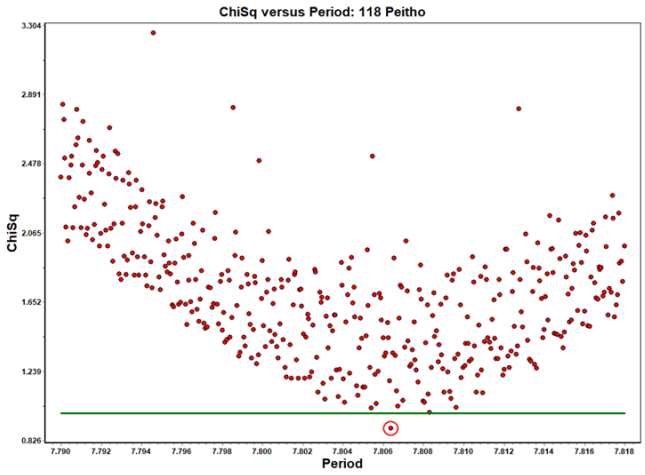


Figure 3. The period search for 118 Peitho shows one isolated sidereal period with Chi-Sq values within 10% of the lowest value.

The pole search consisted of looking at 312 discrete, fixed pole positions while allowing the previously found sidereal period to "float." From this step we found two roughly mirrored lower Chi-Sq solutions (Figure 4) separated by about 180° in longitude at ecliptic longitude-latitude pairs (180°, 60°) and (345°, 45°).

The subsequent "fine" search, centered on these rough positions, allowed us to refine the position of the pole (Figure 5). The analysis shows two set of clustered solutions within 10° of radius that had Chi-Sq values within 10% of the lowest value, centered at ecliptic longitude-latitude (179°, 59°) and (345°, 40°).

The two best solutions (lower Chi-Sq) are reported in Table II. The sidereal period was obtained by averaging the two solutions found in the pole search process. Typical errors in the pole solution are ± 10° and the uncertainty in sidereal period has been evaluated as a rotational error of 20° over the total time span of the dense data set. Figure 6 shows the shape model (first solution) while Figure 7 shows the fit between the model (black line) and some observed lightcurves (red points).

| λ ° | β ° | Sidereal Period (hours) | RMS |
|---|---|---|---|
| 179 | 60 | 7.806397 ± 0.000009 | 0.0172 |
| 345 | 39 | | 0.0174 |

Table II. The two spin axis solutions for 118 Peitho (ecliptic coordinates) with an uncertainty of ± 10 degrees. The sidereal period was the average of the two solutions found in the pole search process.

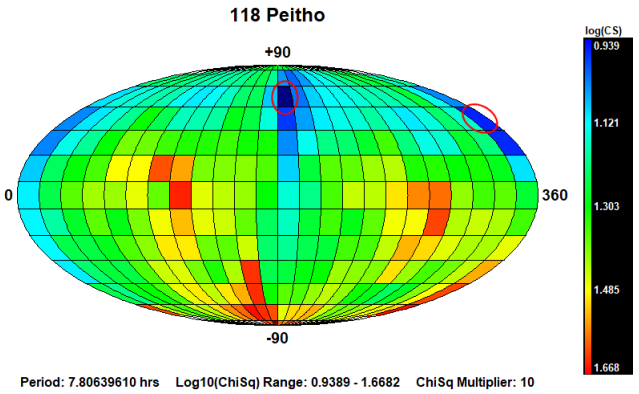


Figure 4. Pole search distribution. The dark blue region indicates the smallest Chi-Sq value while the dark red region indicates the largest.

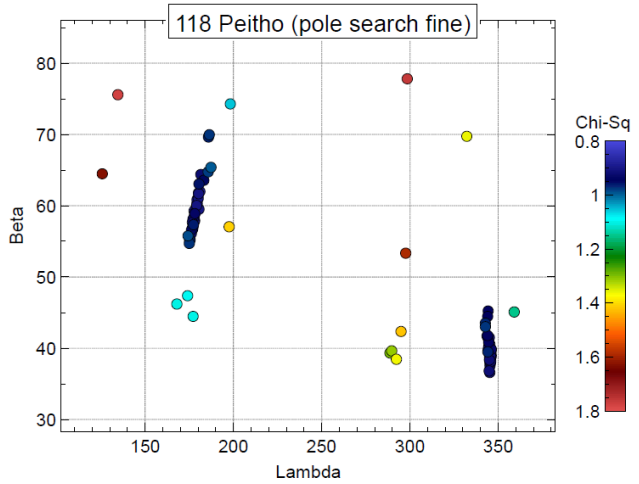


Figure 5. The "fine" pole search shows two clustered solutions centered at the ecliptic longitude/latitude (179°, 59°) and (345°, 40°) with radius approximately of 10° and Chi-Sq values within 10% of the lowest value.

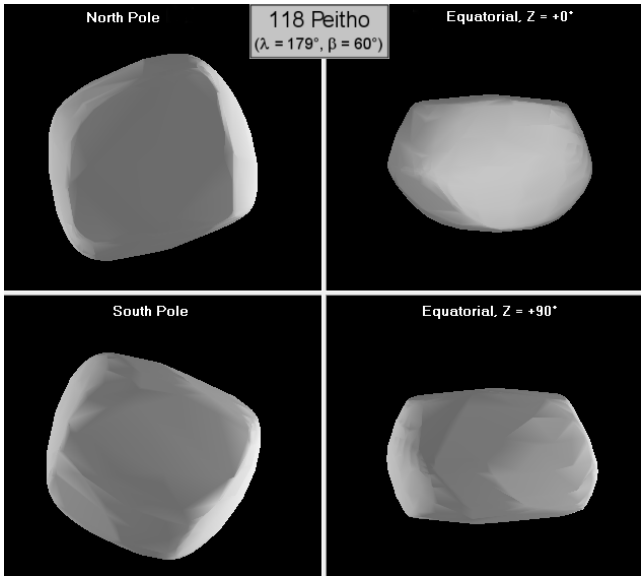


Figure 6: The shape model for 118 Peitho (λ = 179°, β = 60°).

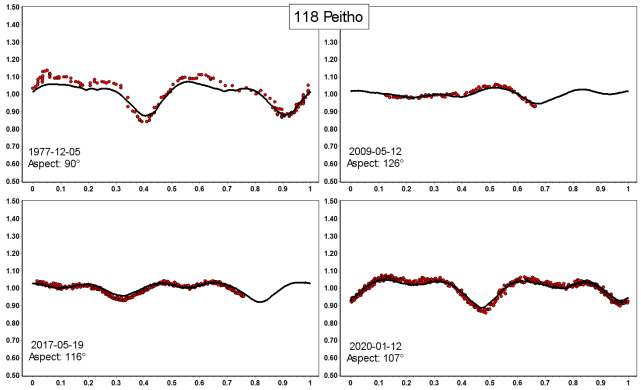


Figure 7: Model fit (black line) versus observed lightcurves (red points) for (λ = 179°, β = 60°) solution.

## References


ALCDEF (2019). Asteroid Lightcurve Data Exchange Format web site. *http://www.alcdef.org/*

APC (1993). Asteroid Photometric Catalogue v.1.1. *https://pds.nasa.gov/ds-view/pds/viewProfile.jsp?dsid=EAR-A-3-DDR-APC-LIGHTCURVE-V1.1*

AstDyS-2 (2020). Asteroids - Dynamic Site. *https://newton.spacedys.com/astdys/*

BDW Publishing (2016). *http://www.minorplanetobserver.com/MPOSoftware/MPOLCInvert.htm*

Durech, J.; Sidorin, V.; Kaasalainen, M. (2010). "DAMIT: a database of asteroid models." *Astron. Astrophys.* **513**, A46.

Franco, L. et. al. (2020). "Collaborative Asteroid Photometry from UAI: 2020 January - March." *Minor Planet Bulletin* **47**, 242-246.

Pilcher, F. (2017). "Rotation Period Determination for 46 Hestia, 118 Peitho, 333 Badenia, 356 Liguria, and 431 Nephele." *Minor Planet Bulletin* **44**, 294-297.

Pilcher, F. (2020). "Lightcurve and Rotation Periods of 83 Beatrix, 86 Semele, 118 Peitho, 153 Hilda, 527 Euryanthe, and 549 Jessonda." *Minor Planet Bulletin* **47**, 192-195.

Stanzel, R.; Schober, H.J. (1980). "The asteroids 118 Peitho and 952 CAIA - Rotation periods and lightcurves from photoelectric observations." *Astron Astrophys Suppl. Series* **39**, 3-5.

Warner, B.D. (2009). "Asteroid Lightcurve Analysis at the Palmer Divide Observatory: 2009 March-June." *Minor Planet Bulletin* **36**, 172-176.

Warner, B.D.; Harris, A.W.; Pravec, P. (2009). "The asteroid lightcurve database." *Icarus* **202**, 134-146. Updated 2020 March. *http://www.minorplanet.info/lightcurvedatabase.html*

## PHOTOMETRIC LIGHTCURVES OF EIGHT MAIN-BELT ASTEROIDS

Andrea Ferrero
Bigmuskie Observatory (B88)
via Italo Aresca 12
14047 Mombercelli, Asti, ITALY
bigmuskie@outlook.com

(Received: 2020 April 14)

In this paper, we present the results of photometric work on eight asteroids:
455 Bruchsalia, $P$ = 11.839 ± 0.001 h, $A$ = 0.42 mag;
862 Franzia, $P$ = 7.523 ± 0.001 h, $A$ = 0.13 mag;
2898 Neuvo, $P$ = 17.591 ± 0.012 h, $A$ = 0.06 mag;
3166 Klondike, $P$ =150.19 ± 0.03 h, $A$ =0.81 mag;
3373 Koktebelia, $P$ = 405.33 ± 0.54 h, $A$ = 0.67 mag,
4857 Altgamia, $P$ = 9.040 ± 0.002 h, $A$ = 0.25 mag;
5042 Colpa, $P$ = 169.64 ± 0.13 h, $A$ = 0.93 mag; and
9100 Tomohisa, $P$ = 9.421 ± 0.003 h, $A$ = 0.09 mag.

Starting in 2019 December, Bigmuskie Observatory worked on eight main-belt asteroids to determinate their rotational periods. They were selected using the CALL website ephemeris generator

*http://www.minorplanet.info/PHP/call_OppLCDBQuery.php*

which allowed finding asteroids near opposition in a given month that had no previous or insecure periods in the asteroid lightcurve database (LCDB; Warner et al., 2009). The final observing list contained 455 Bruchsalia, 862 Franzia, 2898 Neuvo, 3166 Klondike, 3373 Koktebelia, 4857 Altgamia, 5042 Colpa, and 9100 Tomohisa.

The setup used at the Bigmuskie Observatory is a Marcon 0.30-meter *f*/8 Ritchey-Chretién telescope coupled with a Moravian G3 01000 CCD camera, which is equipped with a KAF-1001E CCD chip (1024×1024×24 microns). The combination gave a pixel scale of exactly 2 arcsec/pixel and a field-of-view of 36×36 arcmin. Exposures were all unguided and taken through a Toptec R filter. Telescope and camera control were carried out using *Maxim DL* (*http://diffractionlimited.com/product/maxim-dl/*) and *The Sky 6 Pro* (*http://www.bisque.com*). The program Voyager (*http://software.starkeeper.it*) automated the entire observatory. All photometric reductions were done with *MPO Canopus* v10.7.12.9 (*http://bdwpublishing.com*), which allows precise night-to-night zero-point calibration using the Comparison Star Selector utility.

455 Bruchsalia. This target was reported on the CALL website with a period of period $P$ = 11.85 h and U = 2+. This means there is a small chance that the true period is something other than the one being reported. The final result found at the Bigmuskie Observatory was $P$ = 11.839 ± 0.001 h with an amplitude of $A$ = 0.42 mag. This is in good agreement to the earlier result.

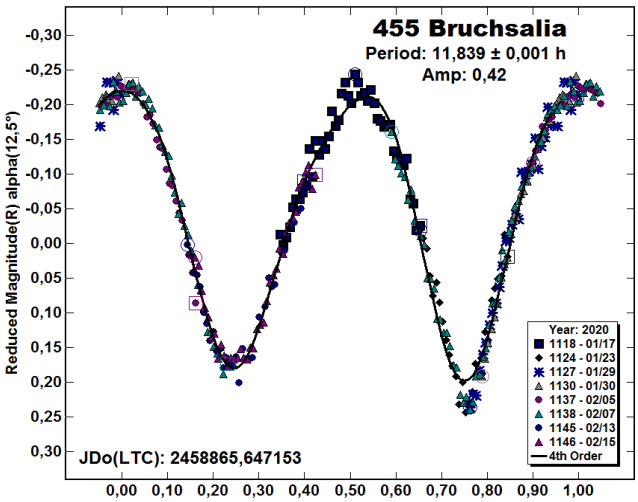


862 Franzia was reported on the CALL website as having a period of $P$ = 7.52 h and flagged U = 2. The photometric observations at the Bigmuskie Observatory led to a fairly complex lightcurve that required to set *MPO Canopus* to use a 10th order Fourier fit to better match the data. The final period is $P$ = 7.523 ± 0.001 h, $A$ = 0.13 mag, or nearly the same as the previous result.

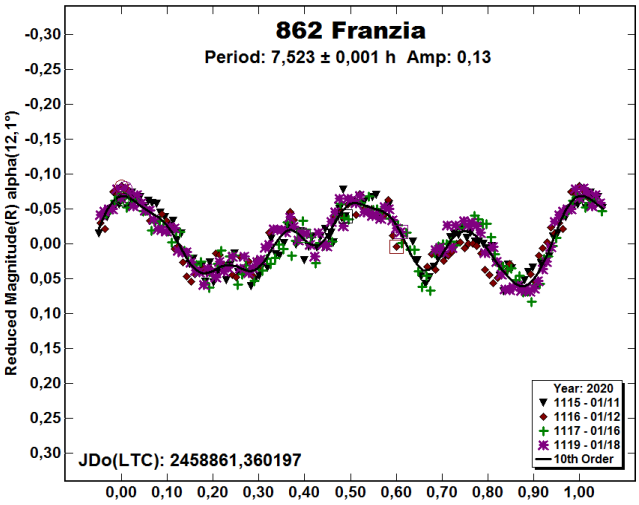


| Number | Name | yyyy mm/dd | Phase | $L_{PAB}$ | $B_{PAB}$ | Period(h) | P.E. | Amp | A.E. | Grp |
|---|---|---|---|---|---|---|---|---|---|---|
| 455 | Bruchsalia | 2020 01/17-02/15 | 12.7,5.9 | 156 | 13 | 11.839 | 0.001 | 0.42 | 0.05 | MB |
| 862 | Franzia | 2020 01/11-01/18 | 11.8,14.1 | 84 | 8 | 7.523 | 0.001 | 0.13 | 0.05 | MB |
| 2898 | Neuvo | 2020 03/20-04/10 | 8.1,10.7 | 184 | 17 | 17.591 | 0.012 | 0.06 | 0.05 | MB |
| 3166 | Klondike | 2019 12/25-02/21 | 14.5,17.5 | 119 | 5 | 150.19 | 0.03 | 0.81 | 0.05 | MB |
| 3373 | Koktebelia | 2019 12/26-03/01 | 14.8,20.1 | 119 | 3 | 405.33 | 0.54 | 0.67 | 0.10 | MB |
| 4857 | Altgamia | 2020 02/27-03/07 | 21.4,21.9 | 152 | 30 | 9.040 | 0.002 | 0.25 | 0.05 | MB |
| 5042 | Colpa | 2020 02/20-04/01 | 11.4,7.1 | 179 | 13 | 169.64 | 0.13 | 0.93 | 0.05 | MB |
| 9100 | Tomohisa | 2020 03/16-04/11 | 8.1,13.5 | 181 | 11 | 9.421 | 0.003 | 0.09 | 0.10 | MB |

Table I. Observing circumstances and results. The phase angle is given for the first and last date. If preceded by an asterisk, the phase angle reached an extrema during the period. $L_{PAB}$ and $B_{PAB}$ are the approximate phase angle bisector longitude/latitude at mid-date range (see Harris et al., 1984). Grp is the asteroid family/group (Warner et al., 2009).

2898 Neuvo. The was no previous period reported for this asteroid. It proved to be a fairly difficult target due to its relative faintness for the equipment used, the sky quality at the observatory, and, most of all, the very low amplitude of the curve. The period is $P$ = 17.591 ± 0.012 h with amplitude $A$ = 0.06 mag.

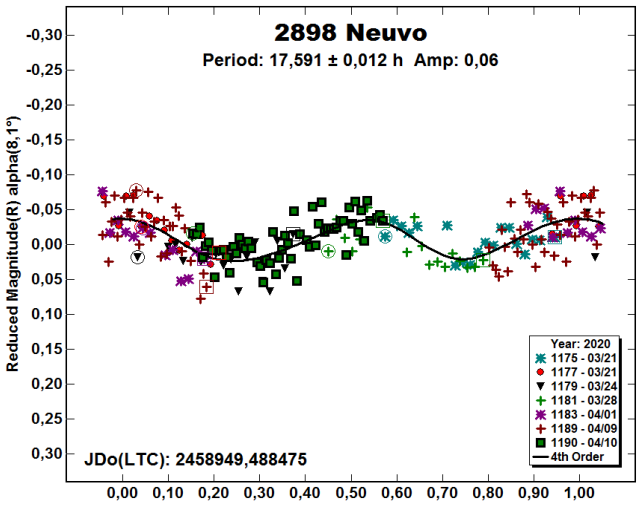


3166 Klondike. This was another target reported on the CALL website with a flag of U = 2. The period reported was 20 h, but after three months of observations at Big Muskie, the final period is completely different. The asteroid proved to be a slow rotator with $P$ = 150.19 ± 0.03 h, $A$ = 0.81 mag.

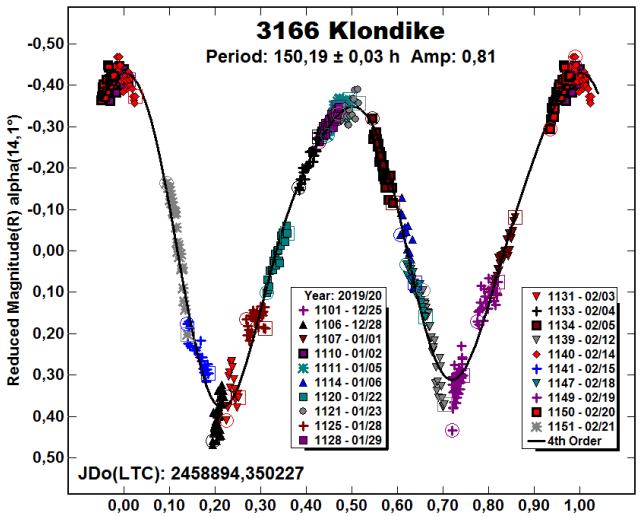


3373 Koktebelia. No period was reported for this target. It took three months of observations to reach the final plot, which shows a long period of $P$ = 405.33 ± 0.54 h and amplitude $A$ = 0.67 mag. Unfortunately, the part of the curve between rotation phase 0.10 - 0.25 is missing. Even so, the lightcurve is well determinated with a different period being unlikely.

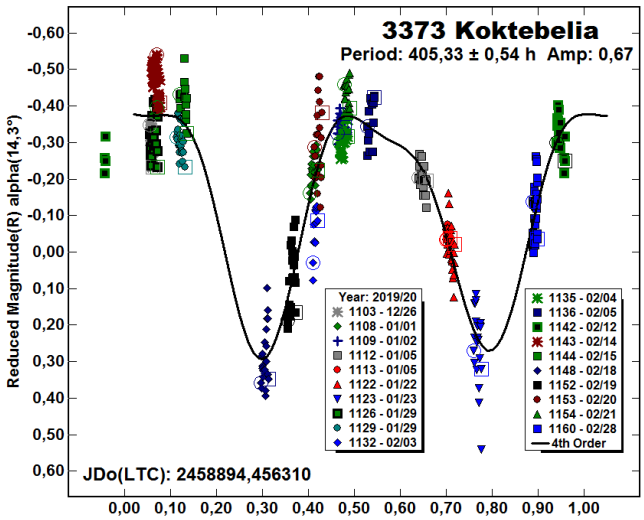


4857 Altagamia. No previous period was reported for this target. After four nights of observations, a clear lightcurve with no alias periods appeared. The final period is $P$ = 9.040 ± 0.002 h and amplitude $A$ = 0.25 mag.

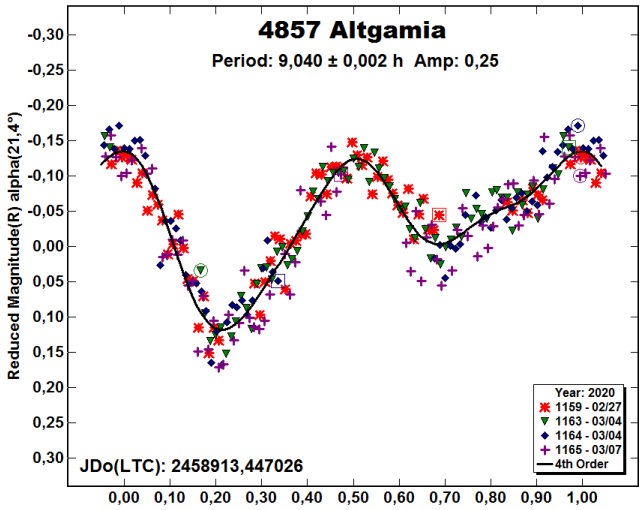

5042 Colpa. There was no previous period found for Colpa, which was observed for two months. This led to a long period lightcurve that is incomplete due to sky conditions. Unfortunately the maximum at phase 0.40 - 0.50 is not well covered but *MPO Canopus* found no other period. The period is $P$ = 169.64 ± 0.13 h and amplitude $A$ = 0.93 mag.

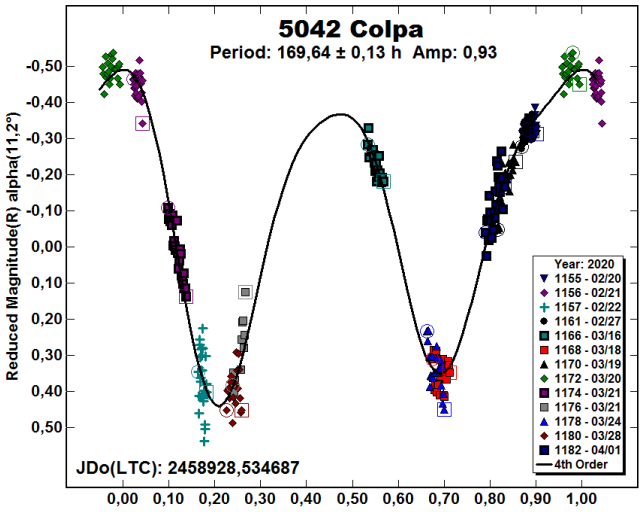


9100 Tomohisa. With no previous period reported, this is the most uncertain result among all the others reported here. The faintness, V ~ 16, and the low amplitude of the curve did not allow finding a secure result. In the end, the most reliable among several possible periods gives a bimodal lightcurve, although *MPO Canopus* slightly prefers the half-period monomodal solution. The adopted period is $P$ = 9.421 ± 0.003 h and amplitude $A$ = 0.09 mag.

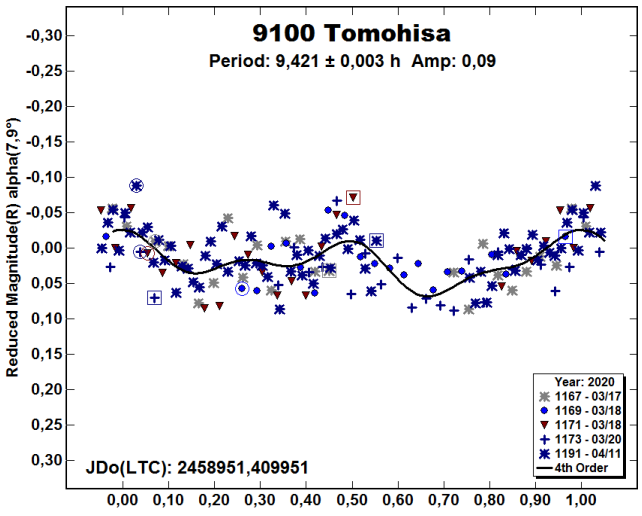


References

Harris, A.W.; Young, J.W.; Scaltriti, F.; Zappala, V. (1984). "Lightcurves and phase relations of the asteroids 82 Alkmene and 444 Gyptis." *Icarus* **57**, 251-258.

Warner, B.D.; Harris, A.W.; Pravec, P. (2009). "The Asteroid Lightcurve Database." *Icarus* **202**, 134-146. Updated 2020 April. *http://www.minorplanet.info/lightcurvedatabase.html*

## DETERMINING THE ROTATIONAL PERIODS AND LIGHTCURVES OF MAIN BELT ASTEROIDS

Shandi Groezinger
Kent Montgomery
Texas A&M University-Commerce
P.O. Box 3011
Commerce, TX 75429-3011
Kent.Montgomery@tamuc.edu

(Received: 2020 Feb 21 Revised: 2020 March 20)

Lightcurves and rotational periods are presented for six main-belt asteroids. The rotational periods determined are 970 Primula (2.777 ± 0.001 h), 1103 Sequoia (3.1125 ± 0.0004 h), 1160 Illyria (4.103 ± 0.002 h), 1188 Gothlandia (3.52 ± 0.05 h), 1831 Nicholson (3.215 ± 0.004 h) and (11230) 1999 JV57 (7.090 ± 0.003 h).

The purpose of this research was to create lightcurves and determine the rotational periods of six asteroids: 970 Primula, 1103 Sequoia, 1160 Illyria, 1188 Gothlandia, 1831 Nicholson and (11230) 1999 JV57. Asteroids were selected for this study from a website that catalogues all known asteroids (CALL). For an asteroid to be chosen in this study, it has to meet the requirements of brightness, declination, and opposition date. For optimum signal to noise ratio (SNR), asteroids of apparent magnitude of 16 or lower were chosen. Asteroids with positive declinations were chosen due to using telescopes located in the northern hemisphere. The data for all the asteroids was typically taken within two weeks from their opposition dates. This would ensure a maximum number of images each night.

Asteroid 970 Primula was discovered by Reinmuth, K. at Heidelberg in 1921. This asteroid has an orbital eccentricity of 0.2715 and a semi-major axis of 2.5599 AU (JPL). Asteroid 1103 Sequoia was discovered in 1928 by Baade, W. at Bergedorf. This asteroid has an orbital eccentricity of 0.0945 and a semi-major axis of 1.9339 AU (JPL). Asteroid 1160 Illyria was discovered in 1929 by Reinmuth, K. at Heidelberg. This asteroid has an orbital eccentricity of 0.1169 and a semi-major axis of 2.5606 AU (JPL). Asteroid 1188 Gothlandia was discovered in 1930 by Comas Sola, J. at Barcelona. This asteroid has an orbital eccentricity of 0.1807 and a semi-major axis of 2.1902 AU (JPL). Asteroid 1831 Nicholson was discovered in 1968 by Wild, P. at Zimmerwald. This asteroid has an orbital eccentricity of 0.1279 and a semi-major axis of 2.2392 AU (JPL). Asteroid (11230) 1999 JV57 was discovered by LINEAR at Socorro in 1999. This asteroid has an orbital eccentricity of 0.1378 and a semi-major axis of 2.1777 AU (JPL).

Two different telescopes were used to collect data for this research. The first one is part of the Southeastern Association for Research in Astronomy (SARA). The SARA-ORM 1.0-m telescope is equipped with an Andor Ikon-L CCD camera and is located at the Observatorio de Roque de los Muchachos located on the island of La Palma in the Canary Isles. The second telescope used was the Texas A&M University-Commerce (TAMUC) 0.7-m telescope equipped with an Andor Ikon-L CCD Camera located at the Research Observatory in Commerce, Texas.

In order to calibrate the CCD images, a set of flats, bias, and dark calibration images were taken each night. The flat field images were taken against the twilight sky at exposures of five to fifteen seconds to ensure proper signal to noise ratio and no shutter artifacts. The darks were exposed for the same time as the

respective light images, with exposures ranging from two minutes to three minutes. The filter used for the SARA-ORM telescope was an IR-blocking and the one for TAMUC telescope was a luminance filter. Both filters transmit the visible portion of the spectrum but block the infrared.

The astronomical software *MaxIm DL* was used to reduce and align all the images to correct for minor image shifts. Afterwards, the program *MPO Canopus v10.2.1.0* (Warner, 2011) was used to perform differential photometry on the reduced data. For each reduced image, five stars were used for brightness comparison to the asteroid. Aperture photometry was used to determine the brightness of these comparison stars and the asteroid. The average of the difference in brightness between the stars and the asteroid was found for each image and then plotted versus time to create a lightcurve. A Fourier transform was then applied to the lightcurve to determine the rotational period and associated error.

970 Primula. The asteroid 970 Primula was imaged 86 times on 2019, September 18, 82 times on 2019, September 25, and 97 on 2019, September 26. All three nights used the TAMUC telescope and the data resulted in a rotational period of 2.777 ± 0.001 h with an amplitude of 0.19 mag. A previous study found a similar rotation period of 2.777 h with an amplitude of 0.18 mag (Sada et al., 2004).

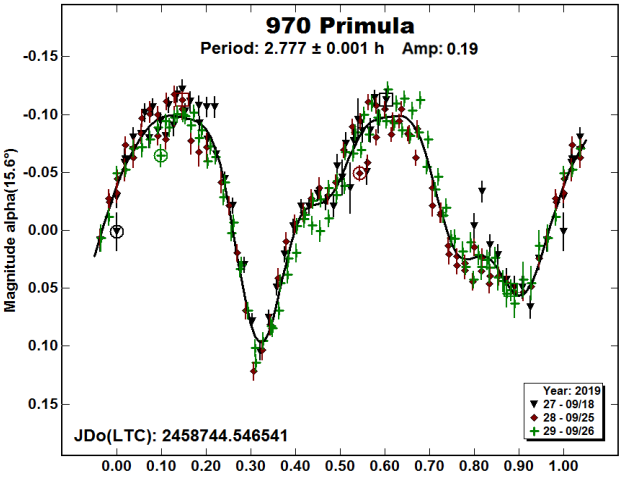


1103 Sequoia. The asteroid 1103 Sequoia was imaged 68 times on 2019, July 24 and 67 times on 2019, August 30. Both nights used the TAMUC telescope and the data resulted in a rotational period of 3.1125 ± 0.0004 h with an amplitude of 0.37 mag. A previous study found a similar rotation period of 3.04 h with an amplitude of 0.34 mag (Lecrone et al., 2004).

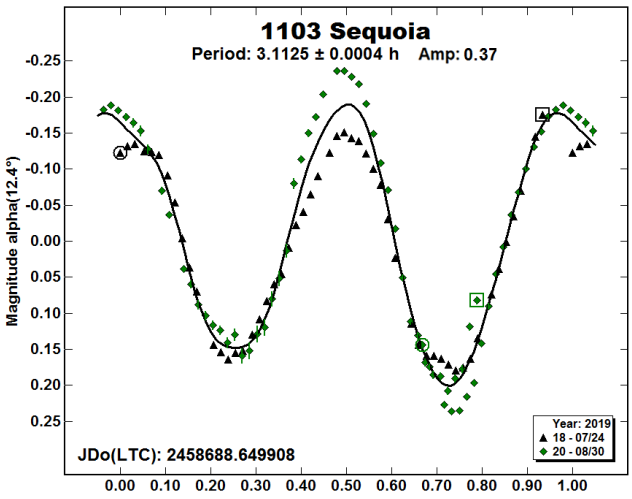


1160 Illyria. The asteroid 1160 Illyria was imaged 92 times on 2019, October 2, 120 times on 2019, October 3, and 42 times on 2019, October 18. All three nights used the TAMUC telescope and the data resulted in a rotational period of 4.103 ± 0.002 h with an amplitude of 0.88 mag. A previous study found a similar rotation period of 4.1040 h with an amplitude of 0.58 mag (Bennefeld, et al., 2009).

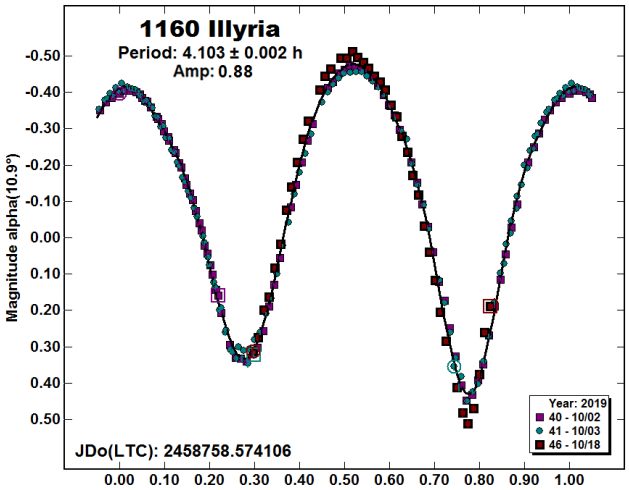


1188 Gothlandia. The asteroid 1188 Gothlandia was imaged 200 times on 2019, January 31. This night used the SARA-ORM telescope and the data resulted in a rotational period of 3.52 ± 0.05 h with an amplitude of 0.64 mag. A previous study found a similar rotation period of 3.4916 h with an amplitude of 0.59 mag (Baker et al., 2012).

| Number | Name | 2019 mm/dd | Phase | $L_{PAB}$ | $B_{PAB}$ | Period(h) | P.E. | Amp | A.E. | Grp |
|---|---|---|---|---|---|---|---|---|---|---|
| 970 | Primula | 09/18-09/26 | 15.4,18.8 | 327 | +2.9 | 2.777 | 0.001 | 0.19 | 0.03 | MB-I |
| 1103 | Sequoia | 07/24-08/30 | 12.3,28 | 295 | +16.6 | 3.1125 | 0.0004 | 0.37 | 0.04 | H |
| 1160 | Illyria | 10/02-10/18 | 10.8,17.3 | 349 | -2.6 | 4.103 | 0.002 | 0.88 | 0.02 | EUN |
| 1188 | Gothlandia | 01/31 | 6.0 | 121 | +5.8 | 3.52 | 0.05 | 0.64 | 0.02 | FLOR |
| 1831 | Nicholson | 09/27-10/01 | 9.5,11.2 | 384 | -7.6 | 3.215 | 0.004 | 0.27 | 0.03 | FLOR |
| 11230 | 1999 JV57 | 10/23-10/24 | 1.9,2.5 | 27 | -0.7 | 7.090 | 0.003 | 0.22 | 0.02 | |

Table I. Observing circumstances and results. The phase angle is given for the first and last date. $L_{PAB}$ and $B_{PAB}$ are the approximate phase angle bisector longitude/latitude at mid-date range (see Harris et al., 1984). Grp is the asteroid family/group (Warner et al., 2009). Some data is from the JPL SBN website (JPL, 2017). Additional data is from *MPO Canopus v10.2.1.0* (Warner, 2011).

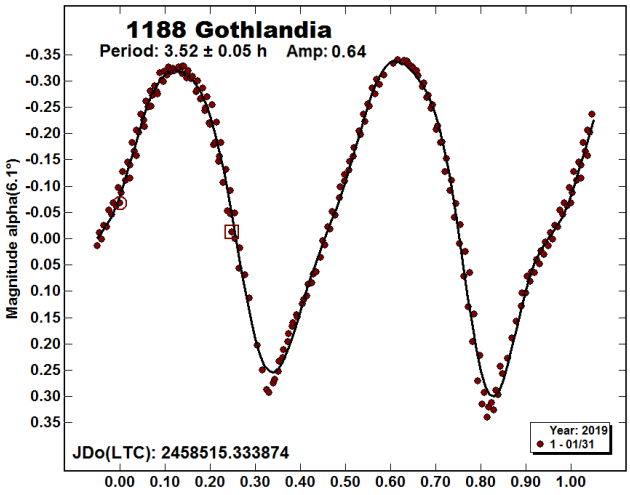


1831 Nicholson. The asteroid 1831 Nicholson was imaged 82 times on 2019, September 27 and 90 times on 2019, October 1. Both nights used the TAMUC telescope and the data resulted in a rotational period of 3.215 ± 0.004 h with an amplitude of 0.27 mag. A previous study found a similar rotation period of 3.2551 h with an amplitude of 0.27 mag (Benishek, 2016).

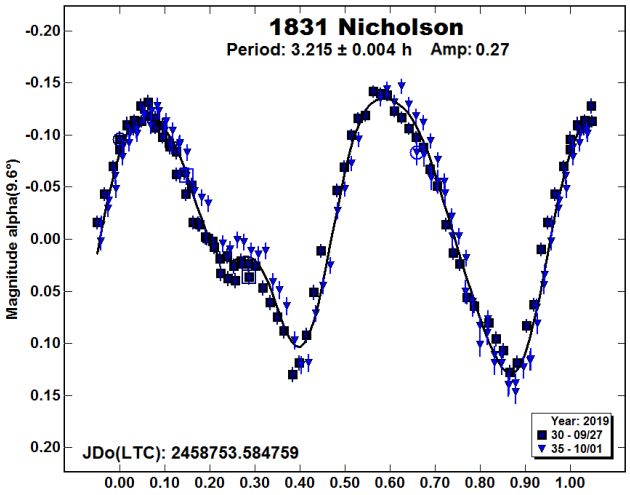


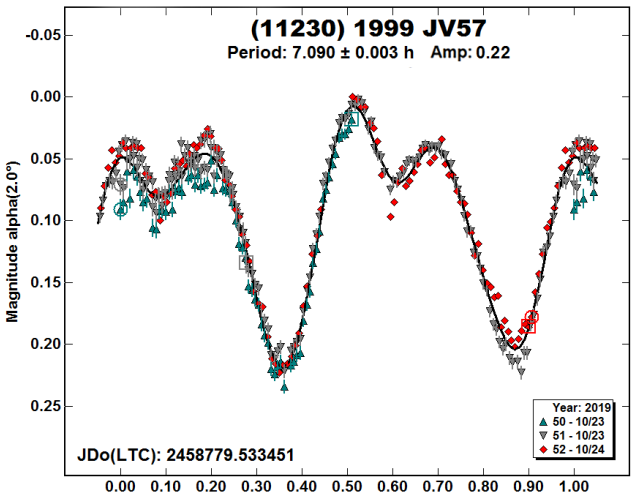


(11230) 1999 JV57. The asteroid 11230 1999 JV57 was imaged 172 times on 2019, October 23 and 116 times on 2019, October 24. The first night used the TAMUC telescope and the second night used the SARA-ORM telescope. This data resulted in a rotational period of 7.090 ± 0.003 h with an amplitude of 0.22 mag. An investigation of the lightcurve database showed no previous lightcurve data (LCDB). A search of JPL's Small Body Database also produced no other lightcurve data on this asteroid (JPL).

Acknowledgements

This research used observations from the SARA Observatory 1.0-m telescope at the Observatorio de Roque de los Muchachos located in the Canary Isles, which is owned by the Southeastern Association for Research in Astronomy at *saraobservatory.org*. One of the authors (S.G.) would like to give a special thanks to Kent Montgomery at Texas A&M University-Commerce for the continued support and the necessary training of the TAMUC telescope; he also provided the training of the multiple software programs listed. This author would like to also give a special thanks to Cristo Sanchez at Texas A&M University-Commerce for the training of how to operate the SARA-ORM telescope.

References

Baker, R.E.; Pilcher, F.; Klinglesmith III, D.A. (2012). "Rotation Period and HG Parameters Determination for 1188 Gothlandia." *Minor Planet Bulletin* **39**, 60-63.

Benishek, V. (2016). "Rotation Periods of 1831 Nicholson, 2929 Harris, 8463 Naomimurdoch, and (34173) 2000 QY37." *Minor Planet Bulletin* **43**, 89-90.

Bennefeld, C.; Bass, S.; Blair, R.; Cunningham, K.; Hill, D.; McHenry, M.; Maxwell, L. (2009). "Asteroid Lightcurve Analysis at Ricky Observatory." *Minor Planet Bulletin* **36**, 147-148.

Collaborative Asteroid Lightcurve Link (CALL): Potential Lightcurve Targets.
*http://www.minorplanet.info/PHP/call_OppLCDBQuery.php*

Harris, A.W.; Young, J.W.; Scaltriti, F.; Zappala, V. (1984). "Lightcurves and phase relations of the asteroids 82 Alkmene and 444 Gyptis." *Icarus* **57**, 251-258.

JPL Small-Body Database Browser.
*http://ssd.jpl.nasa.gov/sbdb.cgi#top*

Lecrone, C.; Duncan, A.; Kirkpatrick, E. (2004). "Lightcurves and periods for asteroids 105 Artemis, 978 Aidamina, and 1103 Sequoia." *Minor Planet Bulletin*, **31**, 77-78.

Lightcurve Database (LCDB)
*http://www.minorplanet.info/lightcurvedatabase.html*

MaxIm DL-Diffraction Ltd. [Online].
*http://diffractionlimted.com/product/maxim-dl/*

Sada, P.V.; Canizales, E.D.; Armada, E.M. (2004). "CCD photometry of asteroids 970 Primula and 1631 Kopff using a remote commercial telescope." *Minor Planet Bulletin*, ***31***, 49-50.

Warner, B.D.; Harris, A.W.; Pravec, P. (2009). "The Asteroid Lightcurve Database." *Icarus* **202**, 134-146. Updated 2019 Dec. *http://www.minorplanet.info/lightcurvedatabase.html*

Warner, B.D. (2011) MPO Canopus software Version 10.2.1.0. Bdw Publishing. *http://www.minorplanetobserver.com/*

# PHOTOMETRIC OBSERVATIONS OF THIRTY MINOR PLANETS

Tom Polakis
Command Module Observatory
121 W. Alameda Dr.
Tempe, AZ 85282
tpolakis@cox.net

(Received: 2020 March 14)

Phased lightcurves and synodic rotation periods for 23 main-belt asteroids are presented, based on CCD observations made from 2019 December through 2020 March. Raw lightcurves are included for an additional 7 asteroids for which no period solution was found. All the data have been submitted to the ALCDEF database.

CCD photometric observations of 30 main-belt asteroids were performed at Command Module Observatory (MPC V02) in Tempe, AZ. Images were taken using a 0.32-m *f*/6.7 Modified Dall-Kirkham telescope, SBIG STXL-6303 CCD camera, and a 'clear' glass filter. Exposure time for all the images was 2 minutes. The image scale after 2×2 binning was 1.76 arcsec/pixel. Table I shows the observing circumstances and results. All of the images for these 30 asteroids were obtained between 2019 December and 2020 March.

Images were calibrated using a dozen bias, dark, and flat frames. Flat-field images were made using an electroluminescent panel. Image calibration and alignment was performed using *MaxIm DL* software.

The data reduction and period analysis were done using *MPO Canopus* (Warner, 2019). The 45′×30′ field of the CCD typically enables the use of the same field center for three consecutive nights. In these fields, the asteroid and three to five comparison stars were measured. Comparison stars were selected with colors within the range of 0.5 < B-V < 0.95 to correspond with color ranges of asteroids. In order to reduce the internal scatter in the data, the brightest stars of appropriate color that had peak ADU counts below the range where chip response becomes nonlinear were selected. The *MPO Canopus* internal star catalogue was useful in selecting comp stars of suitable color and brightness.

Since the sensitivity of the KAF-6303 chip peaks in the red, the clear-filtered images were reduced to Sloan r′ to minimize error with respect to a color term. Comparison star magnitudes were obtained from the ATLAS catalog (Tonry et al., 2018), which is incorporated directly into *MPO Canopus*. The ATLAS catalog derives Sloan griz magnitudes using a number of available catalogs. The consistency of the ATLAS comp star magnitudes and color-indices allowed the separate nightly runs to be often linked with no zero-point offset; others required shifts of only a few hundredths of a magnitude in a series.

A 9-pixel (16 arcsec) diameter measuring aperture was used for asteroids and comp stars. It was typically necessary to employ star subtraction to remove contamination by field stars. For the asteroids described here, I note the RMS scatter on the phased lightcurves, which gives an indication of the overall data quality including errors from the calibration of the frames, measurement of the comp stars, the asteroid itself, and the period-fit. Period determination was done using the *MPO Canopus* Fourier-type FALC fitting method (cf. Harris et al., 1989). Phased lightcurves show the maximum at phase zero. Magnitudes in these plots are apparent and scaled by *MPO Canopus* to the first night.

Most asteroids were selected from the CALL website (Warner, 2011a) using the criteria of magnitude greater than 15.0 and quality of results, U, less than 2+. In this set of observations, 9 of the 30 asteroids had no previous period analysis, 1 had U = 1, and 15 had U = 2. The Asteroid Lightcurve Database (LCDB; Warner et al., 2009) was consulted to locate previously published results. All the new data for these asteroids can be found in the ALCDEF database.

445 Edna. This outer-belt asteroid was discovered by Edwin Coddington in 1899 at Mt. Hamilton. Its high eccentricity and inclination brought it to a favorable opposition at a northerly declination in late 2019. Malcolm (2002) reported a period of 19.97 ± 0.01 h and Pilcher (2019) computed 19.959 ± 0.003 h. During five nights, 482 images were taken, resulting in a synodic period of 19.960 ± 0.007 h, agreeing with previous assessments. The amplitude is 0.26 mag, with an RMS error of 0.021 mag.

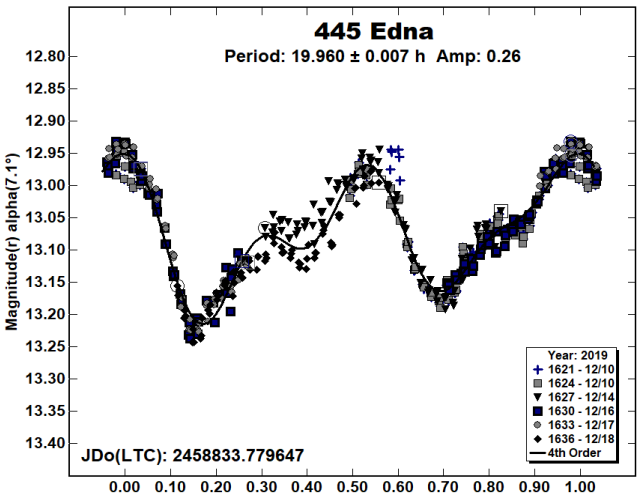


527 Euryanthe was discovered by Max Wolf at Heidelberg in 1904. Brinsfield (2010) reported a period of 26.06 ± 0.01 h and Polakis (2019a) found 42.986 ± 0.021 h. During nine nights, 615 images were gathered to compute a period of 43.40 ± 0.13 h, in line with Polakis's previous value. The amplitude of the lightcurve is 0.14 mag, with an RMS error of 0.028 mag.

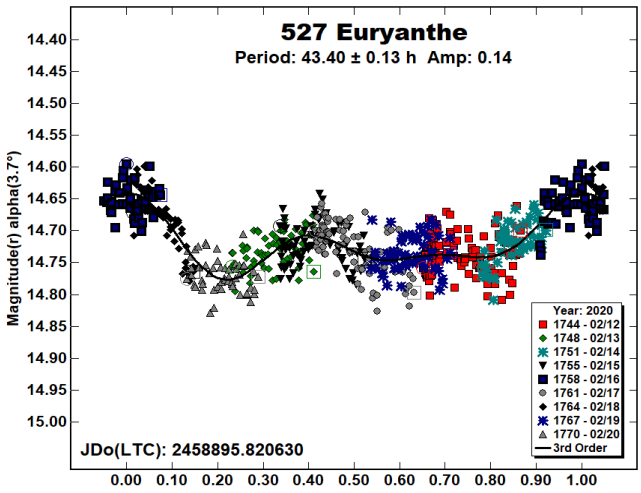

820 Adriana is an outer main-belt asteroid discovered in 1916 by Max Wolf at Heidelberg. It has a low albedo of 0.02. Only one period determination is found in the LCDB, that of Ditteon et al. (2018), who published 6.527 ± 0.006 h. After three nights and 203 images, it became apparent that these data are too flat to obtain a period solution. The raw lightcurve is presented.

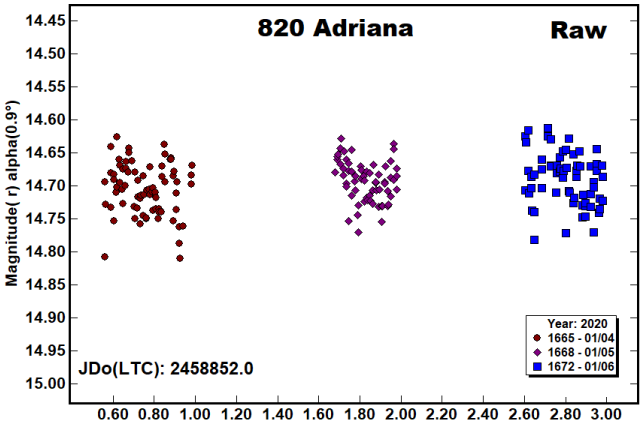


862 Franzia. This is another of Max Wolf's discoveries, made in 1917 at Heidelberg. Several period solutions are published. Warner (2010) found a period of 7.65 ± 0.01 h, Brinsfield (2011) computed 5.014 ± 0.001 h, and Aznar Macias et al. (2016) calculated 16.299 ± 0.013 h. A total of 188 data points were obtained in three nights, yielding a period of 7.520 ± 0.008 h, in agreement with Warner's solution. The amplitude is 0.12 mag, with an RMS error of 0.022 mag.

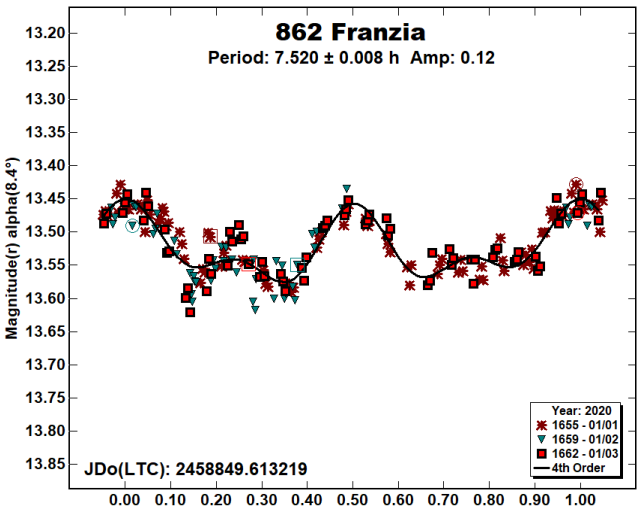


903 Nealley was discovered by Johann Palisa at Vienna in 1918. Warner (2012) obtained a period of 19.72 ± 0.02 h. Observations made on four nights totaling 222 data points were unable to produce a period solution.

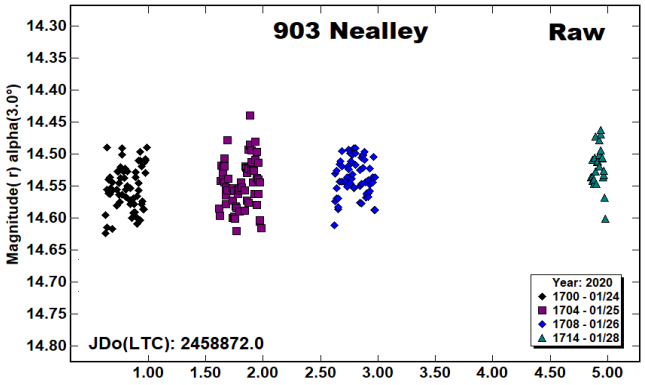


1027 Aesculapia. This Themis-family asteroid was discovered at Yerkes Observatory in 1923 by George Van Biesbroeck. Multiple discordant period solutions are found: Maleszewski and Clark (2004) 6.83 ± 0.10 h; Ehlert and Kingerly (2015), 9.791 ± 0.002 h; Waszczak et al. (2015), 19.506 ± 0.1501 h; and Hess et al. (2017), 13.529 ± 0.042 h. During six nights, 383 observations were made, resulting in a solution of 19.90 ± 0.06 h, in agreement with Waszczak. The RMS error of 0.054 mag is significant relative to the amplitude of 0.19 mag.

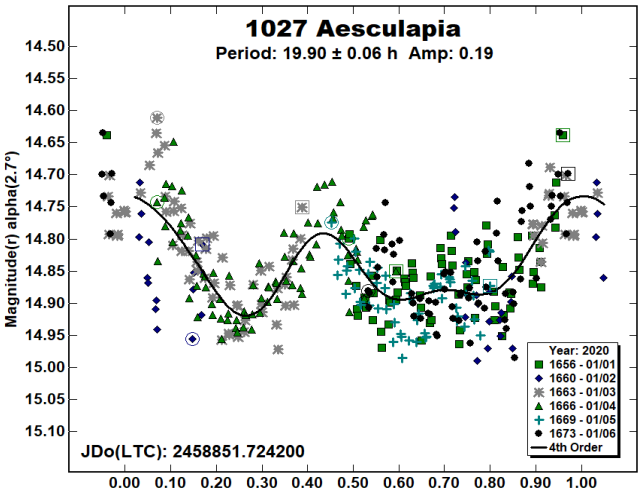


1048 Feodosia was discovered by Karl Reinmuth at Heidelberg in 1924. Schober et al. (1994) determined a period of 10.46 h, while Aznar Macias et al. (2016) shows 35.20 ± 0.23 h. Over the course of three nights, 218 images were taken, yielding a solution of 10.42 ± 0.02 h, agreeing with Schober. The amplitude is 0.15 ± 0.023 mag. A monomodal solution with a period of 5.204 ± 0.008 h is also viable.

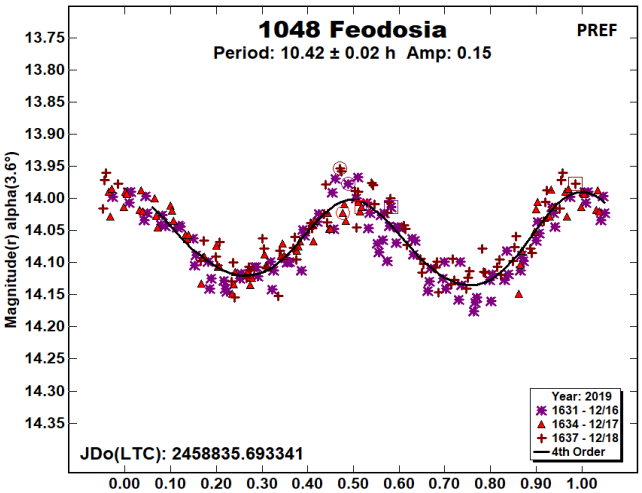


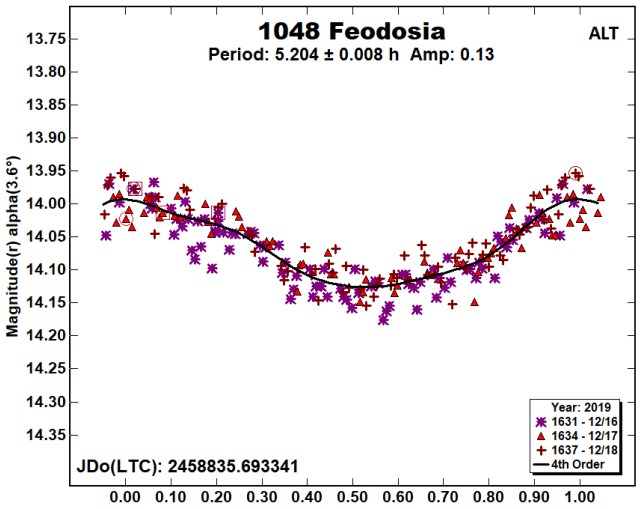


1079 Mimosa. This Koronis-family asteroid was discovered at Yerkes Observatory by George Van Biesbroeck in 1927. Binzel (1987) published a period of 7.3 h and Silvan et al. (2008) obtained 64.6 ± 0.5 h. A total of 353 observations were made on five nights, but the period spectrum revealed no solutions.

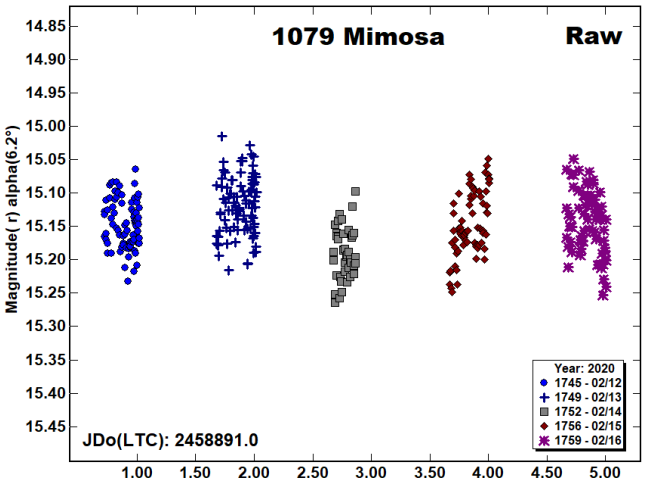


1109 Tata is another of Karl Reinmuth's discoveries, found in 1929 from Heidelberg. Behrend (2005web) shows a period of 8.277 ± 0.002 h. The asteroid was observed on 11 nights, during which 612 data points were obtained. The best period fit is 55.50 ± 0.12 h, disagreeing with Behrend's result. The fit is poor, with an RMS error of 0.049 mag. Despite large nightly amplitude ranges, no shorter periods were apparent in the period spectrum.

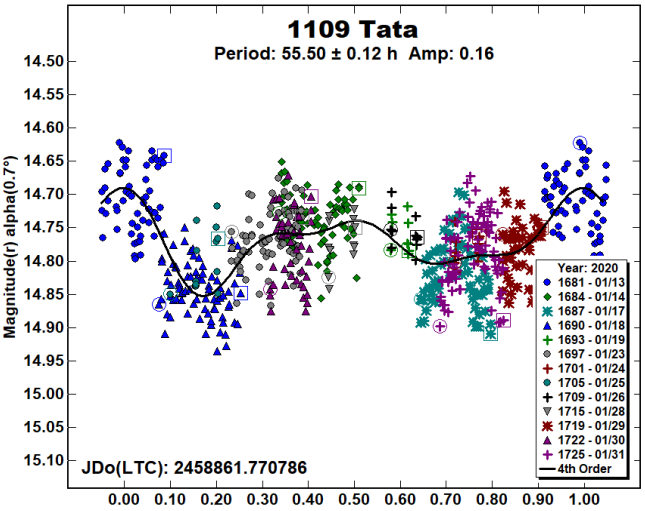


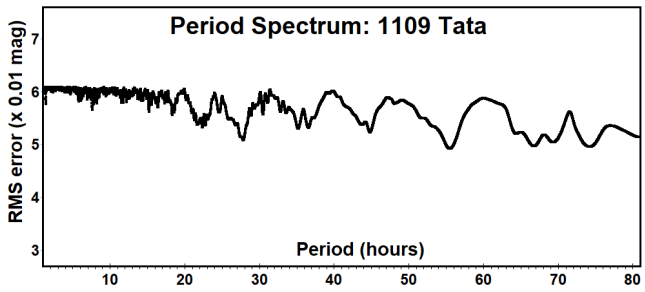


1112 Polonia is an asteroid in the Eos family. It was discovered by Grigory Shajn in 1928 at Simeis. Warner (2008) calculated a period of 82.5 ± 0.5 h, and Behrend (2018web) obtained 18.605 ± 0.002 h. During five nights 322 data points were used to compute a period of 18.71 ± 0.04 h. The amplitude is 0.12 ± 0.021 mag.

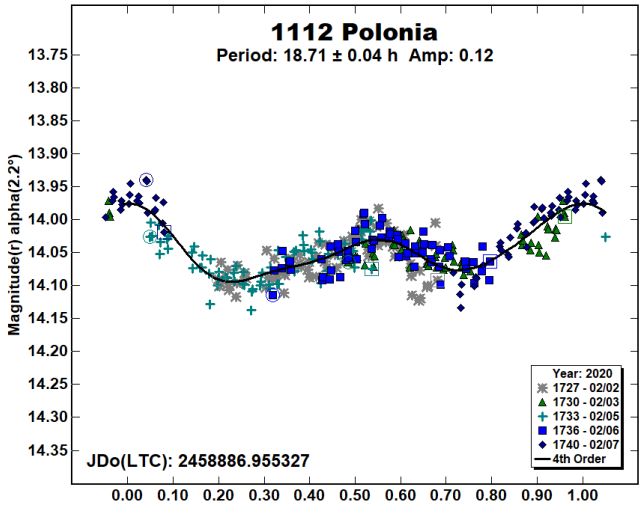

1124 Stroobantia was discovered in 1928 at Uccle by Eugène Joseph Delporte. Two uncertain solutions appear in the LCDB: those of Gil-Hutton (1988), 16.39 h; and Behrend (2016web), 17.0 ± 0.2 h. During two widely separated nights, 167 images were sufficient to reveal that a period solution would elude detection with the small telescope.

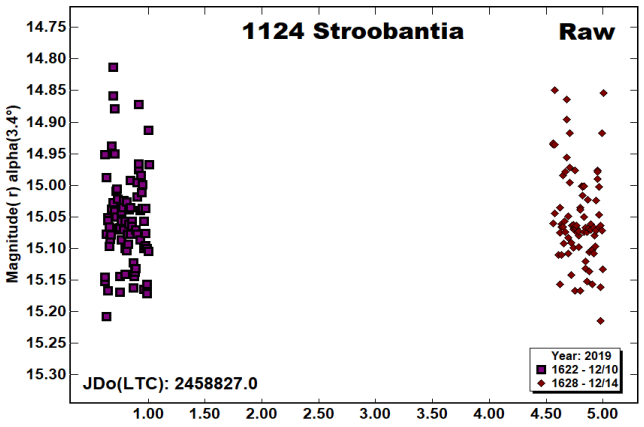


1149 Volga was discovered by E.F. Skvortsov at Simeis in 1929. Binzel (1987) produced a period solution of 27.5 h, and Polakis (2019b) obtained 27.262 ± 0.049 h. A total of 383 data points in six nights were used to compute a synodic period of 27.63 ± 0.07 h, agreeing with previous values. The amplitude is 0.20 mag, with an RMS error of 0.029 mag.

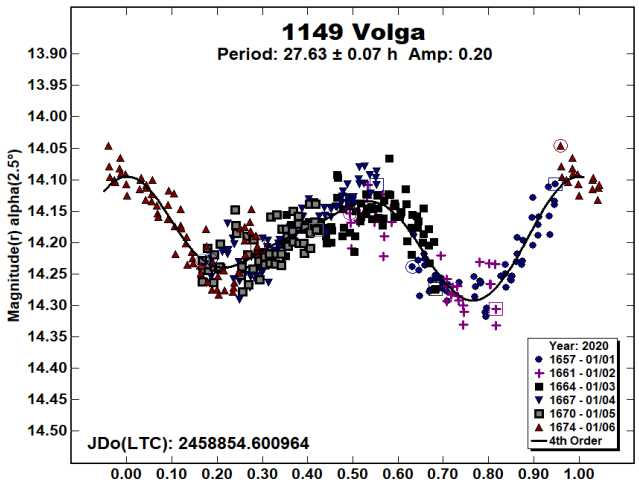


1169 Alwine. This asteroid was discovered at Heidelberg in 1930 by Max Wolf and Laurent Ferrero.

The LCDB shows no period solutions for it. In only two nights, 192 images were sufficient to obtain a period of 2.927 ± 0.003 h. The amplitude of the lightcurve is 0.25 ± 0.046 mag.

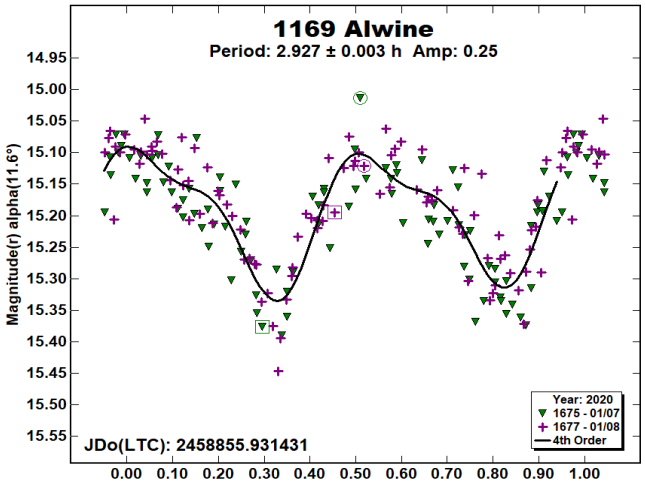


1170 Siva lies in a highly eccentric and inclined orbit. Its discovery was made by Johann Delporte at Uccle in 1930. Several discordant period solutions are published. Behrend (2001web) shows 5.22 ± 0.01 h, Szekely et al. (2005) calculated 3.5 h, and Durech et al. (2018) gives 15.92947 ± 0.00002 h. During two nights, 192 data points were gathered, producing a period of 3.135 ± 0.002 h, disagreeing with published values. The amplitude is 0.30 ± 0.029 mag.

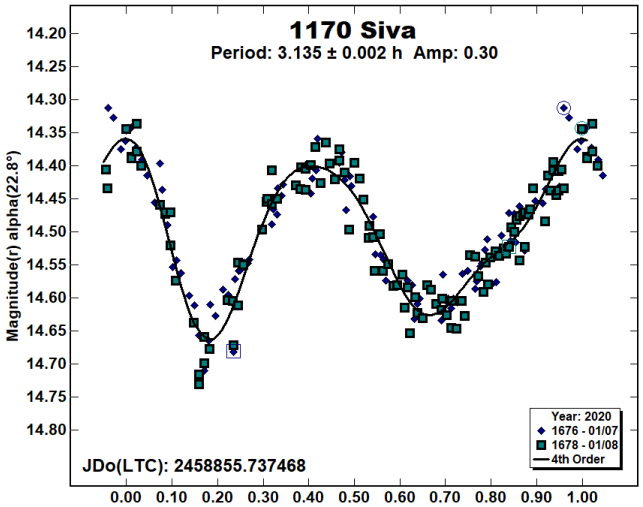


1302 Werra. Karlreinmuth found this Themis-family asteroid while working at Heidelberg in 1924. The only entry in the LCDB is that of Polakis (2019a): 14.03 ± 0.012 h. A total of 269 images were taken in four nights, producing a synodic period of 13.94 ± 0.02 h, agreeing with the earlier result. The amplitude is 0.19 ± 0.034 mag.

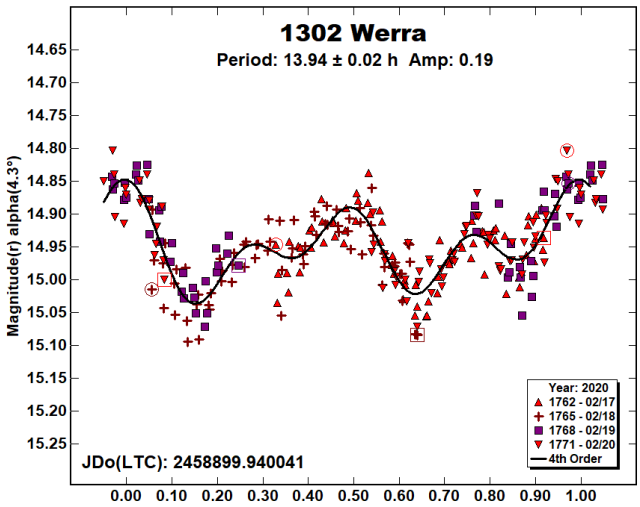


1359 Prieska. Cyril Jackson discovered this asteroid at Johannesburg in 1935. No solutions appear in the LCDB. After three nights, 195 data points failed to yield a period solution.

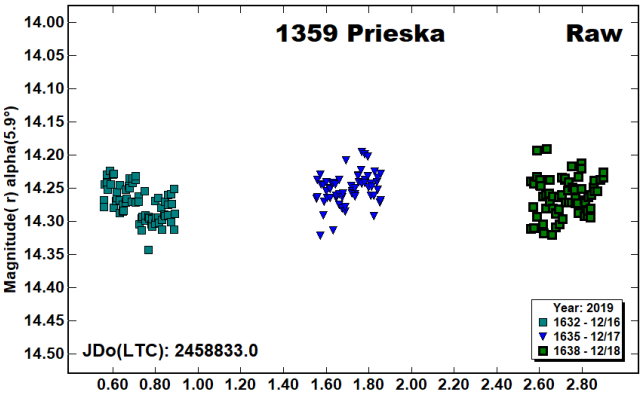


1385 Gelria. Hendrik Van Gent discovered this outer-belt asteroid in 1935, while working at Johannesburg. Polakis (2019a) published a period of 2.3118 ± 0.0007 h, while Benishek (2019) computed nearly double this value: 4.6234 ± 0.0003. A total of 205 points were gathered in three nights. The minimum in the period spectrum agreed much better with the longer period; the result is 4.624 ± 0.011 h, with an amplitude of 0.08 ± 0.029 mag.

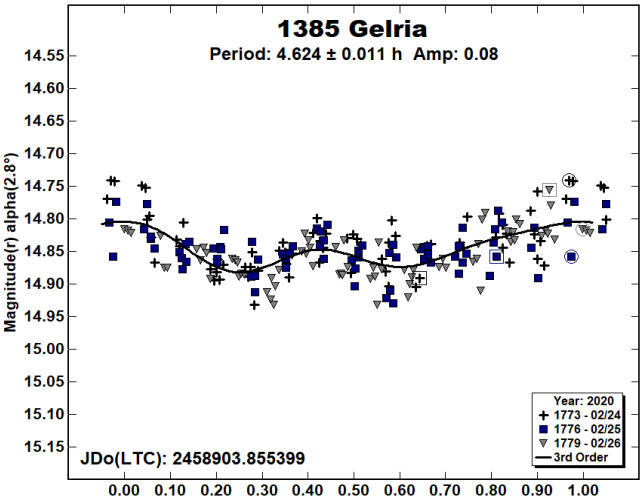


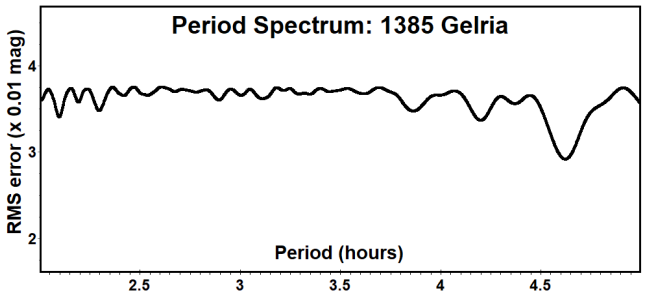


1415 Maulautra is a Flora-family asteroid, discovered in Algiers by Louis Boyer in 1937. The only period solution in the LCDB is that of Behrend (2007web), who shows >12 h. A total of 329 images were taken during seven nights. The slow rotator has a synodic period of 154.9 ± 0.5 h, and an amplitude of 0.57 ± 0.030 mag.

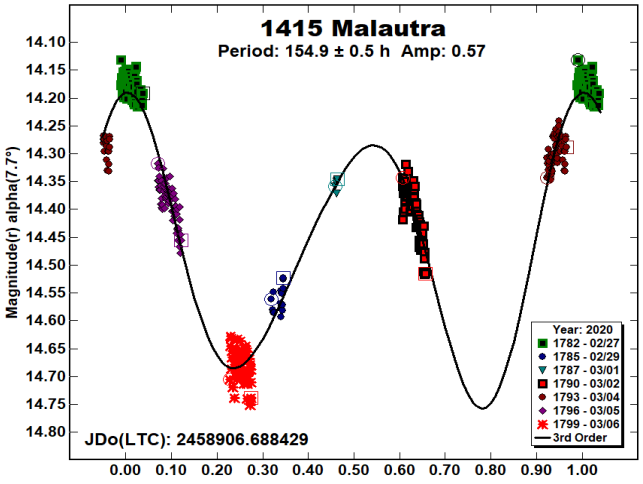


1539 Borrelly was discovered at Nice in 1940. A period of 15.922 ± 0.007 h was computed by Polakis (2019b). Behrend (2018web) found a period of 23.844 ± 0.004 h. In three nights, 230 images were taken, yielding a period solution of 23.84 ± 0.02 h, which is closer to Behrend's result. The asteroid's Earth-day commensurate period prevented coverage of two of the extrema.

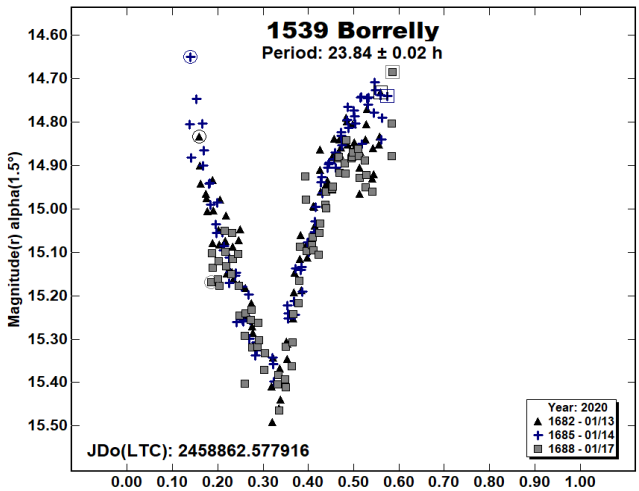

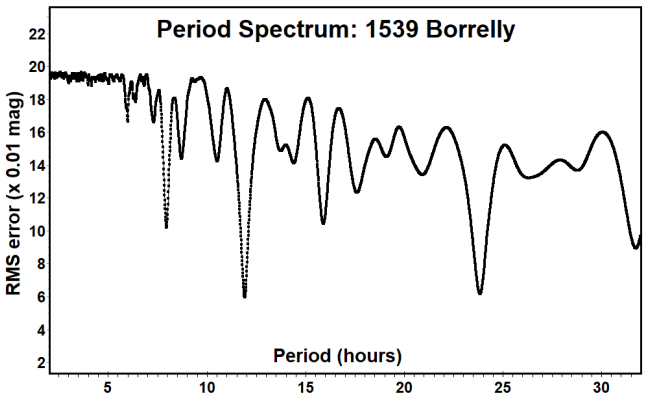


1579 Herrick. Observing at Uccle in 1948, Sylvain Arend found this outer-belt asteroid. The LCDB shows no period solutions. The asteroid was observed on six nights, producing 304 images. A rotation period of 21.33 ± 0.09 h was obtained. The amplitude is 0.18 mag, with an RMS error on the fit of 0.039 mag.

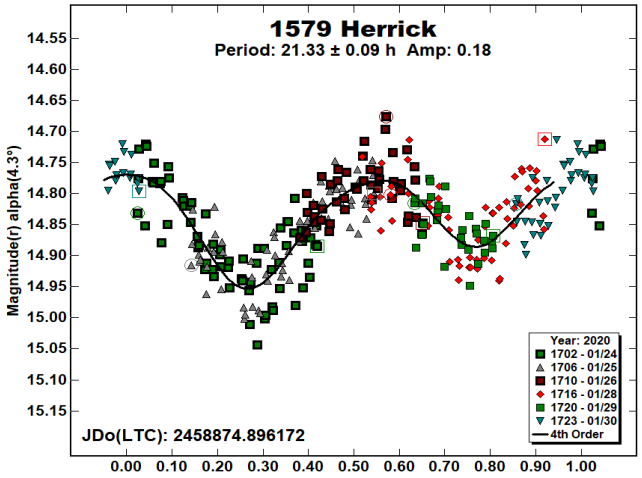


1665 Gaby is an inner-belt asteroid in an eccentric orbit. Its discovery was made by Karl Reinmuth in 1930 at Heidelberg. Hanus et al. (2011) shows a period of 67.905 ± 0.005 h, and Hanus et al. (2016) computed a similar value of 67.911 ± 0.005 h.

In ten observing nights, 593 images were taken. The period spectrum showed a longer period that disagreed with both of these values: 155.4 ± 0.2 h. The amplitude is 0.67 ± 0.030 mag.

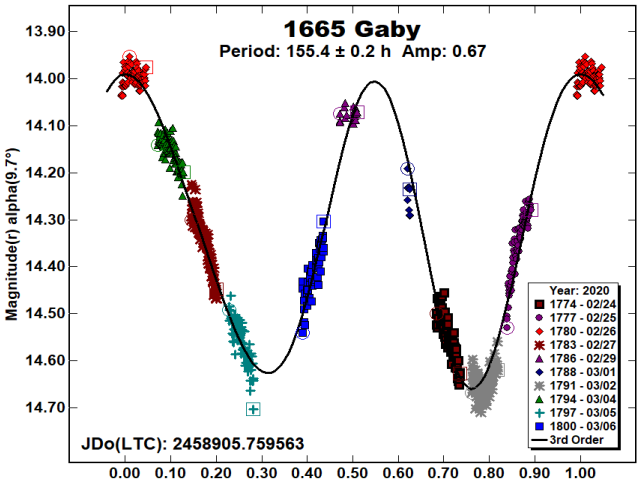


2075 Martinez is a member of the Phocea family. It was discovered in 1974 at Felix Aguilar Observatory.

Menke et al. (2008) published a rotation period of 4.755 ± 0.002 h. In two nights, 191 images were used to compute a period of 4.749 ± 0.004 h, in close agreement with Menke's result. The lightcurve has an amplitude of 0.22 ± 0.030 mag.

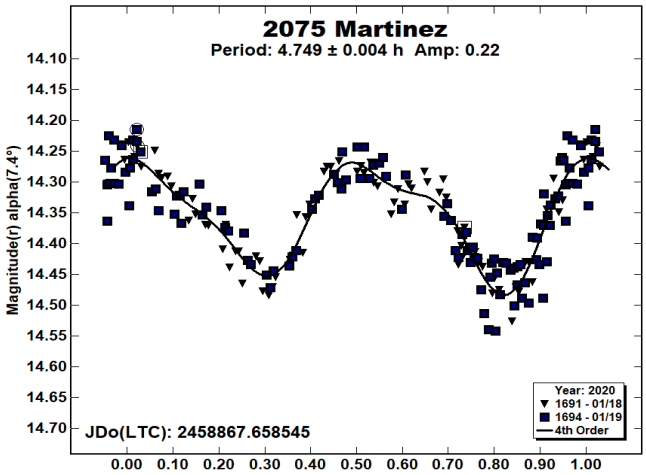


2326 Tololo. This outer-belt asteroid was discovered in 1965 at Brooklyn. Percy (2019) computed a synodic period of 9.488 ± 0.001 h. A total of 115 data points obtained in two nights produced a period solution of 9.49 ± 0.05 mag, agreeing with Percy's value. The amplitude is 0.14 ± 0.020 mag.

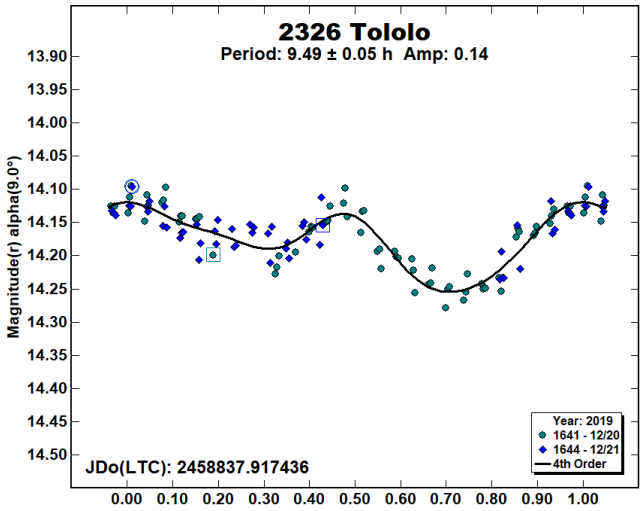


2859 Paganini was discovered by Lyudmila Chernykh at Nauchnyj in 1978. No period solutions appear in the LCDB. In five nights, 341 images were taken. The resulting data was too flat to determine the period.

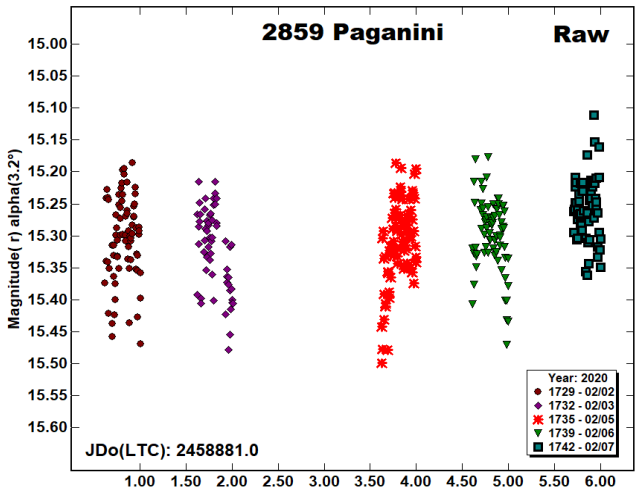


3156 Ellington. Alfred Schmitt discovered this asteroid at Uccle in 1953. Warner (2011b) found a rotation period of 3.53 ± 0.08 h, and Menke et al. (2008) computed 8.33 ± 0.01 h. In four nights, 318 data points did not reveal any rotation periods in the period spectrum.

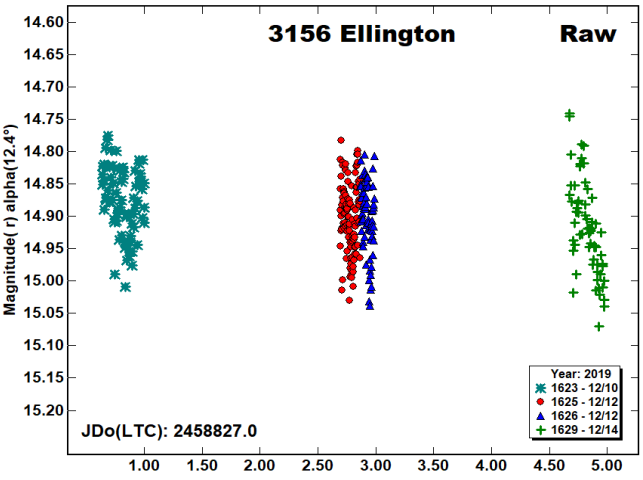


3166 Klondike. Yrjö Väisälä discovered this Flora-family asteroid at Turku in 1940. Sauppe et al. (2007) found a period of 11.72 ± 0.05 h.

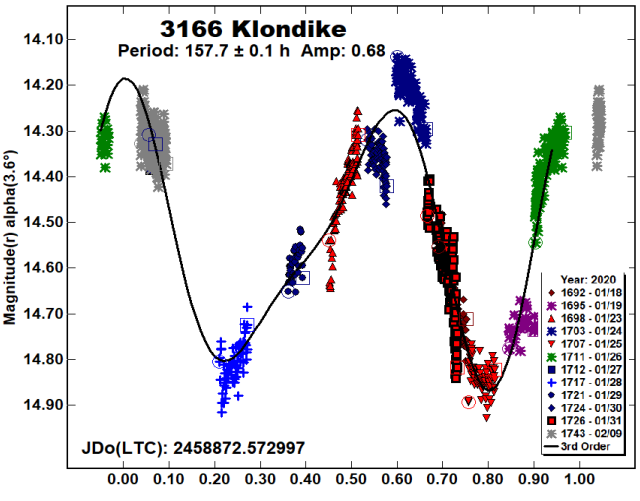


During 12 nights, 1011 images were obtained. The resulting rotation period is 157.7 ± 0.1 h, in disagreement with Sauppe. The amplitude is 0.68 mag, with an RMS error on the fit of 0.068 mag. Misalignment of the points along the Fourier curve is an indication of tumbling.

4421 Kayor was discovered at Heidelberg in 1942 by Karl Reinmuth. There are no period solutions in the LCDB. After 11 nights, 417 images were used to determine a rotation period of 91.4 ± 0.2 h. The amplitude of the phased lightcurve is 0.43 ± 0.054 mag.

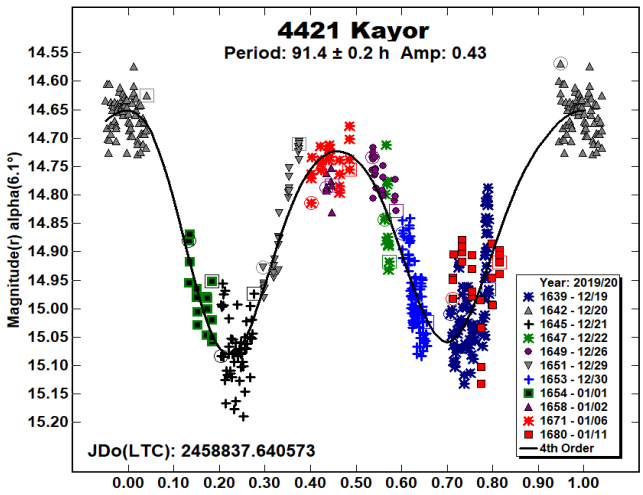


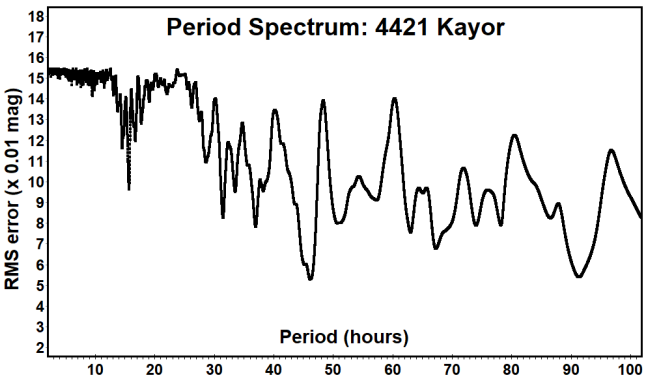


4700 Carusi. Edward Bowell discovered this minor planet at Flagstaff in 1986. The LCDB contains no period solutions for it.

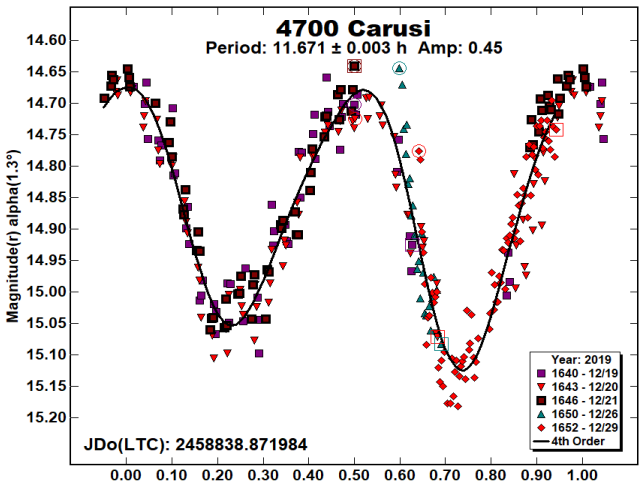

A total of 311 images were obtained in five nights, producing a period of 11.671 ± 0.003 h. The amplitude is 0.45 mag, and the RMS error is 0.045 mag.

4931 Tomsk is an inner main-belt object with a high inclination that was discovered in 1983 by Henri Debehogne at La Silla.

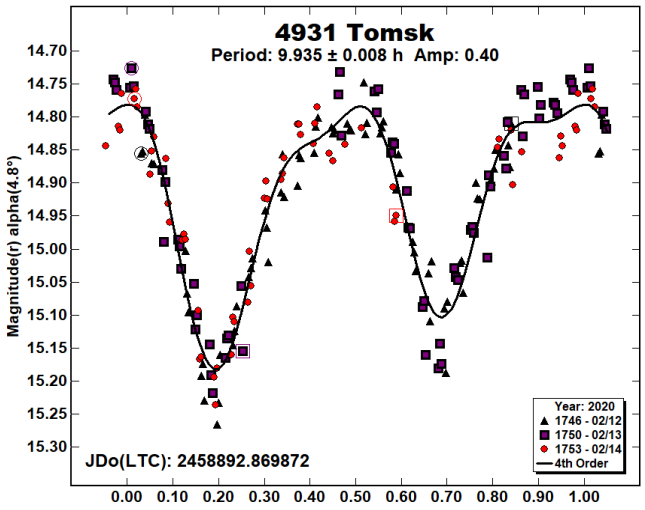


The only published period is that of Durkee et al. (2016), who shows 7.020 ± 0.01 h. In three nights, 187 data points revealed a period of 9.935 ± 0.008 h disagreeing with Durkee's value. The amplitude is 0.40 ± 0.039 mag.

5438 Lorre was discovered by Elanor Helin at Palomar in 1990. Behrend (2002web) shows a period of 26 h. During seven nights, 467 images were obtained. The resulting period is 25.30 ± 0.02 h, agreeing with Behrend's value. The amplitude is 0.68 ± 0.091 mag.

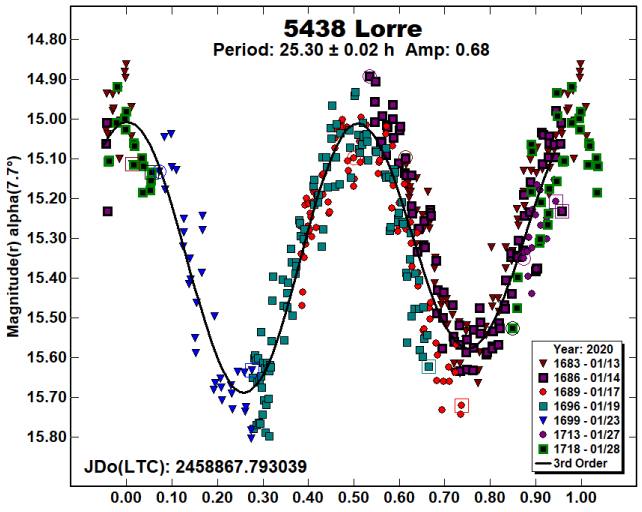


Acknowledgements

The author would like to express his gratitude to Brian Skiff for his indispensable mentoring in data acquisition and reduction. Thanks also go out to Brian Warner for support of his *MPO Canopus* software package.

References

Aznar Macias, A.; Carreno Garcerain, A.; Arce Masego, E.; Brines Rodriques, P.; Lozano de Haro, J.; Fornas Silva, A.; Fornas Silva, G.; Mas Martinez, V.; Rodrigo Chiner, O.; Herrero Porta, D. (2016). "Twenty-one Asteroid Lightcurves at Group Observadores de Asteroides (OBAS): Late 2015 to Early 2016." *Minor Planet Bull.* **43**, 257-263.

Behrend, R. (2001web, 2002web, 2005web, 2007web, 2016web, 2018web). Observatoire de Geneve website. *http://obswww.unige.ch/~behrend/page_cou.html*

Benishek, V. (2019). "Asteroid Lightcurve and Synodic Period Determinations: 2018 October-December."*Minor Planet Bull.***46**, 208-210.

Binzel, R.P. (1987). "A photoelectric survey of 130 asteroids." *Icarus* **72**, 135-208.

Brinsfield, J.W. (2010). "Asteroid Lightcurve Analysis at Via Capote Observatory: 4th Quarter 2009." *Minor Planet Bull.* **37**, 50-53.

Brinsfield, J.W. (2011). "Asteroid Lightcurve Analysis at the Via Capote Observatory: 1st Quarter 2011." *Minor Planet Bull.* **38**, 154-155.

Ditteon, R.; Black, S.; Masner, Z.; Osborne, J.; Trent, L. (2018). "Lightcurve Analysis of Minor Planets Observed at the Oakley Southern Sky Observatory: 2017 August-September." *Minor Planet Bull.* **45**, 338-340.

Durech, J.; Hanus, J.; Ali-Lagoa, V. (2018). "Asteroid models reconstructed from the Lowell Photometric Database and WISE data." *Astron. Astrophys.* **617**, A57.

Durkee, R.I.; Houghton, J.L.; Eggleston, C.L. (2016). "The Rotation Period of Asteroids 4931 Tomsk and 4232 Jordaens." *Minor Planet Bull.* **43**, 284-285.

Ehlert, S.; Kingery, A. (2015). "New Lightcurves of 1027 Aesculapia and 3395 Jitka." *Minor Planet Bull.* **42**, 211.

Gil-Hutton, R. (1998). "Photometry of Asteroids 558 Carmen, 613 Ginevra, and 1124 Stroobantia." *Rev. Mexicana Astron. Astrof.* **34**, 9-11.

Hanus, J.; Durech, J.; Broz, M.; Warner, B.D.; Pilcher, F.; Stephens, R.; Oey, J.; Bernasconi, L.; Casulli, S.; Behrend, R.; Polishok, D.; Henych, T.; Lehky, M; Yoshida, F.; Ito, T. (2011). "A study of asteroid pole-latitude distribution based on an extended set of shape models derived by the lightcurve inversion method." *Astron. Astrophys.* **530**, A134.

Hanus, J.; Durech, J.; Oszkiewicz, D.A.; Behrend, R.; et al. (2016). "New and updated convex shape models of asteroids based on optical data from a large collaboration network." *Astron. Astrophys.* **586**, A108.

Harris, A.W.; Young, J.W.; Scaltriti, F.; Zappala, V. (1984). "Lightcurves and phase relations of the asteroids 82 Alkmene and 444 Gyptis." *Icarus* **57**, 251-258.

| Number | Name | 20yy/mm/dd | Phase | $L_{PAB}$ | $B_{PAB}$ | Period(h) | P.E. | Amp | A.E. | Grp |
|---|---|---|---|---|---|---|---|---|---|---|
| 445 | Edna | 19/12/10-19/12/18 | 7.2,8.0 | 74 | 16 | 19.960 | 0.007 | 0.26 | 0.02 | MB-O |
| 527 | Euryanthe | 20/02/12-20/02/20 | 3.6,6.5 | 133 | 3 | 43.40 | 0.13 | 0.14 | 0.03 | MB-O |
| 820 | Adriana | 20/01/04-20/01/06 | 0.8,1.3 | 102 | -2 | -- | -- | -- | -- | MB-O |
| 862 | Franzia | 20/01/01-20/01/03 | 8.3,9.0 | 84 | 10 | 7.520 | 0.008 | 0.12 | 0.02 | MB-O |
| 903 | Nealley | 20/01/24-20/01/28 | 3.0,2.9 | 125 | 8 | -- | -- | -- | -- | MB-O |
| 1027 | Aesculapia | 20/01/01-20/01/06 | 2.5,4.5 | 93 | 1 | 19.90 | 0.06 | 0.19 | 0.05 | THM |
| 1048 | Feodosia | 19/12/16-19/12/18 | 3.6,3.8 | 82 | 10 | [A]10.42 | 0.02 | 0.15 | 0.02 | MB-O |
| 1079 | Mimosa | 20/02/12-20/02/16 | 6.3,4.7 | 158 | 0 | -- | -- | -- | -- | KOR |
| 1109 | Tata | 20/01/13-20/01/31 | 0.6,6.1 | 111 | -2 | 55.50 | 0.12 | 0.16 | 0.05 | MB-O |
| 1112 | Polonia | 20/02/02-20/02/07 | 2.3,1.1 | 138 | -3 | 18.71 | 0.04 | 0.12 | 0.02 | EOS |
| 1124 | Stroobantia | 19/12/10-19/12/14 | 3.5,3.2 | 81 | 8 | -- | -- | -- | -- | MB-O |
| 1149 | Volga | 20/01/01-20/01/06 | 2.4,4.3 | 95 | -4 | 27.63 | 0.07 | 0.20 | 0.03 | MB-O |
| 1169 | Alwine | 20/01/07-20/01/08 | 11.7,11.2 | 125 | -4 | 2.927 | 0.003 | 0.25 | 0.05 | FLO |
| 1170 | Siva | 20/01/07-20/01/08 | 22.9,22.7 | 117 | 32 | 3.135 | 0.002 | 0.30 | 0.03 | MC |
| 1302 | Werra | 20/02/17-20/02/20 | 4.4,3.2 | 158 | 3 | 13.94 | 0.02 | 0.19 | 0.03 | THM |
| 1359 | Prieska | 19/12/16-19/12/18 | 5.8,6.6 | 69 | 2 | -- | -- | -- | -- | MB-O |
| 1385 | Gelria | 20/02/24-20/02/26 | 2.8,3.4 | 150 | 5 | 4.624 | 0.011 | 0.08 | 0.03 | MB-O |
| 1415 | Malautra | 20/02/27-20/03/06 | 7.8,3.3 | 170 | -2 | 154.9 | 0.5 | 0.57 | 0.03 | FLOR |
| 1539 | Borrelly | 20/01/13-20/01/17 | 1.6,0.4 | 116 | -1 | 23.84 | 0.02 | 0.70 | -- | THM |
| 1579 | Herrick | 20/01/24-20/01/30 | 4.3,3.4 | 130 | -9 | 21.33 | 0.09 | 0.18 | 0.04 | MB-O |
| 1665 | Gaby | 20/02/24-20/03/06 | *9.7,8.9 | 163 | 15 | 155.4 | 0.2 | 0.67 | 0.03 | MB-I |
| 2075 | Martinez | 20/01/18-20/01/19 | 7.5,7.2 | 124 | -8 | 4.749 | 0.004 | 0.22 | 0.03 | PHO |
| 2326 | Tololo | 19/12/20-19/12/21 | 9.0,8.9 | 90 | -18 | 9.49 | 0.05 | 0.14 | 0.02 | MB-O |
| 2859 | Paganini | 20/02/02-20/02/07 | 3.4,1.7 | 137 | -3 | -- | -- | -- | -- | MB-I |
| 3156 | Ellington | 19/12/10-19/12/14 | 12.4,11.7 | 92 | 21 | -- | -- | -- | -- | MB-O |
| 3166 | Klondike | 20/01/18-20/02/09 | 3.6,11.8 | 120 | 6 | 157.7 | 0.1 | 0.68 | 0.06 | FLOR |
| 4421 | Kayor | 19/12/19-20/01/11 | *6.3,7.1 | 98 | 1 | 91.4 | 0.2 | 0.43 | 0.05 | MB-O |
| 4700 | Carusi | 19/12/19-19/12/29 | *1.5,5.0 | 89 | 2 | 11.671 | 0.003 | 0.45 | 0.05 | MB-I |
| 4931 | Tomsk | 20/02/12-20/02/14 | *4.8,4.8 | 142 | -8 | 9.935 | 0.008 | 0.40 | 0.04 | MB-I |
| 5438 | Lorre | 20/01/13-20/02/28 | 7.6,18.1 | 101 | 8 | 25.30 | 0.02 | 0.68 | 0.09 | MB-O |

Table I. Observing circumstances and results. [A]Ambiguous (preferred solution). The phase angle is given for the first and last date. If preceded by an asterisk, the phase angle reached an extrema during the period. $L_{PAB}$ and $B_{PAB}$ are the approximate phase angle bisector longitude/latitude at mid-date range (see Harris et al., 1984). Grp is the asteroid family/group (Warner et al., 2009).


Harris, A.W.; Young, J.W.; Bowell, E.; Martin, L.J.; Millis, R.L.; Poutanen, M.; Scaltriti, F.; Zappala, V.; Schober, H.J.; Debehogne, H.; Zeigler, K.W. (1989). "Photoelectric Observations of Asteroids 3, 24, 60, 261, and 863." *Icarus* **77**, 171-186.

Hess, K.; Bruner, M.; Ditteon, R. (2017). "Asteroid Lightcurve Analysis at the Oakley Southern Sky Observatory: 2015 February - March." *Minor Planet Bull.* **44**, 3-5.

JPL (2017). Small-Body Database Browser. *http://ssd.jpl.nasa.gov/sbdb.cgi#top*

Malcolm, G. (2002). "Rotational Periods and Lightcurves of 445 Edna, 1817 Katanga and 1847 Stobbe." *Minor Planet Bull.* **29**, 28-29.

Maleszewski, C.; Clark, M. (2004). "Bucknell University Observatory lightcurve results for 2003-2004." *Minor Planet Bull.* **31**, 93-94.

Menke, J.; Cooney, W.; Gross, J.; Terrell, D. (2008). "Asteroid Lightcurve Analysis at Menke Observatory." *Minor Planet Bull.* **35**, 155-160.

Percy, S.C. (2019). "Rotation Period for 2326 Tololo." *Minor Planet Bull.* **46**, 13-14.

Pilcher, F. (2019). "New Lightcurves of 156 Xanthippe, 445 Edna, and 676 Melitta." *Minor Planet Bull.* **46**, 58-60.

Polakis, T. (2019a). "Lightcurve Analysis of Eleven Main-belt Minor Planets." *Minor Planet Bull.* **46**, 132-137.

Polakis, T. (2019b). "Lightcurve Analysis for Seven Main-belt Minor Planets." *Minor Planet Bull.* **46**, 78-80.

Sauppe, J.; Torno, S.; Lemke-Oliver, R.; Ditteon, R. (2007). "Asteroid Lightcurve Analysis at the Oakley Observatory - March/April 2007." *Minor Planet Bull.* **34**, 119-122.

Schober, H.J.; Erikson, A.; Hahn, G.; Lagerkvist, C.-I.; Albrecht, R.; Schroll, A.; Stadler, M. (1994). "Physical studies of asteroids. XXVIII. Lightcurves and photoelectric photometry of asteroids 2, 14, 51, 105, 181, 238, 258, 369, 377, 416, 487, 626, 679, 1048 and 2183." *Astron. Astrophys. Suppl. Ser.* **105**, 281-300.

Slivan, S.M.; Binzel, R.P.; Boroumand, S.C.; Pan, M.W.; Simpson, C.M.; Tanabe, J.T.; Villastrigo, R.M.; Yen, L.L.; Ditteon, R.P.; Pray, D.P.; Stephens, R.D. (2008). "Rotation rates in the Koronis family, complete to H≈11.2." *Icarus* **195**, 226-276.

Székely, P.; Kiss, L.L.; Szabó, Gy.M.; Sárneczky, K.; Csák, B.; Váradi, M.; Mészáros, Sz. (2005). "CCD photometry of 23 minor planets." *Planet. Space Sci.* **53**, 925-936.

Tonry, J.L.; Denneau, L.; Flewelling, H.; Heinze, A.N.; Onken, C.A.; Smartt, S.J.; Stalder, B.; Weiland, H.J.; Wolf, C. (2018). "The ATLAS all-sky stellar reference catalog." *Astrophys. J.* **867**, A105.

VizieR (2017) *http://vizier.u-strasbg.fr/viz-bin/VizieR*

Warner, B.D. (2008). "Asteroid Lightcurve Analysis at the Palmer Divide Observatory: September-December 2007." *Minor Planet Bull.* **35**, 67-71.

Warner, B.D.; Harris, A.W.; Pravec, P. (2009). "The Asteroid Lightcurve Database." *Icarus* **202**, 134-146. Updated 2016 Feb. *http://www.minorplanet.info/lightcurvedatabase.html*

Warner, B.D. (2010). "Upon Further Review: I. An Examination of Previous Lightcurve Analysis from the Palmer Divide Observatory." *Minor Planet Bull.* **37**, 127-130.

Warner, B.D. (2011a). Collaborative Asteroid Lightcurve Link website. *http://www.minorplanet.info/call.html*

Warner, B.D. (2011b). Asteroid Lightcurve Research at PDO *http://www.minorplanetobserver.com/PDO/PDOLightcurves.htm*

Warner, B.D. (2012). "Asteroid Lightcurve Analysis at the Palmer Divide Observatory: 2011 June - September." *Minor Planet Bull.* **39**, 16-21.

Warner, B.D. (2019). *MPO Canopus* software. *http://bdwpublishing.com*

Waszczak, A.; Chang, C.-K.; Ofeck, E.O.; Laher, R.; Masci, F.; Levitan, D.; Surace, J.; Cheng, Y-C.; Ip, W.-H.; Kinoshita, D.; Helou, G.; Prince, TA.; Kulkarni, S. (2015). "Asteroid Light Curves from the Palomar Transient Factory Survey: Rotation Periods and Phase Functions from Sparse Photometry." *Astron. J.* **150**, A75.

## LIGHTCURVE ANALYSIS FOR THREE MAIN-BELT ASTEROIDS

Giovanni Battista Casalnuovo, Benedetto Chinaglia
Filzi School Observatory D12
Laives, ITALY
gb.minorplanet@gmail.com

(Received: 2020 April 11)

Photometric observations of three main-belt asteroids, 1755 Lorbach, 3566 Levitan, (64163) 2001 TB49, were made at the Filzi School Observatory (School in country Laives - Italy) MPC code D12.

We report CCD photometric observations made at the Filzi School Observatory. All measurements reported are with an R filter, except 1755 Lorbach, made without filter (clear). All images were obtained with a 0.35-m reflector telescope reduced to *f*/8.0, a QHY9 CCD camera, and then calibrated with dark and flat-field frames. The pixel scale was 1.56 arcsec when binned at 4x4 pixels. All exposures were 120 seconds. The computer clock was synchronized with an Internet time server before each session. Differential photometry and period analysis were done using *MPO Canopus* version 10.7.12.9 (Warner, 2014). Solar-type stars from CMC15 catalog in R band were used as comparison stars.

1755 Lorbach. This main-belt asteroid was reported as a lightcurve photometry opportunity for 2020 March on the MinorPlanet.info web site (*http://www.MinorPlanet.info*; hereafter referenced as MPI). 1755 Lorbach was discovered in the year 1936 (November 08) by Laugier M. at Nice. It is a main-belt asteroid with a semi-major axis of 3.09 AU, eccentricity 0.046, inclination 10.7 deg, and orbital period of 5.43 yr. Its absolute magnitude is H = 10.80. We studied Lorbach for six nights (for a total of 756 images), finding a derived synodic period of P = 7.980 ± 0.002 h with an amplitude of A = 0.43 ± 0.06 mag. There were no previous entries in the LCDB (Warner et al., 2009) for this asteroid.

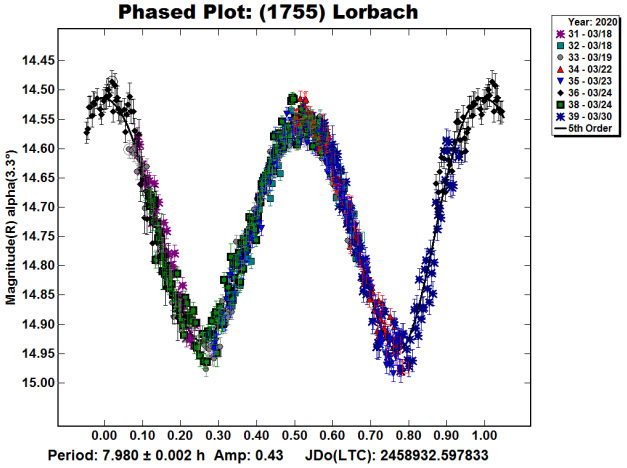


| Number | Name | yyyy mm/dd | Phase | | $L_{PAB}$ | $B_{PAB}$ | Period(h) | P.E. | Amp | A.E. | Grp |
|---|---|---|---|---|---|---|---|---|---|---|---|
| 1755 | Lorbach | 2020 03/18-03/30 | 2.9 | 7.3 | 170.8 | 3.7 | 7.980 | 0.002 | 0.43 | 0.06 | MB |
| 3566 | Levitan | 2020 02/12-02/20 | 1.1 | 4.8 | 142.7 | -1.8 | 5.612 | 0.002 | 0.50 | 0.10 | MB |
| 64163 | 2001 TB49 | 2020 01/23-01/27 | 6.4 | 9.3 | 113.6 | 0.3 | 4.230 | 0.002 | 0.30 | 0.11 | MB |

Table I. Observing circumstances and results. The phase angle is given for the first and last date. If preceded by an asterisk, the phase angle reached an extrema during the period. $L_{PAB}$ and $B_{PAB}$ are the approximate phase angle bisector longitude/latitude at mid-date range (see Harris et al., 1984). Grp is the asteroid family/group (Warner et al., 2009).

3566 Levitan. This main-belt asteroid was reported as a lightcurve photometry opportunity for 2020 February on the MinorPlanet.info web site (*http://www.MinorPlanet.info*). 3566 Levitan, it was discovered in the year 1979 (December 24) by Zhuravleva, L. at Nauchnyj. It is a main-belt asteroid with a semi-major axis of 2.36 AU, eccentricity 0.126, inclination 2.27 deg, and orbital period of 3.63 yr. Its absolute magnitude is H = 13.10. It was studied for four nights (for a total of 387 images). The derived synodic period was P = 5.612 ± 0.002 h with an amplitude of A = 0.50 ± 0.10 mag. Durech et al. (2018) reported (LCDB: *http://www.minorplanet.info/PHP/lcdbsummaryquery.php*) a period of 5.61403 h., which is in very close agreement with the result given here.

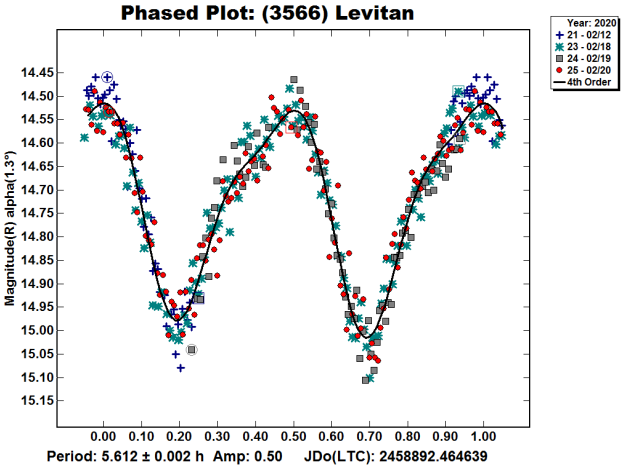


(64163) 2001 TB49. This main-belt asteroid was reported as a lightcurve photometry opportunity for 2020 January on the MinorPlanet.info web site (*http://www.MinorPlanet.info*). It was discovered in the year 2001 (October 15) by survey LINEAR at Socorro. It is a main-belt asteroid with a semi-major axis of 2.32 AU, eccentricity 0.231, inclination 26.79 deg, and orbital period of 3.55 years, absolute magnitude is H= 14.30. It was studied for three nights (for a total of 87 images, following bad weather, no other sessions were made to improve the period). The derived synodic period was P = 4.230 ± 0.002 h with an amplitude of A = 0.30 ± 0.10 mag. There were no entries in the LCDB (Warner et al., 2009) for this asteroid.

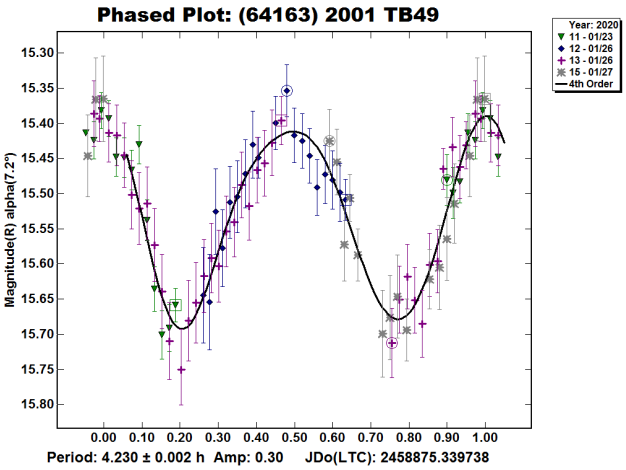


References

Durech, J.; Hanus, J.; Ali-Lagoa, V. (2018). "Asteroid models reconstructed from the Lowell Photometric Database and WISE data." *Astron. Astrophys.* **617**, A57.

Harris, A.W.; Young, J.W.; Scaltriti, F.; Zappala, V. (1984). "Lightcurves and phase relations of the asteroids 82 Alkmene and 444 Gyptis." *Icarus* **57**, 251-258.

LCDB. *http://www.minorplanet.info/PHP/lcdbsummaryquery.php*

Minor Planet Call. *http://www.minorplanet.info/PHP*

Minorplanet.Info.
*http://www.minorplanet.info/lightcurvedatabase.html*

Warner, B.D.; Harris, A.W.; Pravec, P. (2009). "The Asteroid Lightcurve Database." *Icarus* **202**, 134-146. Updated 2018 June. *http://www.minorplanet.info/lightcurvedatabase.html*

Warner, B.D. (2014). *MPO Software, MPO Canopus* version 10.7.12.9. *Bdw Publishing. http://minorplanetobserver.com*

# ASTEROID PHOTOMETRY AND LIGHTCURVE ANALYSIS AT GORA'S OBSERVATORIES

Milagros Colazo
Facultad de Matemática, Astronomía y Física,
Universidad Nacional de Córdoba, ARGENTINA
milirita.colazovinovo@gmail.com

César Fornari, Marcos Santucho, Aldo Mottino, Carlos Colazo, Raúl Melia, Nicolás Vasconi, Daniela Arias, Claudio Pittari, Néstor Suarez, Eduardo Pulver, Guillermo Ferrero, Andrés Chapman, Carla Girardini, Elisa Rodríguez, Guillermo Amilibia, Marcos Anzola, Marina Tornatore, Ricardo Nolte, Sergio Morero
Grupo de Observadores de Rotaciones de Asteroides (GORA)
ARGENTINA
*https://aoacm.com.ar/gora/index.php*

Estación Astrofísica Bosque Alegre (MPC 821)
Bosque Alegre, Córdoba, ARGENTINA

Observatorio Astronómico Córdoba (MPC 822)
Córdoba Capital, Córdoba, ARGENTINA

Observatorio Astronómico El Gato Gris (MPC I19)
Tanti, Córdoba, ARGENTINA

Observatorio Cruz del Sur (MPC I39)
San Justo, Buenos Aires, ARGENTINA

Observatorio Galileo Galilei (MPC X31)
Oro Verde, Entre Ríos, ARGENTINA

Observatorio Antares (MPC X39)
Pilar, Buenos Aires, ARGENTINA

Observatorio de Aldo Mottino (OAM)
Rosario, Santa Fe, ARGENTINA

Observatorio Punto Azul (OPA)
Villa María, Córdoba, ARGENTINA

Observatorio Astro Pulver (OAP)
Rosario, Santa Fe, ARGENTINA

Grupo de Astrometría y Fotometría (GAF)
Córdoba Capital, Córdoba, ARGENTINA

Julian Oey
Blue Mountains Observatory (MPC Q68)
Leura, NSW, AUSTRALIA

(Received: 2020 March 26)

Synodic rotation periods and amplitudes are reported for 179 Klytaemnestra, 372 Palma, 504 Cora, 739 Mandeville, 749 Malzovia, 925 Alphonsina, 1015 Christa, 1086 Nata, and 1794 Finsen.

In this paper we present the collaborative work of amateur astronomers and undergraduate students belonging to the argentine group G.O.R.A (Grupo de Observadores de Rotaciones de Asteroides). GORA is a continuity of collaborative experience between argentine amateur observers initially joined under the name of "Asociación de Observatorios Argentinos de Cuerpos Menores" (AOACM), and dedicated to perform astrometry and photometry of minor bodies. Since 2019 March, an increasing number of members were incorporated to GORA to perform asteroid observations. To validate our working methodology, we first chose asteroids with known rotation periods. We will progressively select more complex challenges, as our learning consolidates. The observatories and equipment used are summarized in Table I. The results and observing circumstances are in Table II.

Image acquisition was performed without filters and with exposure times of a few minutes. All images used were corrected using dark frames and in some cases bias and flat-field also were used. Differential photometry measurements were performed using *FotoDif* software and for the analysis we employed *Periodos* software (Mazzone, 2012).

Below, we present the results for each asteroid under study. The lightcurve figures contain the following information: 1) the estimated period and amplitude, 2) a 95% confidence interval regarding the period estimate, 3) RMS of the fitting, 4) estimated amplitude and amplitude error, 5) Julian time corresponding to 0 rotation phase, and 6) the number of data points. In the reference boxes the columns represent, respectively, the marker, observatory MPC code, session date, session off-set, and number of data points. (Mazzone et al., 2014).

Targets were selected based on the following criteria: 1) those asteroids with magnitudes accessible to the equipment of all participants, 2) those with favorable observation conditions from Argentina i.e. with negative declinations and 3) objects with few periods reported in the literature and/or with Lightcurve Database (LCDB; Warner et al., 2009) quality codes (U) of less than 3.

179 Klytaemnestra. This asteroid belongs to the Telramund family and is classified as an S-type asteroid in the Tholem taxonomy. The last reported period was of 11.17342 ± 0.00005 h (Hanuš et al., 2016). We observed this asteroid from 2019 May 25 to August 8. The main difficulty that arose was the wealth of background stars that made us hesitate several times to continue observing this object. Despite this, we obtained a rotation period of 11.168 ± 0.008 h, quite similar to that of LCDB records. The last amplitude measurement in the databases corresponds to Ditteon and Hawkins (2007) and was of 0.55 ± 0.02 mag, whereas ours was of 0.07 ± 0.01 mag. The difference between these values may be an indicator of a noticeable change in the aspect angle of this asteroid.

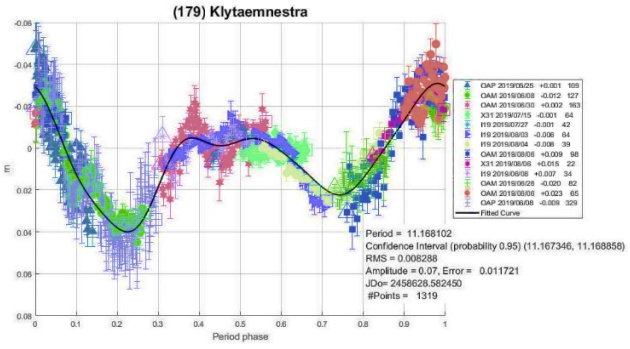


372 Palma is a B-type asteroid. The last reported period was of 8.57964 ± 0.00005 h (Hanuš et al., 2016) and the last reported amplitude was of 0.10 ± 0.01 mag (Behrend, 2011). This asteroid was chosen because its brightness (V ~ 12.6) and declination (δ ~ –31 °) allowed it to be observed with culminations close to the local zenith of the observatories involved. Analysis of our data resulted in a period of 8.582 ± 0.009 h and amplitude of 0.07 ± 0.01 mag, which is in concordance with previously published data.

| Observatory | Telescope | Camera |
|---|---|---|
| Estación Astrofísica Bosque Alegre | Newtonian telescope (D=1540mm; f=4.9) | CCD APOGEE Alta U9 |
| Observatorio Astronómico Córdoba | Celestron SCT14 (D=355mm; f=11.0) | CCD SBIG ST7 + F.R. |
| Observatorio El Gato Gris | Celestron SCT14 (D=355mm; f=10.6) | CCD SBIG STF8300M |
| Observatorio Cruz del Sur | Newtonian telescope (D=200mm; f=4.0) | CCD Atik 414Ex |
| Observatorio Galileo Galilei (2019) | Celestron SCT14 (D=355mm; f=11.0) | CCD SBIG STF8300MT |
| Observatorio Galileo Galilei (2020) | RC ap (D=405mm; f=8.0) | CCD SBIG STF8300M |
| Observatorio Antares | Newtonian telescope (D=200mm; f=5.0) | CCD QHY9 Mono |
| Observatorio de Aldo Mottino | Newtonian telescope (D=250mm; f=4.7) | CCD SBIG STF8300M |
| Observatorio Punto Azul | Newtonian telescope (D=254mm; f=5.0) | CCD QHY6 Mono |
| Observatorio Astro Pulver | Celestron SCT8 (D=203mm; f=10.0) | CMOS QHY5 LII M + F.R. |
| Blue Mountains Observatory | SCT Edge (D=355m; f=7.0) | CCD SBIG STF8300M. |

Table I. List of observatories and equipment.

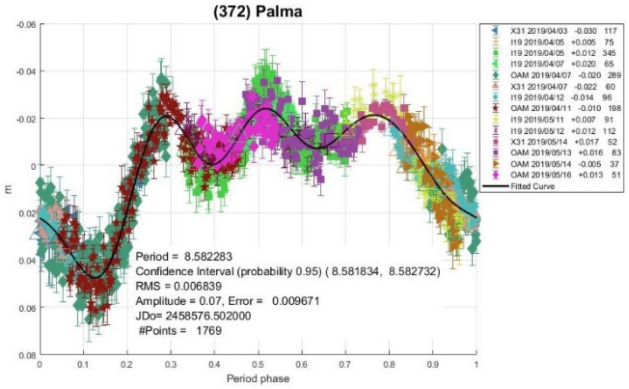


504 Cora. On the Tholen taxonomic scheme, as well as by the NEOWISE mission of NASA's Wide-field Infrared Survey Explorer (WISE), Cora is classified as a metallic M-type asteroid (Mainzer et al., 2011). The last periods registered in the literature were of 7.5915 ± 0.0043 h and 7.5882 ± 0.0023 h, with amplitudes of 0.15 mag and 0.17 mag, respectively (Waszczak et al., 2015). Seven GORA members observed this asteroid between 2019 August 10 and September 26. Despite some stretches with large dispersions and some discordant junctions, our data derived a period of rotation of 7.59 ± 0.02 h and amplitude of 0.22 ± 0.03 mag, quite similar to those found in the literature. The small difference in amplitude may be due to the aspect angle of the asteroid being progressively changing.

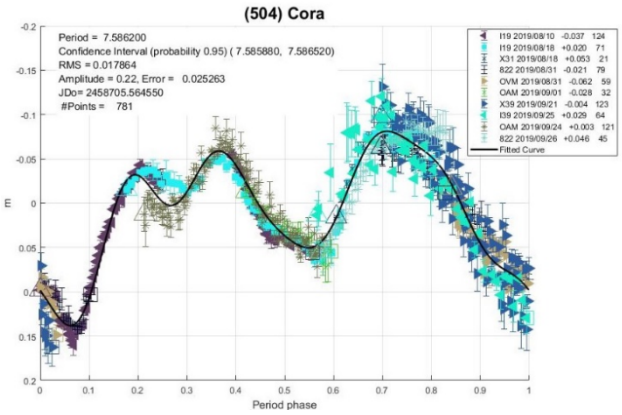


739 Mandeville is classified as type X in the Tholen taxonomy. There are three periods reported in the literature with marked differences: 15.9 h (Zappalá, 1983), 11.931 ± 0.010 h (Harris and Zappalá, 1989) and 24 ± 1 h (Behrend, 2005). The last amplitude reported is 0.14 ± 0.03 mag (Melton et al., 2012). This asteroid was the one in which we invested the largest number of observations because we had to deal with candidate periods that were multiple or divisors of 24 h. We observed it from 2019 September 18 to November 21. We requested and received the generous and valuable collaboration of Julian Oey, who contributed observations from Australia. As a final result, we found a period of 23.92 ± 0.02 h and amplitude of 0.22 ± 0.02 mag.

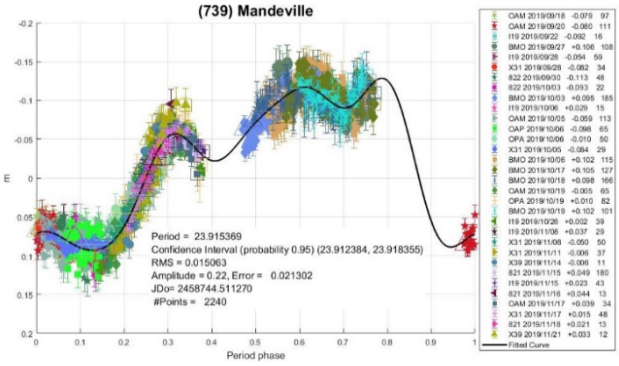


749 Malzovia. This S-type asteroid has a reported period of 5.9275 ± 0.0002 h with amplitude of 0.30 ± 0.03 mag (Oey, 2016). It was observed between 2014 May 1 and June 8. As with 1794 Finsen, the studies were performed before GORA's consolidation, so we decided to include it in this paper. We obtained a period of 5.928 ± 0.008 h and amplitude of 0.32 ± 0.01 mag, similar to the data found in literature.

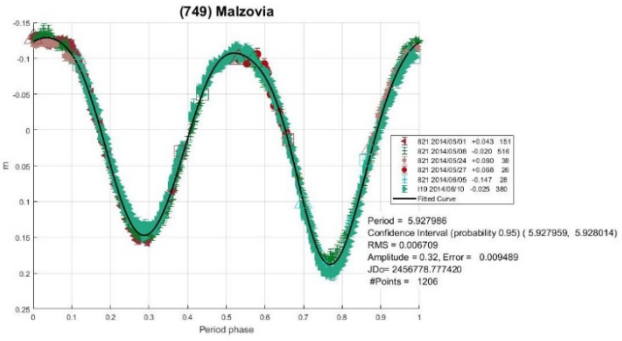


925 Alphonsina is a Hansian asteroid from the central region of the asteroid belt. The last reported period in the literature of this S-type asteroid was 7.87754 ± 0.00005 h (Durech et al., 2011; Hanuš et al., 2011). The last reported amplitude was of 0.30 ± 0.01 mag (Hamanowa and Hamanowa, 2011). We studied this asteroid between 2018 March 8-24, with the novelty of participation of three amateur observatories in association. Analysis of our data resulted in a period of 7.88 ± 0.01 h, which is in concordance with previously published data. Our calculated amplitude, however, was 0.11 ± 0.02 mag, which clearly differs from that published by Hamanowa and Hamanowa (2011).

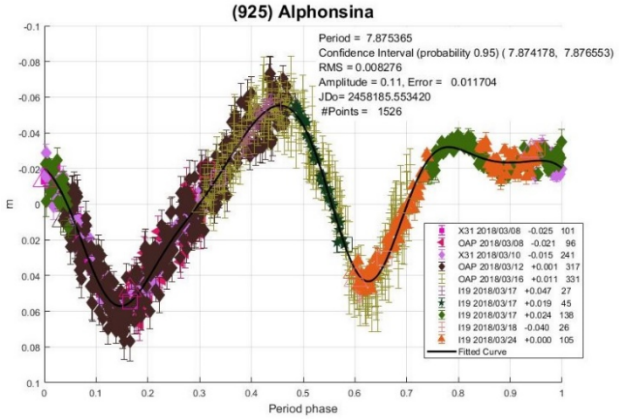


1015 Christa. Christa is a non-family asteroid from the main-belt background population. In the Tholen classification, Christa is a common C-type asteroid. Two different periods were reported in the literature: 12.189 ± 0.001 h (Behrend, 2005) and 11.230 ± 0.004 h (Warner, 2009). The respective reported amplitudes were 0.20 ± 0.01 mag and 0.12 ± 0.01 mag. Observations made by GORA from 2019 November 7 to December 5 provided a rotation period of 11.23 ± 0.03 h and an amplitude of 0.20 ± 0.04 mag, in good agreement with the period reported by Warner (2009).

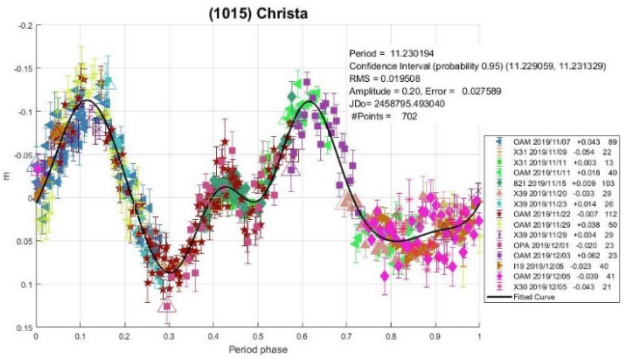


1086 Nata is a member of the Veritas family and has an estimated diameter of 72 ± 11 km. The only reported period we found in the literature is 18.074 ± 0.002 h with an amplitude 0.17 ± 0.03 mag (Sheridan, 2002). We started observing Nata on 2020 January 30 and concluded on March 6, obtaining a period of 18.05 ± 0.02 h and amplitude of 0.18 ± 0.02 mag.

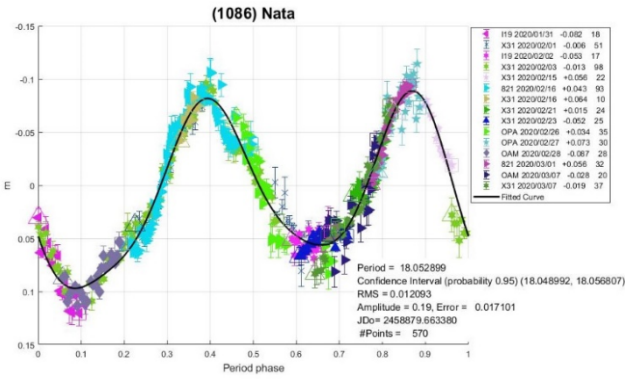


1794 Finsen. This C-type asteroid has a reported period of 12.3495 ± 0.0055 h and amplitude of 0.38 mag (Waszczak et al, 2015). It was observed from 2014 March 21 to June 20. However, the corresponding report was never published by the AOACM, so that we decided to include it here. Our data resulted in a period of rotation of 12.347 ± 0.009 h and amplitude of 0.49 ± 0.01 mag, quite similar to those found in the literature.

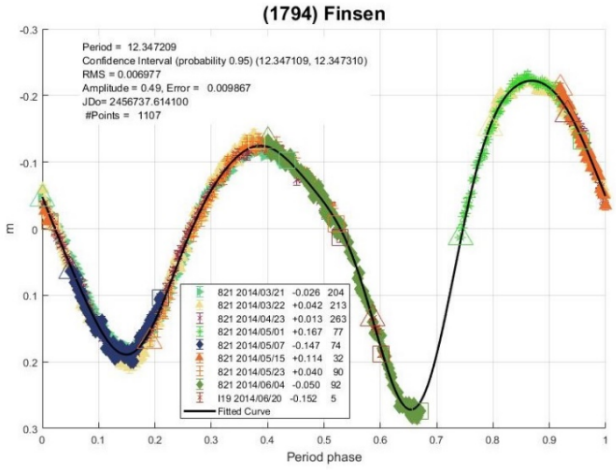


Acknowledgements

We want to thank Julio Castellano as we use his *FotoDif* program for preliminary analyses and to Fernando Mazzone for his *Periods* program, used in final analyses. This research has made use of the Small Bodies Data Ferret (*http://sbn.psi.edu/ferret/*), supported by the NASA Planetary System. This research has made use of data and/or services provided by the International Astronomical Union's Minor Planet Center.

| Number | Name | yyyy mm/dd | Phase | $L_{PAB}$ | $B_{PAB}$ | Period(h) | P.E. | Amp | A.E. |
|---|---|---|---|---|---|---|---|---|---|
| 179 | Klytaemnestra | 2019/05/25-08/08 | *7.9,17.2 | 264 | 2 | 11.1682 | 0.008 | 0.07 | 0.01 |
| 372 | Palma | 2019/04/03-05/16 | 7.8,12.9 | 197 | -23 | 8.582 | 0.009 | 0.07 | 0.01 |
| 504 | Cora | 2019/08/10-09/26 | *12.4,13.0 | 335 | -15 | 7.59 | 0.02 | 0.22 | 0.03 |
| 739 | Mandeville | 2019/09/18-11/21 | 5.8,17.7 | 348 | -15 | 23.92 | 0.02 | 0.22 | 0.02 |
| 749 | Malzovia | 2014/05/01-06/08 | *16.9,7.7 | 246 | 6 | 5.928 | 0.008 | 0.32 | 0.01 |
| 925 | Alphonsina | 2018/03/08-03/24 | 9.6,13.2 | 162 | -20 | 7.88 | 0.01 | 0.11 | 0.02 |
| 1015 | Christa | 2019/11/07-12/05 | 13.1,18.2 | 10 | -11 | 11.23 | 0.03 | 0.20 | 0.04 |
| 1086 | Nata | 2020/01/30-03/06 | *7.5,6.4 | 149 | -3 | 18.05 | 0.02 | 0.18 | 0.02 |
| 1794 | Finsen | 2014/03/21-06/20 | *8.1,21.9 | 197 | -5 | 12.347 | 0.009 | 0.49 | 0.01 |

Table II. Observing circumstances. The phase angle ($\alpha$) is given at the start and end of each date range. If there is an asterisk before the first phase value, the phase angle reached a maximum or minimum during the period. $L_{PAB}$ and $B_{PAB}$ are, respectively the average phase angle bisector longitude and latitude (see Harris et al.,1984).

References

Behred, R. (2005, 2011). Observatoire de Geneve web site. *http://obswww.unige.ch/~behrend/page_cou.html*

Ditteon, R.; Hawkins, S. (2007). "Asteroid Lightcurve Analysis at the Oakley Observatory – November 2006." *Minor Planet Bull*. **34,** 59-64.

Durech, J.; Kaasalainen, M.; Herald, D.; Dunham, D.; Timerson, B.; Hanuš, J.; Frappa, E.; Talbot, J.; Hayamizu, T.; Warner, B.D.; Pilcher, F.; Galád, A. (2011). "Combining asteroid models derived by lightcurve inversion with asteroidal occultation silhouettes." *Icarus* **214**, 652-670.

Hamanowa, H.; Hamanowa, H. (2011).
*http://www2.ocn.ne.jp/~hamaten/astlcdata.htm*

Hanuš, J.; Durech, J.; Broz, M.; Warner, B.D.; Pilcher, F.; Stephens, R.; Oey, J.; Bernasconi, L.; Casulli, S.; Behrend, R.; Polishook, D.; Henych, T.; Lehký, M.; Yoshida, F.; Ito, T. (2011). "A study of asteroid pole-latitude distribution based on an extended set of shape models derived by the lightcurve inversion method." *Astron. Astrophys.* **530**, A134.

Hanuš, J. and 168 colleagues (2016). "New and updated convex shape models of asteroids based on optical data from a large collaboration network." *Astron. Astrophys.* **586,** A108.

Harris, A.W.; Zappalá, V. (1989). "Photoelectric Photometry Opportunities". *Minor Planet Bull.* **16**
"February–April" 10.
"May–July" 23.
"August–October" 38.
"November–January" 46.

Harris, A.W.; Young, J.W.; Scaltriti, F.; Zappala, V. (1984). "Lightcurves and phase relations of the asteroids 82 Alkmene and 444 Gyptis." *Icarus* **57**, 251-258.

Mainzer, A.; Grav, T.; Masiero, J.; Hand, E.; Bauer, J.; Tholen, D.; McMillan, R.S.; Spahr, T.; Cutri, R.M.; Wright, E.; Watkins, J.; Mo, W.; Maleszewski, C. (2011). "NEOWISE Studies of Spectrophotometrically Classified Asteroids: Preliminary Results." *Astrophys. J.* **741**, 90.

Mazzone, F.D. (2012). Periodos sotware, version 1.0.
*http://www.astrosurf.com/salvador/Programas.html*

Mazzone, F.; Colazo, C.; Mina, F.; Melia, R.; Spagnotto, J.; Bernal, A. (2014). "Collaborative asteroid photometry and lightcurve analysis at observatories OAEGG, OAC, EABA and OAS." *Minor Planet Bull.* **41**, 17-18.

Melton, E.; Carver, S.; Harris, A.; Karnemaat, R.; Klaasse, M.; Ditteon, R. (2012). "Asteroid Lightcurve Analysis at the Oakley Southern Sky Observatory: 2011 November–December". *Minor Planet Bull.* **39**, 131-133.

Oey, J. (2016). "Lightcurve Analysis of Asteroids from Blue Mountains Observatory in 2014." *Minor Planet Bull.* **43**, 45-51.

Sheridan, E.E. (2002). "Rotational Periods and Lightcurve Photometry of 697 Galilea, 1086 Nata, 2052 Tamriko, 4451 Grieve, and (27973) 1997 TR25." *Minor Planet Bull.* **29**, 32-33.

Warner, B.D. (2009). "Asteroid Lightcurve Analysis at the Palmer Divide Observatory: 2008 December - 2009 March." *Minor Planet Bull.* **36**, 109-116.

Warner, B.D.; Harris, A.W.; Pravec, P. (2009). "The Asteroid Lightcurve Database." Icarus **202**, 134-146. Updated 2016 Sep. *http://www.minorplanet.info/lightcurvedatabase.html*

Waszczak, A.; Chang, C.-K.; Ofeck, E.O.; Laher, F.; Masci, F.; Levitan, D.; Surace, J.; Cheng, Y.; Ip, W.; Kinoshita, D.; Helou, G.; Prince, T.A.; Kulkarni, S. (2015). "Asteroid Light Curves from the Palomar Transient Factory Survey: Rotation Periods and Phase Functions from Sparse Photometry." *Astron. J.* **150**, A75.

Zappalá, V. (1983). "Photoelectric Investigations of Asteroids: The Contributions of Small Telescopes." *Minor Planet Bull.* **10**, 17-18.

# LIGHTCURVES AND ROTATION PERIODS OF 83 BEATRIX, 86 SEMELE, 118 PEITHO, 153 HILDA, 527 EURYANTHE, AND 549 JESSONDA

Frederick Pilcher
Organ Mesa Observatory (G50)
4438 Organ Mesa Loop
Las Cruces, NM 88011 USA
fpilcher35@gmail.com

(Received: 2020 March 26)

Synodic rotation periods and amplitudes are found for 83 Beatrix: 10.111 ± 0.001 h, 0.08 ± 0.01 mag; 86 Semele: 16.641 ± 0.001 h, 0.13 ± 0.01 mag; 118 Peitho: 7.8060 ± 0.0001 h, 0.21 ± 0.02 mag; 153 Hilda: 5.958 ± 0.002 h, 0.09 ± 0.01 mag; 527 Euryanthe: 42.93 ± 0.01 h, 0.15 ± 0.01 mag; 549 Jessonda: 2.9713 ± 0.0002 h, 0.09 ± 0.01 mag with three maxima and minima per cycle. For 86 Semele *V-R* = 0.28, *H* = 8.539 ± 0.025, and *G* = 0.152 ± 0.041.

Observations to produce the results reported in this paper were made at the Organ Mesa Observatory with a Meade 35-cm LX200 GPS Schmidt-Cassegrain, SBIG STL-1001E CCD, unguided. For the bright targets 86 Semele (Dec 16 – Jan 4) and 118 Peitho, exposures were through an R filter. For all other targets, including 86 Semele after Jan. 4, exposures were through a clear filter. Image measurement and lightcurve construction were with *MPO Canopus* software with all calibration star magnitudes from the CMC15 catalog reduced to the Cousins R band. To reduce the number of data points on the lightcurves and make them easier to read, data points have been binned in sets of 3 with maximum time difference 5 minutes.

83 Beatrix. Two previously published rotation periods are by Zappala et al. (1983), 10.16 h; and by Behrend (2005), 15.36 h. Six new sessions (2020 January 6 - 27) can be fit to a synodic rotation period 10.111 ± 0.001 h, amplitude 0.08 ± 0.01 mag (Fig. 1).

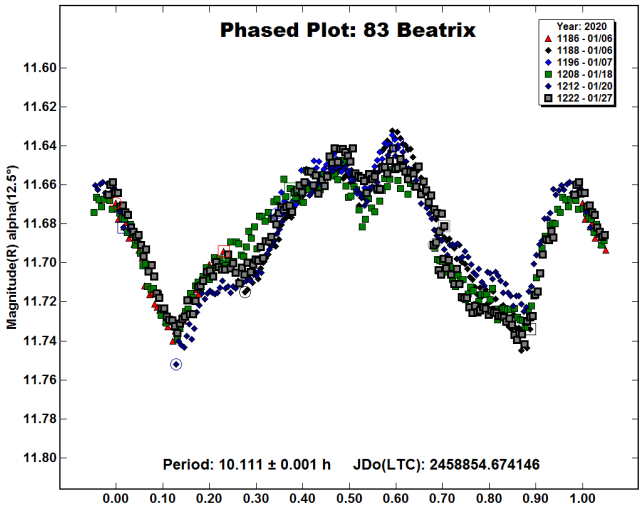


Fig. 1. Lightcurve of 83 Beatrix.

There are some misfits among the sessions. A split-halves plot to the double period of 20.222 hours (Fig. 2) shows that these misfits apply to the same halves of the double period, and are not evidence in favor of the double period. The 10.111-hour period is consistent with Zappala (1983), rules out the period by Behrend (2005), and can be considered secure.

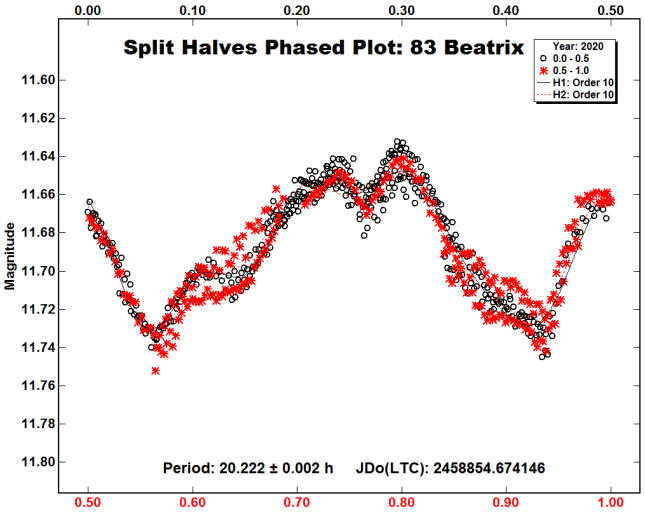


Fig. 2. Split-halves plot of the double period of 83 Beatrix.

86 Semele. Two previously published rotation periods are by Surdej et al. (1983), 16.634 h; and by Behrend (2010), 18.24 h. New sessions on 10 nights (2019 Dec 16 – 2020 Jan 25) provide a good fit to a lightcurve with period 16.641 ± 0.001 h, amplitude 0.13 ± 0.01 mag (Fig. 3). This period is consistent with Surdej et al. (1983) but not with Behrend (2010).

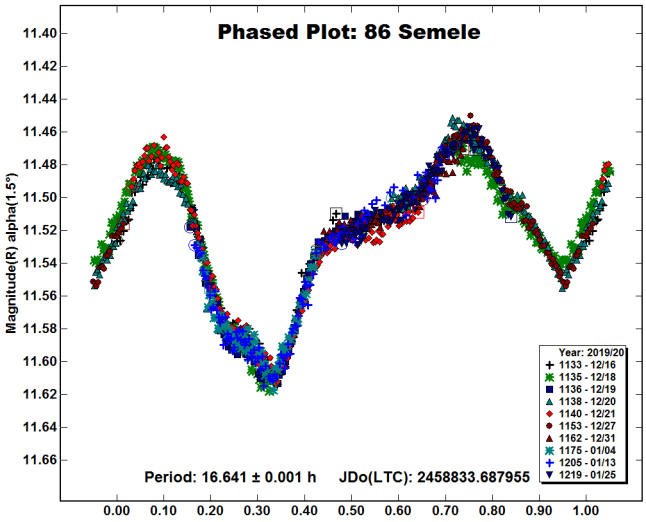


Fig. 3. Lightcurve of 86 Semele.

The double period of 33.273 h was completely sampled over the interval 2019 Dec 16 – 21. The corresponding split-halves plot to the double period (Fig. 4) shows that the two halves are identical within photometric error and rules out the double period. On 2020 Jan 2, twenty exposures were obtained alternating between the R and V filters. A raw lightcurve of both sessions shows that *V-R* = 0.28 (Fig. 5). An *H-G* plot from phase angle 0.1 to 17.9 degrees in the *V* magnitude band shows *H* = 8.539 ± 0.025 and *G* = 0.152 ± 0.041 using mid-light (Fig. 6).

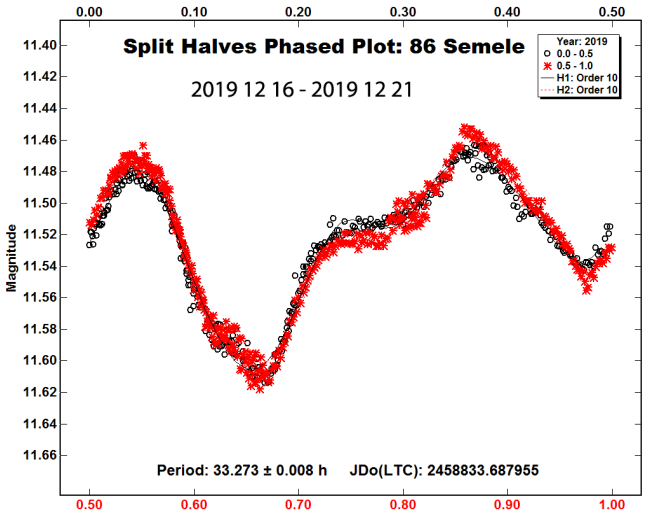


Fig. 4. Split-halves plot of the double period of 86 Semele.

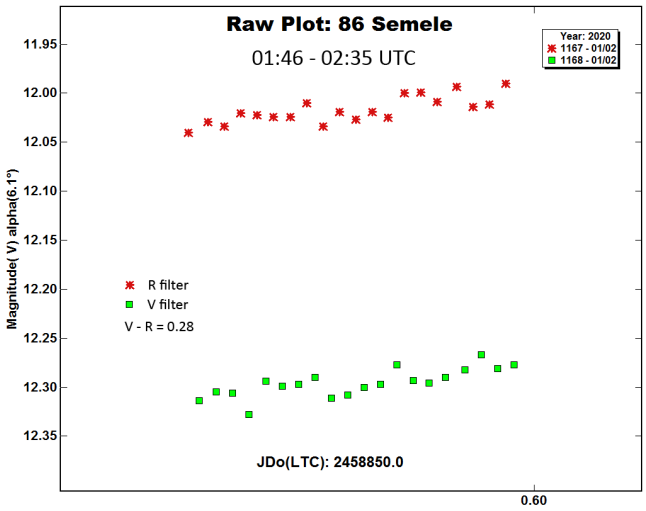


Fig. 5. Lightcurve of sessions on 86 Semele 2020 01 02 in *R* and *V* filters.

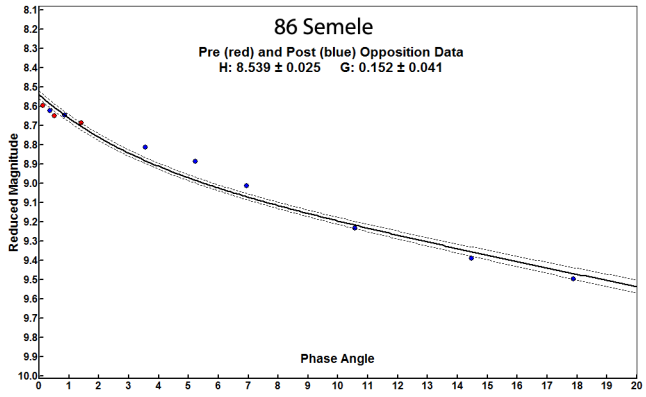


Fig. 6. *H-G* plot for 86 Semele.

118 Peitho. The Lightcurve Data Base (Warner et al., 2009) lists six previously published rotation periods all near 7.8055 h. Two sessions, each nearly 10 hours, were obtained on consecutive nights on 2020 Jan 11 – 12. They provide a good fit to a synodic period 7.807 ± 0.002 h, amplitude 0.20 ± 0.01 mag (Fig. 7). It should be noted that for a period near 8 hours, and a double period near 16 hours, observations on consecutive nights about 24 hours apart show opposite sides of the double period.

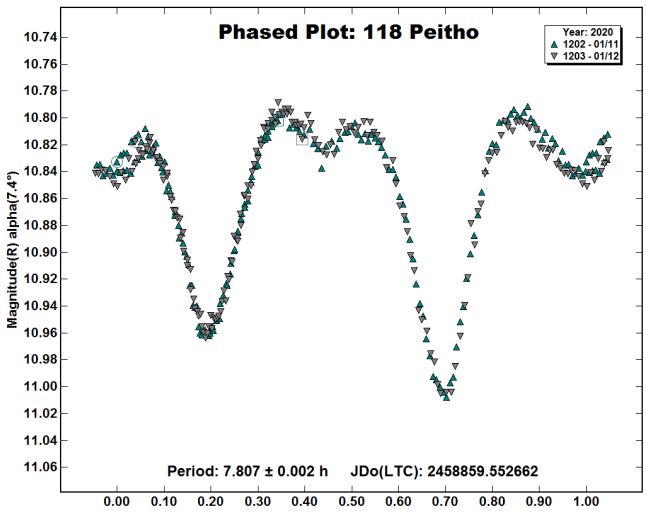


Fig. 7. Lightcurve of 118 Peitho 2020 01 11 and 2020 01 12.

The two sessions on the plot to 7.807 hours are a de facto split-halves plot. That they are nearly identical rules out the double period. The 7.807-hour period is secure but aligning lightcurve segments separated by only 3 rotational cycles does not have great accuracy. A single additional session was obtained 28 days, 86 rotational cycles, later on 2020 Feb 9. A good fit to a period 7.8060 ± 0.0001 h is made showing the changes in lightcurve shape commonly found with changing phase angle (Fig. 8).

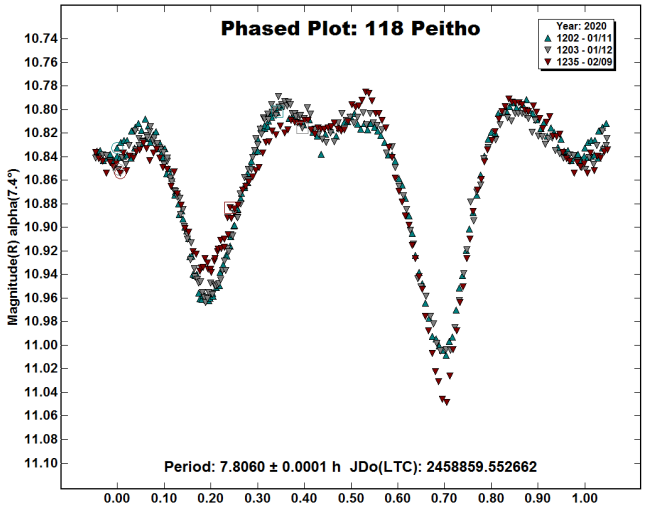


Fig. 8. Lightcurve of 118 Peitho 2020 01 11 to 2020 02 09.

For sessions separated by 86 rotational cycles, the accuracy of the period is very good. But there is considerable chance of a miscount of the number of intervening cycles, or rotational alias. The period spectrum (Fig. 9) shows the deepest minimum at 7.806 h. Other minima corresponding to 87, 86.5, 85.5, 85, etc., cycles in the 28-day interval are shallower and symmetrically placed about the 86-cycle minimum. This symmetry shows that the 7.8060-hour period is very likely the correct one. Hence, I conclude that synodic rotational period of 118 Peitho is 7.8060 ± 0.0001 h, amplitude 0.21 ± 0.02 mag, a result that is consistent with all previous results.

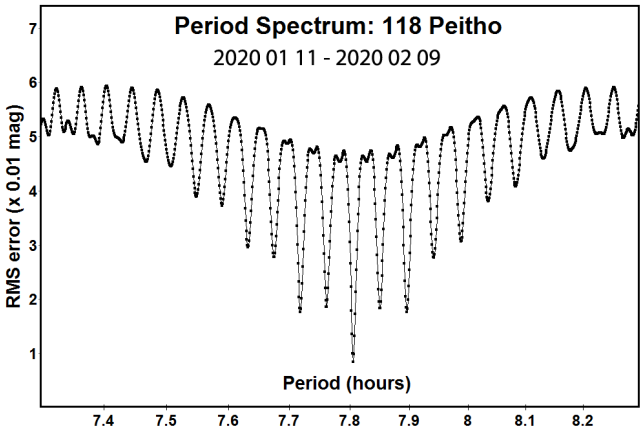


Fig. 9. Period spectrum for 118 Peitho.

153 Hilda. The Lightcurve Data Base (Warner et al. 2009) lists eight previously published rotation periods, all near 5.9585 h. New sessions on three nights (2020 Jan 14 – 23), each covering the complete rotational cycle, were obtained to contribute to future lightcurve inversion (LI) modeling. They provide a good fit to a synodic period 5.958 ± 0.002 h, amplitude 0.09 ± 0.01 mag (Fig. 10). This result is consistent with all previous results.

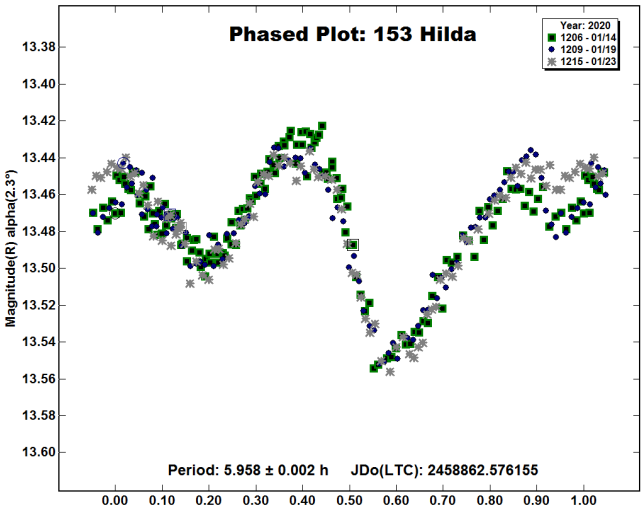


Fig. 10. Lightcurve of 153 Hilda.

527 Euryanthe. Two previously published rotation periods are by Brinsfield (2010), 26.06 h; and by Polakis and Skiff (2019), 42.986 h. New sessions on 13 nights (2019 Dec 28 – 2020 Feb 2) provide a good fit to an irregular lightcurve with period 42.93 ± 0.01 h, amplitude 0.15 ± 0.02 mag (Fig. 11). A period spectrum between 40 h and 90 h (Fig. 12) shows that all periods within this range, except 42.93 h and the double period of 85.88 h, can be ruled out. The data cover about 90% of the double period. The split-halves plot of the double period (Fig. 13) shows that the covered segments are almost identical within usual photometric error. The 42.93 h period is consistent with Polakis and Skiff (2019) and rules out Brinsfield (2010).

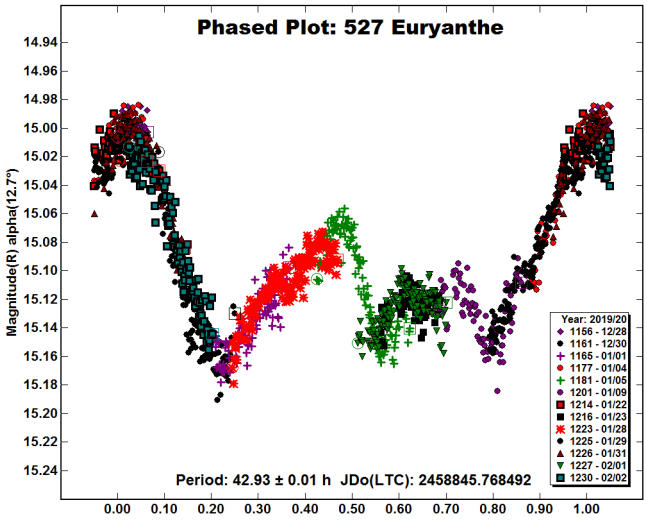


Fig. 11. Lightcurve of 527 Euryanthe phased to 42.93 h.

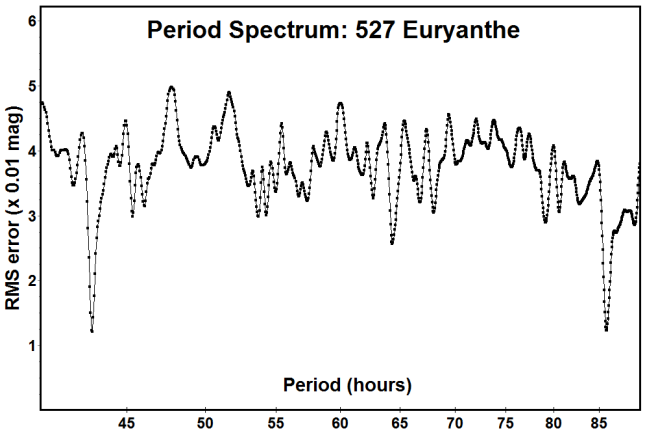


Fig. 12. Period spectrum for 527 Euryanthe between 40 and 90 h.

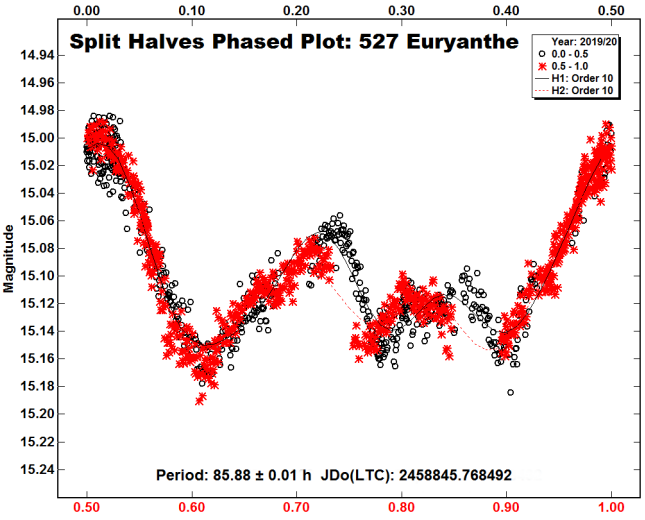


Fig. 13. Split-halves plot of the double period of 527 Euryanthe.

| Number | Name | yyyy/mm/dd | Phase | $L_{PAB}$ | $B_{PAB}$ | Period(h) | P.E. | Amp | A.E. |
|---|---|---|---|---|---|---|---|---|---|
| 83 | Beatrix | 2020/01/06-2020/01/27 | 12.5,4.0 | 130 | 6 | 10.111 | 0.001 | 0.09 | 0.01 |
| 86 | Semele | 2019/12/16-2020/01/25 | 0.1,17.9 | 88 | 1 | 16.641 | 0.001 | 0.13 | 0.01 |
| 118 | Peitho | 2020/01/11-2020/02/09 | 7.4,19.3 | 104 | 10 | 7.8060 | 0.0001 | 0.21 | 0.02 |
| 153 | Hilda | 2020/01/14-2020/01/23 | 2.3,4.1 | 107 | -8 | 5.958 | 0.002 | 0.10 | 0.01 |
| 527 | Euryanthe | 2019/12/28-2020/02/02 | 12.7,1.0 | 134 | 2 | 42.93 | 0.01 | 0.15 | 0.02 |
| 549 | Jessonda | 2020/03/05-2020/03/24 | 11.0,3.3 | 118 | -5 | 2.9713 | 0.0002 | 0.09 | 0.01 |

Table I. Observing circumstances and results. Pts is the number of data points. The phase angle is given for the first and last date, unless a minimum (second value) was reached. $L_{PAB}$ and $B_{PAB}$ are the approximate phase angle bisector longitude and latitude at mid-date range (see Harris et al., 1984).

549 Jessonda. Previously published rotation periods begin with Behrend (2002), 2.97 h; Behrend (2005), 2.9709 h; and Warner (2006), 5.958 h. Warner (2011) corrected the 2006 period to 2.971 h, amplitude 0.10 mag with one large and one small maximum per rotational cycle near phase angle bisector longitude ($L_{PAB}$) 55 degrees. Stephens (2015) published a rotation period 2.962 h near $L_{PAB}$ = 78 degrees with a lightcurve nearly identical in shape to the lightcurve by Warner (2011). New observations obtained on four nights 2020 Mar 5 – 24 near $L_{PAB}$ = 118 degrees provide a good fit to a lightcurve with period 2.9713 ± 0.0002 h, amplitude 0.09 ± 0.01 mag, and three unequal maxima and minima per rotational cycle (Fig. 14).

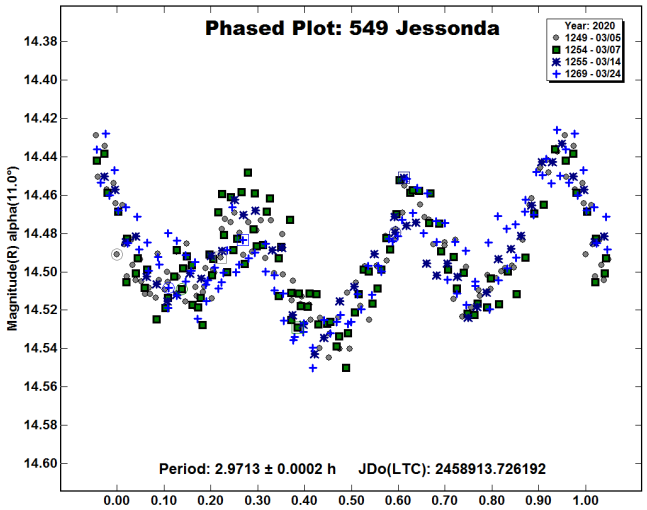


Fig. 14. Lightcurve of 549 Jessonda.

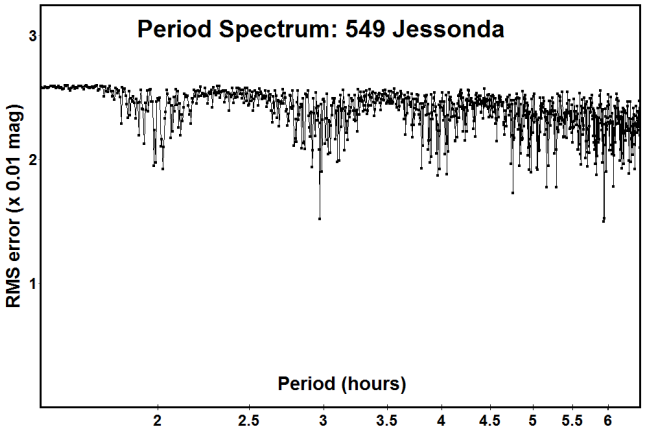


Fig. 15. Period spectrum for 549 Jessonda between 1.5 and 6.5 h.

A split-halves plot to the double period 5.94 h, not published, shows that the two halves are almost identical and rules out the double period. A period spectrum between 1.5 and 6.5 h (Fig. 15) shows that minima corresponding to 3 and 6 maxima and minima per cycle, respectively, are deeper than minima corresponding to 2, 4, and 5 maxima and minima per cycle, respectively. The combination of all evidence shows that all periods except 2.9713 h can now be ruled out, and the 2.9713-hour period is secure. This result is consistent with previously published periods.

## References


Behrend, R. (2002, 2005, 2010). Observatoire de Geneve web site. *http://*obswww.unige.ch/*~behrend/page_cou.html*.

Brinsfield, J.W. (2010). "Asteroid lightcurve analysis at the Via Capote Observatory: 4th quarter." *Minor Planet Bull.* **37**, 50-53.

Harris, A.W.; Young, J.W.; Scaltriti, F.; Zappala, V. (1984). "Lightcurves and phase relations of the asteroids 82 Alkmene and 444 Gyptis." *Icarus* **57**, 251-258.

Polakis, T.; Skiff, B. (2019). "Lightcurves of eleven main-belt minor planets." *Minor Planet Bull.* **46**, 152-157.

Stephens, R. (2015). "Asteroids observed from CS3: 2014 October – December." *Minor Planet Bull.* **42**, 104-106.

Surdej, J.; Surdej, A.; Louis, B. (1983). "UBV photometry of the minor planets 86 Semele, 521 Brixia, 53 Kalypso, and 113 Amalthea." *Astron. Astrophys. Suppl. Ser.* **52**, 203-211.

Warner, B.D. (2006). "Asteroid lightcurve analysis at the Palmer Divide Observatory – late 2005 and early 2006." *Minor Planet Bull.* **33**, 58-62.

Warner, B.D.; Harris, A.W.; Pravec, P. (2009). "The Asteroid Lightcurve Database." *Icarus* **202**, 134-146. Updated 2019 August. *http://www.minorplanet.info/lightcurvedatabase.html*

Warner, B.D. (2011). "Upon further review: VI. An examination of previous lightcurve analysis from the Palmer Divide Observatory." *Minor Planet Bull.* **38**, 96-101.

Zappala, V.; Scaltriti, F.; Di Martino, M. (1983). "Photoelectric photometry of 21 asteroids." *Icarus* **56**, 325-344.

# LIGHTCURVE ANALYSIS OF HILDA ASTEROIDS AT THE CENTER FOR SOLAR SYSTEM STUDIES: 2019 DECEMBER - 2020 APRIL

Brian D. Warner
Center for Solar System Studies / MoreData!
446 Sycamore Ave.
Eaton, CO 80615 USA
brian@MinorPlanetObserver.com

Robert D. Stephens
Center for Solar System Studies / MoreData!
Rancho Cucamonga, CA

(Received: 2020 April 7)

CCD photometric observations of ten Hilda asteroids were made at the Center for Solar System Studies (CS3) in 2019 December to provide additional lightcurves for modeling.

CCD photometric observations of ten Hilda asteroids were made at the Center for Solar System Studies (CS3) from 2019 December to 2020 April as part of an ongoing study of this family/group, which is located between the outer main-belt and Jupiter Trojans in a 3:2 orbital resonance with Jupiter. The goal is to determine the spin rate statistics of the Hildas and to find pole and shape models when possible. We also look to examine the degree of influence that the YORP (Yarkovsky–O'Keefe–Radzievskii–Paddack) effect (Rubincam, 2000) has on distant objects and to compare the spin rate distribution against the Jupiter Trojans, which can provide evidence that the Hildas are more "comet-like" than main-belt asteroids.

| Telescopes | Cameras |
|---|---|
| 0.30-m *f*/6.3 Schmidt-Cass | FLI Microline 1001E |
| 0.35-m *f*/9.1 Schmidt-Cass | FLI Proline 1001E |
| 0.35-m *f*/11 Schmidt-Cass | SBIG STL-1001E |
| 0.40-m f/10 Schmidt-Cass | |
| 0.50-m *f*/8.1 Ritchey-Chrétien | |

Table I. List of available telescopes and CCD cameras at CS3. The exact combination for each telescope/camera pair can vary due to maintenance or specific needs.

Table I lists the telescopes and CCD cameras that are combined to make observations. Up to nine telescopes can be used for the campaign, although seven is more common. All the cameras use CCD chips from the KAF blue-enhanced family and so have essentially the same response. The pixel scales ranged from 1.24-1.60 arcsec/pixel. All lightcurve observations were unfiltered since a clear filter can result in a 0.1-0.3 magnitude loss. The exposures varied depending on the asteroid's brightness.

To reduce the number of times and amounts of adjusting nightly zero points, we use the ATLAS catalog r´ (SR) magnitudes (Tonry et al., 2018). Those adjustments are usually ≤ 0.03 mag. The few corrections that were greater may have been related in part to using unfiltered observations, poor centroiding of the reference stars, and not correcting for second-order extinction.

The Y-axis values are ATLAS SR "sky" (catalog) magnitudes. During period analysis, the magnitudes were normalized to the comparison stars used in the earliest session and to the phase angle given in parentheses using $G$ = 0.15. If "Reduced" is seen, the magnitudes were converted to unity distances by using $-5\log_{10}(r\Delta)$ where $r\Delta$ is the product of the Sun-asteroid and Earth-asteroid distances in au. The X-axis shows rotational phase from –0.05 to 1.05. If the plot includes the amplitude, e.g., "Amp: 0.65", this is the amplitude of the Fourier model curve and *not necessarily the adopted amplitude for the lightcurve*.

Our initial search for previous results started with the asteroid lightcurve database (LCDB; Warner et al., 2009) found on-line at *http://www.minorplanet.info/lightcurvedatabase.html*. Readers are strongly encouraged to obtain, when possible, the original references listed in the LCDB. From here on, we'll use only "LCDB" to reference the paper by Warner et al. (2009).

1202 Marina. Dahlgren et al. (1998) reported a period of 9.45 h based on data from 1993. Our period is similar to theirs but is based on a denser data set.

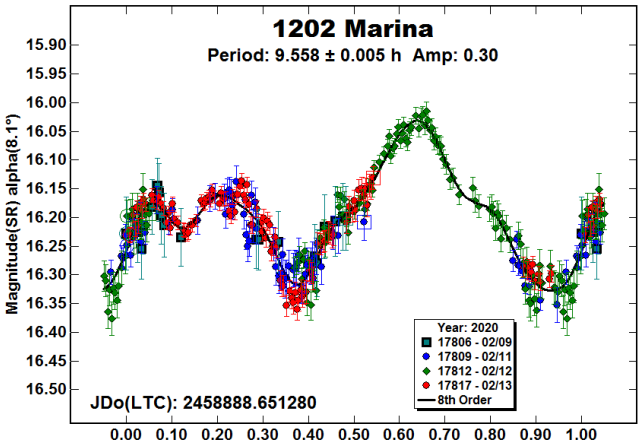


1212 Francette. Previous results for the 82-km Francette are 22.433 h (Warner and Stephens, 2017) and 16.2879 h (Pál et al., 2020) using data from TESS. Our data show a strong preference for a period near 32 h, or double that from Pál et al. (2020).

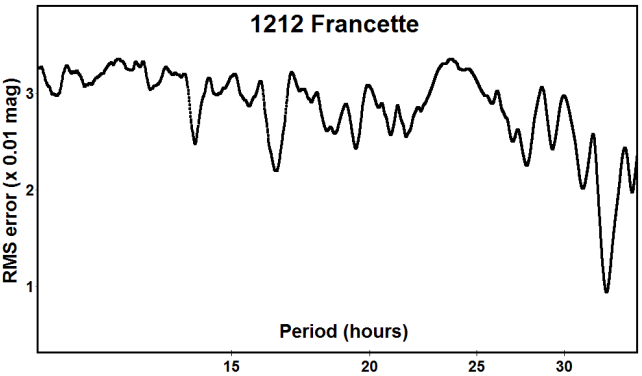


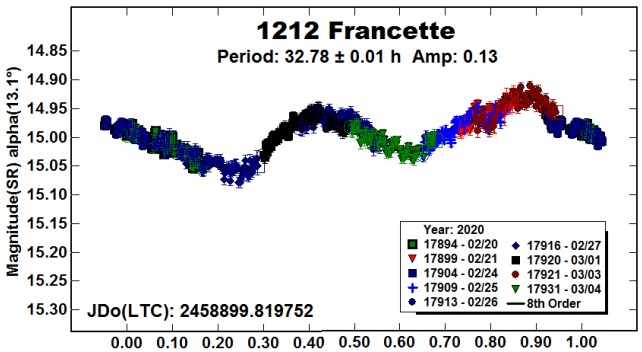

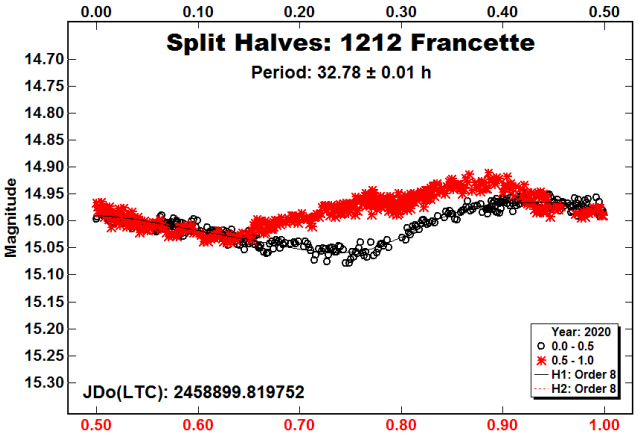


A split-halves plot for our period indicates that the 16 h period does not fit the data. It's worth noting that the 22.433 h period from Warner and Stephens (2017), is close to a 3:2 integer ratio with the period adopted here.

1345 Potomac. Dahlgren et al. (1998) found a period of 11.40 h and Brinsfield (2010) found a period of 11.41 h. Our result is in good agreement with those earlier works.

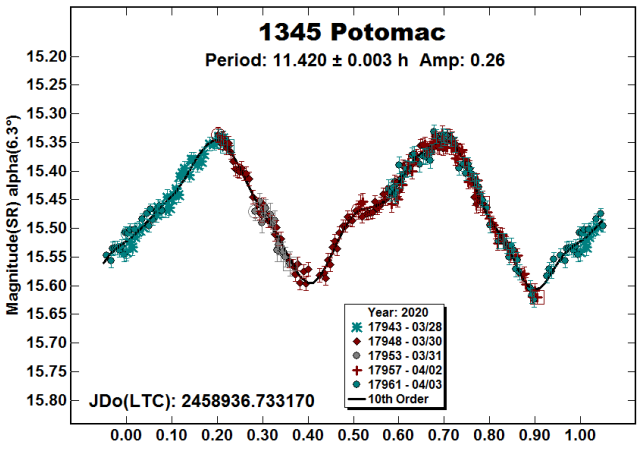


1439 Vogtia. We found a period of 12.898 h using data from 2016 (Warner et al., 2017) and then 12.944 h from the 2017 apparition (Warner et al., 2018). The latest result is consistent with those earlier findings.

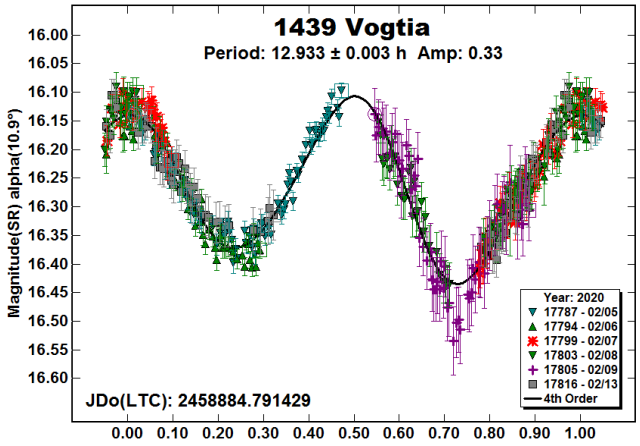


1941 Wild. Waszczak et al. (2015) used data from the Palomar Transient Factory (PTF) to find a period of 45.649 h, which is rated U = 1 in the LCDB. Our result is only marginally better since the data do not cover the full lightcurve and were acquired over a span of almost two months.

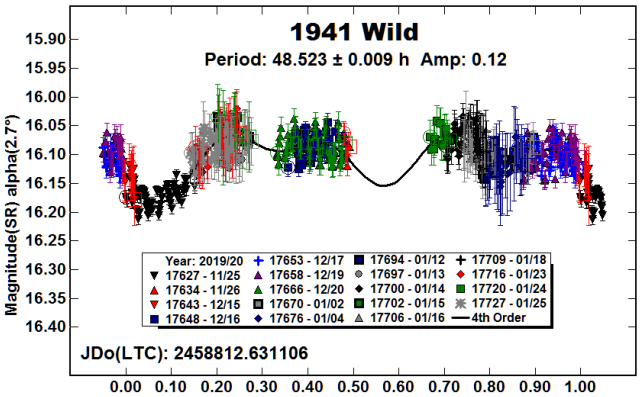


3202 Graff. Stephens (2016) observed this 35-km Hilda in 2015 and found a period of 17.32 h. Pál et al. (2020) reported $P$ = 17.3548 h. Our period is consistent with those earlier results.

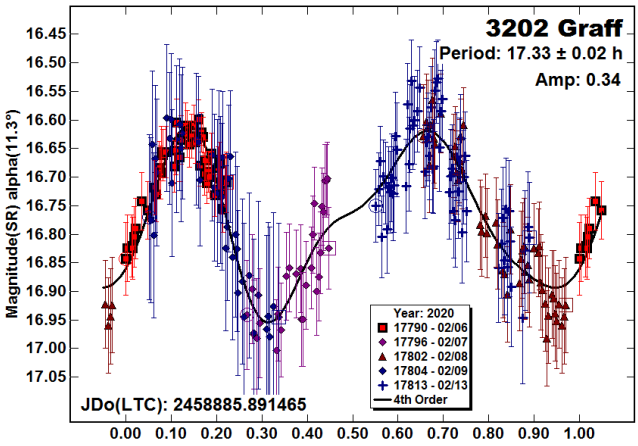


3571 Milanstefanik. A definitive period for 39-km Milanstefanik has proved elusive. Using data from 2016, we found a period of 421.1 h (Warner and Stephens, 2017). Our data from 2020 could not be fit to any period $P$ > 400 h; it did fit well with $P$ ~ 360 h, but only after some significant adjustments to nightly zero points.

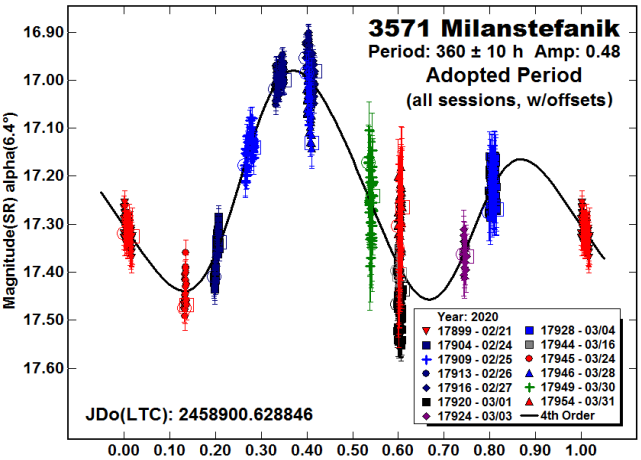

A raw plot of the data without adjustments and excluding two sessions shows no overt signs of tumbling, although it would seem probable given the period and size (Pravec et al., 2005; 2014). The two excluded sessions were too far "off the curve" too quickly to have been due to tumbling. Other than some sort of calibration error, we don't have an explanation for the anomalous sessions.

Given the new results, we returned to the data from 2016. After resetting all nightly zero points and changing the comparison star magnitudes from APASS V (Henden et al., 2009) to ATLAS SR, we redid the period analysis to see if the data would fit the shorter period.

In fact, they did and with very little zero-point adjustments ("2016 A"). However, the lightcurve shape seems highly improbable given the amplitude and low phase angle (Harris et al., 2014). A search above 400 h found a best fit of $P$ = 472 h ("2016 B") with something closer to the expected bimodal lightcurve. The lack of coverage from the second minimum to maximum makes the solution tentative at best.

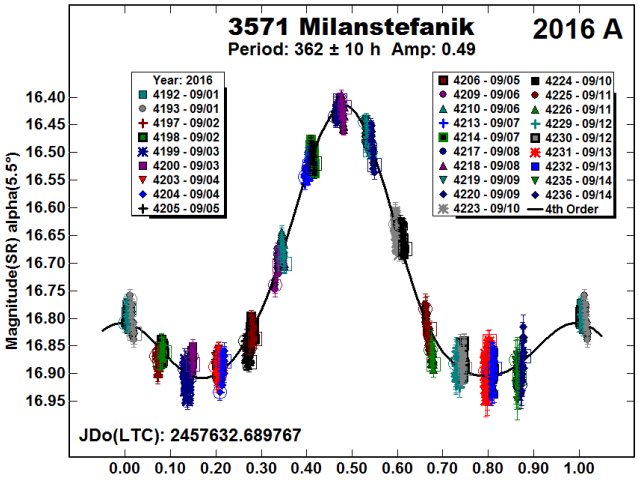


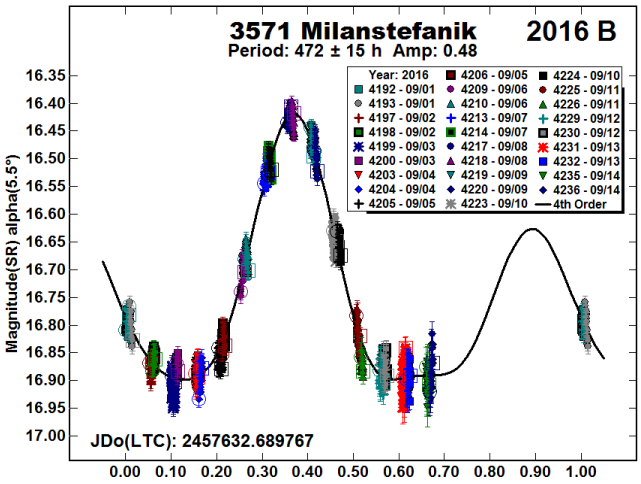


To solve the ambiguity will likely require a collaboration among individual or groups of observers who are well-separated in longitude.

(23186) 2000 PO8. We observed this asteroid in 2017 (Warner and Stephens, 2018). Analysis of the data found a period of 5.003 h. Our 2020 data set led to $P$ = 5.0165 h, which is in good agreement with our earlier result.

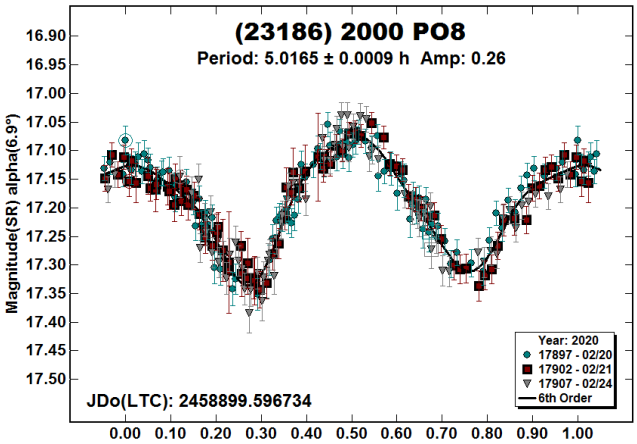


(32395) 2000 QV213. Waszczak et al. (2015) reported a period of 15.349h. Analysis of our denser data set found $P$ = 15.372 h.

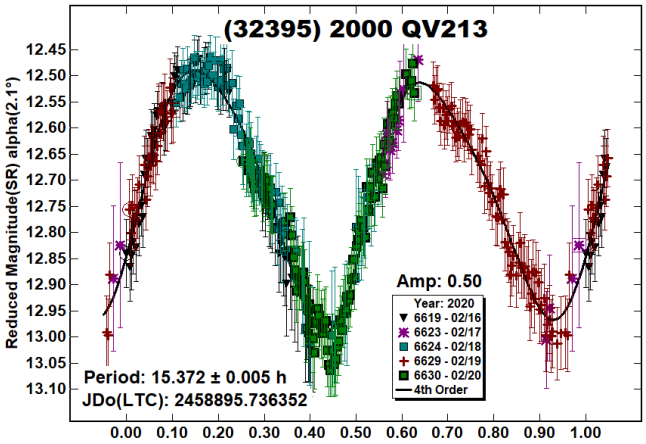


(77892) 2001 SZ250. This appears to be the first reported period for 2001 SZ250, which has an estimated diameter of 13 km. The "notch" at 0.25 rotation phase was seen on several occasions and so appears to have a physical cause.

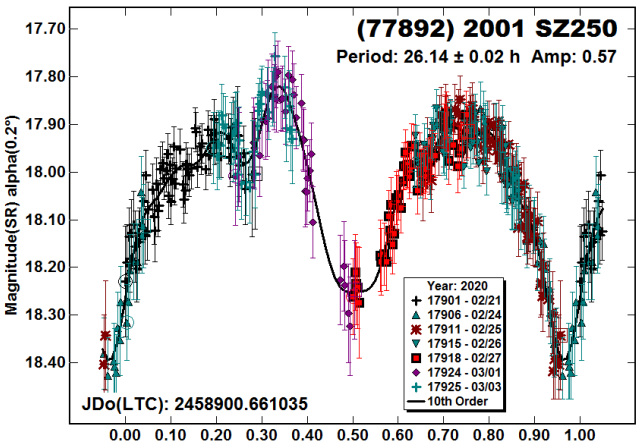


Acknowledgements

Funding for observations at CS3 and work on the asteroid lightcurve database (Warner et al., 2009) and ALCDEF database (*alcdef.org*) are supported by NASA grant 80NSSC18K0851.

This work includes data from the Asteroid Terrestrial-impact Last Alert System (ATLAS) project. ATLAS is primarily funded to search for near earth asteroids through NASA grants NN12AR55G, 80NSSC18K0284, and 80NSSC18K1575; byproducts of the NEO search include images and catalogs from the survey area. The ATLAS science products have been made possible through the contributions of the University of Hawaii Institute for Astronomy, the Queen's University Belfast, the Space Telescope Science Institute, and the South African Astronomical Observatory.

The authors gratefully acknowledge Shoemaker NEO Grants from the Planetary Society (2007, 2013). These were used to purchase some of the telescopes and CCD cameras used in this research.

References

Brinsfield, J.W. (2010). "Asteroid Lightcurve Analysis at Via Capote Observatory: 4th Quarter 2009." *Minor Planet Bull*. **37**, 50-53.

Dahlgren, M.; Lahulla, J.F.; Lagerkvist, C.-I.; Lagerros, J.; Mottola, S.; Erikson, A.; Gonano-Beurer, M.; Di Martino, M. (1998). "A Study of Hilda Asteroids. V. Lightcurves of 47 Hilda Asteroids." *Icarus* **133**, 247-285.

Harris, A.W.; Young, J.W.; Scaltriti, F.; Zappala, V. (1984). "Lightcurves and phase relations of the asteroids 82 Alkmene and 444 Gyptis." *Icarus* **57**, 251-258.

Harris, A.W.; Pravec, P.; Galad, A.; Skiff, B.A.; Warner, B.D.; Vilagi, J.; Gajdos, S.; Carbognani, A.; Hornoch, K.; Kusnirak, P.; Cooney, W.R.; Gross, J.; Terrell, D.; Higgins, D.; Bowell, E.; Koehn, B.W. (2014). "On the maximum amplitude of harmonics on an asteroid lightcurve." *Icarus* **235**, 55-59.

Henden, A.A.; Terrell, D.; Levine, S.E.; Templeton, M.; Smith, T.C.; Welch, D.L. (2009). *http://www.aavso.org/apass*

Pál, A.; Szakáts, R.; Kiss, C.; Bódi, A.; Bognár, Z.; Kalup, C.; Kiss, L.L.; Marton, G.; Molnár, L.; Plachy, E.; Sárneczky, K.; Szabó, G.M.; Szabó, R. (2020). "Solar System Objects Observed with TESS—First Data Release: Bright Main-belt and Trojan Asteroids from the Southern Survey." *Ap. J. Supl. Ser*. **247**, id.26.

Pravec, P.; Harris, A.W.; Scheirich, P.; Kušnirák, P.; Šarounová, L.; Hergenrother, C.W.; Mottola, S.; Hicks, M.D.; Masi, G.; Krugly, Yu.N.; Shevchenko, V.G.; Nolan, M.C.; Howell, E.S.; Kaasalainen, M.; Galád, A.; Brown, P.; Degraff, D.R.; Lambert, J.V.; Cooney, W.R.; Foglia, S. (2005). "Tumbling asteroids." *Icarus* **173**, 108-131.

Pravec, P.; Scheirich, P.; Durech, J.; Pollock, J.; Kusnirak, P.; Hornoch, K.; Galad, A.; Vokrouhlicky, D.; Harris, A.W.; Jehin, E.; Manfroid, J.; Opitom, C.; Gillon, M.; Colas, F.; Oey, J.; Vrastil, J.; Reichart, D.; Ivarsen, K.; Haislip, J.; LaCluyze, A. (2014). "The tumbling state of (99942) Apophis." *Icarus* **233**, 48-60.

Rubincam, D.P. (2000). "Relative Spin-up and Spin-down of Small Asteroids." *Icarus* **148**, 2-11.

Stephens, R.D. (2016). "Asteroids Observed from CS3: 2015 July - September." *Minor Planet Bull*. **43**, 52-56.

Tonry, J.L.; Denneau, L.; Flewelling, H.; Heinze, A.N.; Onken, C.A.; Smartt, S.J.; Stalder, B.; Weiland, H.J.; Wolf, C. (2018). "The ATLAS All-Sky Stellar Reference Catalog." *Astrophys. J.* **867**, A105.

Warner, B.D.; Harris, A.W.; Pravec, P. (2009). "The Asteroid Lightcurve Database." *Icarus* **202**, 134-146. Updated 2020 March. *http://www.minorplanet.info/lightcurvedatabase.html*

Warner, B.D.; Stephens, R.D. (2017). "Lightcurve Analysis of Hilda Asteroids at the Center for Solar System Studies: 2016 June-September." *Minor Planet Bull*. **44**, 36-41.

Warner, B.D.; Stephens, R.D. (2018). "Lightcurve Analysis of Hilda Asteroids at the Center for Solar System Studies: 2017 July through September." *Minor Planet Bull*. **45**, 35-39.

Warner, B.D.; Stephens, R.D.; Coley, D.R. (2017). "Lightcurve Analysis of Hilda Asteroids at the Center for Solar System Studies: 2016 September-December." *Minor Planet Bull*. **44**, 130-137.

Warner, B.D.; Stephens, R.D.; Coley, D.R. (2018). "Lightcurve Analysis of Hilda Asteroids at the Center for Solar System Studies: 2017 October-December." *Minor Planet Bull*. **45**, 147-161.

Waszczak, A.; Chang, C.-K.; Ofek, E.O.; Laher, R.; Masci, F.; Levitan, D.; Surace, J.; Cheng, Y.-C.; Ip, W.-H.; Kinoshita, D.; Helou, G.; Prince, T.A.; Kulkarni, S. (2015). "Asteroid Light Curves from the Palomar Transient Factory Survey: Rotation Periods and Phase Functions from Sparse Photometry." *Astron. J.* **150**, A75.

| Number | Name | 2020/mm/dd | Phase | $L_{PAB}$ | $B_{PAB}$ | Period(h) | P.E. | Amp | A.E. |
|---|---|---|---|---|---|---|---|---|---|
| 1202 | Marina | 02/09-02/13 | 8.2,9.0 | 107 | 3 | 9.558 | 0.005 | 0.30 | 0.03 |
| 1212 | Francette | 02/20-03/04 | 13.1,10.2 | 196 | 6 | 32.78 | 0.01 | 0.13 | 0.01 |
| 1345 | Potomac | 03/28-04/03 | 6.3,5.1 | 207 | 12 | 11.420 | 0.003 | 0.26 | 0.02 |
| 1439 | Vogtia | 02/05-02/13 | 10.9,9.0 | 174 | 4 | 12.933 | 0.003 | 0.37 | 0.03 |
| 1941 | Wild | 11/25-01/25 | 2.7,17.0 | 58 | 0 | 48.523 | 0.009 | 0.12 | 0.02 |
| 3202 | Graff | 02/06-02/13 | 11.4,9.9 | 178 | -7 | 17.33 | 0.02 | 0.34 | 0.04 |
| 3571 | Milanstefanik | 2016/09/01-09/14 | 5.5,2.6 | 356 | 9 | 362 | 10 | 0.49 | 0.05 |
| | | | | | | [A]472 | 15 | 0.48 | 0.05 |
| 3571 | Milanstefanik | 2020/02/21-03/31 | 6.4,12.7 | 128 | -8 | 360 | 10 | 0.50 | 0.05 |
| 23186 | 2000 PO8 | 02/20-02/24 | 6.9,7.9 | 129 | 9 | 5.0165 | 0.0009 | 0.26 | 0.03 |
| 32395 | 2000 QV213 | 02/16-02/20 | 2.1,1.0 | 153 | 2 | 15.372 | 0.005 | 0.50 | 0.03 |
| 77892 | 2001 SZ250 | 02/21-03/03 | 0.2,3.9 | 152 | 0 | 26.14 | 0.02 | 0.57 | 0.04 |

Table II. Observing circumstances. [A]Alternate period. The phase angle ($\alpha$) is given at the start and end of each date range. $L_{PAB}$ and $B_{PAB}$ are the average phase angle bisector longitude and latitude (see Harris *et al*., 1984). An amplitude in italics overrides the value in the plot.

# NEAR-EARTH ASTEROID LIGHTCURVE ANALYSIS AT THE CENTER FOR SOLAR SYSTEM STUDIES: 2019 DECEMBER - 2020 APRIL

Brian D. Warner
Center for Solar System Studies / MoreData!
446 Sycamore Ave.
Eaton, CO 80615 USA
brian@MinorPlanetObserver.com

Robert D. Stephens
Center for Solar System Studies / MoreData!
Rancho Cucamonga, CA 91730

(Received: 2020 April 6 Revised: 2020 May 14)

Lightcurves for 32 near-Earth asteroids (NEAs) obtained at the Center for Solar System Studies (CS3) from 2019 December to early 2020 April were analyzed for rotation period, peak-to-peak amplitude, and signs of satellites or tumbling.

CCD photometric observations of 32 near-Earth asteroids (NEAs) were made at the Center for Solar System Studies (CS3) from 2019 September to early 2020 January. Table I lists the telescopes and CCD cameras that are combined to make observations.

Up to nine telescopes can be used for the campaign, although seven is more common. All the cameras use CCD chips from the KAF blue-enhanced family and so have essentially the same response. The pixel scales ranged from 1.24-1.60 arcsec/pixel.

| Telescopes | Cameras |
|---|---|
| 0.30-m *f*/6.3 Schmidt-Cass | FLI Microline 1001E |
| 0.35-m *f*/9.1 Schmidt-Cass | FLI Proline 1001E |
| 0.40-m *f*/10 Schmidt-Cass | SBIG STL-1001E |
| 0.40-m *f*/10 Schmidt-Cass | |
| 0.50-m *f*/8.1 Ritchey-Chrétien | |

Table I. List of available telescopes and CCD cameras at CS3. The exact combination for each telescope/camera pair can vary due to maintenance or specific needs.

All lightcurve observations were unfiltered since a clear filter can cause a 0.1-0.3 mag loss. The exposure duration varied depending on the asteroid's brightness and sky motion. Guiding on a field star sometimes resulted in a trailed image for the asteroid.

Measurements were made using *MPO Canopus*. The Comp Star Selector utility in *MPO Canopus* found up to five comparison stars of near solar-color for differential photometry. Comp star magnitudes were taken from ATLAS catalog (Tonry et al., 2018a), which has Sloan *griz* magnitudes that were derived from the GAIA and Pan-STARR catalogs, among others, and are the "native" magnitudes of the catalog.

To reduce the number of times and amount of resetting nightly zero points, we use the ATLAS r′ (SR) magnitudes. Those adjustments are mostly ≤ 0.03 mag. The occasions where larger corrections were required may have been related in part to using unfiltered observations, poor centroiding of the reference stars, and not correcting for second-order extinction terms.

Unless otherwise indicated, the Y-axis of lightcurves are ATLAS SR or V "sky" (catalog) magnitudes. During period analysis, the magnitudes were normalized to the comparison stars used in the earliest session and to the phase angle given in parentheses using $G = 0.15$. If "Reduced" is seen, the magnitudes were converted to unity distances by using $-5\log_{10}(r\Delta)$, where $r\Delta$ is the product of the Sun-asteroid and Earth-asteroid distances in au. The X-axis shows rotational phase from –0.05 to 1.05. If the plot includes the amplitude, e.g., "Amp: 0.65", this is the amplitude of the Fourier model curve and *not necessarily the adopted amplitude for the lightcurve*.

Our initial search for previous results started with the asteroid lightcurve database (LCDB; Warner et al., 2009) found on-line at *http://www.minorplanet.info/lightcurvedatabase.html*. Readers are strongly encouraged to obtain, when possible, the original references listed in the LCDB. From here on, we'll use only "LCDB" to reference the paper by Warner et al. (2009).

1627 Ivar. This 8-km NEA has been studied numerous times in the past, enough so that a pole solution within a few degrees of ($\lambda$ = 335°, $\beta$ = +38°) has been established (Kaasalianen et al., 2004; Hanus et al., 2015; Crowell et al., 2017). The amplitude of the elongated asteroid ranges from 0.25 to 1.48 mag (LCDB), which means the 2020 observations were nearly pole-on.

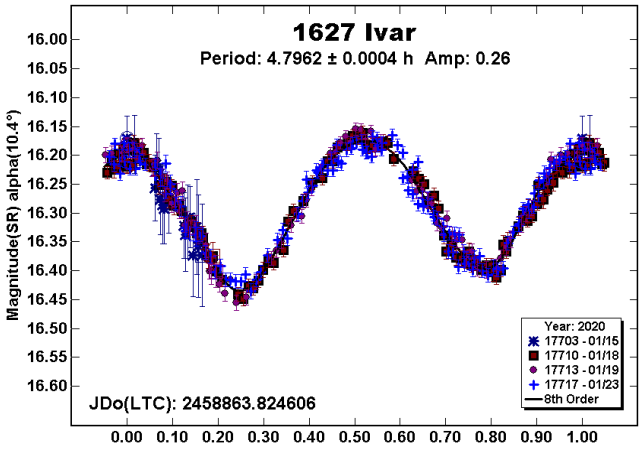


1864 Daedalus. Pravec et al. (1995web) found a period of 8.572 h. That result has been confirmed several times since, including by our data analysis from the 2020 February observations. The lowest amplitude in the LCDB is 0.72 mag so, as with 1627 Ivar, the observations were made looking close to the asteroid's north or south pole.

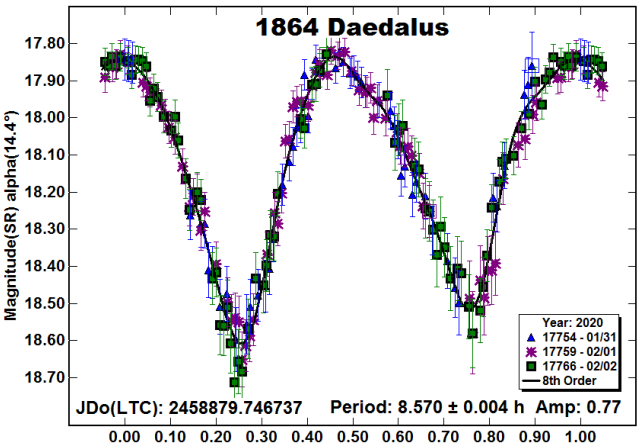


5626 Melissabrucker. We observed this asteroid in late 2019 (Warner and Stephens, 2020b) and found a period of 2.2574 h but it was not a fully secure solution. Analysis of our newest data

found $P$ = 2.48611 h. Despite the unusual shape of the lightcurve, we believe the solution to be correct even though it does not agree within error bars of previous results, e.g., Krugly et al. (2002, 2.4606 h) and Fornas et al. (2018, 2.813 h).

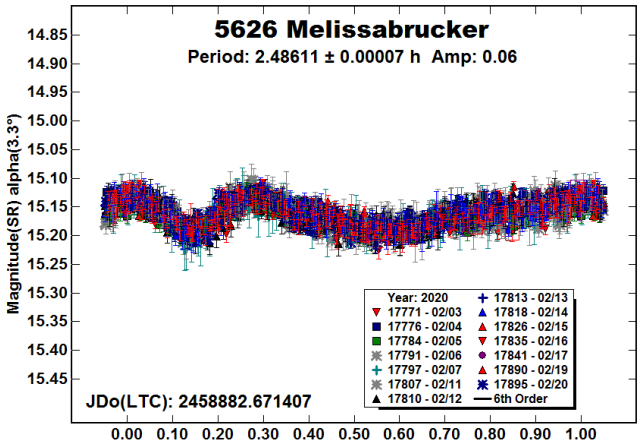


In particular, it did not agree with Warner (2017) who found a period of 133.6 h. At the time it was a suspected *very wide binary*, which is where the primary period is $P$ > 100 h and the secondary period usually ranges from 2-15 h. To confirm those earlier results, the comparison star magnitudes were changed from APASS V magnitudes (Henden et al., 2009) to ATLAS SR magnitudes (Tonry et al., 2018). The quality of each comparison star was reviewed, e.g., if its magnitude was a significant outlier when subtracted from the average of the others, and then the analysis was done anew.

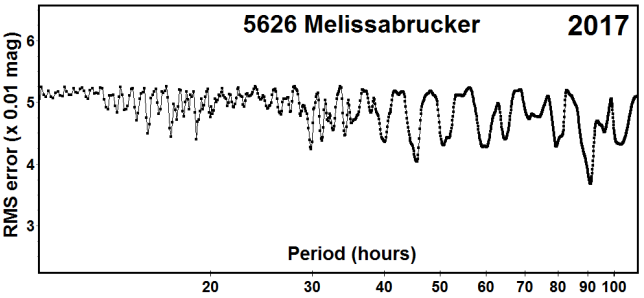


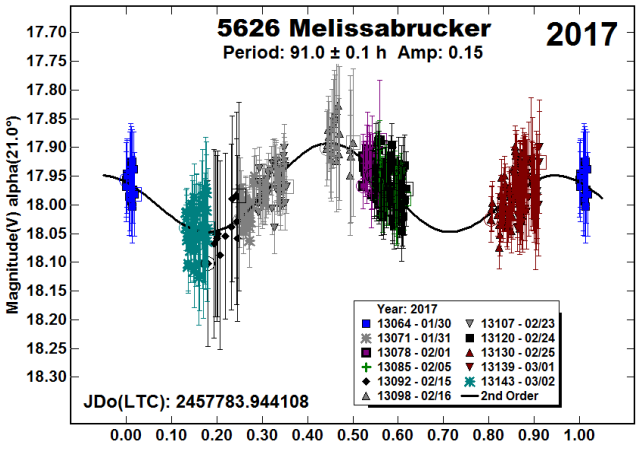


The result was yet a different solution that was not close to the others. Note that the 91 h period is close to a 3:2 ratio with the 133 h found by Warner (2017). Zero point adjustments were all < 0.04 mag, save one session that required a much larger offset. Why that was the case is not known, but tumbling was not considered likely.

We also returned to the 2019 data and reset those comparison stars to use ATLAS SR. With very little zero-point adjusting, we found a period compatible with the 2020 result.

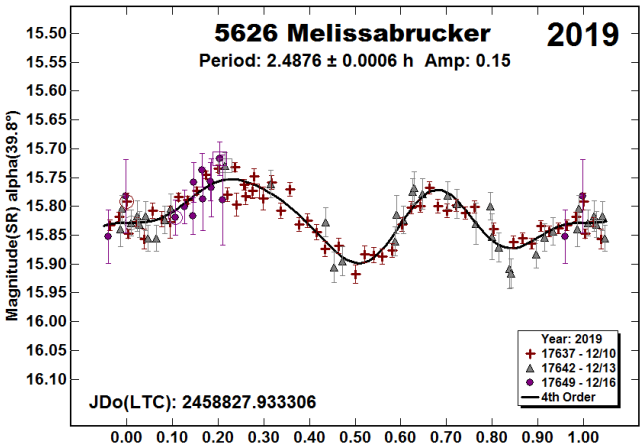


(5693) 1993 EA. Warner (2017) found a period of 2.496 h and reported a possible secondary period of 16.55 h. No signs of a satellite, let alone a second period, were seen.

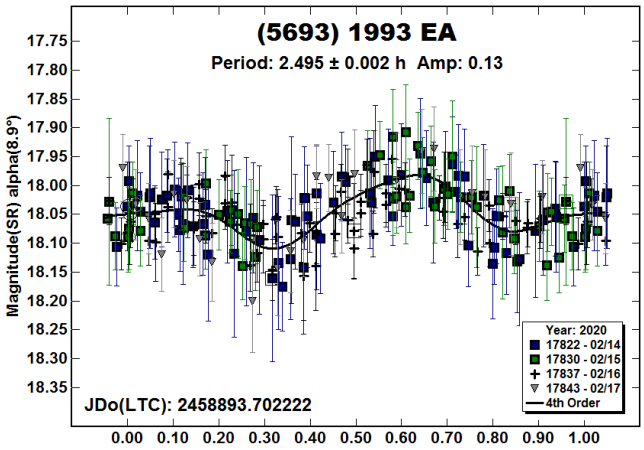


7088 Ishtar. Pravec et al. (2006web) reported this to be a binary asteroid with a primary period of $P_1$ = 2.6790 h and satellite orbital period of $P_2$ = 20.65h. The effective secondary-primary diameter ratio was $Ds/Dp$ > 0.42. Pravec et al. (2016) updated their results a decade later with $P_1$ = 2.6786 h and $P_2$ = 20.63 h.

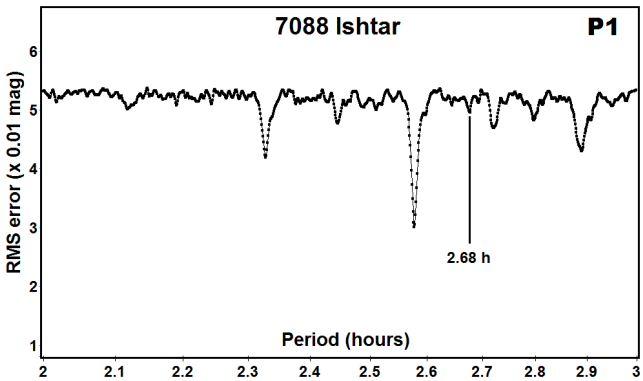

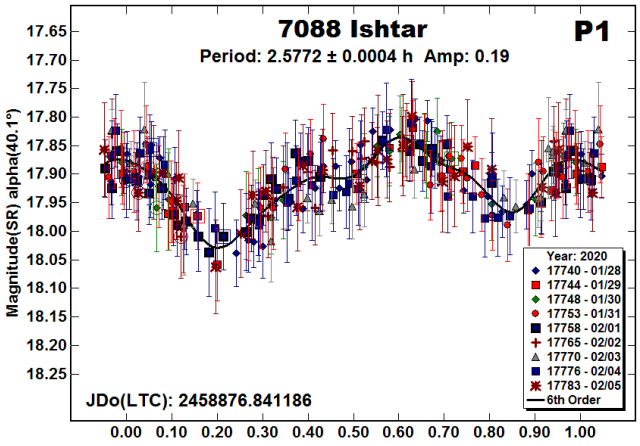


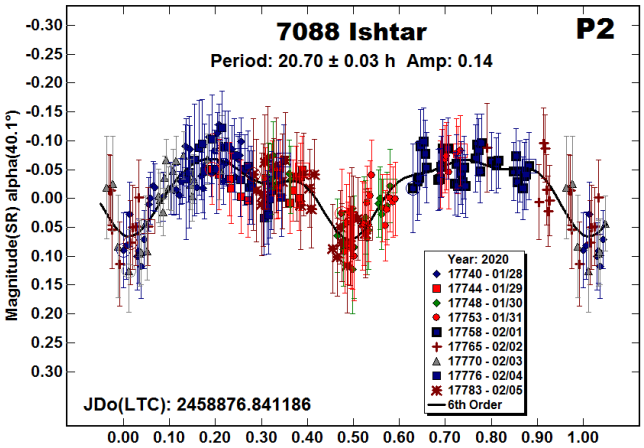


Our observations in 2020 were made to help with modeling of the binary system. The data analysis found $P_1$ = 2.5772 h, which is significantly different from the earlier works. No amount of zero point adjustments allowed finding a period near 2.68 h. In the period spectrum, our solution is a "side band" of the 2.68 h period, meaning that it might be harmonically related. In fact, the two periods *are* related to one another, differing by one rotation every 68 hours. Our secondary lightcurve period, $P_2$ = 20.70 h, is similar to Pravec et al. (2016). Our estimate of $Ds/Dp > 0.37 \pm 0.04$ is a little smaller than Pravec et al. (2016), but within the error bars of the two results.

(8566) 1996 EN. There were no previous period entries in the LCDB for this 1.6 km NEA. Thomas et al. (2014) classified it as a type V ("Vestoid") asteroid.

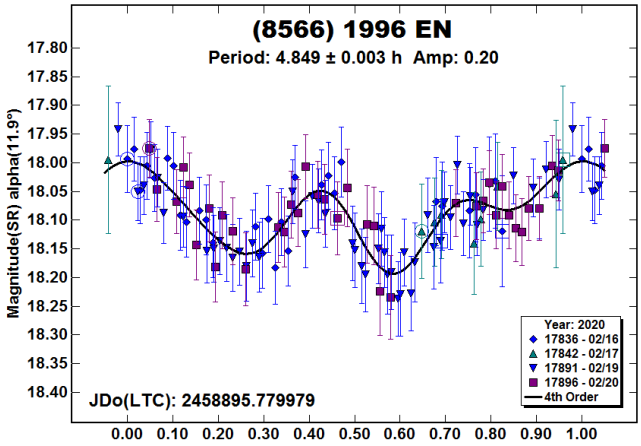


11066 Sigurd. Pravec et al. (1998) and Warner (2015c) both found a period close to 8.50 h. The latest result is in good agreement.

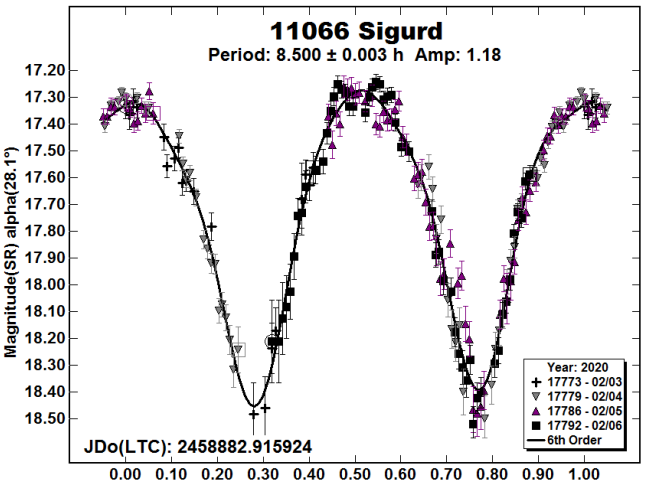


(11405) 1999 CV3. Pravec et al. (1999web) established the rotation period to be close to 6.50 h. We found similar results at two following apparitions: Warner (2013, 6.504 h; 2014, 6.501 h). The new data from 2020 were obtained at a different viewing aspect from the previous works and so we tried to model the asteroid using our dense data and sparse data from the Catalina Sky Survey (2020) downloaded from the AstDys-2 (2020) web site and sparse data from the ATLAS survey (2018b) that were available in the Asteroid Lightcurve Data Exchange Format (ALCDEF; 2020) database. The dense lightcurves are from the same period as the model vs. data plots in Figures 5 and 6.

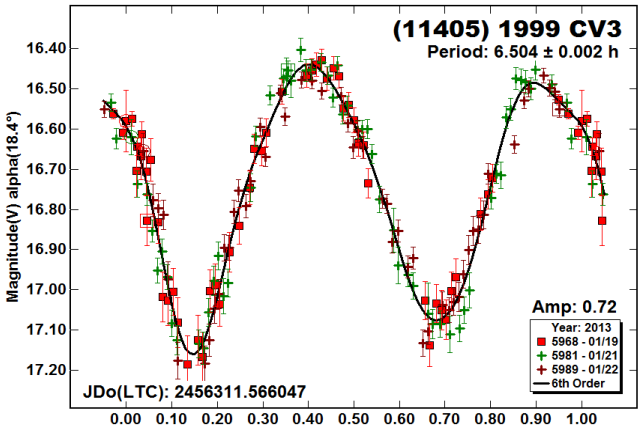


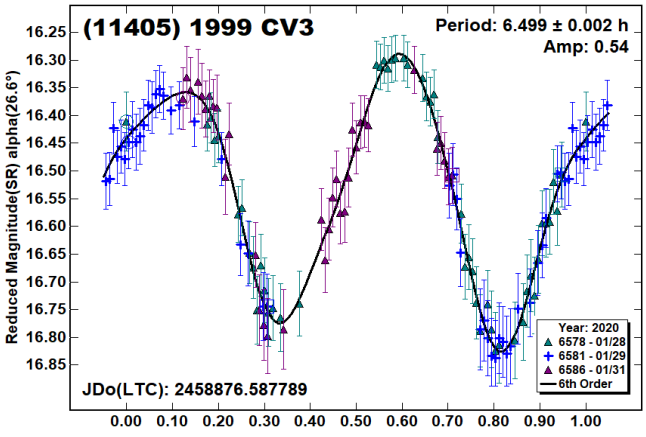

# SPIN/SHAPE MODEL FOR (11405) 1999 CV3

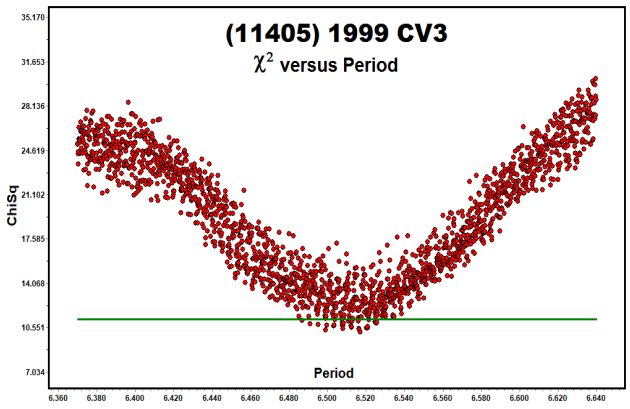


Figure 1. The initial period search results.

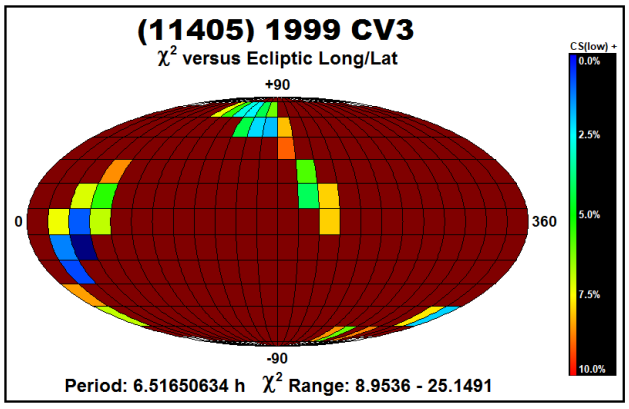


Figure 2. The pole search found two probable solutions.

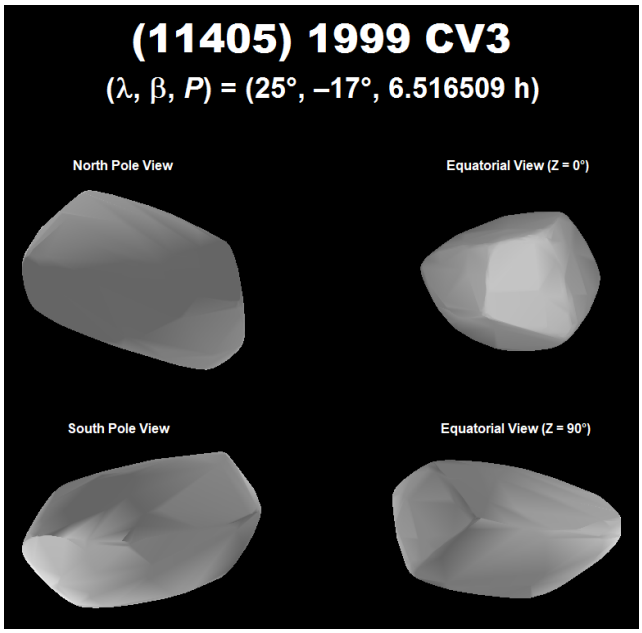


Figure 3. The shape of the asteroid based on the preferred pole solution.

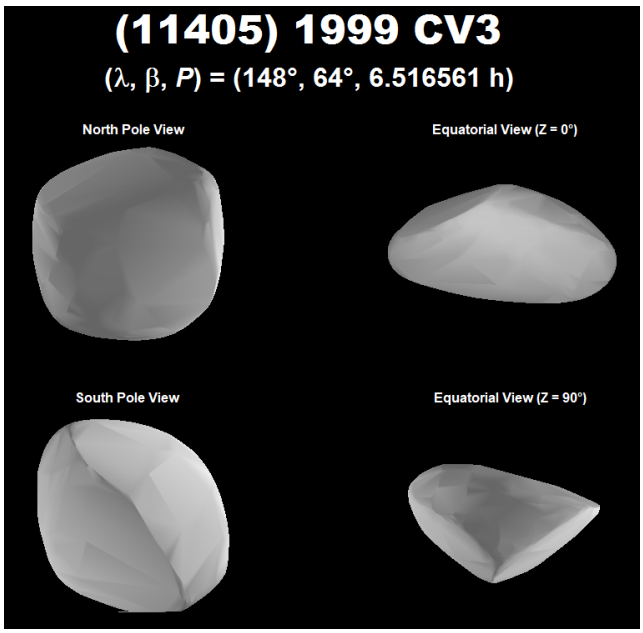


Figure 4. The secondary solution shape is less elongated when looking at the asteroid's north and south poles.

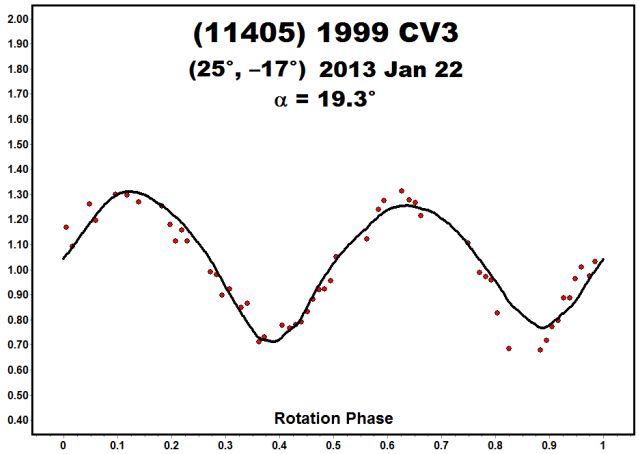


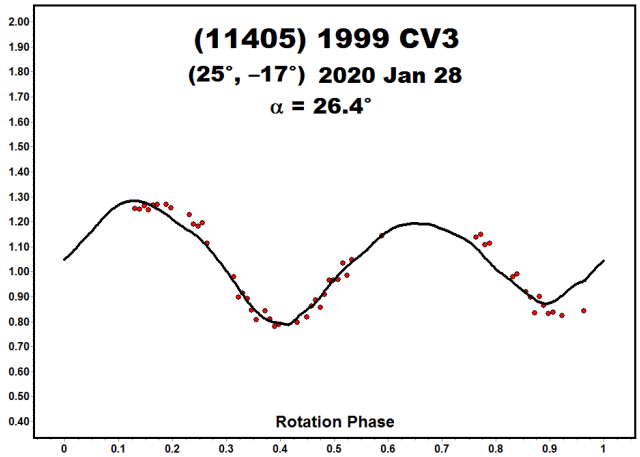


Figure 5/6. The comparison plots are against the preferred pole solution. The red dots indicate the data used for modeling while the black line is the smoothed lightcurve for generated by the shape at the time of the observations. The match is very close on both occasions, which gives confidence in the shape/spin axis model. Also, by virtue of the data being "in phase" some seven years apart, either the asteroid's rotation rate is not being affected by YORP, or the effect is too small for the available data and time span.

The references to figures in the following discussion are to the plots from the modeling process shown in Figures 1-6. The initial period search (Figure 1) found a number of solutions with 10% of the lowest $\chi^2$ value. A narrower search range found the most likely period from among the initial possibilities. The pole search (Figure 2) tested 312 discrete, fixed pole positions but allowed the sidereal period from period search to "float." The result was two possible solutions separated by about 180° in longitude and were on opposite sides of the equator. In Figure 2, the dark red regions had $\chi^2$ values more than 1.1x the lowest $\chi^2$ value.

Models were built using the poles of $(\lambda, \beta, P)_1$ = (25°, –17°, 6.516509 h; Figure 3) and $(\lambda, \beta, P)_2$ = (148°, +64°, 6.516561 h; Figure 4) with the former being the preferred solution. Figures 5 and 6 compare the model lightcurve (black line) against the data (red dots) at specific times. It's important to note that the vertical axis in the dense lightcurves shown above is in magnitudes while the vertical axis of the model comparisons is in units of intensity and so they don't have the same amplitude or shape as the dense lightcurves.

(18172) 2000 QL7. Kluwak (2020) reported a period of 2.3767 h based on data obtained in 2019 October. Additional data obtained on 2020 Jan 8 through Feb 1 produced nearly identical results. This differed significantly from our result of 2.509 h, which was based on data obtained in 2019 August (Warner and Stephens, 2020a). Private communications with Kluwak prompted a re-analysis of our data.

Before doing any new analysis, we changed the magnitudes for the comparison stars used in 2019 from ATLAS V to ATLAS SR. As noted in the introduction, the latter are native magnitudes, i.e., they are not derived from conversion formulae. We also reset the 2019 and 2020 nightly zero-point offsets to 0. Doing this did not change the overall results but did increase confidence in them.

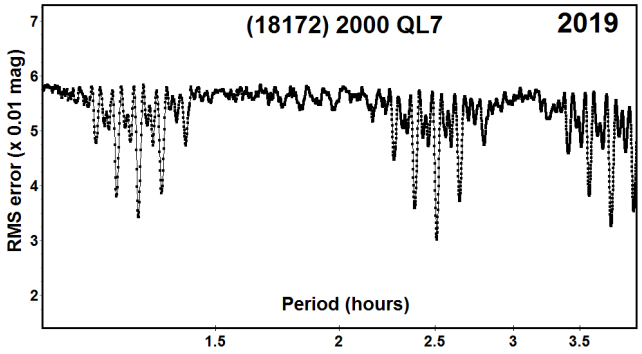


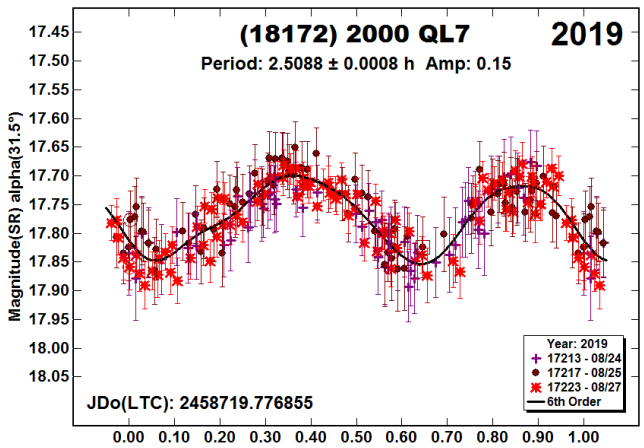


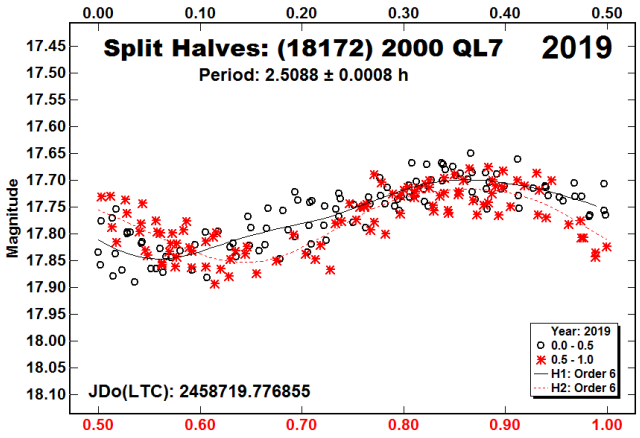


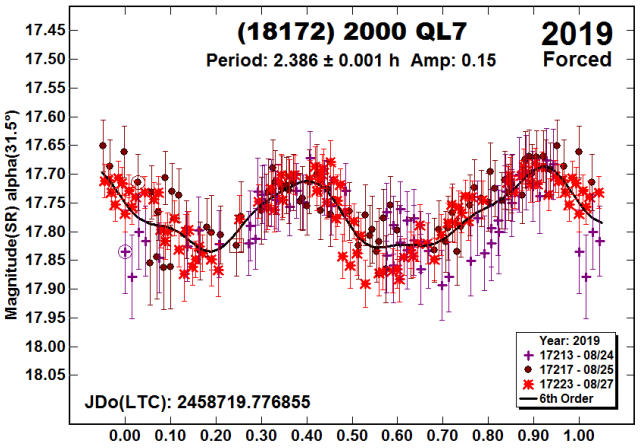


The period spectrum for 2019 clearly shows that a period of about 2.5088 h is favored. There is a less likely result close to the Kluwak period of 2.3767 h. If taken to sufficient precision, the two disparate periods differ by almost exactly one rotation over 45 hours. If the lightcurve was symmetrical about the two halves, it would be easy to argue for a case of *rotational aliasing*, which is where the true number of rotations over a given time is ambiguous.

However, for our 2019 results, the lightcurve shape is sufficiently *asymmetrical* so as to make rotational aliasing less likely. However, the close integral difference of rotations every 45 hours, which is nearly commensurate with an Earth day, strengthens the argument *for* rotational aliasing.

We attempted to fit the 2019 data to the Kluwak period near 2.3767 h. The best fit we could get after working with nightly zero-point adjustments gave a close, but still not convincing, fit when compared to the solution at 2.5088 h.

Using the 2020 data produced opposite results, i.e., a shorter period of 2.3710 h was even more strongly favored over one near 2.5 h. The data set in 2020 had a little more scatter than the set from 2019, but the differences seemed too minor to lead to the opposing results. Forcing the 2020 data to a period near 2.50 h shows a decided mismatch between the data and model lightcurve.

Despite the period spectrum's favoring a shorter period, it's worth comparing the split-halves plots from each year. The 2019 plot shows a distinct difference in the two halves at 0.1/0.6 rotation phase. On the other hand, in the 2020 plot, the two Fourier curves remain much closer throughout a full rotation. The difference near 0.0/0.5 rotation is almost within the noise in the data.

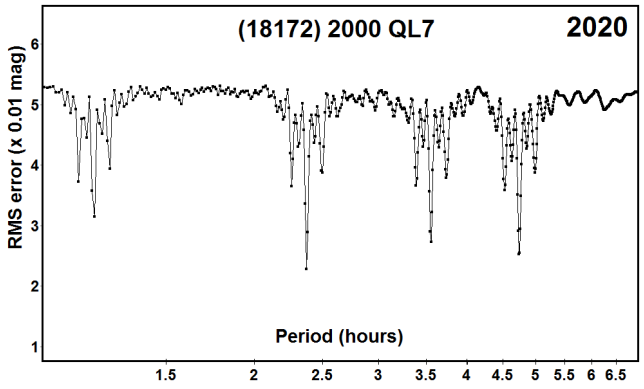


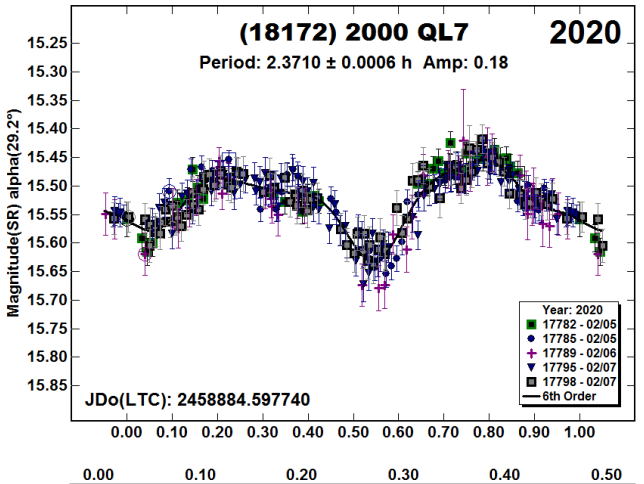


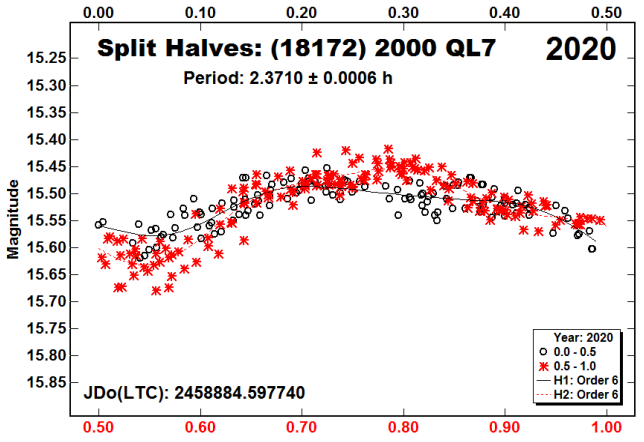


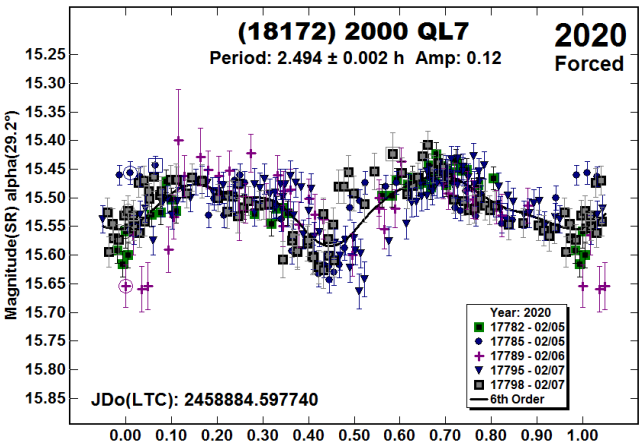


Kluwak (private communications) was able to fit our 2.509 h period to his data, but the fit was visibly worse but the RMS fits differed by only 0.013 mag. Given that his data set has much higher scatter and lower SNR, the visual difference between the two solutions using his data may be more an aesthetic than actual one.

We found two solutions that have a nearly integral ratio. The best solution is "More Data!," i.e., high-quality observations (≤ 0.02 mag) at future apparitions are needed to solve the conundrum. Ideally, they would be part of a campaign involving individual or groups of observers that are well-separated in longitude. This would help solve the problem of the period being nearly commensurate with an Earth day.

(34613) 2000 UR13. The period spectrum showed several, nearly equal fits in the range of 5-12 hours. We chose the longest one since it produced a bimodal lightcurve with the extrema properly spaced. Harris et al. (2014) showed that this is not always the best assumption, so additional observations are required.

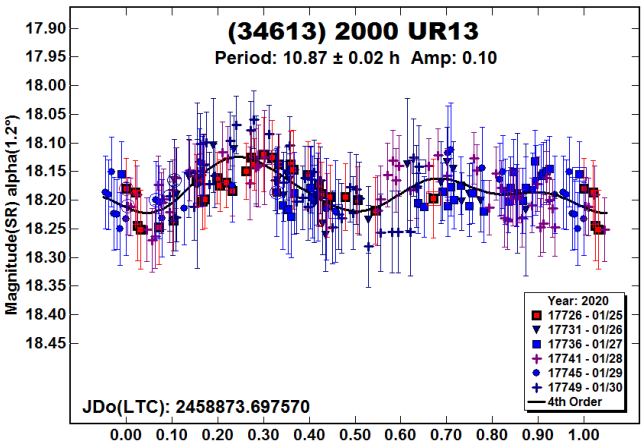


(35107) 1991 VH. Pravec et al. (1997) were first to discover that this is a binary asteroid. Later (Pravec et al., 2006), they found that the asteroid may be a multiple system with periods of 2.6239, 12.836 h, and a satellite orbital period of 32.63 h.

An unprocessed lightcurve with our 2020 data shows a primary period of about 2.62 h and several deviations that bear the traits of *mutual events* (occultations/eclipses) due to main (first) satellite.

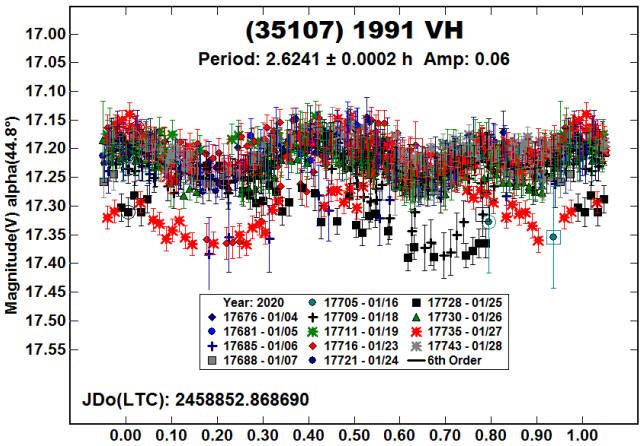

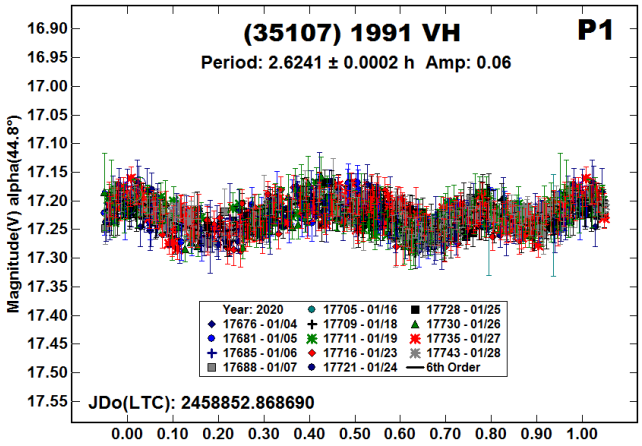


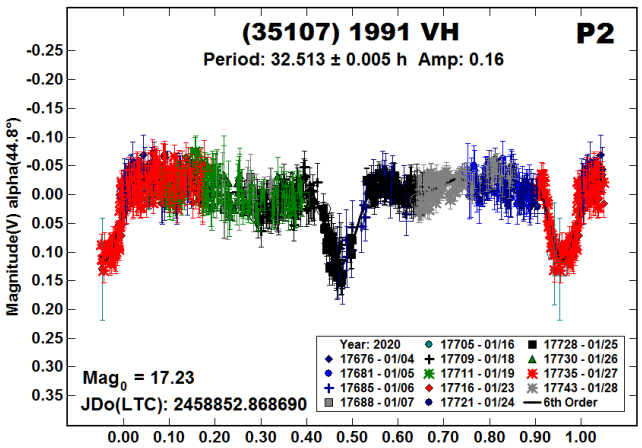


We used the iterative dual-period search in *MPO Canopus* to find the period of the primary, $P_1$ = 2.6241 h, and reveal the mutual events due to the satellite that has an orbital period of $P_2$ = 32.513 h. We did not find any evidence of a third period, though it's possible its lightcurve was hidden within the noise.

(36284) 2000 DM8. Linder et al. (2013) reported a period of 3.848 h. Our result is essentially identical. The original lightcurve showed more scatter than we liked, so we used the dual-period search in *MPO Canopus* to check on the possibility of a satellite: no evidence of such was found. However, using a high-frequency Fourier search created a "noise filter" that produced a better lightcurve and slightly different period.

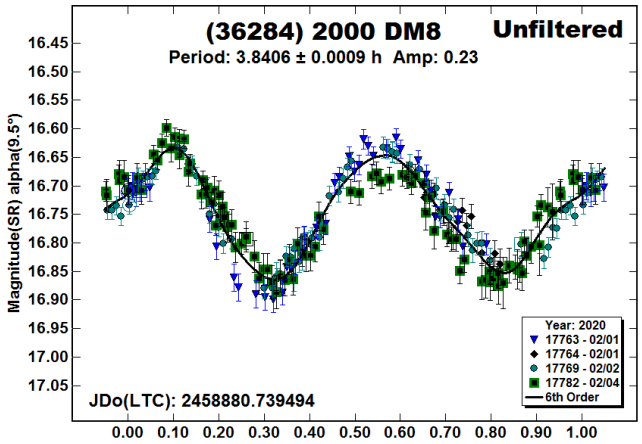


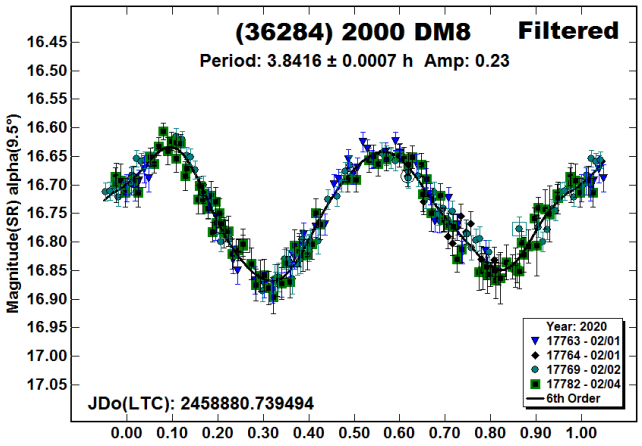


(52768) 1998 OR2. Skiff et al. (2019) found a period of 4.1120 h using data from 2009. Our $P$ = 4.106 h is statistically the same.

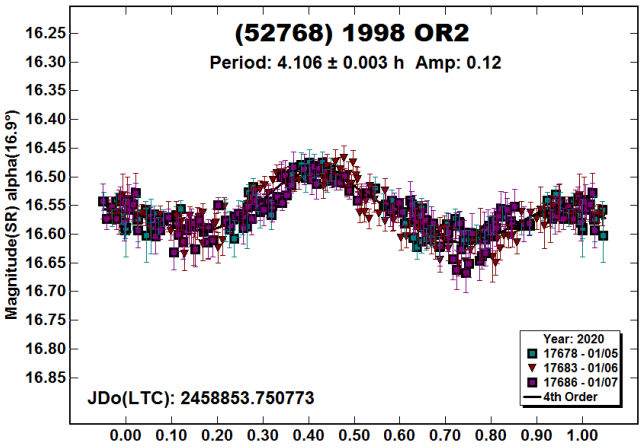


(54686) 2001 DU8. When a data set spans several days or even weeks and there are few times when observing sessions are on consecutive nights, a period search will likely find numerous possible solutions, with several being nearly likely. This is seen in the period spectrum for 2001 DU8 where the observations covered 15 days. There were some contiguous (night-to-night) sessions, but the long breaks between led to the ambiguous results.

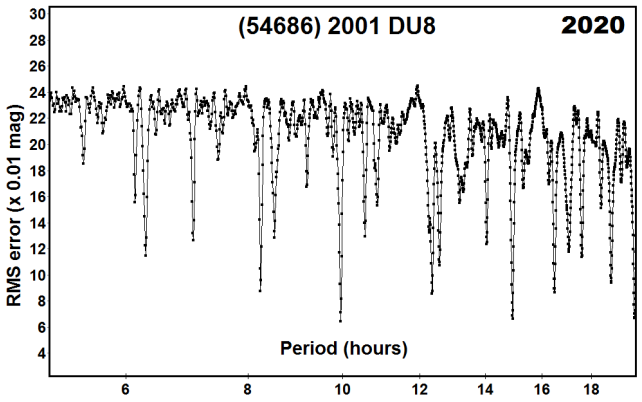


We chose a period of 9.958 h because it gives a nearly symmetrical bimodal lightcurve. The large amplitude at relatively low solar phase angles makes this assumption almost a certainty (Harris et al., 2014).

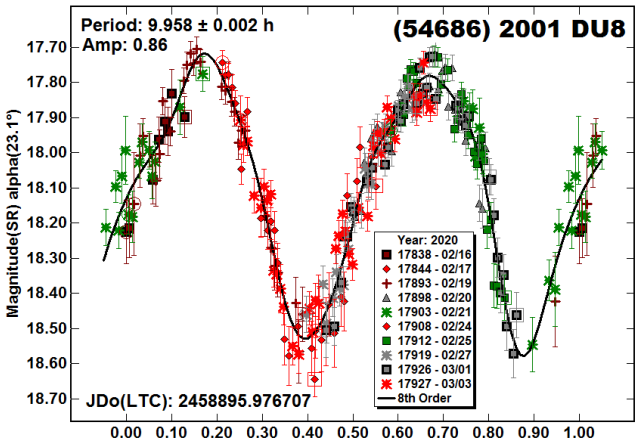


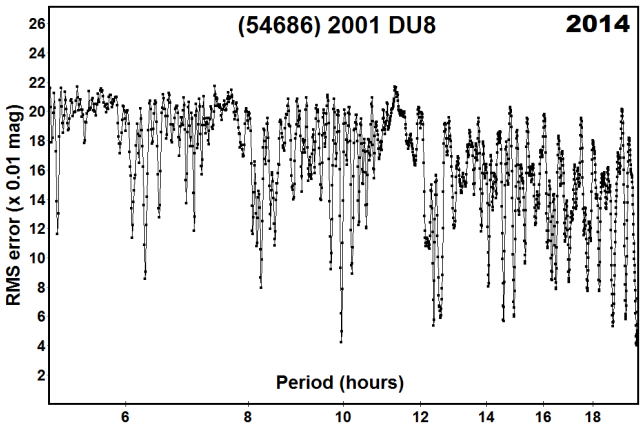


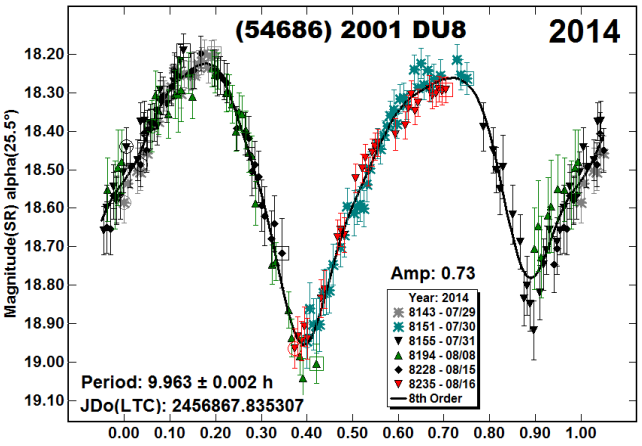


Warner (2015a) found a period of 12.552 h using data from 2014 August. That result has a near integral ratio with the adopted period of 9.958 h. We re-examined the 2014 data after changing the comparison star magnitudes to ATLAS SR. The result was a period of 9.963 h, which is nearly identical to the 2020 result.

(65690) 1991 DG. There were no previous entries in the LCDB for this NEA, which has an estimated diameter of about 500 meters. As we did with (36284) 2000 DM8, we used a high-frequency Fourier noise filter after first checking for signs of a satellite. Given the somewhat noisy data, it was unlikely one could have been found. The plots show that the period and period precision were significantly improved after applying the filter.

After submitting this paper, Petr Pravec (private communications) reported a different, more likely solution of 7.1125 h based on data obtained in 2020 February and March. During the full period through early April for the two observers, the asteroid went through a large phase angle range of about 19 to 75 degrees. As might be expected, the shape and amplitude of the lightcurve changed significantly over that time. In the case of the CS3 data, obtained mostly at large phase angles, the adopted period of 7.1111 h produced a trimodal lightcurve. While unusual, such a curve is not unexpected at large phase angles. No noise filter was applied to the 7.1111 h lightcurve.

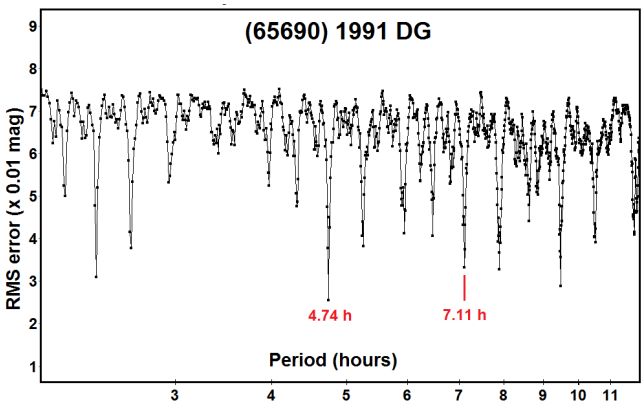


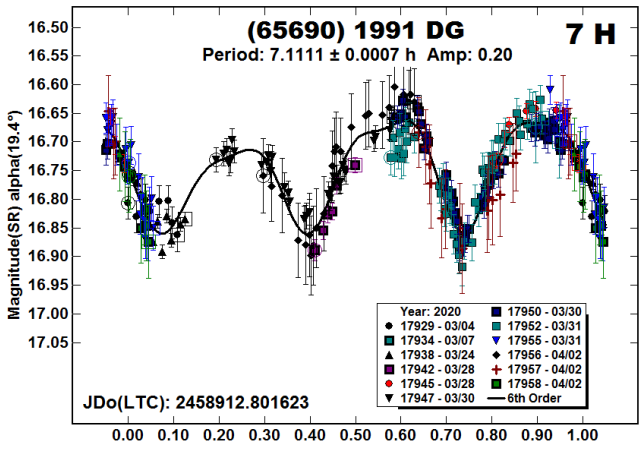


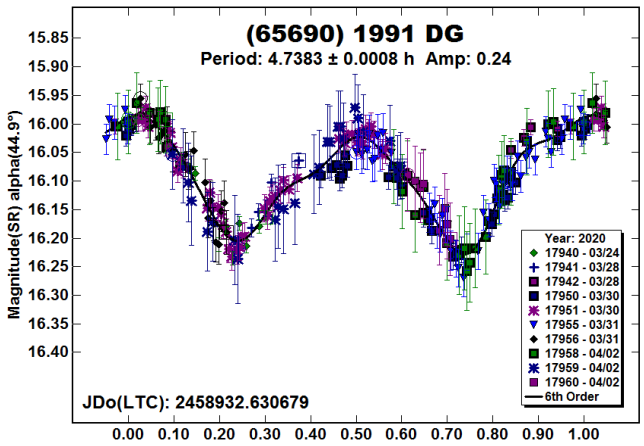


(90075) 2002 VU94. We worked this asteroid at three apparitions: once in 2014 (Warner, 2015c; 7.88 h), twice in 2017 Warner, 2017, 7.878 h; Warner, 2018, 7.879 h), and again in 2020. The results were essentially the same. The 2020 period may be a little longer because the data set doesn't fully cover the lightcurve and so the Fourier analysis found a local minimum RMS value instead of the global minimum.

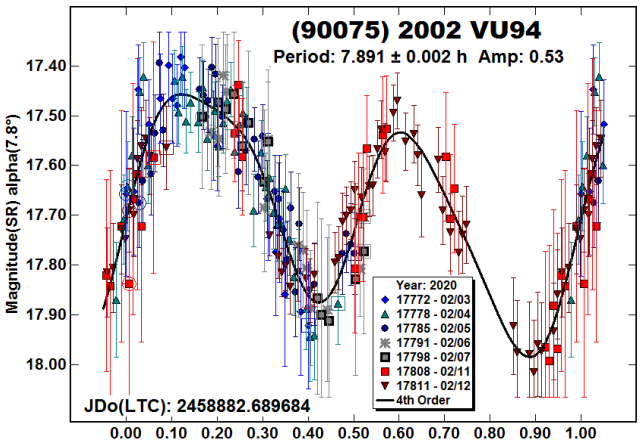


(103067) 1999 XA143. Galad et al. (2005) were apparently the first to report a period (9.8490 h) for 1999 XA143. Warner (2015b) reported 9.85 h based on data from early 2015. Our 2020 result of $P$ = 9.855 h is within the error bars of Galad et al. (2005) and Warner (2015b).

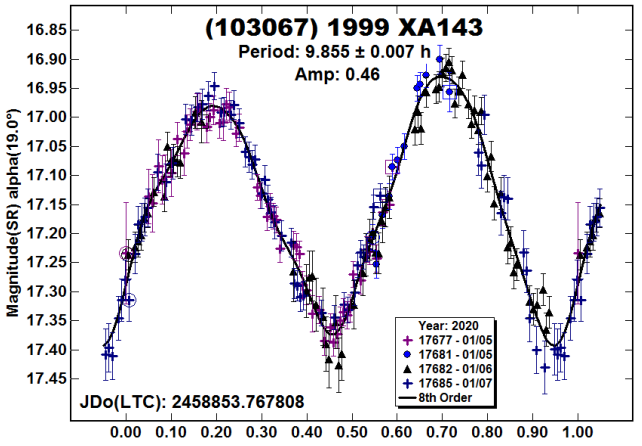


(154993) 2005 EA94. There were no previous period results in the LCDB for this 800-m NEA. Given the noisy data and long spells between some sessions, the period is likely, but not secure.

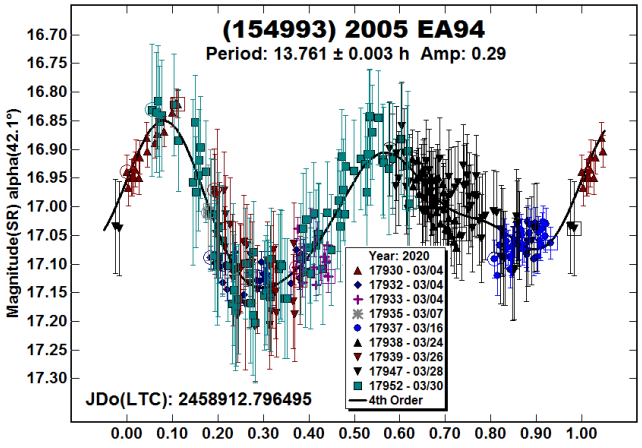


(163373) 2002 PZ39. Pravec et al. (2020web) reported a period of 148.9 h, but it is rated 1+ in the LCDB. The best solution we could find was a long period of 186 h. There were some indications of a second period in the data, so a dual-period search using *MPO Canopus* was run by subtracting the long-period lightcurve from the data. The $P_2$ period spectrum shows some strong possibilities, the most prominent being at 14.35 h.

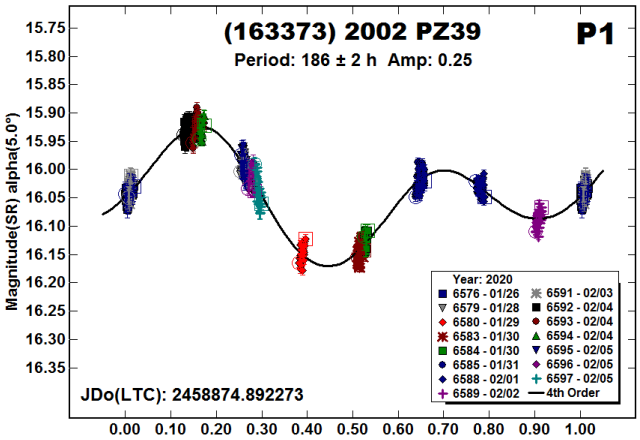


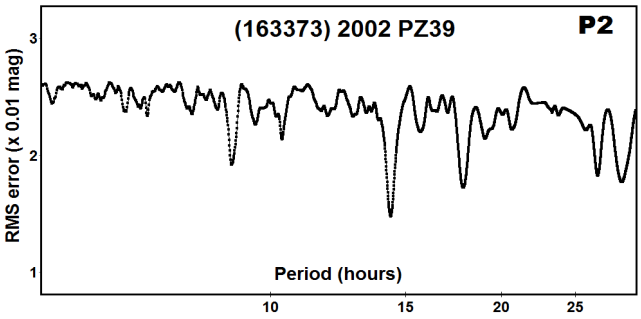


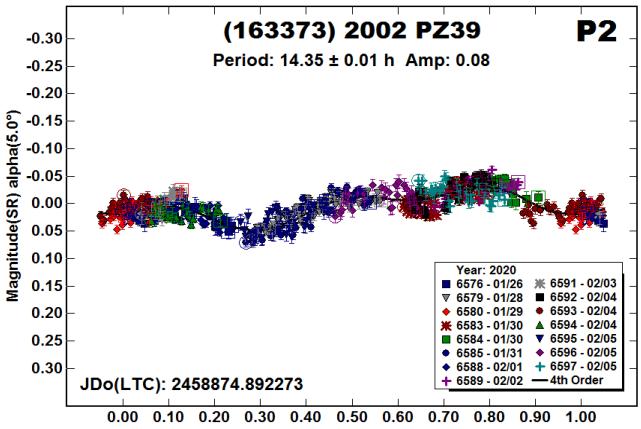


The shape of the $P_2$ lightcurve is asymmetrical and the period, 14.35 h, is almost exactly a 13:1 ratio with the long period. This often means that the Fourier analysis is finding some kind of harmonic of the long period. The asteroid's diameter and long period make it a good candidate for tumbling (see Pravec et al., 2014; 2005), so it's possible that the short period is an indication of low-level tumbling.

(214088) 2004 JN13. Warner (2015b) observed this asteroid in 2014. The data were separated into two sets. Analysis of one set found a reliable period of 6.336 h and 0.20 mag amplitude. The other set produced a less reliable, but still useful, period of 6.33 h and 0.17 mag amplitude. The result from the 2020 data is secure and is in good agreement with the earlier results and Vaduvescu et al. (2017; 6.336 h, 0.30 mag).

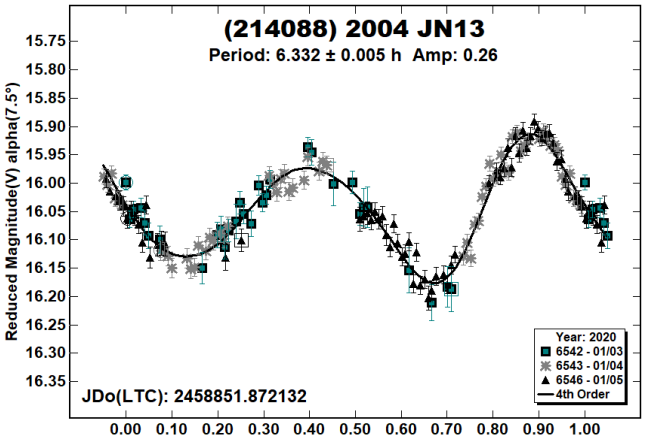


(416591) 2004 LC2, (437316) 2013 OS3, (474223) 2001 CC32. These appear to be the first reported lightcurves for the three NEAs. The estimated diameter of 2004 LC2 is 0.6 km. For 2013 OS3, the estimated diameter is also about 0.6 km while 2013 OS has an estimated diameter of 0.5 km.

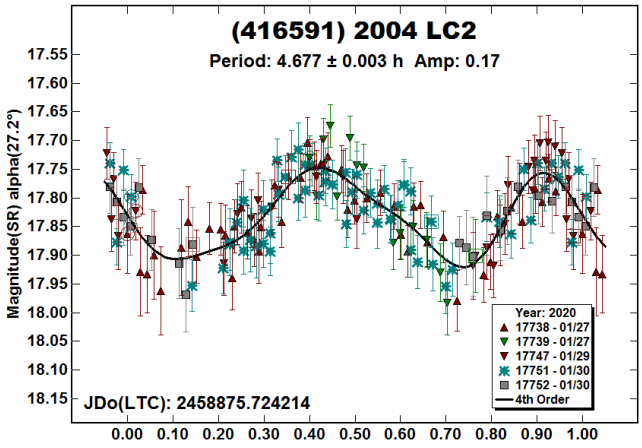


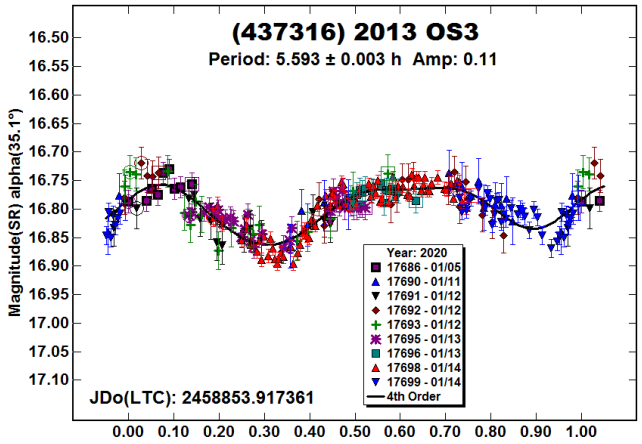


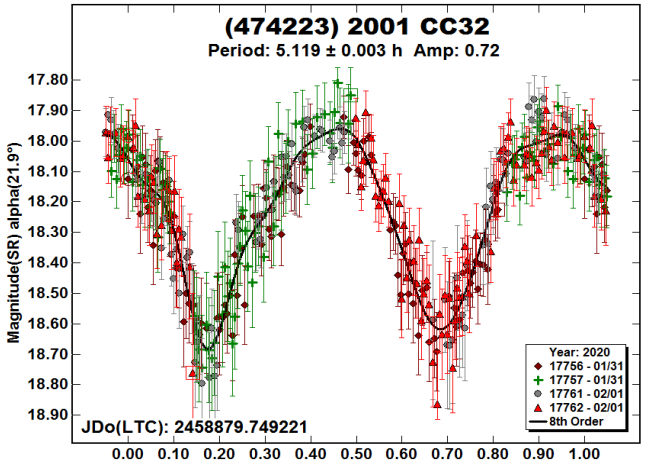


(489486) 2007 GS3. Pravec et al. (2019) were first to discover that this is a binary asteroid. They found a primary period of 3.497 h and satellite orbital period of 41.36 h. Our 2020 data showed no signs of the short period or that the asteroid might be binary. However, our data did lead directly to a period of 41.5 h, which is in good agreement with Pravec et al. (2019).

Their secondary period lightcurve showed attenuations of 0.21 and 0.32 mag, which indicated a satellite-to-primary effective diameter ratio of $Ds/Dp > 0.46$. Assuming the amplitude of our lightcurve can be used to estimate $Ds/Dp$, we found 0.42 ± 0.04.

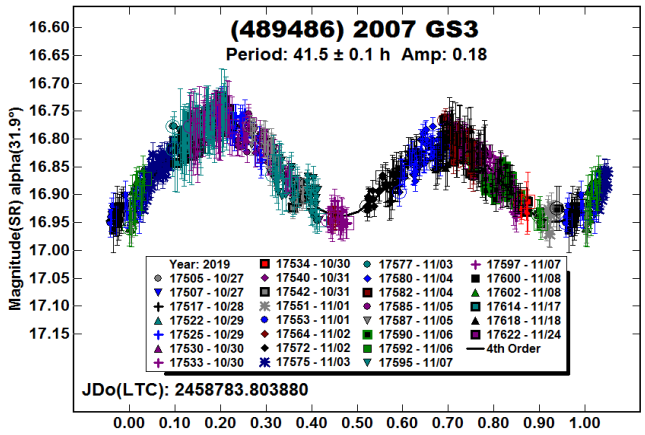


(500094) 2012 BC20. There were no previous entries of any kind in the LCDB for this NEA.

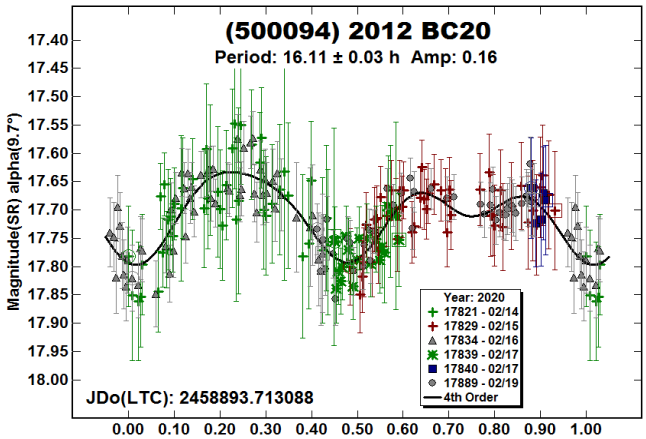

The estimated diameter is 0.54 km. Because of the gap in the data and an amplitude < 0.20 mag, the assumption of a bimodal lightcurve could be wrong (Harris et al, 2014) but no other possible period produced a believable result.

(512245) 2016 AU8. We made observations of 2016 AU8 in 2018 December to 2019 January (Warner and Stephens, 2019a). A period of 4.516 h was found. The latest result is in good agreement.

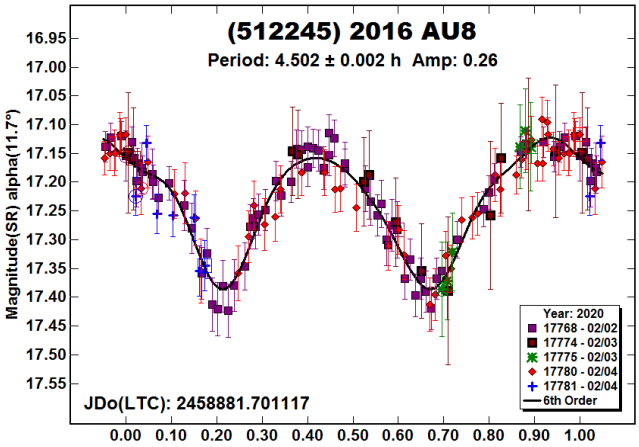


2011 CT4. Pravec et al. (2020web) reported a period 3.930 h that is rated U = 1+ in the LCDB. We didn't fare any better. Looking at the raw data for individual nights showed what appeared to be only noise. Sometimes a very short period is hidden in such data sets and so we extended our period search to go from 0.01 h to 5.5 h in steps that grew geometrically from 0.001 h.

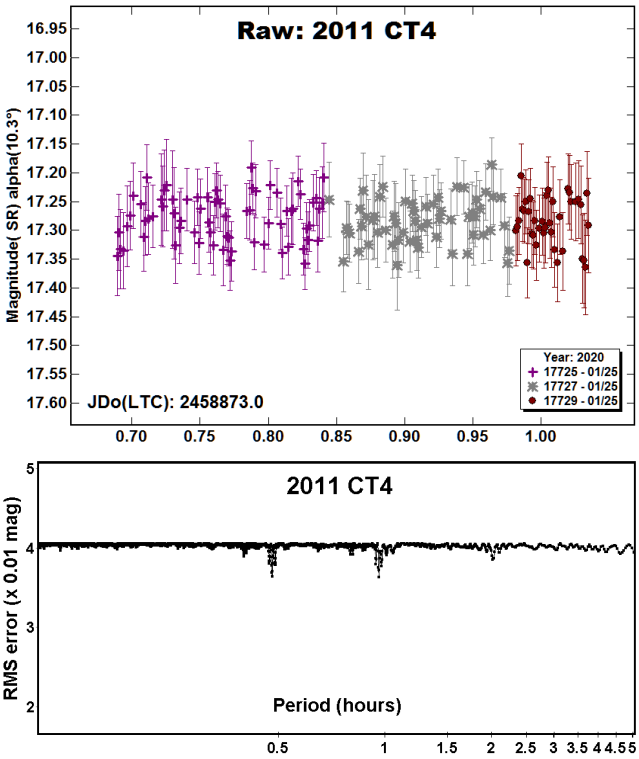


The period spectrum shows two possible candidates. We adopted the bimodal lightcurve with a period of 0.9601 h for this paper. However, the noise in the data is about the same as the lightcurve amplitude, so the solution is far from secure.

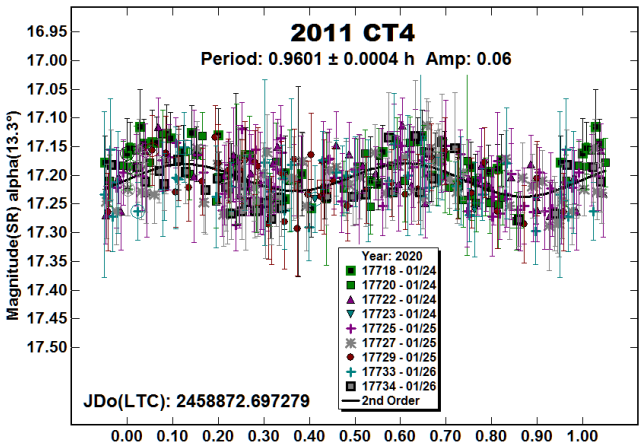


2019 CH. Pravec et al. (2019web) observed 2019 CH in early 2019 March. We observed the asteroid about a month later and originally reported a period of 6.772 h (Warner and Stephens, 2019b). While reviewing previous results for this work, we found the discrepancy and re-examined our 2019 data set.

Before redoing period analysis, comparison star magnitudes were changed to ATLAS SR and all zero-points reset to 0.0. This led to a revised period of 7.881 h and amplitude of 0.68 mag. The period is in closer agreement with Pravec et al. The small difference is probably due to our data not fully covering the lightcurve.

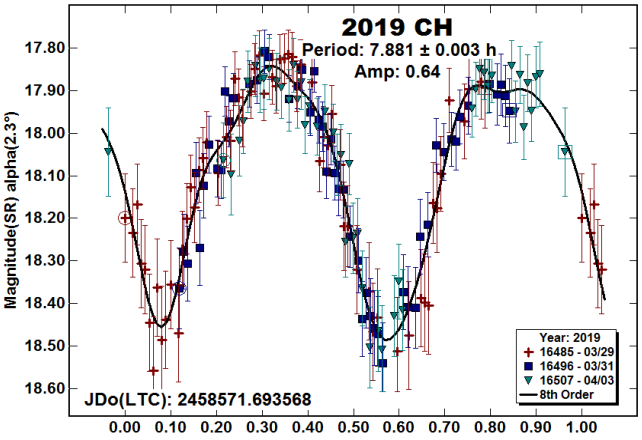


2019 XG1. The period spectrum indicated two likely solutions at about 12 and 24 hours. We adopted the shorter period mostly because of the large gaps in the lightcurve with a period near 24 h.

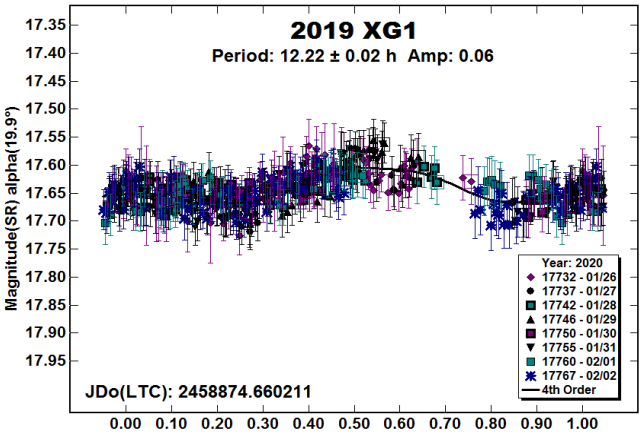

This longer result could easily be attributed to a *fit by exclusion*, which is where the Fourier analysis finds a local minimum by minimizing the number of overlapping data points.

2019 WB6, 2020 DD, 2020 BZ11. There were no previous entries in the LCDB for these three NEAs.

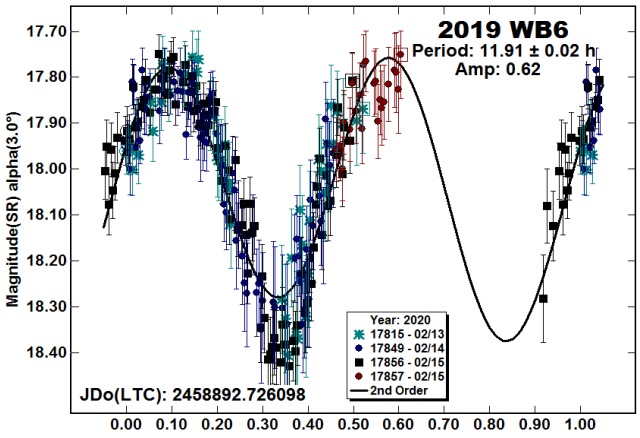


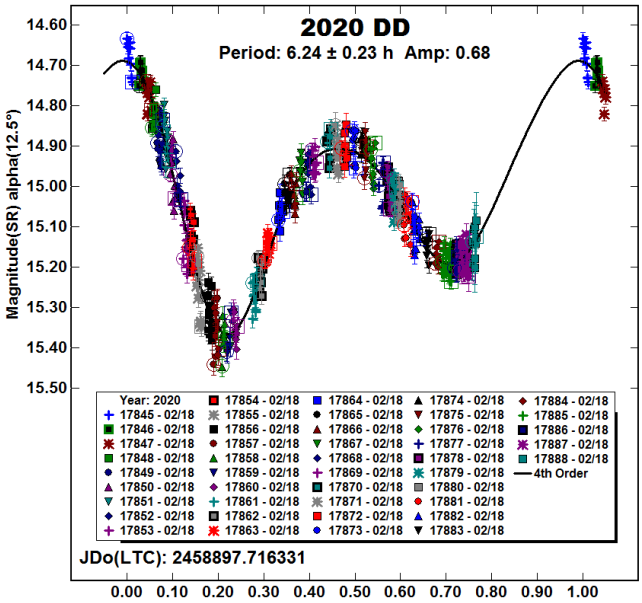


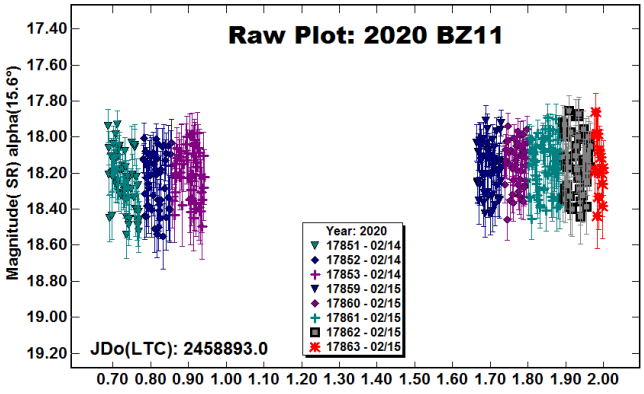


The lightcurves for 2019 WB6 and 2020 DD are incomplete because their periods are nearly commensurate with an Earth day. It would have taken some weeks to fill in the curve for 2019 WB6. It was not possible for 2020 DD since it was within reach of our equipment for only one night.

2020 BZ11 is an example of a campaign that failed. The raw data appeared to be just noise. A search for periods $0.01 < P < 1$ h was made to no avail. We show the data here to put it on the record and note that they are available on the ALCDEF (2020) web site.

Acknowledgements

Funding for observations at CS3 and work on the asteroid lightcurve database (Warner et al., 2009) and ALCDEF database (*alcdef.org*) are supported by NASA grant 80NSSC18K0851. The authors gratefully acknowledge Shoemaker NEO Grants from the Planetary Society (2007, 2013). These were used to purchase some of the telescopes and CCD cameras used in this research. This work includes data from the Asteroid Terrestrial-impact Last Alert System (ATLAS) project. ATLAS is primarily funded to search for near earth asteroids through NASA grants NN12AR55G, 80NSSC18K0284, and 80NSSC18K1575; byproducts of the NEO search include images and catalogs from the survey area. The ATLAS science products have been made possible through the contributions of the University of Hawaii Institute for Astronomy, the Queen's University Belfast, the Space Telescope Science Institute, and the South African Astronomical Observatory.

References

References from web sites should be considered transitory, unless from an agency with a long lifetime expectancy. Sites run by private individuals, even if on an institutional web site, do not necessarily fall into this category.

ALCDEF (2020). Asteroid Lightcurve Data Exchange Format web site. *http://alcdef.org*.

AstDys-2 (2020). Web site.
*https://newton.spacedys.com/astdys2/*

Catalina Sky Survey (2020). Web site.
*https://catalina.lpl.arizona.edu/*

Crowell, J.L.; Howell, E.S.; Magri, C.; Nolan, M.C.; Fernández, Y.R.; Richardson, J.E.; Warner, B.D.; Marshall, S.E.; Springmann, A.; Vervack, R.J. (2017). "Radar and Lightcurve Shape Model of Near-Earth Asteroid (1627) Ivar." *Icarus* **291**, 254-267.

Fornas, G.; Carreño, A.; Arce, E.; Flores, A.; Mas, V.; Rodrigo, O.; Brines, P.; Fornas, A.; Herrero, D.; Lozano, J. (2018). "Seven Near-Earth Asteroids at Asteroids Observers (OBAS) - MMPD: 2017 Jan-May." *Minor Planet Bull*. **45**, 45-47.

Galád, A.; Pravec, P.; Kušnirák, P.; Gajdoš, Š.; Kornoš, L.; Világi, J. (2005). "Joint Lightcurve Observations of 10 Near-Earth Asteroids from Modra and Ondřejov." *Earth Moon, and Planets* **97**, 147-163.

Hanus, J.; Delbo, M.; Durech, J.; Ali-Lagoa, V. (2015). "Thermophysical modeling of asteroids from WISE thermal infrared data - Significance of the shape model and the pole orientation uncertainties." *Icarus* **256**, 101-116.

| Number | Name | 2020 mm/dd | Phase | $L_{PAB}$ | $B_{PAB}$ | Period(h) | P.E. | Amp | A.E. |
|---|---|---|---|---|---|---|---|---|---|
| 1627 | Ivar | 01/15-01/23 | 10.4,6.8 | 137 | 0 | 4.7962 | 0.0004 | 0.26 | 0.02 |
| 1864 | Daedalus | 01/31-02/02 | 14.4,13.7 | 152 | 19 | 8.570 | 0.004 | 0.77 | 0.03 |
| 5626 | Melissabrucker | 02/03-02/20 | *3.3,11.1 | 135 | -4 | 2.48611 | 0.00007 | 0.06 | 0.01 |
| | | 2017/01/30-03/02 | 21.0,6.9 | 175 | 0 | 91.0 | 0.1 | 0.15 | 0.03 |
| | | 2019/12/10-12/19 | 39.8,19.5 | 126 | -6 | 2.4876 | 0.0006 | 0.15 | 0.02 |
| 5693 | 1993 EA | 02/14-02/17 | 9.0,6.9 | 154 | 7 | 2.495 | 0.002 | 0.13 | 0.03 |
| 7088 | Ishtar | 01/28-02/05 | 40.2,36.1 | 170 | 11 | 2.5772 | 0.0004 | 0.18 | 0.03 |
| | Sat. orbital period | | | | | 20.70 | 0.03 | 0.14 | 0.02 |
| 8566 | 1996 EN | 02/16-02/20 | 11.9,10.1 | 155 | -14 | 4.849 | 0.003 | 0.20 | 0.03 |
| 11066 | Sigurd | 02/03-02/06 | 28.1,26.8 | 178 | 5 | 8.500 | 0.003 | 1.18 | 0.05 |
| 11405 | 1999 CV3 | 01/28-01/31 | 26.6,28.1 | 97 | -19 | 6.499 | 0.002 | 0.54 | 0.02 |
| | Pole (λ, β, P) | **(25°, -17°, 6.516509 h)** | (148°, +64°, 6.516561 h) | | | | **a/b: 1.596** | **a/c: 1.745** | |
| 18172 | 2000 QL7 | 02/05-02/07 | 29.2,28.7 | 119 | 20 | 2.3710 | 0.0006 | 0.18 | 0.02 |
| | | 2019/08/24-08/27 | 31.5,31.3 | 14 | 9 | 2.5088 | 0.0008 | 0.15 | 0.02 |
| 34613 | 2000 UR13 | 01/25-01/30 | *1.2,2.6 | 126 | 1 | 10.87 | 0.02 | 0.10 | 0.03 |
| 35107 | 1991 VH | 01/04-01/27 | 44.9,26.2 | 146 | -6 | 2.6241 | 0.0002 | 0.06 | 0.01 |
| | Sat. orbital period | | | | | 32.513 | 0.005 | 0.16 | 0.02 |
| 36284 | 2000 DM8 | 02/01-02/02 | 9.5,8.7 | 143 | 6 | 3.8416 | 0.0007 | 0.23 | 0.02 |
| 52768 | 1998 OR2 | 01/05-01/07 | 17.0,16.2 | 121 | 10 | 4.106 | 0.003 | 0.12 | 0.02 |
| 54686 | 2001 DU8 | 02/16-03/03 | 23.2,12.2 | 176 | 5 | 9.958 | 0.002 | 0.86 | 0.05 |
| | | 2014/07/29-08/16 | 25.5,16.0 | 337 | 14 | 9.963 | 0.002 | 0.73 | 0.05 |
| 65690 | 1991 DG | 03/04-04/02 | 19.4,70.4 | 156 | 1 | 7.1111 | 0.0007 | 0.20 | 0.02 |
| | | | | | | [A]4.7383 | 0.0008 | 0.24 | 0.02 |
| 90075 | 2002 VU94 | 02/03-02/12 | 7.9,10.0 | 134 | -13 | 7.891 | 0.002 | 0.53 | 0.04 |
| 103067 | 1999 XA143 | 01/05-01/07 | 19.1,17.5 | 124 | -3 | 9.855 | 0.007 | 0.46 | 0.03 |
| 154993 | 2005 EA94 | 03/04-03/30 | *42.2,26.7 | 171 | 24 | 13.761 | 0.003 | 0.29 | 0.04 |
| 163373 | 2002 PZ39 | 01/26-02/05 | *5.1,16.1 | 128 | 2 | 186 | 2 | 0.25 | 0.02 |
| | Secondary period | | | | | 14.35 | 0.01 | 0.08 | 0.01 |
| 214088 | 2004 JN13 | 01/03-01/05 | 7.6,6.8 | 108 | 8 | 6.332 | 0.005 | 0.26 | 0.02 |
| 416591 | 2004 LC2 | 01/27-01/30 | 27.2,23.9 | 137 | 20 | 4.677 | 0.003 | 0.17 | 0.03 |
| 437316 | 2013 OS3 | 01/05-01/14 | 35.2,27.5 | 105 | 19 | 5.593 | 0.003 | 0.11 | 0.02 |
| 474223 | 2001 CC32 | 01/31-02/01 | 21.9,21.0 | 149 | -1 | 5.119 | 0.003 | 0.72 | 0.05 |
| 489486 | 2007 GS3 | 2019/10/27-11/24 | *32.1,32.0 | 53 | -10 | 41.5 | 0.1 | 0.18 | 0.03 |
| 500094 | 2012 BC20 | 02/14-02/19 | 9.7,3.6 | 153 | -2 | 16.11 | 0.03 | 0.16 | 0.03 |
| 512245 | 2016 AU8 | 02/02-02/04 | 11.8,11.0 | 138 | -7 | 4.502 | 0.002 | 0.26 | 0.03 |
| | 2011 CT4 | 01/24-01/26 | 13.0,7.4 | 131 | 0 | 0.9601 | 0.0004 | 0.06 | 0.02 |
| | 2019 CH | 03/29-04/03 | 2.3,4.3 | 190 | -2 | 7.881 | 0.003 | 0.64 | 0.04 |
| | 2019 XG1 | 01/27-02/02 | 20.3,23.2 | 127 | 16 | 12.22 | 0.02 | 0.06 | 0.02 |
| | 2019 WB6 | 02/13-02/15 | 3.1,2.4 | 147 | 1 | 11.91 | 0.02 | 0.62 | 0.05 |
| | 2020 DD | 02/18-02/18 | 15.2 | 147 | -8 | 6.24 | 0.23 | 0.68 | 0.05 |
| | 2020 BZ11 | 02/14-02/15 | 16.0,19.5 | 141 | 10 | - | - | - | - |

Table II. Observing circumstances. [A]Alternate period in ambiguous solution. The phase angle (α) is given at the start and end of each date range. If there is an asterisk before the first phase value, the phase angle reached a maximum or minimum during the period. $L_{PAB}$ and $B_{PAB}$ are, respectively the average phase angle bisector longitude and latitude (see Harris et al.,1984). For (11405) 1999 CV3, the preferred pole results are in bold text.


Harris, A.W.; Young, J.W.; Scaltriti, F.; Zappala, V. (1984). "Lightcurves and phase relations of the asteroids 82 Alkmene and 444 Gyptis." *Icarus* **57**, 251-258.

Harris, A.W.; Pravec, P.; Galad, A.; Skiff, B.A.; Warner, B.D.; Vilagi, J.; Gajdos, S.; Carbognani, A.; Hornoch, K.; Kusnirak, P.; Cooney, W.R.; Gross, J.; Terrell, D.; Higgins, D.; Bowell, E.; Koehn, B.W. (2014). "On the maximum amplitude of harmonics on an asteroid lightcurve." *Icarus* **235**, 55-59.

Henden, A.A.; Terrell, D.; Levine, S.E.; Templeton, M.; Smith, T.C.; Welch, D.L. (2009). *http://www.aavso.org/apass*

Kaasalainen, M.; Pravec, P.; Krugly, Y.N.; Šarounová, L.; Torppa, J.; Virtanen, J.; Kaasalainen, S.; Erikson, A.; Nathues, A.; Ďurech, J.; Wolf, M.; Lagerros, J.S.V.; Lindgren, M.; Lagerkvist, C.-I.; Koff, R.; Davies, J.; Mann, R.; Kušnirák, P.; Gaftonyuk, N.M.; Shevchenko, V.G.; Chiorny, V.G.; Belskaya, I.N. (2004). "Photometry and models of eight near-Earth asteroids." *Icarus* **167**, 178-196.

Kluwak, T. (2020). "Rotation Period and Amplitude Determination of (18172) 2000 QL7: A Fast Rotator." *Minor Planet Bull.* **47**, 92-93.

Krugly, Yu.N.; Belskaya, I.N.; Shevchenko, V.G.; Chiorny, V.G.; Velichko, F.P.; Mottola, S.; Erikson, A.; Hahn, G.; Nathues, A.; Neukum, G.; Gaftonyuk, N.M.; Dotto, E. (2002). "The Near-Earth Objects Follow-up Program. IV. CCD Photometry in 1996-1999." *Icarus* **158**, 294-304.

Linder, T.; Sampson, R.; Holmes, R. (2013). "Astronomical Research Institute Photometric Results." *Minor Planet Bull*. **40**, 4-6.

Pravec, P.; Wolf, M.; Sarounova, L. (1995web, 1999web, 2006web, 2019web, 2020web).
*http://www.asu.cas.cz/~ppravec/neo.htm*

Pravec, P.; Wolf, M.; Sarounova, L. (1997). *IAUC* **6607**.

Pravec, P.; Wolf, M.; Sarounova, L. (1998). "Lightcurves of 26 Near-Earth Asteroids." *Icarus* **136**, 124-153.

Pravec, P.; Harris, A.W.; Scheirich, P.; Kušnirák, P.; Šarounová, L.; Hergenrother, C.W.; Mottola, S.; Hicks, M.D.; Masi, G.; Krugly, Yu.N.; Shevchenko, V.G.; Nolan, M.C.; Howell, E.S.; Kaasalainen, M.; Galád, A.; Brown, P.; Degraff, D.R.; Lambert, J.V.; Cooney, W.R.; Foglia, S. (2005). "Tumbling asteroids." *Icarus* **173**, 108-131.

Pravec, P.; Scheirich, P.; Kusnirák, P.; Sarounová, L.; Mottola, S.; Hahn, G.; Brown, P.; Esquerdo, G.; Kaiser, N.; Krzeminski, Z.; and 47 coauthors (2006). "Photometric survey of binary near-Earth asteroids." *Icarus* **181**, 63-93.

Pravec, P.; Scheirich, P.; Durech, J.; Pollock, J.; Kušnirák, P.; Hornoch, K.; Galád, A.; Vokrouhlicky, D.; Harris, A.W.; Jehin, E.; Manfroid, J.; Opitom, C.; Gillon, M.; Colas, F.; Oey, J.; Vrastil, J.; Reichart, D.; Ivarsen, K.; Haislip, J.; LaCluyze, A. (2014). "The tumbling state of (99942) Apophis." *Icarus* **233**, 48-60.

Pravec, P.; Scheirich, P.; Kusnirak, P.; Hornoch, K.; and 45 coauthors (2016). "Binary asteroid population. 3. Secondary rotations and elongations." *Icarus* **267**, 267-295.

Pravec, P.; Kusnirak, P.; Hornoch, K.; Fatka, P.; Kucakova, H. (2019). *CBET* **4701**.

Skiff, B.A.; McLelland, K.P.; Sanborn, J.; Pravec, P.; Koehn, B.W. (2019). "Lowell Observatory Near-Earth Asteroid Photometric Survey (NEAPS): Paper 4." *Minor Planet Bull*. **46**, 458-503.

Thomas, C.A.; Emery, J.P.; Trilling, D.E.; Delbó, M.; Hora, J.L.; Mueller, M. (2014). "Physical characterization of Warm Spitzer-observed near-Earth objects." *Icarus* **228**, 217-246.

Tonry, J.L.; Denneau, L.; Flewelling, H.; Heinze, A.N.; Onken, C.A.; Smartt, S.J.; Stalder, B.; Weiland, H.J.; Wolf, C. (2018a). "The ATLAS All-Sky Stellar Reference Catalog." *Ap. J.* **867**, A105.

Tonry, J.L.; Denneau, L. Heinze, A.N.; Stalder, B.; Smith, K.W.; Smartt, S.J.; Stubbs, C.W.; Weiland, H.J.; Rest, A. (2018b). "ATLAS: A High-cadence All-sky Survey System." *PASP* **130**, 064505.

Vaduvescu, O.; Aznar Macias, A.; Tudor, V.; Predatu, M.; Galád, A.; Gajdoš, Š.; Világi, J.; Stevance, H.F.; Errmann, R.; Unda-Sanzana, E.; Char, F.; Peixinho, N.; Popescu, M.; Sonka, A.; Cornea, R.; Suciu, O.; Toma, R.; Santos-Sanz, P.; Sota, A.; Licandro, J.; Serra-Ricart, M.; Morate, D.; Mocnik, T.; Diaz Alfaro, M.; Lopez-Martinez, F.; McCormac, J.; Humphries, N. (2017). "The EURONEAR Lightcurve Survey of Near-Earth Asteroids." *Earth Moon, and Planets* **120**, 41-100.

Warner, B.D.; Harris, A.W.; Pravec, P. (2009). "The Asteroid Lightcurve Database." *Icarus* **202**, 134-146. Updated 2019 July. *http://www.minorplanet.info/lightcurvedatabase.html*

Warner, B.D. (2013). "Asteroid Lightcurve Analysis at the Palmer Divide Observatory: 2013 January - March." *Minor Planet Bull*. **40**, 137-145.

Warner, B.D. (2014). "Near-Earth Asteroid Lightcurve Analysis at CS3-Palmer Divide Station: 2013 June-September." *Minor Planet Bull*. **41**, 41-47.

Warner, B.D. (2015a). "Near-Earth Asteroid Lightcurve Analysis at CS3-Palmer Divide Station: 2014 June-October." *Minor Planet Bull*. **42**, 41-53.

Warner, B.D. (2015b). "Near-Earth Asteroid Lightcurve Analysis at CS3-Palmer Divide Station: 2014 October-December." *Minor Planet Bull*. **42**, 115-127.

Warner, B.D. (2015c). "Near-Earth Asteroid Lightcurve Analysis at CS3-Palmer Divide Station: 2015 January - March." *Minor Planet Bull*. **42**, 172-183.

Warner, B.D. (2017). "Near-Earth Asteroid Lightcurve Analysis at CS3-Palmer Divide Station: 2016 December thru 2017 April." *Minor Planet Bull*. **44**, 223-237.

Warner, B.D. (2018). "Near-Earth Asteroid Lightcurve Analysis at CS3-Palmer Divide Station: 2017 July through October." *Minor Planet Bull*. **45**, 19-34.

Warner, B.D.; Stephens, R.D. (2019a). "Near-Earth Asteroid Lightcurve Analysis at the Center for Solar System Studies: 2018 September-December." *Minor Planet Bull*. **46**, 144-152.

Warner, B.D.; Stephens, R.D. (2019b). "Near-Earth Asteroid Lightcurve Analysis at the Center for Solar System Studies: 2019 January-April." *Minor Planet Bull*. **46**, 304-314.

Warner, B.D.; Stephens, R.D. (2020a). "Near-Earth Asteroid Lightcurve Analysis at the Center for Solar System Studies: 2019 July-September." *Minor Planet Bull*. **47**, 23-34.

Warner, B.D.; Stephens, R.D. (2020b). "Near-Earth Asteroid Lightcurve Analysis at the Center for Solar System Studies: 2019 September – 2020 January." *Minor Planet Bull*. **47**, 105-120.

# ON TRYING TO FIND COLOR INDICES USING ONLY UNFILTERED OBSERVATIONS

Brian D. Warner
Center for Solar System Studies / MoreData!
446 Sycamore Ave.
Eaton, CO 80615 USA
brian@MinorPlanetObserver.com

(Received: 2020 March 30)

It will be shown why, if using only unfiltered observations, it is not possible to find the true color index of an asteroid without knowing its actual sky (catalog) magnitude, or the reverse, i.e., finding the sky magnitude without knowing the true color index.

A simple and often used method to find the sky magnitude of an asteroid is to use differential photometry and the formula

$$M_a = (m_a - m_c) + M_c \quad (1)$$

where $M_a$ asteroid sky (catalog) magnitude
$m_a$, $m_c$ instrumental magnitude of, respectively, the asteroid and comp star.
$M_c$ comp star sky (catalog) magnitude

To find the magnitude in different colors, the appropriate magnitudes of the comparison stars are used, e.g., B magnitudes to find $B_a$ and V magnitudes to find $V_a$.

Usually, several comp stars are used to overcome a single bad value and/or noise from one or more sources. The mean and standard deviation of the sum of the several $M_a$ values are found and then reported as a single magnitude and its error. However, this faithfully serves only if the color index of the asteroid and every comp star is exactly the same, i.e., the difference in color index is 0.0 for every asteroid/comp pair.

A more complete formula corrects for a color difference between the asteroid and each comp star:

$$M_a = (m_a - m_c) + T_f(\Delta CI) + M_c \quad (2)$$

where $T_f$ transform to convert instrumental to catalog magnitudes for a given color
$\Delta CI$ $CI_a - CI_c$ (CI: color index; e.g., B-V)

Note that a second-order extinction correction is missing. With similar color indices and an air mass (X) ~ 1, it can often, but not always, be ignored. Also note that when using unfiltered observations, the value $(m_a - m_c)$ is constant for a given asteroid/comp pair regardless of the two colors being used.

Eq. 2 has two unknowns: $M_a$ and $CI_a$. Mathematically, there are an infinite number of solutions, i.e., changing one value causes a proportional change in the other. One of the two values *must* be known to find the other but, in most cases, *neither* value is.

In the simplest example, assume that

$$(m_a - m_c) = 0, (CI_a - CI_c) = 0$$

The CI values change depending on the color bands being used, e.g., B-V, V-R, etc., but the *difference* is still 0. This is entirely possible given the infinite number of solutions of Eq. 2.

Therefore, for each session, the average of the several asteroid/comp values is just the average of the comp star sky magnitudes. Changing the zero point of one lightcurve to match the other doesn't find the target CI. Instead, it finds the difference between the two averages of comp star magnitudes.

Figure 1 shows a real-world example using 1600 Vyssotsky, which is an A-type asteroid and so should have a value of B-V ~ 1.0. Here $(m_a - m_c)$ and $(CI_a - CI_c)$ are non-zero and different for each asteroid/comp star pair. However, the net result is the same: the difference between the B and V magnitudes of the asteroid (~0.66 mag) is not the color index of the asteroid but the difference between the average value of the comparison stars in the B and V sessions.

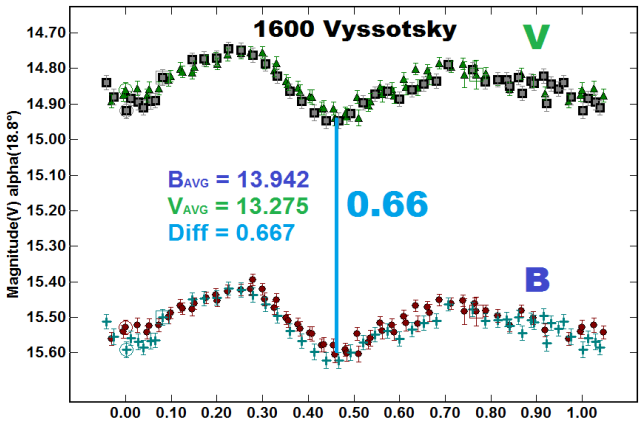


Figure 1: The "AVG" values are the average sky magnitudes of the comp stars in each session. B: blue; V: visual.

Ramirez et al. (2012) give $B\text{-}V_{Sun}$ = 0.653. If using near solar-color comparison stars, the average for the comps in the sessions using B and V magnitudes will never lead to B-V ~ 1.0. Even so, the B-V color index would not be for the asteroid but for the difference in comp star averages.

## Conclusion

To find the actual color index of an asteroid, observations in two colors ("clear" is not a color) *must* be made. In other words, the value $(m_a - m_c)$ must be different from one color to another when measuring the same object and comp star. Only a few observations in two filters are needed to find the true sky magnitude of the asteroid in each color; this leads to a unique color index for the asteroid. See Binzel (2005) or Warner (2016) for detailed steps.

With at least two color indices for an asteroid, e.g., B-V and V-R, it *might be possible* to assign a taxonomic classification, but only in a broad sense, i.e., S but not Sk vs. Sa. The considerations, complications, and cautions using color indices to classify an asteroid are for another time but should *not* be ignored.

## References

Binzel, R.P. (2005). "A simplified method for standard star calibration." *Minor Planet Bull*. **32**, 93-95.

Ramirez, I.; Michel, R.; Sefako, R.; Tucci Maia, M.; Schuster, W.J.; van Wyk, F.; Melendez, J.; Casagrande, L.; Castilho, B.V. (2012). "$UBV(RI)_C$ Colors of the Sun." *Astrophys. J.* **752**, A5.

Warner, B.D. (2016). *A Practical Guide to Lightcurve Photometry and Analysis*. Springer, Geneva. pp. 433.

# PHOTOMETRIC OBSERVATIONS OF MAIN-BELT ASTEROIDS 1755 LORBACH, 4857 ALTGAMIA, AND (48540) 1993 TW8

Stephen M. Brincat
Flarestar Observatory (MPC 171)
Fl.5/B, George Tayar Street,
San Gwann SGN 3160, MALTA
stephenbrincat@gmail.com

Kevin Hills
Tacande Observatory
El Paso, La Palma, SPAIN

Charles Galdies
Znith Observatory
Naxxar, MALTA

(Received: 2020 April 2)

Photometric observations of three main-belt asteroids were made from Malta and Spain in order to determine their synodic rotation periods. For 1755 Lorbach we found a period of 7.973 ± 0.001 h, amplitude 0.45 mag. For 4857 Altgamia the results show a period of 9.034 ± 0.003 h and 0.26 mag. and for (48540) 1993 TW8 we report a period of 25.037± 0.004 h with an amplitude of 0.24 mag.

Photometric observations of asteroids (1755) Lorbach, (4857) Altgamia and (48540) 1993 TW8 were carried out from the three observatories shown in Table I. During the time of observation, a notification to the CALL website was sent in order to notify other observers and avoid any duplication of work (Warner, 2011a).

| Observatory (Location) | Telescope | CCD Sensor | Pixel Scale/ Binning |
|---|---|---|---|
| Flarestar Obs. (San Gwann, Malta) | 0.25-m SCT | Moravian G2 1600/KAF 1603ME | 0.99″ / 1x1 |
| Tacande Observatory (La Palma, Spain) | 0.5-m Optimized Dall Kirkham | FLI ML3200/ KAF3200ME | 0.98″ / 1x1 |
| Znith Obs. (Naxxar, Malta) | 0.2-m SCT | Moravian G2-1600/KAF 1603ME | 1.17″ / 1x1 |

Table I. Observatories and Equipment

The telescopes and cameras located in Malta were controlled remotely via *Sequence Generator Pro* (Main Sequence Software, 2020) while Tacande Observatory was programmed remotely over the internet via *ACP Software* (DC-3 Dreams, 2020). Photometric reduction, lightcurve construction and analyses were derived through *MPO Canopus* software (Warner, 2020). Differential aperture photometry was utilized and photometric measurements were derived through the use of *MPO Canopus (Ver 10.8.1.1)*. Near-solar color comparisons stars were selected through the Comparison Star Selector (CSS) as used by the same software. All measurements were based on the ATLAS catalogue (Tonry et al., 2018) based on R-magnitudes. All images were dark subtracted and flat-fielded.

1755 Lorbach is an outer main-belt asteroid discovered on 1936 November 8 by Laugier, M. at Nice and named in honour of Anne Lorbach Herget, who worked as an assistant at the Cincinnati Observatory. She had been in charge for assigning minor planet provisional designations and had keyed-in almost of all the material in the MPC's early work (Schmadel, 2012). (1755) Lorbach orbit has an eccentricity of 0.047 with a semi-major axis of 3.090 AU. This asteroid rotates around the Sun every 5.43 years. Its absolute magnitude is H = 10.8 with an albedo of 0.140 ± 0.024 and a diameter of about 25 km (JPL, 2020).

A search of the asteroid lightcurve database (LCDB; Warner et al., 2009) did not find any synodic period value reported. Our photometric data for this asteroid, that were obtained over 5 nights from Flarestar Observatory, have been acquired on 2020 February 7, 8, 15, 20 and 22. With a total of 222 data points, we obtained a lightcurve and determined a rotation period of 7.973 ± 0.001 h with an amplitude of 0.45 ± 0.03 mag.

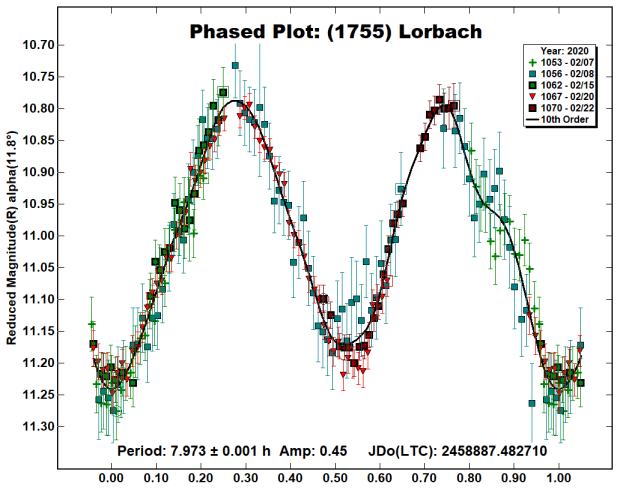


4857 Altgamia belongs to the Phocaea (PHO) asteroid family and resides within the main-belt asteroid region. Discovered on 1984 March 29 by C.S. Shoemaker at Palomar, this asteroid was named after Andrew L.T. and Angela Maria Chiarappa Green, son and wife of D.W.E. Green who took an active role for the discovery of this minor planet by taking the discovery films and its identification on the photographic plates (Schmadel, 2012).

Asteroid Altgamia's orbit has a semi-major axis of 2.357 AU, eccentricity of 0.228 and orbital period of 3.62 years (JPL, 2020). The JPL Small-Bodies Database Browser lists the diameter of this asteroid as 6.19 ± 0.07 km based on an absolute magnitude (H) of 13.2 (JPL, 2020).

This asteroid was observed from 2020 February 7 to 15. Observations have been obtained from Znith Observatory, Malta over 4 nights. The phased lightcurve comprises 253 data points. Based on this data, we determined the synodic period of (4857) Altgamia as 9.034 ± 0.003 h with an amplitude of 0.26 ± 0.05 mag. No published period was found on the LCDB database.

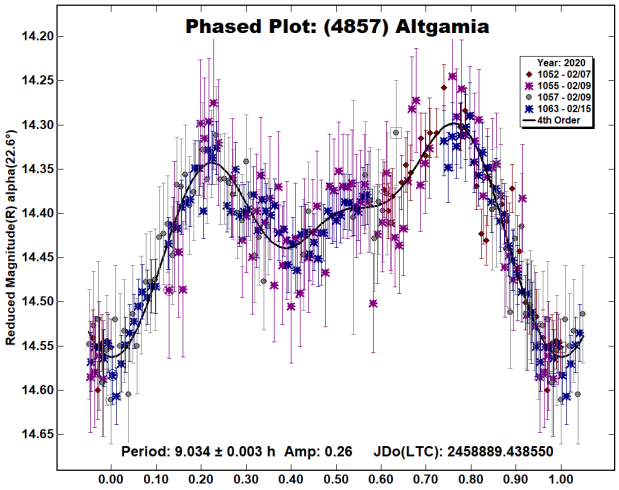


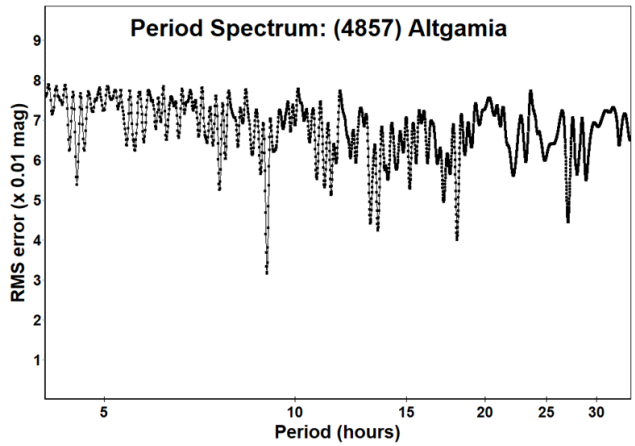


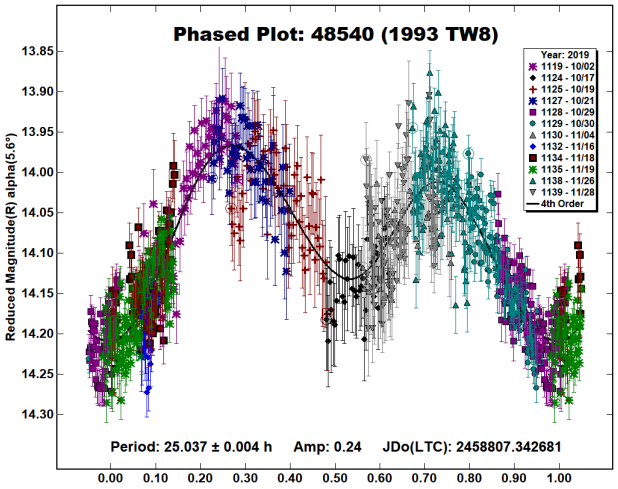


(48540) 1993 TW8 is a main-belt asteroid that was discovered on 1993 October 11 by Spacewatch at Kitt Peak. The asteroid orbits the sun with a semi-major axis of 2.664 AU, eccentricity 0. 254, and orbital period of 4.35 years (JPL, 2020). The JPL Small-Bodies Database Browser lists the diameter of this asteroid as 6.0 ± 0.1 km based on an absolute magnitude (H) of 13.9 (JPL, 2020).

This asteroid was observed from 2019 October 02 to November 28. Observations have been obtained from Flarestar Observatory and Tacande Observatory where each observatory contributed 6 nights. We have gathered 887 data points to generate the lightcurve of this asteroid. We determine the synodic period of (48540) 1993 TW8 as 25.037 ± 0.004 h with an amplitude of 0.24 ± 0.05 mag. No published period was found on the LCDB database.

Acknowledgements

We would like to thank Brian Warner for his work in the development of MPO Canopus and for his efforts in maintaining the CALL website. This research has made use of the JPL's Small-Body Database and the CALL website and the Minorplanet.info website (Warner, 2011b). This work has made use of data from the Asteroid Terrestrial-impact Last Alert System (ATLAS) project. ATLAS is primarily funded to search for near earth asteroids through NASA grants NN12AR55G, 80NSSC18K0284, and 80NSSC18K1575. Byproducts of the NEO search include images and catalogs from the survey area. The ATLAS science products have been made possible through the contributions of the University of Hawaii Institute for Astronomy, the Queen's University Belfast, the Space Telescope Science Institute, and the South African Astronomical Observatory.

References

DC-3 Dreams (2020). ACP Observatory Control Software. *http://acp.dc3.com/index2.html*. Last accessed on 2020 March 24.

Harris, A.W.; Young, J.W.; Scaltriti, F.; Zappala, V. (1984). "Lightcurve and phase relations of the asteroids 82 Alkmene and 444 Gyptis." *Icarus* **57**, 251-258.

JPL (2020). Small-Body Database Browser - JPL Solar System Dynamics web site. *http://ssd.jpl.nasa.gov/sbdb.cgi.* Last accessed: 2020 February 25.

Main Sequence Software (2020). Sequence Generator Pro – SGP. *http://mainsequencesoftware.com/Products/SGPro*. Last accessed on 2020 March 6.

| Number | Name | yyyy mm/dd | Phase | $L_{PAB}$ | $B_{PAB}$ | Period(h) | P.E. | Amp | A.E. | Grp |
|---|---|---|---|---|---|---|---|---|---|---|
| 1755 | Lorbach | 2020 02/07-02/22 | 12.1, 7.2 | 171 | 2.0 | 7.973 | 0.001 | 0.45 | 0.03 | MB-O |
| 4857 | Altgamia | 2020 02/07-02/16 | 22.7,21.7 | 50 | 33.3 | 9.034 | 0.003 | 0.26 | 0.05 | PHO |
| 48540 | 1993 TW8 | 2019 10/02-11/28 | 5.6,23.1 | 020 | 2.1 | 25.037 | 0.004 | 0.24 | 0.05 | MB-M |

Table II. Observing circumstances and results. The phase angle is given for the first and last date. If preceded by an asterisk, the phase angle reached an extrema during the period. $L_{PAB}$ and $B_{PAB}$ are the approximate phase angle bisector longitude/latitude at mid-date range (see Harris et al., 1984). Grp is the asteroid family/group (Warner et al., 2009).

Schmadel, L.D. (2012). *Dictionary of Minor Planet Names*. p. 135. Springer.

Tonry, J.L.; Denneau, L.; Flewelling, H.; Heinze, A.N.; Onken, C.A.; Smartt, S.J.; Stalder, B.; Weiland, H.J.; Wolf, C. (2018). "The ATLAS All-Sky Stellar Reference Catalog." *Astrophys. J.* **867**, A105.

Warner, B.D.; Harris, A.W.; Pravec, P. (2009). "The Asteroid Lightcurve Database." *Icarus* **202**, 134-146. Updated 2016 Sep. *http://www.minorplanet.info/lightcurvedatabase.html*

Warner, B.D. (2011a). Collaborative Asteroid Lightcurve Link website. *http://www.minorplanet.info/call.html*

Warner, B.D. (2011b). Minorplanet.info. *http://www.minorplanet.info/PHP/generateOneAsteroidInfo.php*. Last accessed on 2019 August 8.

Warner, B.D. (2020). MPO Software, MPO Canopus version10.8.1.1 Bdw Publishing. *http://www.minorplanetobserver.com/*

## GENERAL REPORT OF POSITION OBSERVATIONS BY THE ALPO MINOR PLANETS SECTION FOR THE YEAR 2019

Frederick Pilcher
4438 Organ Mesa Loop
Las Cruces, NM 88011 USA
fpilcher35@gmail.com

Observations of positions of minor planets by members of the Minor Planets Section in calendar year 2019 are summarized.

During the year 2019 a total of 2197 observations of 519 different minor planets were reported by members of the Minor Planets Section. Of these, 1892 are approximate visual positions denoted V, and 305 are CCD images denoted C not measured at the time of writing.

The summary lists minor planets in numerical order, the observer and telescope aperture (in cm), UT dates of the observations, and the total number of observations in that interval. When a significant departure from the predicted magnitude was noted, it is stated in the next line below the number of positions. The year is 2019 in each case.

Positional observations were contributed by the following observers:

| Observer, Instrument | Location | Planets | Positions |
|---|---|---|---|
| Faure, Gerard | Col d'Arlezier, | 16 | 52V |
| 9 cm Celestron | Bora Bora, Polynesia | | |
| 20 cm Celestron, 20 cm Newtonian, 25 cm Dobson | Vaison la romaine, France | | |
| 35 cm Meade LX200 | Col de L'Arzelier, France | | |
| Harvey, G. Roger | Concord, North | 468 | 1548V |
| 81 cm Newtonian, | Carolina, USA | | |
| 30 cm Celestron SC at Wildacres, NC USA | | | |
| Pryal, Jim | Ellensburg, WA USA | 9 | 26V |
| 20 cm f/10 SCT | | | |
| Rayon, Jean-Michel | Meylan and | 9 | 5V, 305C |
| 25 cm Quattro | Vaison la romaine, France | | |
| Sony A6000 CCD | | | |
| Werner, Robert | Pasadena, CA USA | 35 | 261V |
| 20 cm Celestron | | | |

CCD observations are labeled C; all others are visual)

| MINOR PLANET | OBSERVER & APERTURE (cm) | OBSERVING PERIOD (2019) | NO. OBS. |
|---|---|---|---|
| 1 Ceres | Werner, 20 | Jul 21-Aug 2 | 6 |
| 2 Pallas | Werner, 20 | Jul 21-Aug 25 | 10 |
| 3 Juno | Werner, 20 | Mar 31-Apr 13 | 3 |
| 6 Hebe | Werner, 20 | Mar 30-Apr 13 | 4 |
| 8 Flora | Faure, 9 | May 8 | 2 |
| | Werner, 20 | May 28-Aug 2 | 13 |
| 9 Metis | Werner, 20 | Dec 16-20 | 2 |
| 11 Parthenope | Faure, 9 | May 8 | 2 |
| | Werner, 20 | May 29-Aug 1 | 9 |
| 16 Psyche | Pryal, 20 | Aug 2-3 | 2 |
| | Werner, 20 | Aug 1-Oct 30 | 31 |
| 18 Melpomene | Werner, 20 | Aug 22-30 | 5 |
| 19 Fortuna | Werner, 20 | May 29-Jun 9 | 3 |
| 20 Massalia | Faure, 9 | May 8 | 2 |
| | Werner, 20 | Jul 21-27 | 3 |
| 21 Lutetia | Werner, 20 | Nov 25-Dec 20 | 3 |
| 24 Themis | Werner, 20 | Jan 25-26 | 2 |
| 29 Amphitrite | Werner, 20 | Oct 21-Nov 2 | 10 |
| 36 Atalante | Werner, 20 | Sep 22-Nov 2 | 20 |

| MINOR | PLANET | OBSERVER & APERTURE (cm) | OBSERVING PERIOD (2019) | NO. OBS. |
|---|---|---|---|---|
| 39 | Laetitia | Pryal, 20 | Aug 2-3 | 2 |
| | | Werner, 20 | Aug 25-Sep 4 | 5 |
| 44 | Nysa | Werner, 20 | May 5-Jun 9 | 7 |
| 45 | Eugenia | Werner, 20 | Aug 1-2 | 2 |
| 51 | Nemausa | Pryal, 20 | Aug 2-3 | 2 |
| | | Werner, 20 | Aug 1-2 | 2 |
| 52 | Europa | Werner, 20 | Oct 21-Nov 2 | 7 |
| 54 | Alexandra | Werner, 20 | Oct 18-Nov 2 | 11 |
| 75 | Eurydike | Pryal, 20 | Aug 2-3 | 2 |
| 130 | Elektra | Werner, 20 | Sep 18-Oct 5 | 8 |
| 135 | Hertha | Werner, 20 | Sep 18-Nov 2 | 25 |
| 216 | Kleopatra | Werner, 20 | Jan 25-26 | 2 |
| 245 | Vera | Pryal, 20 | Sep 2-3 | 3 |
| 247 | Eukrate | Werner, 20 | Sep 22-Nov 25 | 21 |
| 287 | Nephthys | Pryal, 20 | Sep 2-3 | 3 |
| | | Werner, 20 | Sep 18-19 | 2 |
| 304 | Olga | Pryal, 20 | Sep 2-3 | 3 |
| 324 | Bamberga | Werner, 20 | Jan 25-26 | 2 |
| 349 | Dembowska | Werner, 20 | May 25-31 | 4 |
| 405 | Thia | Werner, 20 | May 25-Jun 8 | 4 |
| 410 | Chloris | Werner, 20 | Jul 22-Aug 2 | 5 |
| 433 | Eros | Pryal, 20 | Jan 29 | 3 |
| | | Werner, 20 | Jan 2-Apr 13 | 13 |
| 532 | Herculina | Werner, 20 | May 25-Jun | 8 |
| 607 | Jenny | Harvey, 81 | Jan 10-11 | 6 |
| 675 | Ludmilla | Werner, 20 | Dec 16-20 | 2 |
| 704 | Interamnia | Werner, 20 | Jan 25-Mar 31 | 3 |
| 776 | Berbericia | Werner, 20 | Jan 2-5 | 4 |
| 914 | Palisana | Pryal, 20 | Jul 4-9 | 6 |
| 1035 | Amata | Faure, 35 | Oct 26 | 2 |
| 1061 | Paeonia | Faure, 35 | Oct 26 | 2 |
| 1066 | Lobelia | Faure, 35 | Sep 28 | 2 |
| 1272 | Gefion | Harvey, 81 | Aug 29 | 3 |
| 1598 | Paloque | Harvey, 81 | Sep 4 | 3 |
| 1868 | Thersites | Harvey, 81 | Jul 30 | 3 |
| 1923 | Osiris | Harvey, 81 | Feb 25 | 3 |
| 1941 | Wild | Faure, 35 | Oct 27 | 2 |
| 2008 | Konstitutsiya | Faure, 35 | Sep 29 | 2 |
| | | Rayon, 25 | Sep 19-30 | 40C |
| 2059 | Baboquivari | Faure, 35 | Sep 28 | 5 |
| | | Rayon, 25 | Sep 30 | 20C |
| 2205 | Glinka | Harvey, 81 | Jul 2 | 3 |
| 2223 | Sarpedon | Harvey, 81 | Apr 28 | 3 |
| 2267 | Agassiz | Harvey, 81 | Feb 28 | 6 |
| 2318 | Lubarsky | Harvey, 81 | Jan 9 | 3 |
| 2499 | Brunk | Harvey, 81 | Apr 11 | 3 |
| 2548 | Lelior | Harvey, 81 | Aug 30 | 3 |
| 2628 | Kopal | Harvey, 81 | Aug 31 | 3 |
| 2629 | Rudra | Harvey, 91 | Aug 29 | 3 |
| 2640 | Hallstrom | Harvey, 81 | Mar 28 | 3 |
| 2735 | Ellen | Harvey, 81 | Feb 14 | 3 |
| 2767 | Takenouchi | Harvey, 81 | Nov 2 | 3 |
| 2867 | Steins | Harvey, 81 | Apr 23 | 3 |
| 2918 | Salazar | Harvey, 81 | Sep 3 | 3 |
| 2990 | Trimberger | Harvey, 81 | Mar 6 | 3 |
| 3079 | Schiller | Harvey, 81 | Jan 25 | 3 |
| 3095 | Omarkhayyam | Harvey, 81 | Sep 7 | 3 |
| 3108 | Lyubov | Harvey, 81 | Dec 29 | 3 |
| 3131 | Mason-Dixon | Harvey, 81 | Aug 31 | 3 |
| 3180 | Morgan | Harvey, 81 | Dec 25 | 3 |
| 3219 | Komaki | Harvey, 81 | Feb 14 | 3 |
| 3286 | Anatoliya | Harvey, 81 | Apr 11 | 3 |
| 3302 | Schliemann | Harvey, 81 | Aug 30 | 3 |
| | | | | 0.5f@15.7 |
| 3313 | Mendel | Harvey, 81 | Mar 7 | 3 |
| 3331 | Kvistabeerg | Harvey, 81 | Mar 7 | 3 |
| 3359 | Purcari | Harvey, 81 | Dec 19 | 3 |
| 3393 | Stur | Harvey, 81 | Mar 6 | 3 |
| 3427 | Szentmartoni | Harvey, 81 | Sep 22 | 3 |
| 3487 | Edgeworth | Harvey, 81 | Apr 16 | 3 |
| 3524 | Schulz | Harvey, 81 | Mar 13 | 3 |
| 3539 | Weimar | Harvey, 81 | Apr 3 | 3 |
| 3579 | Rockholt | Harvey, 81 | Apr 3 | 3 |
| 3621 | Curtis | Harvey, 81 | Sep 22 | 3 |
| 3623 | Chaplin | Harvey, 81 | Aug 31 | 3 |
| 3658 | Feldman | Harvey, 81 | Jan 6 | 3 |
| 3709 | Polypoites | Harvey, 81 | Aug 10 | 3 |
| 3743 | Pauljaniczek | Harvey, 81 | Mar 27 | 3 |
| 3796 | Lene | Harvey, 81 | Feb 4 | 3 |
| 3818 | Gorlitza | Harvey, 81 | Aug 30 | 3 |
| 3822 | Segovia | Harvey, 81 | May 7 | 3 |
| 3836 | Lem | Harvey, 81 | Sep 7 | 3 |
| | | | | 0.3f@16.1 |
| 3847 | Sindel | Harvey, 81 | Dec 2 | 3 |
| 3853 | Haas | Harvey, 81 | Dec 31 | 3 |
| 3874 | Stuart | Harvey, 81 | Feb 25 | 3 |
| 3912 | Troja | Harvey, 81 | Jan 9 | 3 |
| 3939 | Huruhata | Harvey, 81 | Mar 28 | 3 |
| 3948 | Bohr | Harvey, 81 | Aug 30 | 3 |
| 3952 | Russelmarks | Harvey, 81 | Feb 25 | 3 |
| | | | | 0.4b@15.9 |
| 3975 | Verdi | Harvey, 81 | Feb 14 | 3 |
| 4021 | Dancey | Harvey, 81 | Sep 22 | 3 |
| | | | | 0.5f@15.5 |
| 4037 | Ikeya | Harvey, 81 | Jan 26 | 3 |
| 4047 | Chang'E | Harvey, 81 | Sep 21 | 3 |
| | | | | 0.4f@16.1 |
| 4118 | Sveta | Harvey, 81 | Nov 3 | 3 |
| 4122 | Ferrari | Harvey, 81 | Aug 30 | 3 |
| 4143 | Huziak | Harvey, 81 | Aug 31 | 3 |
| 4165 | Didkovskij | Harvey, 81 | Sep 7 | 3 |
| 4191 | Assesee | Harvey, 81 | Jul 30 | 3 |
| 4205 | Davidhughes | Harvey, 81 | Dec 16 | 6 |
| 4219 | Nakamura | Harvey, 81 | Feb 25 | 3 |
| 4221 | Picasso | Faure, 35 | Sep 28-29 | 2 |
| | | Rayon, 25 | Sep 19-30 | 40C |
| 4235 | Tatishschev | Harvey, 81 | Oct 3 | 3 |
| 4327 | Ries | Harvey, 81 | May 2 | 3 |
| 4366 | Venikagan | Harvey, 81 | Jan 9 | 3 |
| 4383 | Suruga | Harvey, 81 | Nov 3 | 3 |
| 4387 | Tanaka | Harvey, 81 | Nov 6 | 3 |
| 4407 | Taihaku | Harvey, 81 | Sep 22 | 3 |
| 4422 | Jarre | Faure, 20 | Sep 8 | 2 |
| | | Rayon, 25 | Sep 8-19 | 40C |
| 4425 | Bilk | Harvey, 81 | Feb 1 | 3 |
| 4434 | Nikulin | Harvey, 81 | Aug 31 | 3 |
| | | | | 0.5f@15.8 |
| 4442 | Garcia | Harvey, 81 | Feb 4 | 3 |
| 4445 | Jimstratton | Harvey, 81 | Aug 30 | 3 |
| 4459 | Nusamaibashi | Harvey, 81 | Nov 2 | 3 |
| 4465 | Rodita | Harvey, 81 | Dec 25 | 3 |
| 4488 | Tokitada | Harvey, 81 | Aug 31 | 3 |
| | | | | 0.5f@16.2 |
| 4553 | Doncampbell | Harvey, 81 | Mar 13 | 3 |
| 4554 | Fanynka | Harvey, 81 | Jul 30 | 3 |
| 4594 | Dashkova | Harvey, 81 | Jun 21 | 3 |
| 4604 | Stekarstrom | Harvey, 81 | Sep 7 | 3 |
| 4621 | Tambov | Harvey, 81 | May 14 | 3 |
| 4643 | Cisneros | Harvey, 81 | Sep 3 | 3 |
| 4647 | Syuji | Harvey, 81 | Jul 2 | 3 |
| 4686 | Maisica | Harvey, 81 | Sep 21 | 3 |
| 4689 | Donn | Harvey, 81 | Jan 6 | 3 |
| 4702 | Berounka | Harvey, 81 | Feb 4 | 3 |
| 4743 | Kikuchi | Harvey, 81 | Apr 28 | 3 |
| 4750 | Mukai | Harvey, 81 | Dec 31 | 3 |
| 4784 | Samcarin | Harvey, 81 | Feb 25 | 3 |
| 4795 | Kihara | Harvey, 81 | Jun 21 | 3 |
| 4821 | Bainucci | Harvey, 81 | Jan 27 | 3 |
| 4831 | Baldwin | Harvey, 81 | Mar 27 | 3 |
| 4840 | Otaynang | Harvey, 81 | Jan 11 | 3 |
| 4849 | Ardenne | Harvey, 81 | Nov 26 | 3 |
| 4852 | Pamjones | Harvey, 81 | May 7 | 3 |
| 4923 | Clarke | Harvey, 81 | May 7 | 3 |
| 4974 | Elford | Harvey, 81 | Mar 28 | 3 |
| 4982 | Bartini | Harvey, 81 | Oct 3 | 3 |
| 5014 | Gorchakov | Harvey, 81 | Aug 30 | 3 |
| 5047 | Zanda | Harvey, 81 | Oct 3 | 3 |

| MINOR PLANET | OBSERVER & APERTURE (cm) | OBSERVING PERIOD (2019) | NO. OBS. |
|---|---|---|---|
| 5102 Benfranklin | Harvey, 81 | Sep 22 | 3 |
| 5178 Pattazhy | Harvey, 81 | Feb 1 | 3 |
| 5183 Robyn | Harvey, 81 | Sep 20 | 3 |
| 5250 Jas | Harvey, 81 | Jul 30 | 3 |
| 5296 Friedrich | Harvey, 81 | Apr 3 | 3 |
| 5297 Schinkel | Harvey, 81 | Feb 25 | 3 |
| 5309 MacPherson | Harvey, 81 | Aug 31 | 3 |
| 5314 Wilkickia | Harvey, 81 | Dec 19 | 3 |
| 5328 Nisiyamakoiti | Harvey, 81 | Nov 26 | 3 |
| 5337 Aoki | Harvey, 81 | Mar 27 | 3 |
| 5342 LePoole | Harvey, 81 | Jun 21 | 3 |
| 5368 Vitagliano | Harvey, 81 | Feb 1 | 3 |
| 5410 Spivakov | Harvey, 81 | Jan 9 | 3 |
| 5421 Ulanova | Harvey, 81 | Aug 30 | 3 |
| 5422 Hodgkin | Harvey, 81 | Jan 9 | 3 |
| 5437 1990 DU3 | Harvey, 81 | Aug 31 | 3 |
| 5453 Zakharchenya | Harvey, 81 | Nov 25 | 3 |
| 5480 1989 YK8 | Harvey, 81 | Mar 6 | 3 |
| 5491 Kaulbach | Harvey, 81 | Feb 4 | 3 |
| 5499 1981 SU2 | Harvey, 81 | Dec 20 | 3 |
| | | | 0.3f@16.2 |
| 5533 Bagrov | Harvey, 81 | Nov 3 | 3 |
| 5543 Sharaf | Harvey, 81 | Dec 20 | 3 |
| 5571 Lesliegreen | Harvey, 81 | Feb 4 | 3 |
| 5599 1991 SG1 | Harvey, 81 | Jan 31 | 3 |
| 5640 Yoshino | Harvey, 81 | Sep 21 | 3 |
| 5643 Roques | Harvey, 81 | Jul 30 | 3 |
| 5669 1985 CC2 | Harvey, 81 | Jan 16 | 3 |
| 5671 Chanal | Harvey, 81 | Oct 3 | 3 |
| 5686 Chiyonoura | Harvey, 81 | Sep 23 | 3 |
| 5688 Kleewyck | Harvey, 81 | Nov 6 | 3 |
| 5705 Schumacher | Harvey, 81 | Feb 25 | 3 |
| 5722 Johnscherrer | Harvey, 81 | Apr 16 | 3 |
| 5752 1992 CJ | Harvey, 81 | Mar 13 | 3 |
| 5768 Pittich | Harvey, 81 | Nov 3 | 3 |
| 5773 1989 NO | Harvey, 81 | Apr 11 | 3 |
| 5777 Hanakai | Harvey, 81 | Jan 16 | 3 |
| | | | 0.4f@16.1 |
| 5795 Roshchina | Harvey, 81 | Nov 2 | 3 |
| 5804 Bambinidipraga | Harvey, 81 | Sep 27 | 3 |
| 5810 1988 EN | Harvey, 81 | Aug 10 | 3 |
| 5848 Harutoriko | Harvey, 81 | Dec 31 | 3 |
| 5872 Sugano | Harvey, 81 | Aug 10 | 3 |
| 5877 Toshimaihara | Harvey, 81 | May 27 | 3 |
| 5891 Gehrig | Harvey, 81 | Oct 3 | 3 |
| 5916 van der Woude | Harvey, 81 | Mar 28 | 3 |
| 5935 Ostankino | Harvey, 81 | Mar 7 | 3 |
| 5973 Takimoto | Harvey, 81 | May 2 | 3 |
| | | | 0.4f@16.2 |
| 6022 Jyuro | Harvey, 81 | Dec 20 | 3 |
| 6028 1994 ER1 | Harvey, 81 | May 7 | 3 |
| 6057 Robbia | Harvey, 81 | Sep 4 | 3 |
| 6061 1981 SQ2 | Harvey, 81 | Oct 4 | 3 |
| 6122 Henrard | Harvey, 81 | Sep 7 | 3 |
| 6128 Lasorda | Harvey, 81 | Apr 16 | 3 |
| 6135 Billowen | Harvey, 81 | Jan 25 | 3 |
| 6140 Kubokawa | Harvey, 81 | Nov 4 | 3 |
| 6151 Viget | Harvey, 81 | Jan 25 | 3 |
| 6258 Rodin | Harvey, 81 | Jan 25 | 3 |
| 6319 Beregovoj | Harvey, 81 | Feb 25 | 3 |
| 6332 Vorarlberg | Harvey, 81 | Apr 16 | 3 |
| 6336 Dodo | Harvey, 81 | Sep 23 | 3 |
| 6347 1995 BM4 | Harvey, 81 | Mar 6 | 3 |
| 6356 Tairov | Harvey, 81 | Dec 19 | 3 |
| 6405 Komiyama | Harvey, 81 | Mar 6 | 3 |
| 6407 1992 PF2 | Harvey, 81 | May 25 | 3 |
| 6481 Tenzing | Harvey, 81 | Oct 4 | 3 |
| 6493 Cathybennett | Harvey, 81 | Jan 10 | 4 |
| 6500 Kodaira | Harvey, 81 | Nov 2 | 6 |
| 6527 Takashiito | Harvey, 81 | Nov 2 | 3 |
| 6567 Shigemasa | Harvey, 81 | Jul 30 | 3 |
| 6652 1991 SJ1 | Harvey, 81 | Apr 3 | 3 |
| 6667 Sannaimura | Harvey, 81 | Jan 25 | 3 |
| 6680 1970 WD | Harvey, 81 | Jul 30 | 3 |
| 6722 Bunichi | Harvey, 81 | Jan 16 | 3 |
| 6818 Sessyu | Harvey, 81 | Feb 1 | 3 |
| 6839 Ozenuma | Harvey, 81 | Nov 3 | 3 |
| 6866 Kukai | Harvey, 81 | Apr 28 | 3 |
| 6877 Giada | Harvey, 81 | Nov 3 | 3 |
| | | | 0.3f@16.0 |
| 6917 1993 FR2 | Harvey, 81 | Jan 27 | 3 |
| 6918 Manaslu | Harvey, 81 | Feb 26 | 3 |
| 6945 Dahlgren | Harvey, 81 | Nov 26 | 3 |
| 6946 1980 RX1 | Harvey, 81 | Jan 7 | 3 |
| 6964 Kunihiko | Harvey, 81 | Sep 22 | 3 |
| 6982 Cesarchavez | Harvey, 81 | Oct 14 | 3 |
| 7023 Heiankyo | Harvey, 81 | Jun 22 | 3 |
| 7033 1994 WN2 | Harvey, 81 | Feb 14 | 3 |
| 7116 Mentall | Harvey, 81 | Jan 16 | 3 |
| 7140 Osaki | Harvey, 81 | Nov 3 | 3 |
| 7148 Reinholdbien | Harvey, 81 | Jan 11 | 3 |
| 7189 Kuniko | Harvey, 81 | Dec 20 | 3 |
| 7245 1991 RN10 | Harvey, 81 | Nov 26 | 3 |
| 7261 Yokootakeo | Harvey, 81 | Jan 6 | 3 |
| 7295 Brozovic | Harvey, 81 | Jul 2 | 3 |
| 7300 Yoshisada | Harvey, 81 | Dec 25 | 3 |
| 7343 Ockeghem | Harvey, 81 | Sep 3 | 3 |
| 7365 Sejong | Harvey, 81 | Aug 29 | 3 |
| 7387 Malbil | Harvey, 81 | Dec 2 | 3 |
| 7397 1986 QS | Harvey, 81 | Nov 2 | 3 |
| 7408 Yoshihide | Harvey, 81 | Sep 23 | 3 |
| 7444 1996 TM10 | Harvey, 81 | Sep 3 | 3 |
| 7463 Oukawamine | Harvey, 81 | Aug 29 | 3 |
| 7527 Marples | Harvey, 81 | Sep 21 | 3 |
| 7534 1995 UA7 | Harvey, 81 | Sep 1 | 3 |
| 7560 Spudis | Harvey, 81 | Feb 4 | 3 |
| 7577 1990 QV4 | Harvey, 81 | Jan 26 | 3 |
| 7743 1986 JA | Harvey, 81 | May 29 | 3 |
| 7752 Otauchunokai | Harvey, 81 | Aug 30 | 3 |
| 7759 1990 QD2 | Harvey, 81 | Sep 20 | 3 |
| 7798 1996 CL | Harvey, 81 | Jan 10 | 3 |
| 7868 Barker | Harvey, 81 | Sep 21 | 3 |
| 7929 1987 SK12 | Harvey, 81 | Jan 26 | 3 |
| 7950 Berezov | Harvey, 81 | Sep 7 | 3 |
| 7960 Condorcet | Harvey, 81 | Mar 28 | 3 |
| 7992 Yozan | Harvey, 81 | Dec 2 | 3 |
| 8020 Erzgebirge | Harvey, 81 | Oct 3 | 3 |
| 8028 Joeengle | Harvey, 81 | Oct 3 | 3 |
| 8047 Akikinoshita | Harvey, 81 | Nov 26 | 3 |
| 8087 Kazutaka | Harvey, 81 | Jan 6 | 3 |
| | | | 0.5f@16.0 |
| 8142 Zolotov | Harvey, 81 | Aug 30 | 3 |
| | | | 0.5f@15.8 |
| 8163 Ishizaki | Harvey, 81 | Mar 27 | 3 |
| 8263 1986 QT | Harvey, 81 | Jul 25 | 3 |
| 8271 Imai | Harvey, 81 | Aug 10 | 3 |
| 8291 Bingham | Harvey, 81 | Feb 4 | 3 |
| 8323 Krimigis | Harvey, 81 | Nov 25 | 3 |
| 8420 Angrowna | Harvey, 81 | Feb 25 | 3 |
| 8471 Obrant | Harvey, 81 | Sep 1 | 3 |
| 8527 Katayama | Harvey, 81 | Aug 31 | 3 |
| | | | 0.5f@16.1 |
| 8575 Seishitakeuchi | Harvey, 81 | Oct 4 | 3 |
| 8610 Goldhaber | Harvey, 81 | Dec 31 | 3 |
| 8630 Billprady | Harvey, 81 | Apr 3 | 3 |
| 8660 Sano | Harvey, 81 | Sep 23 | 3 |
| 8785 Boltwood | Harvey, 81 | Sep 3 | 3 |
| 8838 1989 UW2 | Harvey, 81 | Jan 31 | 3 |
| 8842 1990 KF | Harvey, 81 | Sep 7 | 3 |
| | | | 0.6f@15.8 |
| 8861 Jenskandler | Harvey, 81 | May 25 | 3 |
| 8937 Gassan | Harvey, 81 | Jul 2 | 3 |
| 9065 1993 FN1 | Harvey, 81 | Jul 25 | 3 |
| | | | 0.5f@15.9 |
| 9086 1995 SA3 | Harvey, 81 | Nov 3 | 3 |

| MINOR | PLANET | OBSERVER & APERTURE (cm) | OBSERVING PERIOD (2019) | NO. OBS. |
|---|---|---|---|---|
| 9137 | Remo | Harvey, 81 | Feb 25 | 3 |
| 9147 | Kourakuen | Harvey, 81 | Jan 25 | 3 |
| 9148 | Boriszaitsev | Harvey, 81 | Dec 25 | 3 |
| 9158 | Plate | Harvey, 81 | Jul 25 | 3 |
| 9262 | Bordovitsyna | Harvey, 81 | Nov 26 | 3 |
| 9334 | Moesta | Harvey, 81 | Jul 2 | 3 |
| 9348 | 1991 RH25 | Harvey, 81 | Nov 3 | 3 |
| 9352 | 1991 UB4 | Harvey, 81 | Mar 27 | 3 |
| 9367 | 1993 BO3 | Harvey, 81 | Nov 26 | 3 |
| 9459 | 1998 FW113 | Harvey, 81 | Mar 27 | 3 |
| 9565 | Tikhonov | Harvey, 81 | Sep 4 | 3 |
| 9717 | Lyudvasilia | Harvey, 81 | Nov 25 | 3 |
| 9772 | 1993 MB | Harvey, 81 | May 7 | 3 |
| 9963 | Sandage | Harvey, 81 | Jul 3 | 3 |
| 9992 | 1997 TG19 | Harvey, 81 | Jun 22 | 3 |
| 10111 | Fresnel | Harvey, 81 | Jan 25 | 3 |
| | | | | 0.5f@16.0 |
| 10134 | 1993 HL6 | Harvey, 81 | Mar 27 | 3 |
| 10261 | Nikdollezhal' | Harvey, 81 | Sep 20 | 3 |
| 10374 | Etampes | Harvey, 81 | May 2 | 3 |
| 10403 | Marcelgrun | Harvey, 81 | Mar 27 | 3 |
| 10418 | 1998 WZ23 | Harvey, 81 | Sep 23 | 3 |
| 10422 | 1999 AN22 | Harvey, 81 | May 7 | 3 |
| 10512 | Yamandu | Harvey, 81 | Sep 22 | 3 |
| 10516 | Sakurajimi | Harvey, 81 | Sep 22 | 3 |
| 10524 | Maniewski | Harvey, 81 | Mar 28 | 3 |
| 10551 | Goteborg | Harvey, 81 | Jan 9 | 3 |
| 10564 | 1993 XQ2 | Harvey, 81 | Dec 31 | 3 |
| 10615 | 1997 UK3 | Harvey, 81 | Nov 6 | 3 |
| 10720 | Danzl | Harvey, 81 | Sep 21 | 3 |
| 10828 | Tomjones | Harvey, 81 | Oct 3 | 3 |
| 10849 | 1995 BO1 | Harvey, 81 | Apr 23 | 3 |
| 10861 | Ciske | Harvey, 81 | Dec 20 | 3 |
| 10922 | 1998 BG2 | Harvey, 81 | Aug 31 | 3 |
| 10990 | Okunev | Harvey, 81 | Sep 3 | 3 |
| 11026 | 1986 RE1 | Harvey, 81 | Sep 21 | 3 |
| 11116 | 1996 EK | Harvey, 81 | May 29 | 3 |
| 11119 | Taro | Harvey, 81 | Sep 22 | 3 |
| 11155 | Kinpu | Harvey, 81 | Feb 25 | 3 |
| 11549 | 1992 YY | Harvey, 81 | Sep 20 | 3 |
| 11550 | 1993 BN | Harvey, 81 | Jan 16 | 3 |
| 11597 | 1995 KL1 | Harvey, 81 | Feb 4 | 3 |
| 11644 | 1997 BR1 | Harvey, 81 | Feb 4 | 3 |
| 11790 | Goode | Harvey, 81 | Sep 1 | 3 |
| 11808 | Platz | Harvey, 81 | Aug 8 | 3 |
| 11906 | 1992 AE1 | Harvey, 81 | Jan 10 | 3 |
| 11928 | Akimotohiro | Harvey, 81 | Mar 28 | 3 |
| 11933 | Himuka | Harvey, 81 | Feb 25 | 3 |
| 11999 | 1996 BV1 | Harvey, 81 | Feb 4 | 3 |
| 12066 | 1998 FX39 | Harvey, 81 | Jul 3 | 3 |
| 12069 | 1998 FC59 | Harvey, 81 | Jul 2 | 3 |
| | | | | 0.5f@16.0 |
| 12198 | 1980 PJ1 | Harvey, 81 | Jan 6 | 3 |
| 12265 | 1990 FG | Harvey, 81 | Mar 7 | 3 |
| 12338 | 1992 XE | Harvey, 81 | Dec 2 | 3 |
| 12403 | 1995 QD3 | Harvey, 81 | Jan 6 | 3 |
| 12415 | Wakatatakayo | Harvey, 81 | Aug 30 | 3 |
| 12417 | 1995 TC8 | Harvey, 81 | Sep 22 | 3 |
| 12583 | 1998 OH | Harvey, 81 | May 29 | 6 |
| 12724 | 1991 PZ14 | Harvey, 81 | Aug 10 | 3 |
| 13050 | 1990 SY | Harvey, 81 | Sep 3 | 3 |
| 13065 | 1991 PG11 | Harvey, 81 | Sep 23 | 3 |
| 13081 | 1992 EW9 | Harvey, 81 | Oct 3 | 3 |
| 13143 | 1995 AF | Harvey, 81 | Jul 25 | 3 |
| 13320 | Jessicamiles | Harvey, 81 | Sep 1 | 3 |
| 13488 | Savanov | Harvey, 81 | Dec 19 | 3 |
| 13696 | 1998 HU43 | Harvey, 81 | Dec 2 | 3 |
| 13803 | 1998 WU10 | Harvey, 81 | Jul 30 | 3 |
| | | | | 0.6f@16.1 |
| 13915 | Yalow | Harvey, 81 | May 14 | 3 |
| 13928 | Aaronrogers | Harvey, 81 | Sep 1 | 3 |
| | | | | 0.4f@16.0 |
| 13938 | 1989 RP1 | Harvey, 81 | Aug 8 | 3 |
| 13949 | 1990 RN3 | Harvey, 81 | Jun 21 | 3 |
| 14033 | 1994 YR | Harvey, 81 | Nov 6 | 3 |
| 14127 | 1998 QA91 | Harvey, 81 | Sep 23 | 3 |
| 14255 | 2000 AS70 | Harvey, 81 | Jan 27 | 3 |
| 14385 | 1990 QG1 | Harvey, 81 | Sep 7 | 3 |
| 14441 | Atakanoseki | Harvey, 81 | Sep 23 | 3 |
| 14790 | Beletskij | Harvey, 81 | Nov 3 | 3 |
| 14875 | 1990 WZ1 | Harvey, 81 | Sep 4 | 3 |
| 14923 | 1994 TU3 | Harvey, 81 | Nov 4 | 3 |
| 14931 | 1994 WR3 | Harvey, 81 | Dec 25 | 3 |
| 14935 | 1995 BP1 | Harvey, 81 | Dec 5 | 3 |
| 15347 | Colinstuart | Harvey, 81 | Nov 6 | 3 |
| 15415 | Rika | Harvey, 81 | Aug 30 | 3 |
| 15416 | 1998 DZ2 | Harvey, 81 | Jan 6 | 3 |
| 15473 | 1999 BL9 | Harvey, 81 | Feb 1 | 3 |
| 15737 | 1991 CL | Harvey, 81 | Mar 28 | 3 |
| 15815 | 1994 PY18 | Harvey, 81 | Aug 29 | 3 |
| 15914 | 1997 UM3 | Harvey, 81 | Nov 3 | 3 |
| | | | | 0.4f@16.0 |
| 16030 | 1999 FS3 | Harvey, 81 | Jan 26 | 3 |
| 16233 | 2000 FA12 | Harvey, 81 | Dec 2 | 3 |
| 16538 | 1991 PO12 | Harvey, 81 | Dec 31 | 3 |
| 16578 | Essjayess | Harvey, 81 | Feb 25 | 3 |
| 16724 | Ullilotzmann | Harvey, 81 | Jan 6 | 3 |
| 16847 | Sanpoloamosciano | Harvey, 81 | Jan 6 | 3 |
| 16866 | 1998 AR | Harvey, 81 | Dec 31 | 3 |
| 16931 | 1998 EK9 | Harvey, 81 | Dec 31 | 3 |
| 16940 | 1988 GC3 | Harvey, 81 | Jan 11 | 3 |
| 16965 | 1998 RX79 | Harvey, 81 | Dec 19 | 3 |
| 17152 | 1999 JA118 | Harvey, 81 | Jul 25 | 3 |
| 17226 | 2000 CC76 | Harvey, 81 | Mar 27 | 3 |
| 17563 | Tsuneyoshi | Harvey, 81 | Dec 31 | 3 |
| | | | | 0.3f@16.2 |
| 17584 | 1994 XF1 | Harvey, 81 | May 7 | 3 |
| 17712 | Fatherwilliam | Harvey, 81 | Feb 4 | 3 |
| 17966 | 1999 JS43 | Harvey, 81 | Mar 13 | 3 |
| 18057 | 1999 VK10 | Harvey, 81 | Oct 4 | 3 |
| 18130 | 2000 OK5 | Harvey, 81 | Nov 21-25 | 3 |
| 18172 | 2000 QL7 | Harvey, 81 | Nov 2 | 6 |
| 18303 | 1980 PU | Harvey, 81 | Sep 3 | 3 |
| 18348 | 1990 BM1 | Harvey, 81 | Jan 9 | 3 |
| 18652 | 1998 FD15 | Harvey, 81 | Mar 28 | 3 |
| 18736 | 1998 NU | Harvey, 81 | Jan 6 | 3 |
| 18765 | 1999 JN17 | Harvey, 81 | Jul 3 | 3 |
| | | | | 0.5f@15.8 |
| 18906 | 2000 OJ19 | Harvey, 81 | Jul 25 | 3 |
| 19021 | 2000 SC8 | Harvey, 81 | Mar 6 | 3 |
| 19141 | Poelkapelle | Harvey, 81 | Jan 27 | 3 |
| 19281 | 1996 AP3 | Harvey, 81 | Nov 21-25 | 3 |
| 19366 | Sudingqiang | Harvey, 81 | Nov 25 | 3 |
| 19369 | 1997 YO | Harvey, 81 | Dec 19 | 3 |
| 19379 | Labrecque | Harvey, 81 | Jan 6 | 3 |
| 19707 | Tokunai | Harvey, 81 | Sep 1 | 3 |
| 19719 | Glasser | Harvey, 81 | Sep 22 | 3 |
| | | | | 0.4f@16.1 |
| 19953 | Takeo | Harvey, 81 | Apr 23 | 3 |
| 20084 | Buckmaster | Harvey, 81 | Jul 2 | 3 |
| 20295 | 1998 FF75 | Harvey, 81 | Jan 9 | 3 |
| 20408 | 1998 QW31 | Harvey, 81 | Nov 4 | 3 |
| 20423 | 1998 VN7 | Harvey, 81 | May 25 | 4 |
| 20747 | 2000 AM186 | Harvey, 81 | May 2 | 3 |
| 21089 | Mochizuki | Harvey, 81 | Jun 21 | 3 |
| 21122 | 1992 YK | Harvey, 81 | Mar 13 | 3 |
| 21194 | 1994 PN1 | Harvey, 81 | Jan 6 | 3 |
| 21373 | 1997 VF6 | Harvey, 81 | Jan 9 | 3 |
| 21378 | 1998 CJ4 | Harvey, 81 | Jan 25 | 3 |
| 21526 | Mirano | Harvey, 81 | Jun 22-Jul 2 | 4 |
| 21527 | Horton | Harvey, 81 | Sep 1 | 3 |
| 21594 | 1998 VP31 | Harvey, 81 | Mar 27 | 3 |
| 21842 | 1999 TH102 | Harvey, 81 | May 2 | 3 |

| MINOR PLANET | OBSERVER & APERTURE (cm) | OBSERVING PERIOD (2019) | NO. OBS. |
|---|---|---|---|
| 21923 1999 VT52 | Harvey, 81 | May 25 | 3 |
| | | | 0.5f@16.0 |
| 21967 1999 WS9 | Harvey, 81 | May 2 | 3 |
| 21976 1999 XV2 | Harvey, 81 | Jan 6 | 3 |
| 22106 Tomokoarai | Harvey, 81 | Jan 9 | 3 |
| 22303 1990 QE4 | Harvey, 81 | Jul 30 | 3 |
| 22601 1998 DH124 | Harvey, 81 | Apr 28 | 3 |
| | | | 0.3f@16.2 |
| 22722 Timothycooper | Harvey, 81 | Mar 6 | 3 |
| 22790 1999 KP4 | Harvey, 81 | Jan 31 | 3 |
| | | | 0.4b@15.8 |
| 22844 1999 RU111 | Harvey, 81 | Sep 20 | 3 |
| 22952 Hommasachi | Harvey, 81 | Sep 3 | 3 |
| 23167 2000 GL124 | Harvey, 81 | Sep 3 | 3 |
| 23193 2000 OK181 | Harvey, 81 | Nov 25 | 3 |
| 23233 2000 WM72 | Harvey, 81 | Feb 25 | 3 |
| | | | 0.3f@16.2 |
| 23297 2001 AX3 | Harvey, 81 | Jul 30 | 3 |
| 23513 1992 PZ3 | Harvey, 81 | Sep 1 | 3 |
| 23692 1997 KA | Harvey, 81 | Sep 21 | 3 |
| 23796 1998 QK34 | Harvey, 81 | Sep 20 | 3 |
| 23857 1998 RT50 | Harvey, 81 | Mar 13 | 3 |
| 24192 1999 XM30 | Harvey, 81 | Jan 26 | 3 |
| 24284 1999 XJ183 | Harvey, 81 | Feb 4 | 3 |
| 24515 2001 CS4 | Harvey, 81 | Jul 27 | 6 |
| 24602 Mozzhorin | Harvey, 81 | Sep 3 | 3 |
| 24754 Zellyfry | Harvey, 81 | Nov 25 | 3 |
| 24795 1994 AC17 | Harvey, 81 | Apr 2 | 3 |
| 24831 1995 SX4 | Harvey, 81 | Nov 6 | 3 |
| 26355 Grueber | Harvey, 81 | Jan 6 | 3 |
| 26479 2000 AE198 | Harvey, 81 | Apr 3 | 3 |
| 26793 Bolshoi | Harvey, 81 | Nov 6 | 3 |
| 26821 Baehr | Harvey, 81 | Jan 6 | 3 |
| 26851 Sarapul | Harvey, 81 | Aug 8 | 3 |
| | Rayon, 25 | Sep 4 | 35C |
| 27027 1998 QA98 | Harvey, 81 | Jan 26 | 3 |
| 27215 1999 CK128 | Harvey, 81 | Dec 25 | 3 |
| 27355 2000 DB79 | Harvey, 81 | Sep 4 | 3 |
| 27612 2001 KG25 | Harvey, 81 | Sep 7 | 3 |
| 28014 1997 YS5 | Harvey, 81 | Jan 6 | 3 |
| 29032 2059-T1 | Faure, 35 | Sep 28-29 | 2 |
| | Rayon, 25 | Sep 19-30 | 40C |
| 29180 1990 SW1 | Harvey, 81 | Oct 3 | 3 |
| 29422 1997 AH21 | Harvey, 81 | Jan 11 | 3 |
| 29763 1999 CH20 | Harvey, 81 | Sep 21 | 3 |
| 30072 2000 EP93 | Harvey, 81 | Sep 3 | 3 |
| 30963 Mount Banzan | Harvey, 81 | Dec 2 | 3 |
| 31361 1998 VQ29 | Harvey, 81 | Oct 3 | 3 |
| 31560 1999 EQ14 | Harvey, 81 | Nov 4 | 3 |
| 32897 Curtharris | Harvey, 81 | Jul 2 | 3 |
| | | | 0.5f@16.1 |
| 33933 2000 LE29 | Harvey, 81 | Apr 16 | 3 |
| 37652 1994 JS1 | Harvey, 81 | Feb 25 | 3 |
| | | | 0.5f@16.1 |
| 39197 2000 XA | Harvey, 81 | Nov 2 | 3 |
| 45864 2000 UO97 | Harvey, 81 | Jan 27 | 3 |
| 46572 1991 VA5 | Harvey, 81 | Jan 16 | 3 |
| 48540 1993 TW8 | Harvey, 81 | Oct 3 | 3 |
| 50363 2000 CD77 | Harvey, 81 | Sep 7 | 3 |
| 52634 1997 WR28 | Harvey, 81 | Dec 2 | 3 |
| 52930 1998 SK127 | Harvey, 81 | Aug 29 | 3 |
| 53916 2000 GW7 | Harvey, 81 | Nov 25 | 3 |
| 54906 2001 OT80 | Harvey, 81 | Jan 11 | 3 |
| | | | 0.4f@16.3 |
| 57085 2001 OY37 | Harvey, 81 | Feb 4 | 3 |
| 64163 2001 TB49 | Harvey, 81 | Dec 25 | 3 |
| 69270 1989 BB | Harvey, 81 | Jan 26 | 3 |
| 78790 2002 VH120 | Harvey, 81 | Aug 8 | 3 |
| 80593 2000 AG144 | Faure, 20 | Sep 7 | 5 |
| | Harvey, 81 | Aug 8 | 3 |
| | Rayon, 25 | Sep 7-17 | 55C |
| 82676 2001 PV23 | Harvey, 81 | Aug 8 | 3 |
| 85236 1993 KH | Harvey, 81 | Nov 20 | 6 |
| 86402 2000 AB144 | Harvey, 81 | Jan 27 | 3 |
| 87135 2000 NU5 | Harvey, 81 | Dec 3 | 3 |
| 88254 2001 FM129 | Harvey, 81 | Mar 18 | 6 |
| 90403 2003 YE45 | Harvey, 81 | Jan 9-11 | 12 |
| 99248 2001 KY66 | Harvey, 81 | Nov 6 | 6 |
| 99915 1997 TR6 | Harvey, 81 | Aug 29 | 3 |
| 100006 1987 DA7 | Harvey, 81 | Jan 6 | 3 |
| 137199 1999 KX4 | Harvey, 81 | Dec 25 | 6 |
| 141525 2002 PV5 | Harvey, 81 | Apr 22-23 | 12 |
| 141593 2002 HK12 | Harvey, 81 | Sep 8 | 6 |
| 152931 2000 EA107 | Harvey, 81 | Apr 3 | 6 |
| 153842 2001 XT30 | Harvey, 81 | Aug 8 | 3 |
| 159493 2000 UA | Harvey, 81 | Feb 4 | 3 |
| 162082 1998 HL1 | Faure, 35 | Oct 26 | 5 |
| | Harvey, 30 | Oct 17-24 | 12 |
| 162723 2000 VM2 | Harvey, 81 | Nov 25 | 6 |
| | | | 0.5f@16.1 |
| 180186 2003 QZ30 | Harvey, 81 | Jan 26-27 | 12 |
| 216258 2006 WH1 | Harvey, 81 | Dec 16 | 6 |
| 237805 2002 CF26 | Faure, 25 | Sep 8 | 8 |
| | Harvey, 81 | Aug 29 | 6 |
| | Rayon, 25 | Sep 8-17 | 5V, 50C |
| 293054 2006 WP127 | Harvey, 81 | Jul 27 | 6 |
| 306381 1993 RP2 | Harvey, 81 | Jul 25 | 3 |
| | | | 0.8f@16.1 |
| 354030 2001 RB18 | Faure, 35 | Sep 29 | 6 |
| | Rayon, 25 | Sep 19-30 | 40C |
| 381677 2009 BJ81 | Harvey, 81 | Feb 14 | 6 |
| 405212 2003 QC10 | Harvey, 81 | Sep 20 | 6 |
| 454177 2013 GJ35 | Harvey, 81 | Jan 6 | 6 |
| 455432 2003 RP8 | Harvey, 81 | Jul 29 | 6 |
| 481394 2006 SF6 | Harvey, 81 | Nov 2 | 6 |
| 2005 FC3 | Harvey, 81 | Mar 7 | 6 |
| 2006 SK134 | Harvey, 81 | Mar 27 | 6 |
| 2008 HS3 | Harvey, 81 | May 7 | 6 |
| 2011 HP | Harvey, 81 | May 27 | 6 |
| 2013 CW32 | Harvey, 81 | Jan 31-Feb 1 | 12 |
| 2015 JD1 | Harvey, 81 | Nov 2 | 6 |
| 2019 DN | Harvey, 81 | Mar 6 | 6 |
| | | | 0.5b@16.0 |
| 2019 JE | Harvey, 81 | May 6 | 6 |
| 2019 MA2 | Harvey, 81 | Jul 15 | 6 |
| 2019 PZ2 | Harvey, 81 | Aug 17 | 6 |
| 2019 UN12 | Harvey, 81 | Nov 11 | 6 |

## ROTATIONAL PERIOD OF FIVE ASTEROIDS

Roberto Bonamico
BSA Osservatorio (K76)
Strada Collarelle 53
12038 Savigliano
Cuneo, ITALY
info@osservatorioastronomicobsa.it
*http://www.osservatorioastronomicobsa.it*

(Received: 2020 April 7)

CCD photometric observations of five main-belt asteroids were made from 2020 January to March. We report the results of lightcurve analysis for: 1169 Alwine, $P$ = 2.928 ± 0.001 h, $A$ = 0.27 mag; 1755 Lorbach, $P$ = 7.978 ± 0.001 h, $A$ = 0.39 mag; 2227 Otto Struve, $P$ = 5.390 ± 0.001 h, $A$ = 0.19 mag; 2443 Tomeileen, $P$ = 7.954 ± 0.001 h, $A$ = 0.12 mag; 5972 Harryatkinson, $P$ = 3.376 ± 0.001 h, $A$ = 0.11 mag.

From 2020 January to March, the astronomical observatory BSA studied the rotation period of five main-belt asteroids that were chosen from the website at *http://minorplanet.info /call.html*.

Observations at Osservatorio Astronomico BSA were made with a Marcon 0.30-m *f*/5 Newtonian telescope with an Atik 314L+ CCD camera using a Sony ICX285AL sensor (1360×1024, 6.5-microns). *MaximDL* was used for camera control (*http://diffractionlimited.com/product/maxim-dl/*), *The Sky 6 Pro* (*http://www.bisque.com*) controlled the mount, and *Voyager* (*http://software.starkeeper.it*) automated the entire observatory.

All photometric reductions were done with *MPO Canopus* v10.7.12.9 (*http://bdwpublishing.com*). Precise night-to-night zero-point calibration was obtained using the Comparison Star Selector utility in *MPO Canopus*. Whenever possible, five solar-color comparison stars were used from the MPOSC3 catalog supplied with *MPO Canopus*.

1169 Alwine. Two nights of observations were enough to complete the work with good precision, thanks to the short rotation period, the large amplitude, and the long astronomical nights. The final result is $P$ = 2.928 ± 0.001 h with an amplitude of $A$ = 0.27 mag. This seems to be a reliable period with no other alias found.

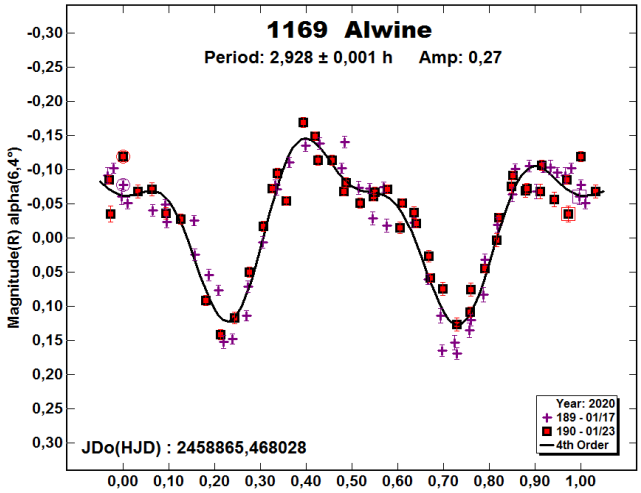


1755 Lorbach. This target was the easiest of the list due to the large amplitude of the curve. Four sessions led to a secure period of $P$ = 7.978 ± 0.001 h and $A$ = 0.39 mag. Moonless nights, the asteroid's brightness, and getting images for the whole rotation period each night facilitated the work and ensured precision.

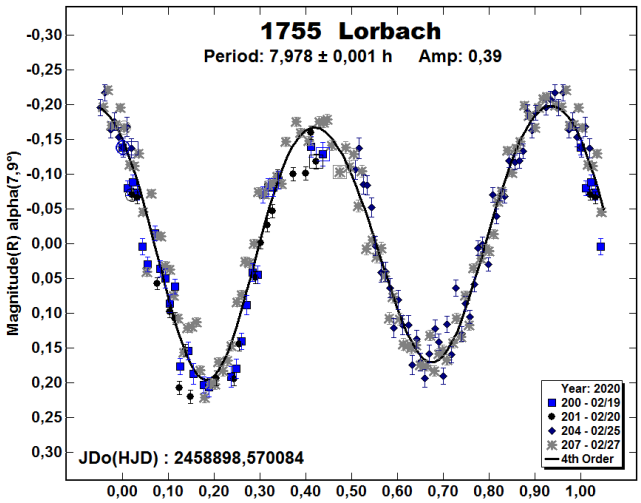


2227 Otto Struve. The observations of this asteroid took place over more than a month due to bad weather. Despite being in crowded star fields during the observation period, which went from 2020 February 3 to March 18, excellent photometric conditions, no moon, and low humidity allowed collecting data that ensured a good rotation period accuracy. Our analysis found $P$ = 5.390 ± 0.001 h and $A$ = 0.19 mag.

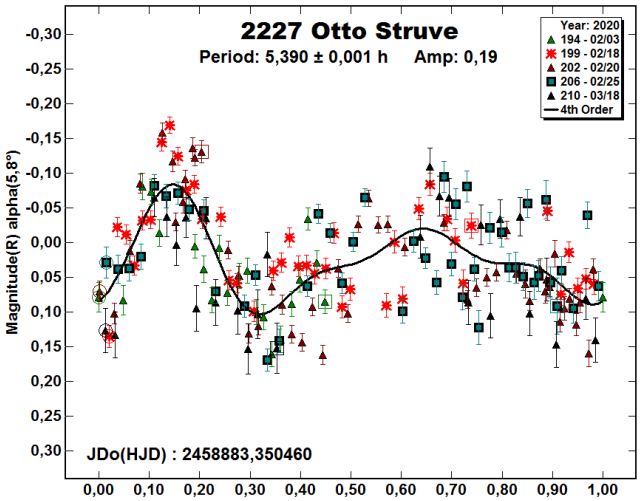


2443 Tomeileen. This main-belt asteroid had three results in the LCDB (Warner et al., 2009). The first was Alvarez-Candal et al. (2004), who found a period of 3.974 h. The second was from Behrend (2006) with a period of 6.822 h. The third was from Aznar (2011) with a period of 4.0 h.

A total of 326 images obtained during 6 nights led to a period $P$ = 7.954 ± 0.001 h with an amplitude of 0.12 mag. Long runs for each night helped assure a secure period.

| Number | Name | yyyy mm/dd | Phase | $L_{PAB}$ | $B_{PAB}$ | Period(h) | P.E. | Amp | A.E. | Grp |
|---|---|---|---|---|---|---|---|---|---|---|
| 1169 | Alwine | 2020 01/17-01/23 | 6.4,3,5 | 125 | -4 | 2.928 | 0.001 | 0.27 | 0.01 | MB |
| 1755 | Lorbach | 2020 02/19-02/27 | 8.2,5.4 | 171 | 2 | 7.978 | 0.001 | 0.39 | 0.01 | MB |
| 2227 | Otto Struve | 2020 02/03-03/18 | 5.4,23.8 | 129 | -5 | 5.390 | 0.001 | 0.19 | 0.02 | MB |
| 2443 | Tomeileen | 2020 01/14-02/12 | 12.4,18.0 | 79 | -7 | 7.954 | 0.001 | 0.12 | 0.01 | MB |
| 5972 | Harryatkinson | 2020 02/26-03/17 | 4.7,5.7 | 166 | 4 | 3.376 | 0.001 | 0.11 | 0.02 | MB |

Table I. Observing circumstances and results. The phase angle is given for the first and last date. If preceded by an asterisk, the phase angle reached an extrema during the period. $L_{PAB}$ and $B_{PAB}$ are the approximate phase angle bisector longitude/latitude at mid-date range (see Harris et al., 1984). Grp is the asteroid family/group (Warner et al., 2009).

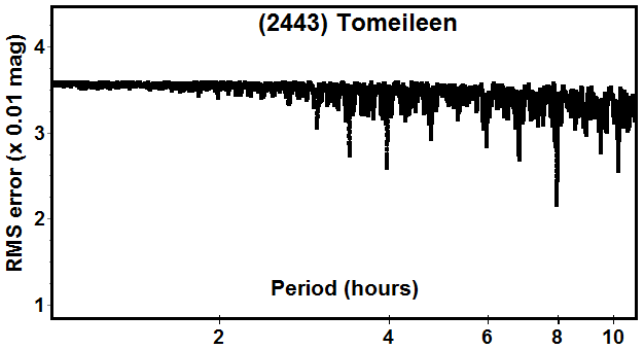


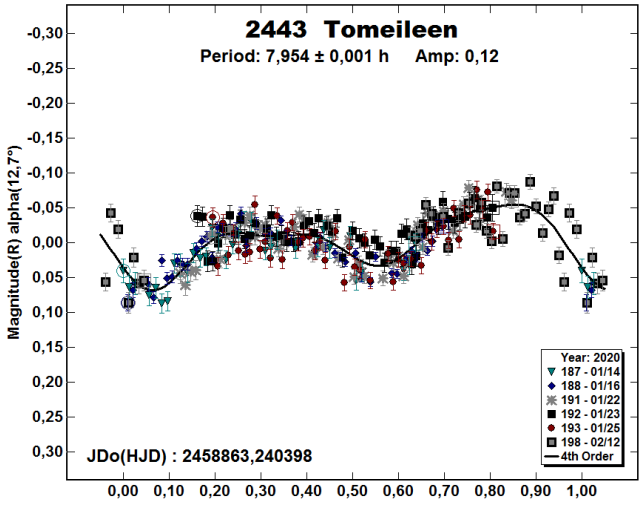


5972 Herryatkinson. This main-belt asteroid, discovered in 1991, is named after New Zealand physicist Harry Atkinson who, among others, chaired the board of the European Space Agency. Data were obtained on six nights from 2020 January 14 to February 12. The analysis found a rotation period of 3.376 ± 0.001 h with a small amplitude of only 0.11 mag.

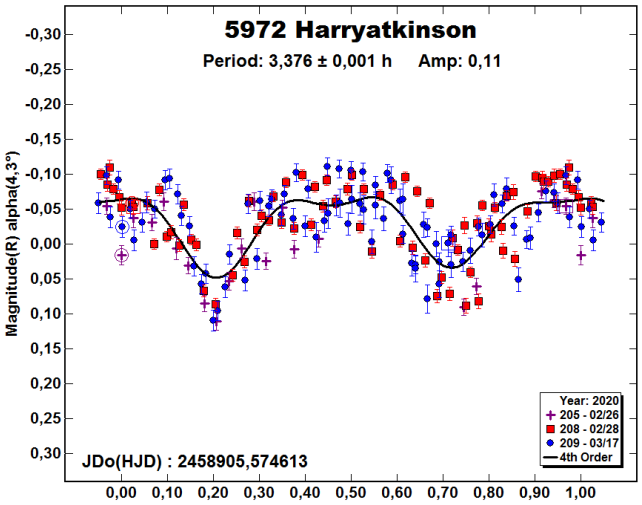


References

Alvarez-Candal, A.; Duffard, R.; Angeli, C.A.; Lazzaro, D.; Fernandez, S. (2004). "Rotational lightcurves of asteroids belonging to families." *Icarus* **172**, 388-401.

Aznar, A. (2011). *http://www.apt.com.es* (no longer valid).

Behrend, R. (2006). Observatoire de Geneve web site. *http://obswww.unige.ch/~behrend/page_cou.html*.

Harris, A.W.; Young, J.W.; Scaltriti, F.; Zappala, V. (1984). "Lightcurves and phase relations of the asteroids 82 Alkmene and 444 Gyptis." *Icarus* **57**, 251-258.

Warner, B.D. (2019). MPO Software. *MPO Canopus* v 17.7.12.9 *http://bdwpublishing.com*

Warner, B.D.; Harris, A.W.; Pravec, P. (2009). "The Asteroid Lightcurve Database." *Icarus* **202**, 134-146. Updated 2020 February. *http://www.minorplanet.info/lightcurvedatabase.html*

# MAIN-BELT ASTEROIDS OBSERVED FROM CS3: 2020 JANUARY TO MARCH

Robert D. Stephens
Center for Solar System Studies (CS3)/MoreData!
11355 Mount Johnson Ct., Rancho Cucamonga, CA 91737 USA
rstephens@foxandstephens.com

Brian D. Warner
Center for Solar System Studies (CS3)/MoreData!
Eaton, CO

(Received: 2020 April 10)

CCD photometric observations of 13 main-belt asteroids were obtained at the Center for Solar System Studies (CS3) from 2020 January to March. An additional 4 main-belt asteroids from prior years are also reported upon or revisited.

The Center for Solar System Studies (CS3) has seven telescopes which are normally used in program asteroid family studies. The focus is on near-Earth asteroids, but when suitable targets are not available, Jovian Trojans and Hildas are observed. When a nearly full moon is too close to the family targets being studied, targets of opportunity amongst the main-belt families were selected.

Table I lists the telescopes and CCD cameras that were used to make the observations. Images were unbinned with no filter and had master flats and darks applied. The exposures depended upon various factors including magnitude of the target, sky motion, and Moon illumination.

| Telescope | Camera |
|---|---|
| 0.30-m f/6.3 Schmidt-Cass | FLI Microline 1001E |
| 0.35-m f/9.1 Schmidt-Cass | FLI Microline 1001E |
| 0.35-m f/9.1 Schmidt-Cass | FLI Microline 1001E |
| 0.35-m f/9.1 Schmidt-Cass | FLI Microline 1001E |
| 0.35-m f/11 Schmidt-Cass | FLI Microline 1001E |
| 0.40-m f/10 Schmidt-Cass | FLI Proline 1001E |
| 0.50-m F8.1 R-C | FLI Proline 1001E |

Table I: List of CS3 telescope/CCD camera combinations.

Image processing, measurement, and period analysis were done using *MPO Canopus* (Bdw Publishing), which incorporates the Fourier analysis algorithm (FALC) developed by Harris (Harris et al., 1989). The Comp Star Selector feature in *MPO Canopus* was used to limit the comparison stars to near solar color. Night-to-night calibration was done using field stars from the ATLAS catalog (Tonry et al., 2018), which has Sloan *griz* magnitudes that were derived from the GAIA and Pan-STARR catalogs, among others and are "native" magnitudes of the catalog.

We used the ATLAS R or r′ (SR) magnitudes. Those adjustments are mostly ≤ 0.03 mag. The occasions where larger corrections were required may have been related in part to using unfiltered observations, poor centroiding of the reference stars, and not correcting for second-order extinction terms.

The magnitudes were normalized to the comparison stars used in the earliest session and to the phase angle given in parentheses using $G = 0.15$. In other words, the data were made to seem that they were all obtained at the same time using the same comparison stars. The X-axis rotational phase ranges from –0.05 to 1.05.

The amplitude indicated in the plots (e.g. Amp. 0.23) is the amplitude of the Fourier model curve and not necessarily the adopted amplitude of the lightcurve.

For brevity, only some of the previously reported rotational periods may be referenced. A complete list is available at the lightcurve database (LCDB; Warner et al., 2009).

463 Lola. For a low numbered asteroid, it is interesting that this inner main-belt asteroid has only three reported rotational periods from the past. Bembrick (2012, 2.206 h), Lecrone et al. (2005, 6.20 h), and Menke (2005, 2.621 h) all found periods similar to our result.

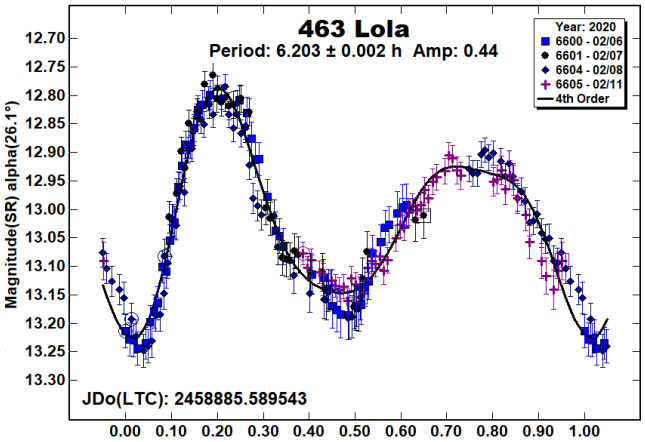


914 Palisana. We originally observed this Phocaea family member in 2008 reporting a period of 15.922 h (Warner, 2009b). Behrend et al. (2019web) observed it in 2019 August reporting a period of 8.681 h; this caused us to reevaluate our 2008 data. The comparison star magnitudes were changed from APASS V magnitudes (Henden et al., 2009) to ATLAS SR magnitudes (Tonry et al., 2018). The quality of each comparison star was reviewed. Our new analysis of the 2008 data showed several aliases including our original period of 15.92 h and a period of 8.686 h, near that found by Behrend et al. (2019web). After this analysis and taking into account the larger amplitude for the Behrend et al. lightcurve, we now slightly favor the 8.686 h period.

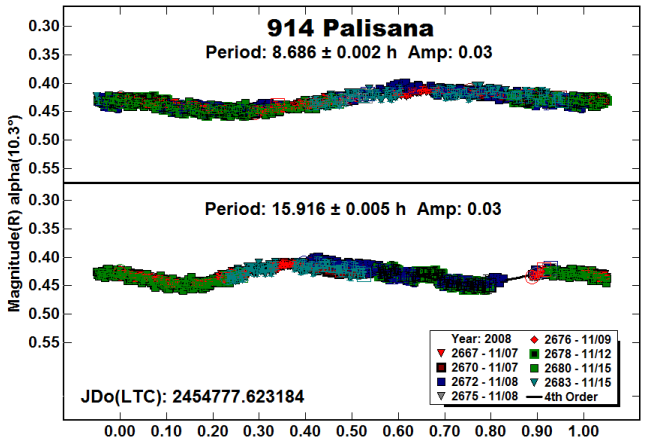

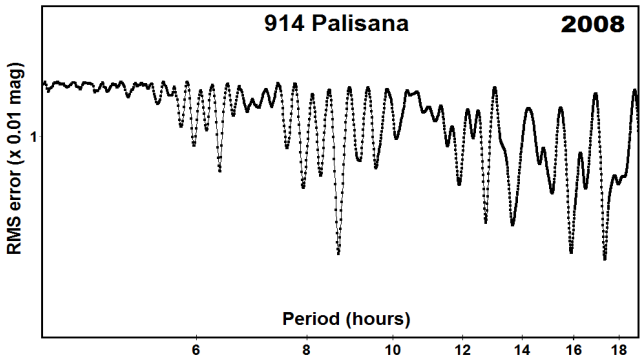


1106 Cydonia. This member of the Eunomia family has been observed twice before. Klinglesmith et al. (2016, 2.679 h) and Aznar (2017, 2.67 h) each found periods similar to our result.

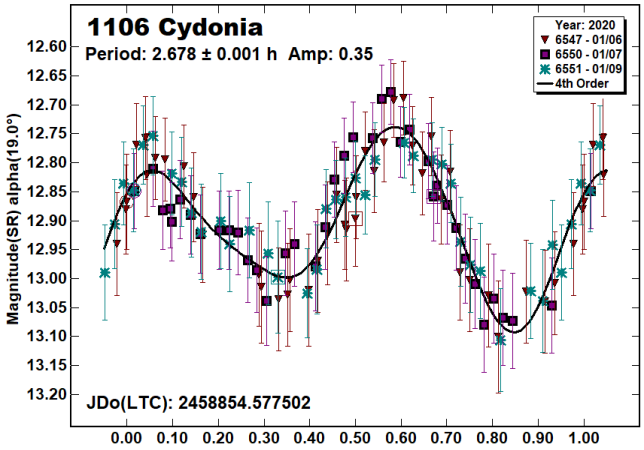


1169 Alwine. This member of the Eunomia family was observed between 2019 December and 2020 March by the Photometric Survey for Asynchronous Binary Asteroids (Pravec, 2020web) as a 'Prime Suspect' of being a binary asteroid. They found a primary period of $P_1$ = 2.9274 h and several attenuations that only roughly fit an orbital period of $P_2$ = 54.45 h.

We observed it from 2020 February to March and used the iterative dual-period search in *MPO Canopus* to find a primary period of $P_1$ = 2.9274 h and reveal the mutual events due to the satellite with an orbital period of $P_2$ = 13.408 h. Our fit was also not very good and is a 4:1 alias of the Pravec $P_2$ result. The next good opposition for the northern hemisphere will be in 2022 October.

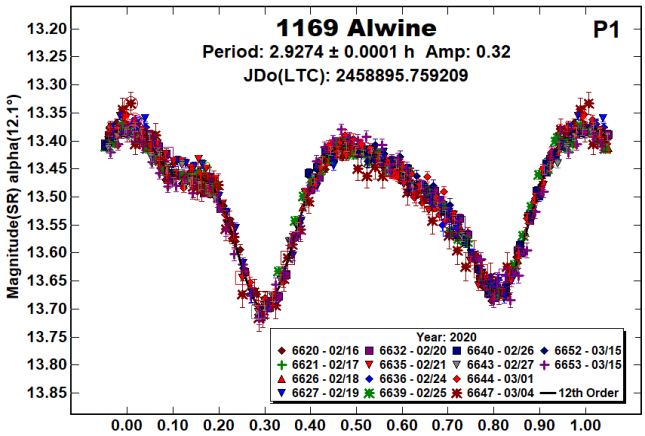


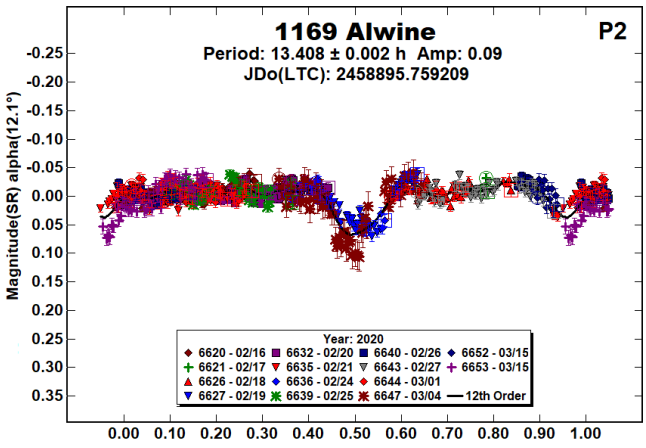


1589 Fanatica. We observed this Vestoid three times in the past (Warner, 2004; Stephens, 2015; Stephens and Warner, 2019) each time finding a period near 2.58 h. This year's result is in good agreement with those prior findings.

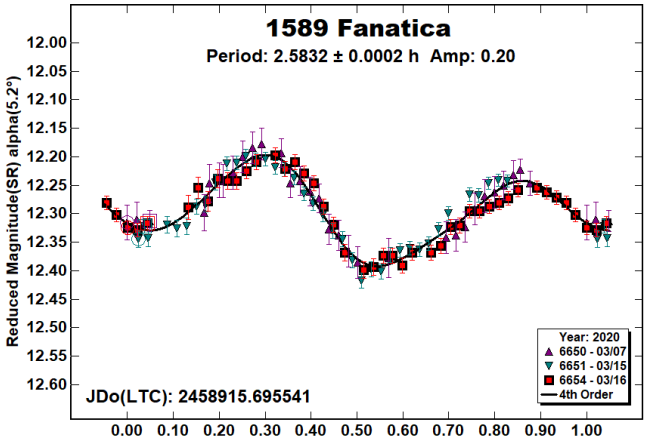


1806 Derice. This member of the Flora family has been observed several times by the Photometric Survey for Asynchronous Binary Asteroids (Pravec, 2009web; 2011web; 2012web; 2016web) as being a 'Prime Suspect' of being a binary asteroid. In the 2009 data, minor deviations from the curve suggested the presence of attenuation events, but an orbital period could not be determined. At each opposition the survey found a primary rotational period near 3.224 h.

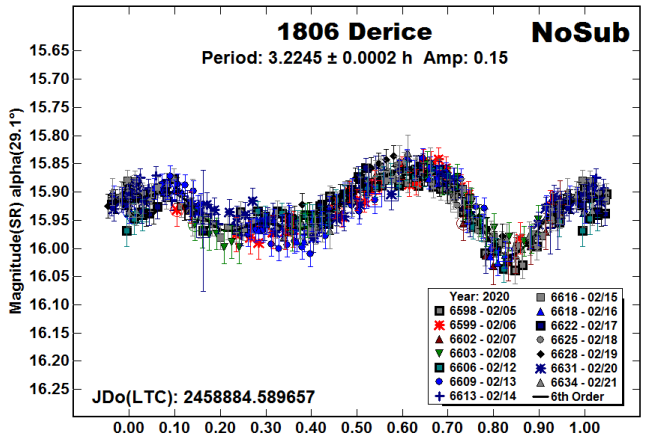

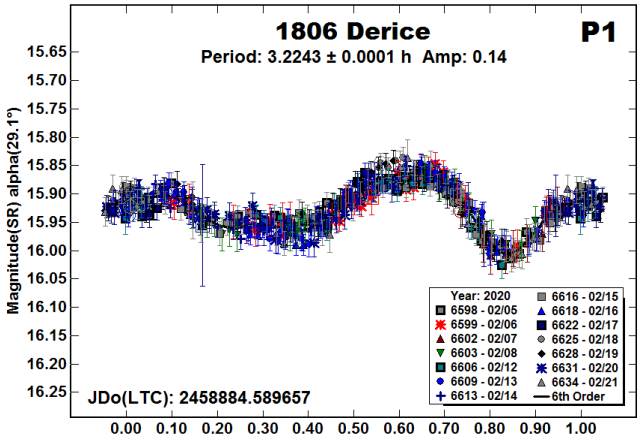


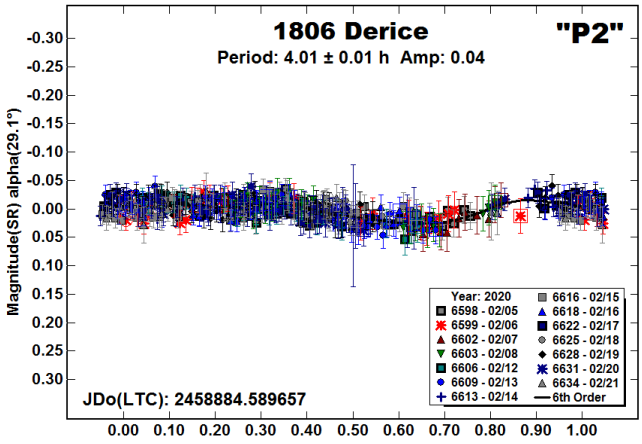


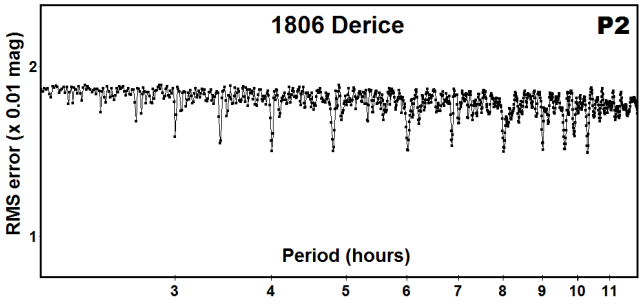


Our data in 2020 February also showed slight deviations from the curve. While promising at the start, more data made the solution increasingly unlikely. Running the dual-period search in *MPO Canopus* acted more as a "noise filter" with $P_2$ having no physical meaning. It is likely the $P_2$ found here is just a harmonic.

2023 Asaph. This outer main-belt asteroid was observed three times in the past. Behrend (2001web; 2006web) reported a period of 9.19 h (U = 1) while Warner (2003) reported a period of 4.74 h. Pál et al. (2020), using data from TESS, reported a period of 88.3197 h. On seeing this new result, we remeasured our images from 2003 using ATLAS SR magnitudes. In 2003, *MPO Canopus* relied on older star catalogs and did not have the Comp Star Selector feature to limit the comparison stars to near solar color. Our new result, although limited by having only four consecutive nights, is close to the Pál et al. result.

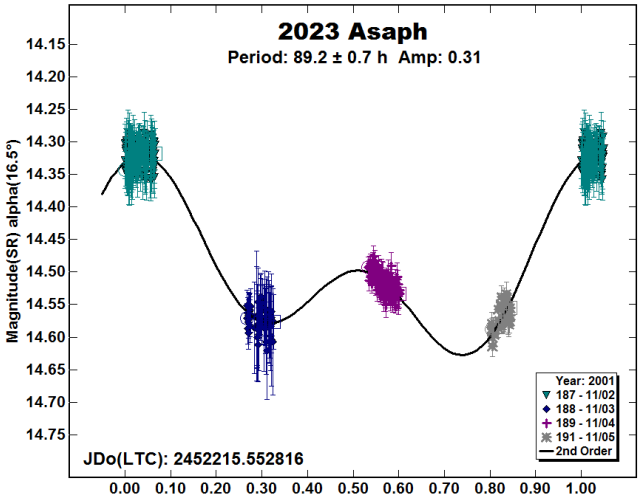


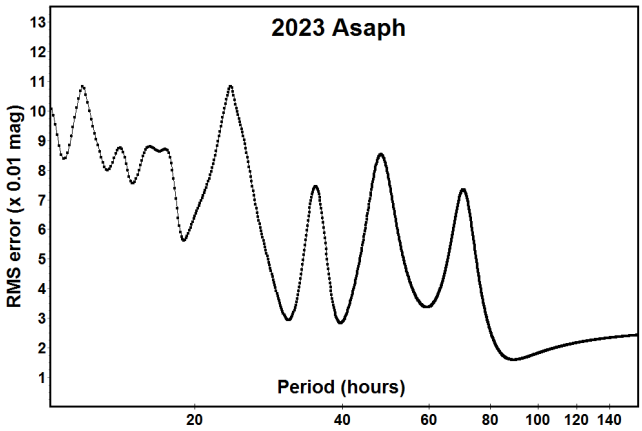


3267 Glo. Pravec et al. (2006web) observed this Mars-crosser and found a synodic rotational period of 6.8782 h. Our period is in good agreement with those results.

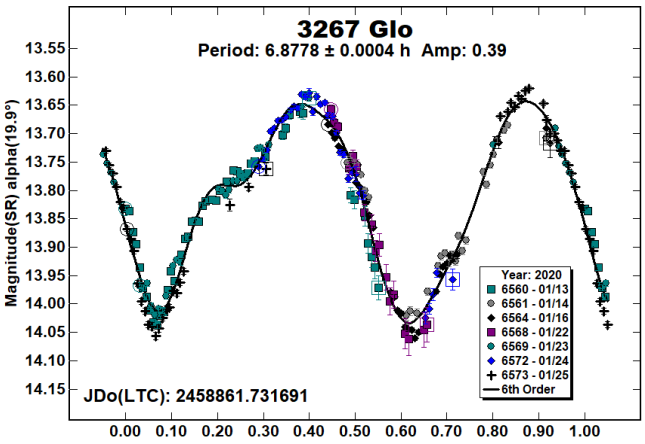


3613 Kunlun. Given the long rotational period, it is not surprising that there are no previously reported lightcurves in the LCDB for this Vestoid. After three weeks of observations, there was sufficient coverage of the lightcurve to have confidence in the primary rotational period, which is longer than the period where tumbling would be more likely than not (Pravec et al., 2005).

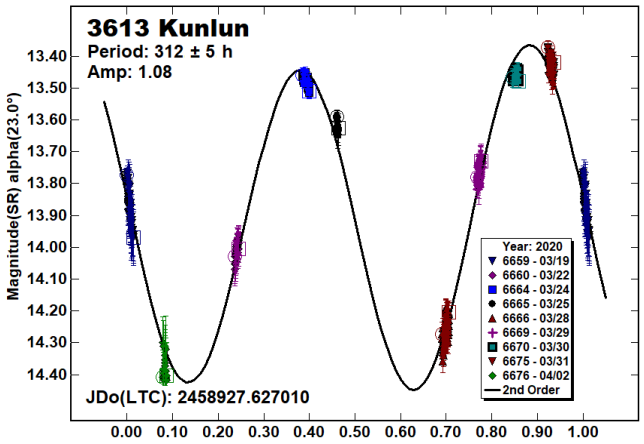


4302 Markeev. The 2019 observations of this 9 km Vestoid escaped publication in our last quarterly article. We previously observed it in 2015 (Stephens, 2016) finding a period of 5.134 h. This year's result is in good agreement.

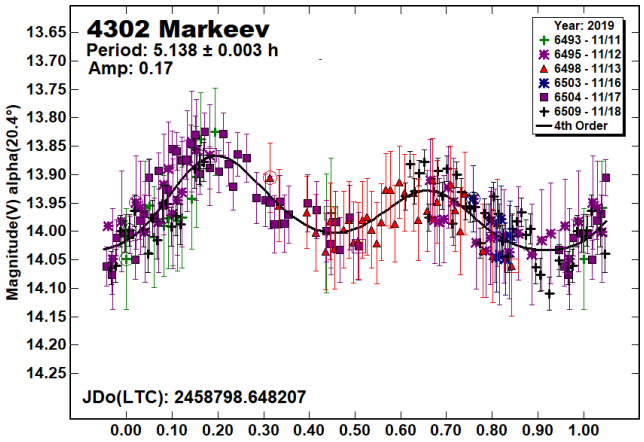


5817 Robertfrazer. Behrend et al. (2004web) and Koff (2005) observed this inner main-belt asteroid determining the rotational period to be 4.051 h. Our initial sessions showed significant deviations that had the traits of *mutual events* (occultations/eclipses) due to a satellite. We used the iterative dual-period search in *MPO Canopus* to find the period of the primary, $P_1$ = 4.05083 h, and reveal the mutual events due to the satellite that has an orbital period of $P_2$ = 28.862 h.

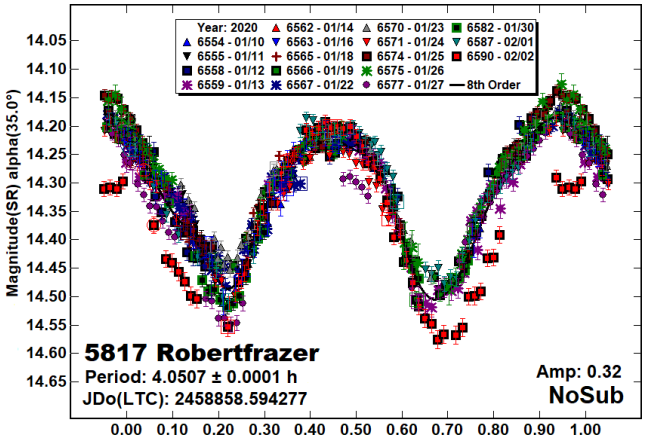


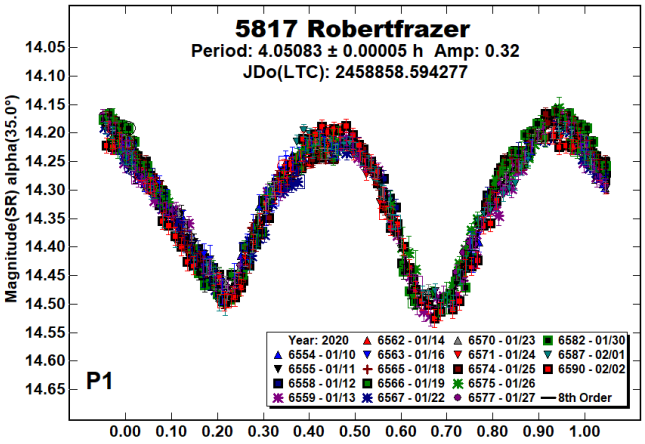


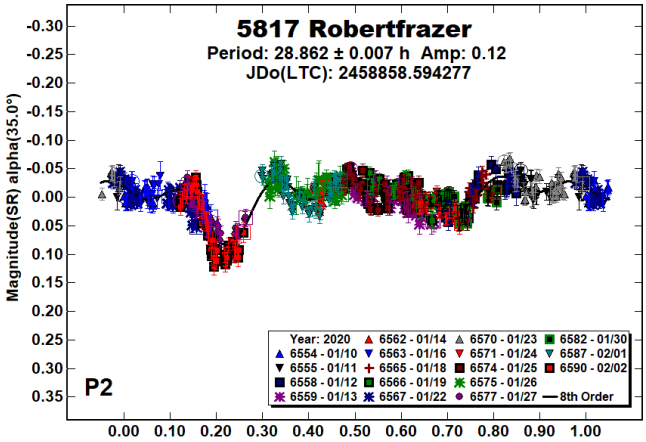


7778 Markrobinson. Behrend (2008web; 2019web) reported periods for this Mars-crosser near 7.23 h. We observed it twice in the past (Warner 2009a; Stephens, 2017) also finding periods near 7.23 h. This year's result is in good agreement with those prior findings and provides additional data for a pole solution.

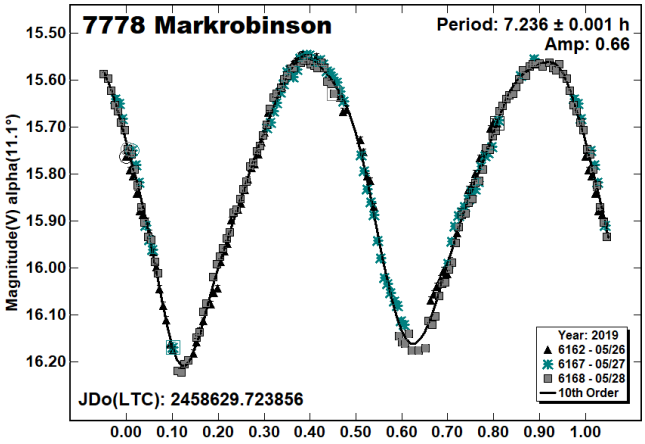


(38181) 1999 JG124. No records were found in the LCDB for this Mars-crosser. Complicating the analysis, winter weather prevented us from getting many consecutive nights of observations. The period spectrum shows many competing aliases, but most were improbable or a fit-by-exclusion. The two periods that seem the most plausible are 9.520 h and 7.936 h. The 7.936 h period is 2/3 of an Earth's day making it impossible to fill in the lightcurve from a single longitude at this opposition. We favor the 9.520 h period because the extrema are 0.50 phase apart and so create a more symmetrical bimodal lightcurve.

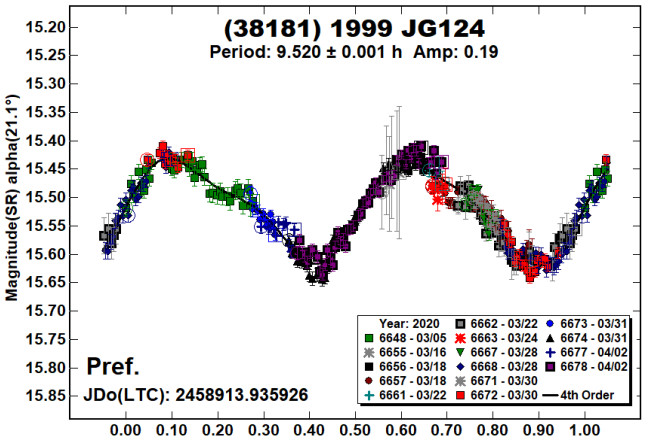


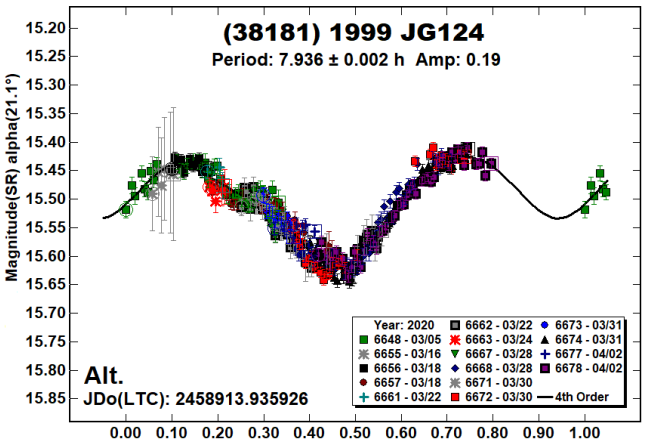


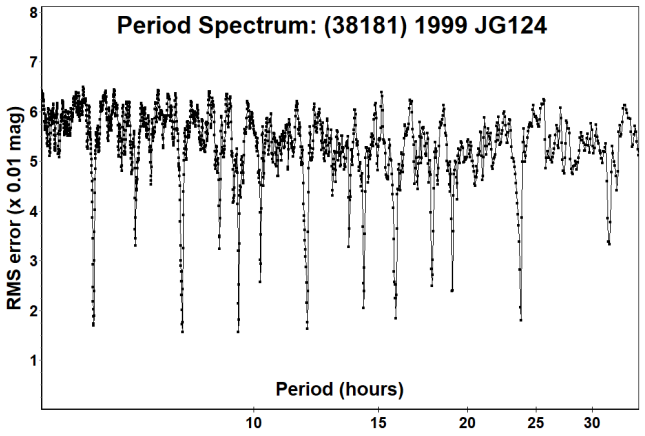


(41475) 2000 PR13. We found no reported lightcurves for this Mars-crosser in the LCDB. Assuming an equatorial view of the asteroid and simple triaxial shape, the 0.62 mag amplitude indicates an a/b ratio of about 1.8:1.

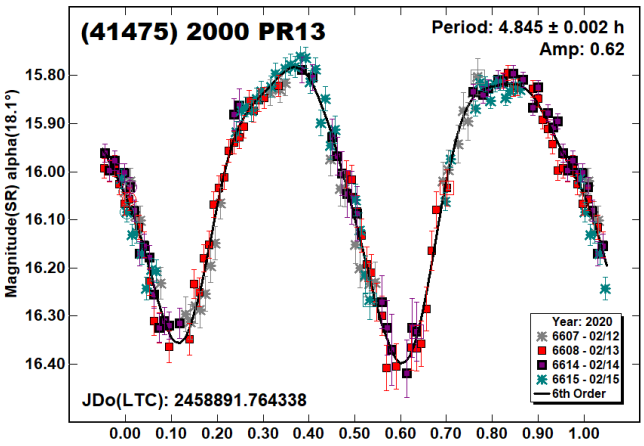


76818 Brianenke. This Hungaria has been well studied in the past, both by us and as part of the Photometric Survey for Asynchronous Binary Asteroids. Pravec et al. (2005web; 2008web) reported a primary period of $P_1$ = 3.16639 h and an orbital period of $P_2$ = 14.11960 h. We previously reported (Warner et al. 2005; 2011; Warner and Stephens, 2009) a primary period of $P_1$ = 3.1666 h and an orbital period of $P_2$ = 14.126 h. To further characterize the system, we undertook observations in 2020 and found primary and orbital periods consistent with prior results.

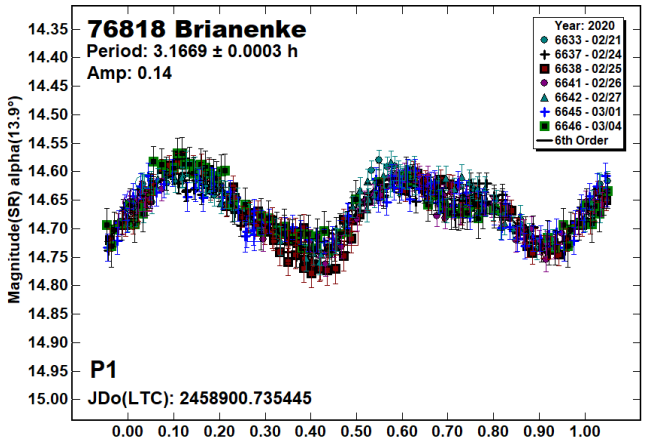


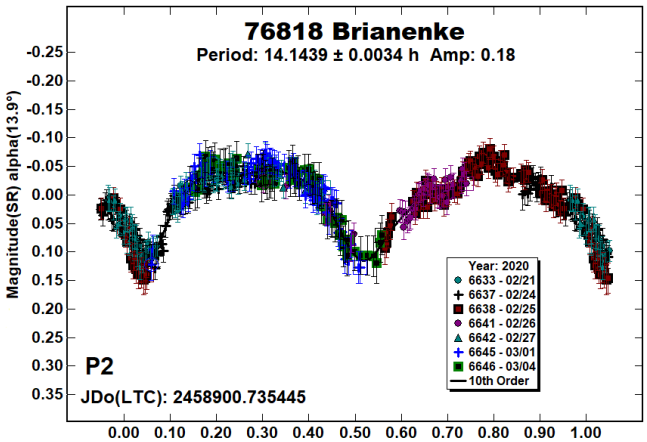

(89776) 2002 AL90. No records were found in the LCDB for this Mars-crosser, making this another new discovery of an asteroid rotational period from CS3.

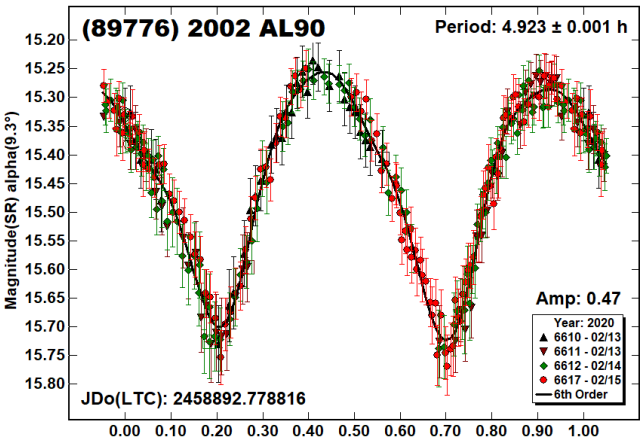


(93040) 2000 SG. Per the LCDB, this Mars-crosser does not have a reported rotational period. Because of winter weather and the encroaching Full Moon, we could get only six nights of observations. The period spectrum showed several possible aliases with the most plausible being near 16 hours (2/3 of an Earth's day). Therefore, it was not possible to complete the lightcurve from a single longitude.

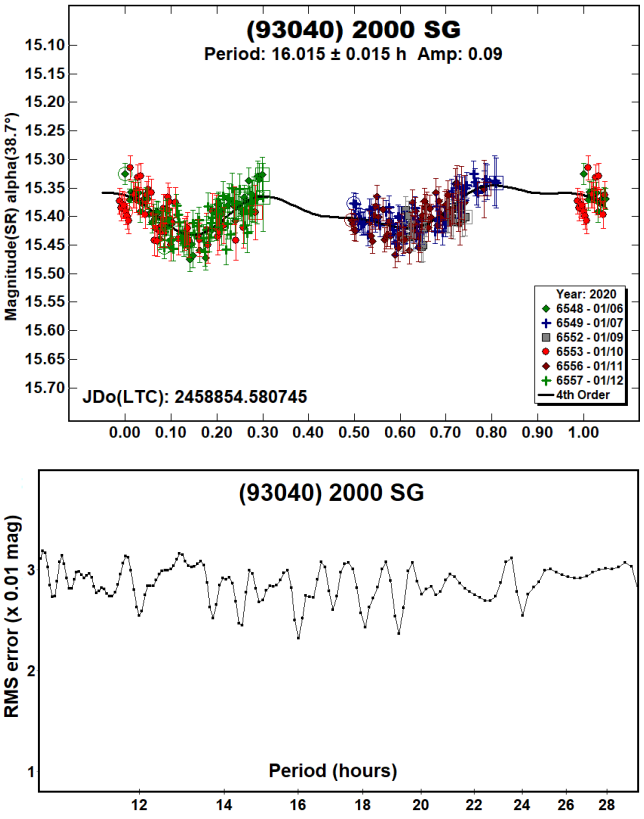


Acknowledgements

Observations at CS3 and continued support of the asteroid lightcurve database (LCDB; Warner et al., 2009) are supported by NASA grant 80NSSC18K0851.

This work includes data from the Asteroid Terrestrial-impact Last Alert System (ATLAS) project. ATLAS is primarily funded to search for near earth asteroids through NASA grants NN12AR55G, 80NSSC18K0284, and 80NSSC18K1575; byproducts of the NEO search include images and catalogs from the survey area. The ATLAS science products have been made possible through the contributions of the University of Hawaii Institute for Astronomy, the Queen's University Belfast, the Space Telescope Science Institute, and the South African Astronomical Observatory.

The purchase of a FLI-1001E CCD cameras was made possible by Gene Shoemaker NEO Grants from the Planetary Society (2007, 2013). These were used to purchase some of the telescopes and CCD cameras used in this research.

References

Aznar, M.A. (2017). "Density and Axis-size Relationship of Five Main-belt Asteroids: 2017 January - March." *Minor Planet Bull.* **44**, 276-279.

Behrend, R. (2001web, 2004web, 2006web, 2008web, 2019web). Observatoire de Geneve web site. *http://obswww.unige.ch/~behrend/page_cou.html*

Bembrick, C. (2005). "Period determination for 463 Lola." *Minor Planet Bull.* **32**, 25.

Harris, A.W.; Young, J.W.; Scaltriti, F.; Zappala, V. (1984). "Lightcurves and phase relations of the asteroids 82 Alkmene and 444 Gyptis." *Icarus* **57**, 251-258.

Harris, A.W.; Young, J.W.; Bowell, E.; Martin, L.J.; Millis, R.L.; Poutanen, M.; Scaltriti, F.; Zappala, V.; Schober, H.J.; Debehogne, H.; Zeigler, K.W. (1989). "Photoelectric Observations of Asteroids 3, 24, 60, 261, and 863." *Icarus* **77**, 171-186.

Henden, A.A.; Terrell, D.; Levine, S.E.; Templeton, M.; Smith, T.C.; Welch, D.L. (2009). *http://www.aavso.org/apass*

Klinglesmith, D.; Hendrickx, S.; Kimber, C.; Madden, K. (2016). "CCD Asteroid Photometry from Etscorn Observatory." *Minor Planet Bull.* **43**, 234-239.

Koff, R. (2005). "Lightcurve photometry of asteroids 212 Medea, 517 Edith, 3581 Alvarez, 5682 Beresford, and 5817 Robertfrazer." *Minor Planet Bull.* **32**, 32-34.

Lecrone, C.; Mills, G.; Ditton, R. (2005). "Lightcurves and periods for asteroids 463 Lola, 523 Ada, 544 Jetta, 642 Clara, 883 Matterania, 6475 Refugium." *Minor Planet Bull.* **32**, 62-64.

Menke, J. (2005). "Asteroid lightcurve results from Menke Observatory." *Minor Planet Bull.* **32**, 85-88.

Pál, A.; Szakáts, R.; Kiss, C.; Bódi, A.; Bognár, Z.; Kalup, C.; Kiss, L.L.; Marton, G.; Molnár, L.; Plachy, E.; Sárneczky, K.; Szabó, G.M.; Szabó, R. (2020). "Solar System Objects Observed with TESS—First Data Release: Bright Main-belt and Trojan Asteroids from the Southern Survey." *Ap. J.* **247**, A26.

Pravec, P.; Wolf, M.; Sarounova, L. (2005web, 2008web, 2006web, 2009web, 2011web, 2012web, 2016web, 2020web). *http://www.asu.cas.cz/~ppravec/neo.htm*

| Number | Name | 2019 mm/dd | Phase | $L_{PAB}$ | $B_{PAB}$ | Period(h) | P.E. | Amp | A.E. | Grp |
|---|---|---|---|---|---|---|---|---|---|---|
| 463 | Lola | 02/06-02/11 | 26.1,26.3 | 72 | 12 | 6.203 | 0.002 | 0.44 | 0.02 | MB-I |
| 914 | Palisana 2008 | 11/07-11/15 | 10.2,11.0 | 40 | 19 | [A]8.686 | 0.002 | 0.03 | 0.01 | PHO |
| | | | | | | 15.916 | 0.005 | 0.03 | 0.01 | |
| 1106 | Cydonia | 01/06-01/09 | 19.0,19.4 | 45 | 15 | 2.678 | 0.001 | 0.35 | 0.03 | EUN |
| 1169 | Alwine | 02/16-03/04 | 12.1,19.2 | 128 | -5 | 2.9274 | 0.0001 | 0.32 | 0.02 | FLOR |
| | Sat. orbital period | | | | | 13.408 | 0.002 | 0.09 | 0.02 | |
| 1589 | Fanatica | 03/07-03/16 | 5.2,3.2 | 176 | 7 | 2.5832 | 0.0002 | 0.20 | 0.02 | V |
| 1806 | Derice | 02/05-02/21 | 29.1,28.8 | 62 | 1 | 3.22443 | 0.0001 | 0.14 | 0.01 | FLOR |
| 2023 | Asaph 2001 | 11/03-01/05 | 16.5,16.8 | 12.2 | 9.3 | 89.2 | 0.7 | 0.31 | 0.02 | MB-O |
| 3267 | Glo | 01/13-01/25 | 19.9,24.4 | 89 | -7 | 6.8778 | 0.0004 | 0.39 | 0.02 | MC |
| 3613 | Kunlun | 03/19-04/02 | 23.0,25.6 | 133 | 9 | 312 | 5 | 0.08 | 1.08 | V |
| 4302 | Markeev 2019 | 11/11-11/18 | 20.5,21.4 | 356 | -4 | 5.138 | 0.003 | 0.17 | 0.02 | V |
| 5817 | Robertfrazer | 01/10-02/02 | 35.0,36.0 | 70 | 28 | 4.05083 | 5.0001 | 0.32 | 0.01 | MC |
| | Sat. orbital period | | | | | 28.862 | 0.007 | 0.12 | 0.02 | |
| 7778 | Markrobinson 2019 | 05/26-05/28 | 11.1,10.8 | 253 | 14 | 7.236 | 0.001 | 0.66 | 0.02 | MC |
| 38181 | 1999 JG124 | 03/05-04/02 | *21.2,22.6 | 188 | 25 | [A]9.520 | 0.001 | 0.19 | 0.02 | MC |
| | | | | | | 7.936 | 0.002 | 0.19 | 0.02 | |
| 41475 | 2000 PR13 | 02/12-02/15 | 18.1,19.9 | 118 | -3 | 4.845 | 0.002 | 0.62 | 0.02 | MC |
| 76818 | Brianenke | 02/21-03/04 | 13.9,19.4 | 137 | -15 | 3.1669 | 0.0003 | 0.14 | 0.01 | H |
| | Sat. orbital period | | | | | 14.1439 | 0.0034 | 0.18 | 0.01 | |
| 89776 | 2002 AL90 | 02/13-02/15 | 9.3,8.1 | 157 | 4 | 4.923 | 0.001 | 0.47 | 0.02 | MC |
| 93040 | 2000 SG | 01/06-01/12 | 38.7,39.1 | 56 | 28 | 16.015 | 0.015 | 0.09 | 0.02 | MC |

Table II. Observing circumstances and results. [A]The preferred period of an ambiguous solution. The phase angle is given for the first and last date. If preceded by an asterisk, the phase angle reached an extrema during the period. $L_{PAB}$ and $B_{PAB}$ are the approximate phase angle bisector longitude/latitude at mid-date range (see Harris et al., 1984). Grp is the asteroid family/group (Warner et al., 2009). For a binary, the first line gives the rotation period of the primary and the second line gives the orbital period of the satellite.


Pravec, P.; Harris, A.W.; Scheirich, P.; Kušnirák, P.; Šarounová, L.; Hergenrother, C.W.; Mottola, S.; Hicks, M.D.; Masi, G.; Krugly, Yu.N.; Shevchenko, V.G.; Nolan, M.C.; Howell, E.S.; Kaasalainen, M.; Galád, A.; Brown, P.; Degraff, D.R.; Lambert, J. V.; Cooney, W.R.; Foglia, S. (2005). "Tumbling asteroids." *Icarus* **173**, 108-131.

Stephens, R.D. (2015). "Asteroids Observed from CS3: 2014 July – September." *Minor Planet Bull.* **42** 70-74.

Stephens, R.D. (2016). "Asteroids Observed from CS3: 2015 July - September." *Minor Planet Bull.* **43**, 52-56.

Stephens, R.D. (2017). "Asteroids Observed from CS3: 2016 October - December." *Minor Planet Bull.* **44**, 120-122.

Stephens, R.D.; Warner, B.D. (2019). "Main-belt Asteroids Observed from CS3: 2018 October - December." *Minor Planet Bull*. **46**, 180-187.

Tonry, J.L.; Denneau, L.; Flewelling, H.; Heinze, A.N.; Onken, C.A.; Smartt, S.J.; Stalder, B.; Weiland, H.J.; Wolf, C. (2018). "The ATLAS All-Sky Stellar Reference Catalog." *Astrophys. J.* **867**, A105.

Warner, B.D. (2003). "Lightcurve analysis of asteroids 331, 795, 886, 1266, 2023, 3285, and 3431." *Minor Planet Bull*. **30**, 61-64.

Warner, B.D. (2004). "Lightcurve analysis for numbered asteroids 1351, 1589, 2778, 5076, 5892, and 6386." *Minor Planet Bull.* **31**, 36-39.

Warner, B.D.; Pravec, P.; Pray, D. (2005). "(76818) 2000 RG_79." *IAU Circ.,* No. 8592, #2.

Warner, B.D. (2009a). "Asteroid Lightcurve Analysis at the Palmer Divide Observatory: 2008 May - September." *Minor Planet Bull.* **36**, 7-13.

Warner, B.D. (2009b). "Asteroid Lightcurve Analysis at the Palmer Divide Observatory: 2008 September - December." *Minor Planet Bull.* **36**, 70-73.

Warner, B.D.; Stephens, R.D. (2009). "Lightcurve Analysis of Two Binary Asteroids: (76818) 2000 RG79 and (185851) 2000 DP107." *Minor Planet Bull*. **36**, 63-63.

Warner, B.D.; Harris, A.W.; Pravec, P. (2009). "The Asteroid Lightcurve Database." *Icarus* **202**, 134-146. Updated 2020 March. *http://www.minorplanet.info/lightcurvedatabase.html*

Warner, B.D.; Pravec, P.; Kusnirak, P.; Harris, A.W.; Cooney Jr., W.R.; Gross, J.; Terrell, D.; Nudds, S.; Vilagi, J.; Gajdos, S.; Masi, G.; Pray, D.P.; Dyvig, R.; Reddy, V. (2011). "Lightcurves from the Initial Discovery of Four Hungaria Binary Asteroids." *Minor Planet Bull*. **38**, 107-109.

# PHOTOMETRY OF 39 ASTEROIDS AT SOPOT ASTRONOMICAL OBSERVATORY: 2019 SEPTEMBER - 2020 MARCH

Vladimir Benishek
Belgrade Astronomical Observatory
Volgina 7, 11060 Belgrade 38, SERBIA
vlaben@yahoo.com

(Received: 2020 April 14)

CCD photometric observations of 39 asteroids were conducted at Sopot Astronomical Observatory (SAO) from 2019 September through 2020 March. A review of the results obtained for synodic rotation periods as well as the established lightcurves is presented here.

Photometric observations of 39 asteroids were conducted at Sopot Astronomical Observatory (SAO) between 2019 September - 2020 March in order to determine their synodic rotation periods. For this purpose, two 0.35-m *f*/6.3 Meade LX200GPS Schmidt-Cassegrain telescopes were employed. The telescopes are equipped with SBIG ST-8 XME and SBIG ST-10 XME CCD cameras. The exposures were unfiltered and unguided for all targets. Both cameras were operated in 2×2 binning mode, which produces image scales of 1.66 arcsec/pixel and 1.25 arcsec/pixel for ST-8 XME and ST-10 XME cameras, respectively. Prior to measurements, all images were corrected using dark and flat field frames.

Photometric reduction, lightcurve construction, and period analysis were conducted using *MPO Canopus* (Warner, 2018). Differential photometry with up to five comparison stars of near solar color ($0.5 \leq$ B-V $\leq 0.9$) was performed using the Comparison Star Selector (CSS) utility. This helped ensure a satisfactory quality level of night-to-night zero-point calibrations and correlation of the measurements within the standard magnitude framework. Field comparison stars were calibrated using standard Cousins R magnitudes derived from the Carlsberg Meridian Catalog 15 (VizieR, 2019) Sloan r′ magnitudes using the formula R = r′ - 0.22. In some instances, small zero-point adjustments were necessary in order to achieve the best match between individual data sets in terms of minimum RMS residual of a Fourier fit.

Some of the targets presented in this paper were observed within the Photometric Survey for Asynchronous Binary Asteroids (BinAstPhot Survey) under the leadership of Petr Pravec from Ondřejov Observatory, Czech Republic.

Table I gives the observing circumstances and results.

1274 Delportia. A search for previous rotation periods in the LCDB (Warner et al., 2009) finds the following results: 5.5 h (Behrend, 2005web), 5.615 h (Sheridan, 2011), and 5.620 h (Waszczak et al., 2015). The dense photometric observations obtained at SAO over a single night in 2020 January led to a synodic period of $P$ = 5.56 ± 0.02 h, which is in good agreement with the previously established periods.

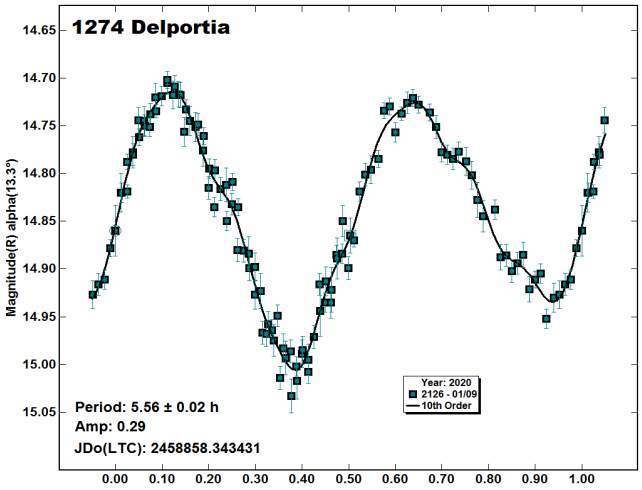


1316 Kasan. Observations made over three consecutive nights in 2019 October yielded a bimodal lightcurve phased to a period of $P$ = 5.843 ± 0.003 h as the most favorable period solution for this Mars-crossing asteroid. This is quite consistent with the results by Warner (2005, 5.83 h) and Stephens (2009, 5.82 h).

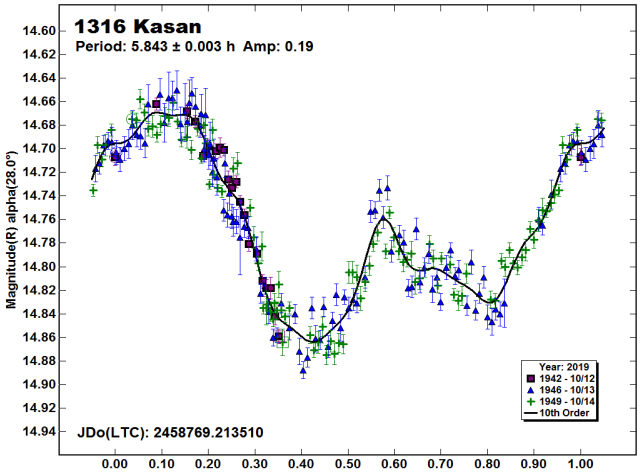


1706 Dieckvoss. Oey (2016) found a rotation period of 2.58944 h for this inner main-belt asteroid. The SAO observations conducted over two nights in 2020 February show a similar result: $P$ = 2.5892 ± 0.0004 h.

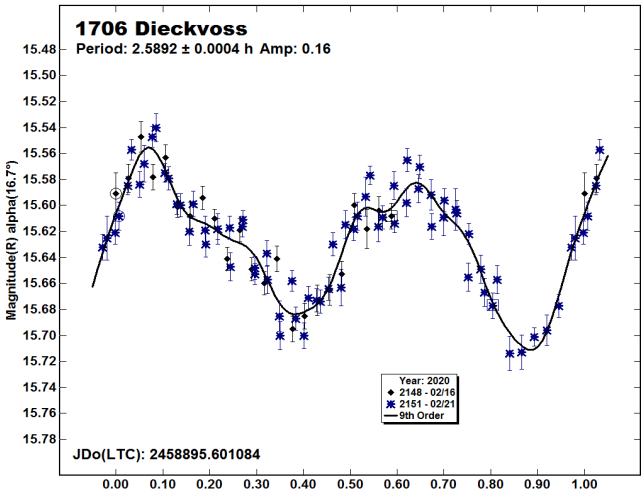

2075 Martinez. The only previous rotation period determination is by Menke et al. (2008, 4.755 h). Period analysis of the SAO data obtained in 2019 December - 2020 January on two nights shows the favored solution to be a bimodal lightcurve with a period of $P = 4.7531 \pm 0.0007$ h and amplitude of 0.27 mag.

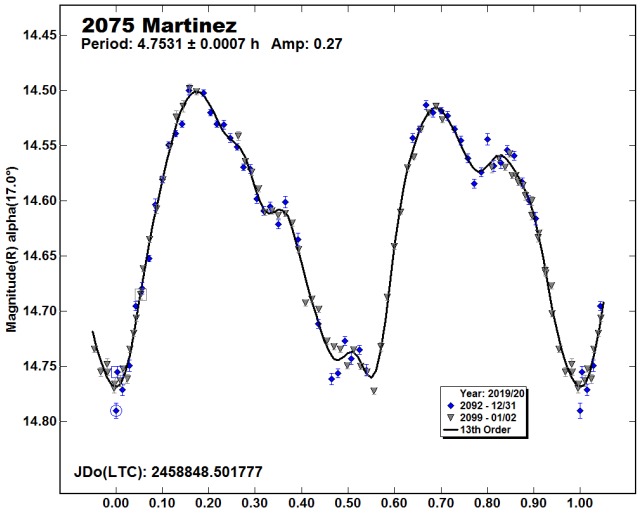


2103 Laverna. Two previous period determinations indicate completely different results: 9.249 h (Klinglesmith et al., 2005) and 11.0 h (Behrend, 2016web), of which the latter is an estimate based on an incomplete lightcurve obtained over a single night.

The SAO observations from 2019 October point to a bimodal period of $P = 9.240 \pm 0.005$ h, which is in a full agreement with that found by Klinglesmith et al. (2005).

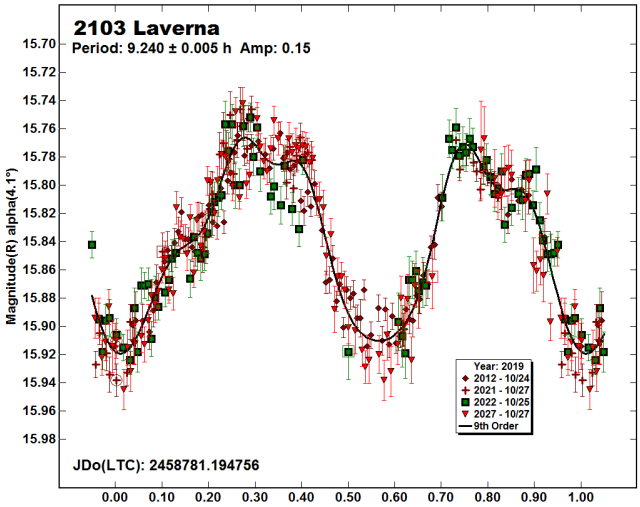


2227 Otto Struve. This was a BinAstPhot Survey target with no previously known rotation period. It was observed solely at SAO on three nights in 2020 January. A unique rotation period solution of $P = 5.397 \pm 0.002$ h was found.

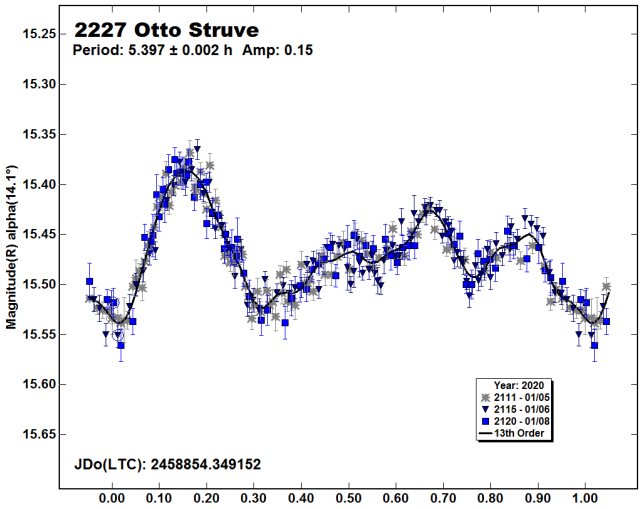


2432 Soomana. The SAO data gathered on three consecutive nights on this Vestoid asteroid in 2019 October show an unambiguous rotation period of $P = 3.2060 \pm 0.0006$ h, associated with a large amplitude (0.42 mag.) bimodal lightcurve.

This period result is fully consistent with two previous results: 3.206 h (Klinglesmith et al., 2013) and 3.207 h (Waszczak et al., 2015).

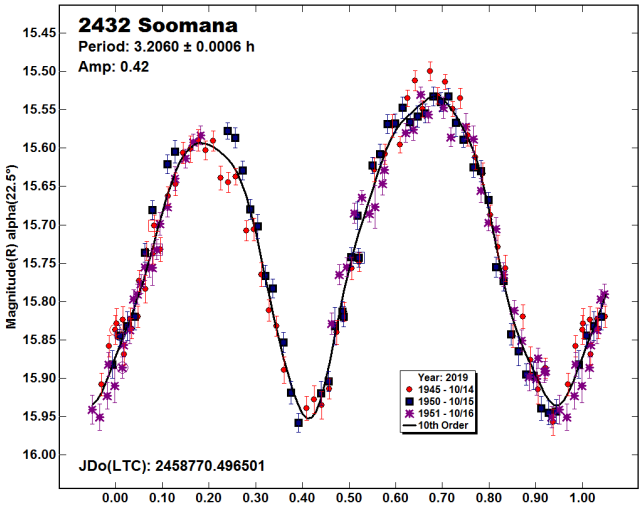


2566 Kirghizia. Montgomery et al. (2013) found the only previously known rotation period, 4.451 h. Photometric data taken on two consecutive nights at SAO yielded a unique bimodal solution of $P = 4.448 \pm 0.002$ h associated with a large amplitude (0.70 mag.) lightcurve.

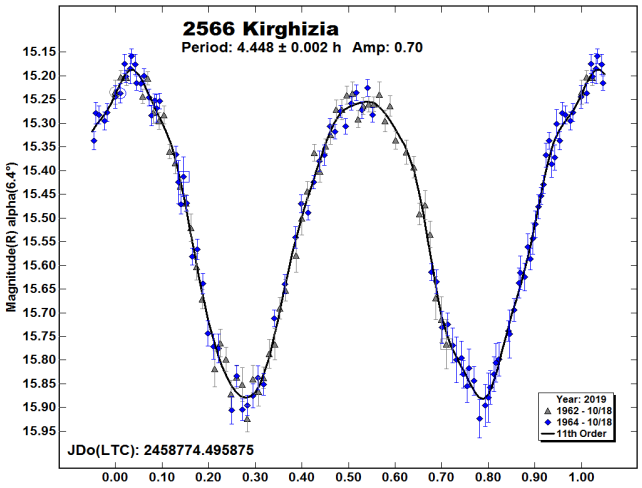


2871 Schober. Yankov and Ditteon (2009) found a synodic rotation period of 2.8674 h. The SAO data collected over nine nights in 2019 December and 2020 January indicate $P$ = 2.85225 ± 0.00005 h, differing slightly from the previous result.

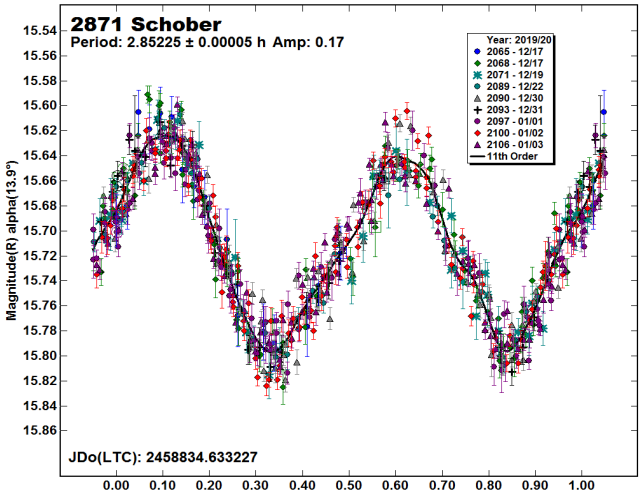


2890 Vilyujsk. Previous period determinations are those of Koff (2003, 3.45 h), Ruthroff (2013, 3.45 h) and Waller (2013, 3.42 h). The SAO observations carried out in 2020 January show a value very close to those earlier ones: $P$ = 3.4610 ± 0.0003 h.

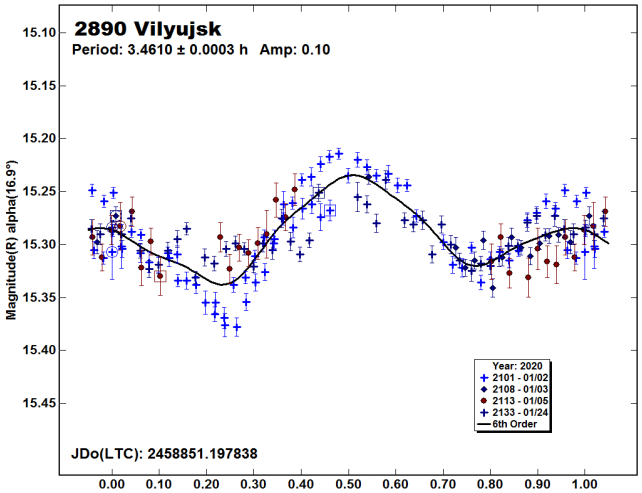


2937 Gibbs. Several rotation period determinations were known for this Mars-crossing asteroid prior to the SAO observations in 2019 October. These include Behrend (2005web; 3.06153 h) and Stephens (2017; 3.189 h). In addition, the most recent results came from the 2019 apparition: Warner and Stephens (2019; 2.982 h) and Benishek (2019; 2.9820 h).

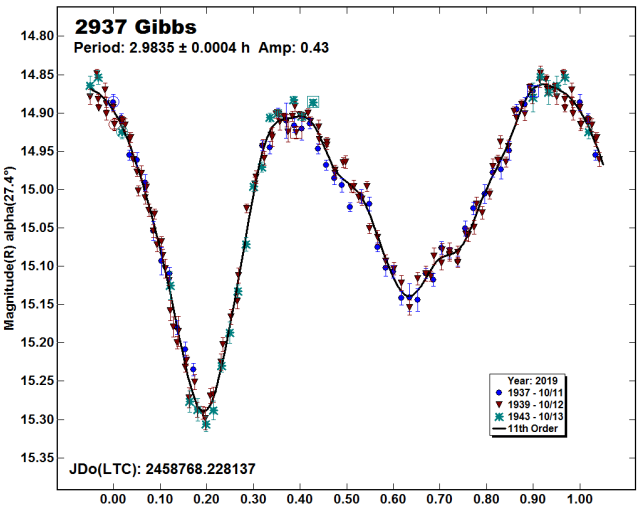


The SAO photometric observations carried out on three consecutive nights resulted in a moderately large amplitude (0.43 mag.) bimodal lightcurve phased to a unique period of $P$ = 2.9835 ± 0.0004 h.

3385 Bronnina. The LCDB records indicate several previously known rotation periods, e.g. by Coley (2012, 2.996 h), Behrend (2014web, 2.93 h) and Dykhuis et al. (2016, 2.95897 h).

This target was observed at two different viewing geometries, first in late 2019 November over a single night and then 2019 January to February 1 on three nights. Hence two, independent lightcurves different in shape were obtained. The single-night 2019 November SAO data indicate a rotation period of 2.974 ± 0.009 h, whilst period analysis of the 2020 January-February data gives a secure period value of 2.95911± 0.00009 h.

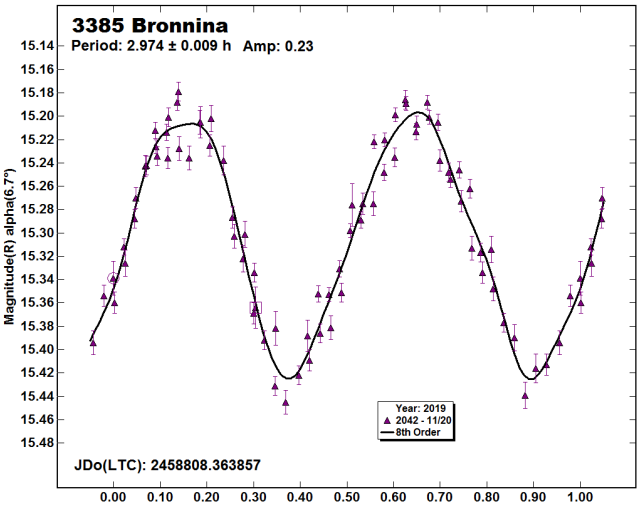

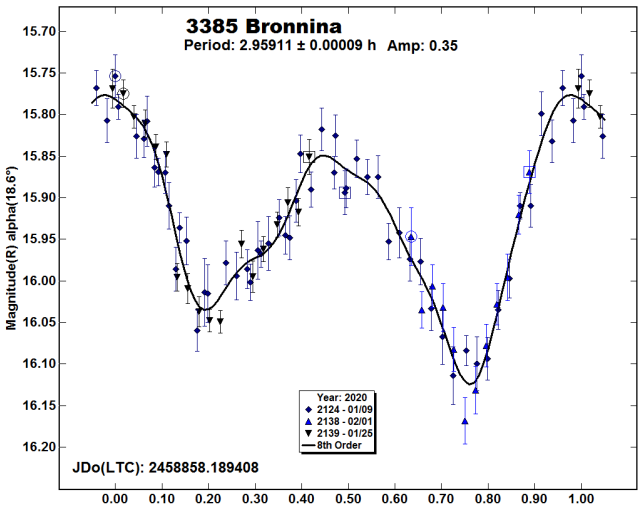


3489 Lottie is a Vestoid type asteroid with no previously known rotation period. Observed over five nights in 2019 October-November at SAO, analysis found an unambiguous bimodal solution of $P = 2.94832 \pm 0.00009$ h.

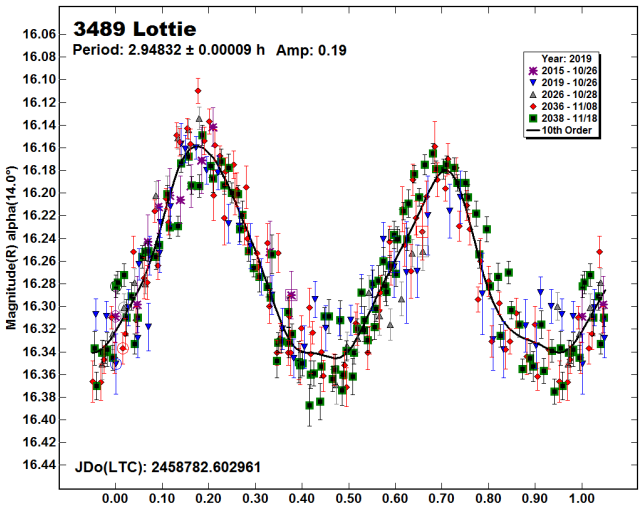


3842 Harlansmith. The only previously determined rotation period was by Han et al. (2013, 2.7938 h).

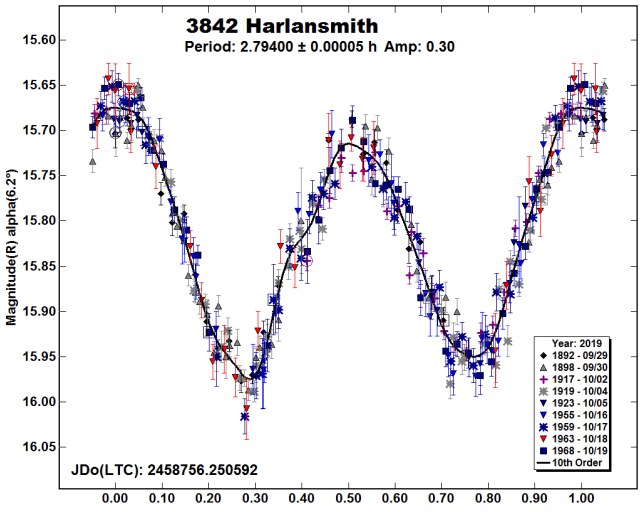


Based on data obtained over nine nights in 2019 September-October at SAO, the most likely solution was a 0.30 mag. amplitude bimodal lightcurve phased to a period of $P = 2.79400 \pm 0.00005$ h

3904 Honda. There were no previously reported rotation period results for this Eunomia family asteroid. Five datasets taken in 2019 October led to a period solution of $P = 8.464 \pm 0.003$ h.

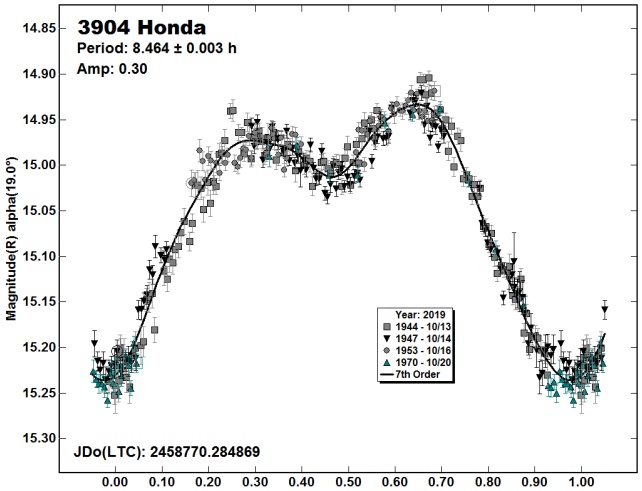


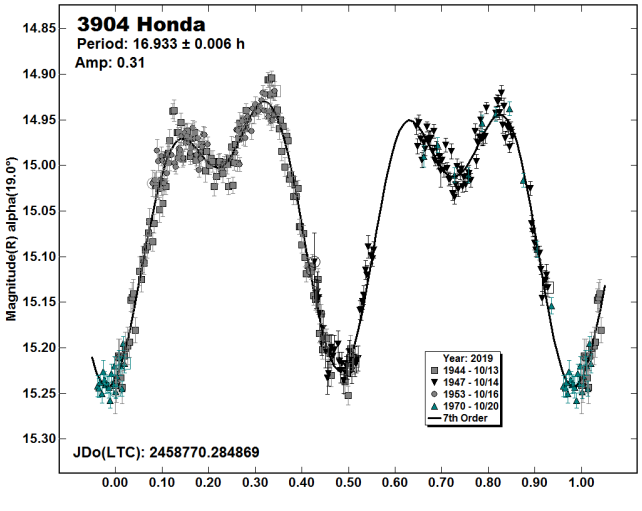


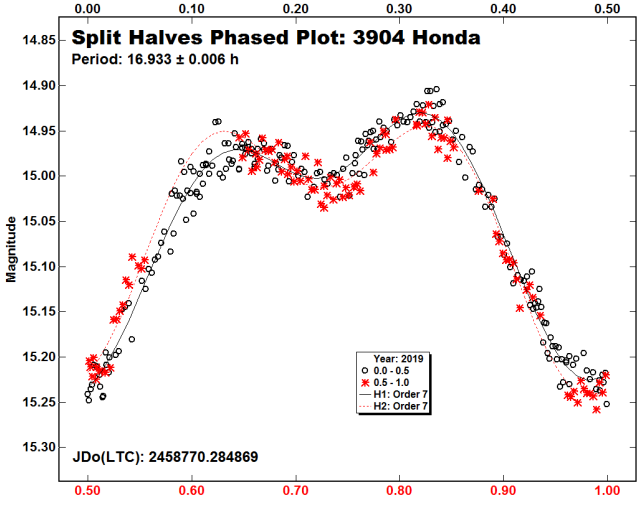

Aside from this solution, a period twice as long of 16.933 h appears in the period spectrum as a possible result, which should not be ruled out given the negligible differences between the two halves of the corresponding lightcurve. Since it is possible that those differences come from a slightly higher noise level in the current data, it would be desirable to observe this target in the future to securely determine which of the two periods is the correct one.

3986 Rozhkovskij. Several earlier rotation period determinations were found in the LCDB: Birlan et al. (1996, 4.26 h) and Warner (2010, 3.548 h). Period analysis of the SAO data taken on two consecutive nights in 2019 October show a unique bimodal solution for a period of $P = 3.549 \pm 0.002$ h.

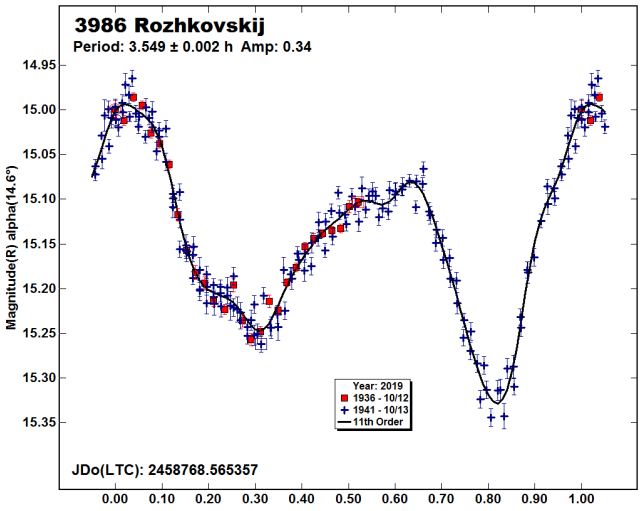


4705 Secchi. No rotation periods were found in the LCDB. The observations were performed over four nights in 2020 March. Due to slightly higher noise level in the obtained data and a relatively low amplitude (0.17 mag.), it is not easy to distinguish between a period of $P = 2.6566 \pm 0.0004$ h and a harmonically related double period of 5.3131 ± 0.0007 h.

The two halves of the lightcurve for the longer period do not fully match, which could be due to higher noise and means that the longer period cannot be formally excluded. The shorter found period is adopted here as more likely. As in other similar cases, only high-quality future observations can give a definitive answer.

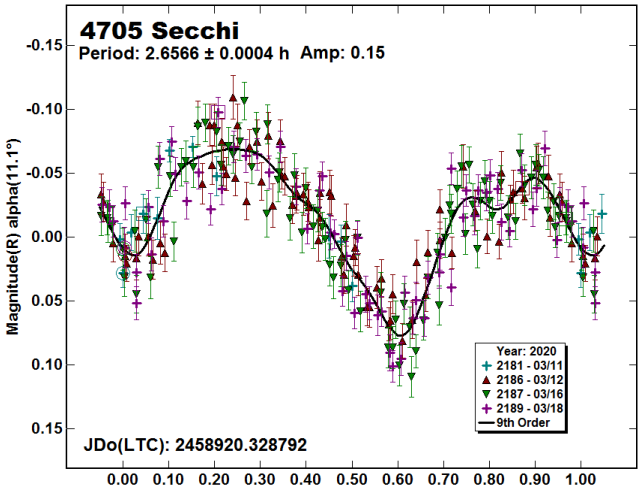


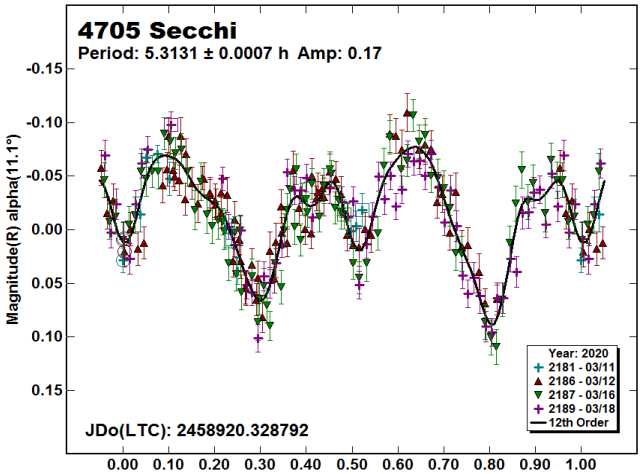


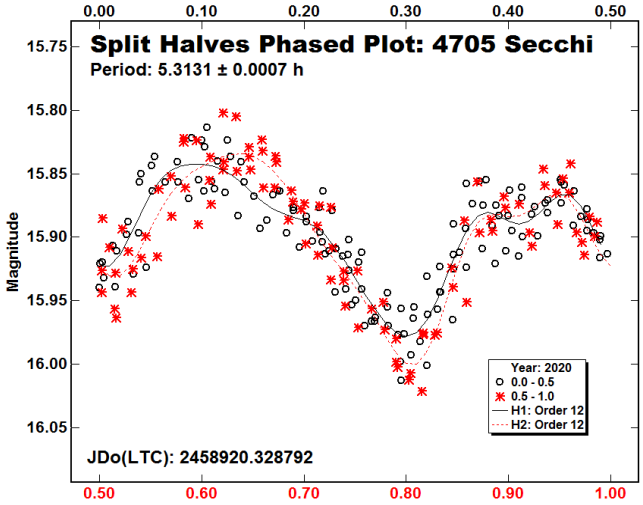


4857 Altgamia. This was a BinAstPhot Survey target with no previously known rotation period. The observations taken at SAO throughout 2020 January revealed a 0.29 mag. lightcurve phased to a period of $P = 9.0357 \pm 0.0004$ h as a most plausible solution.

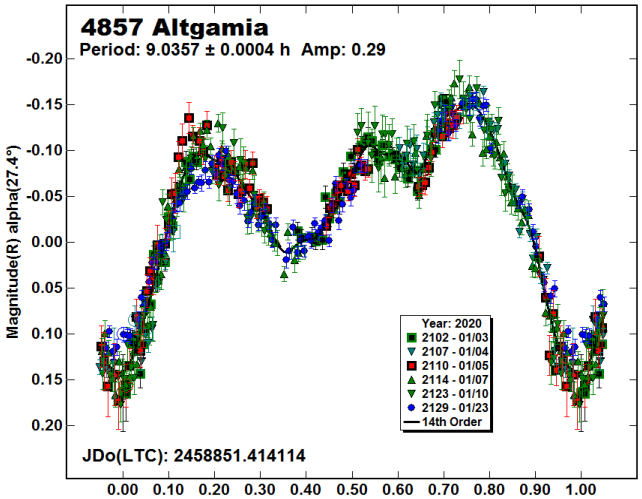


4875 Ingalls. Garceran et al. (2016) found a synodic rotation period of 3.78 h based a somewhat noisy data set (rated U = 2+ in the LCDB). Analysis of the 2019 October SAO observations nevertheless confirm the previous result, showing a unique period of $P = 3.7783 \pm 0.0007$ h.

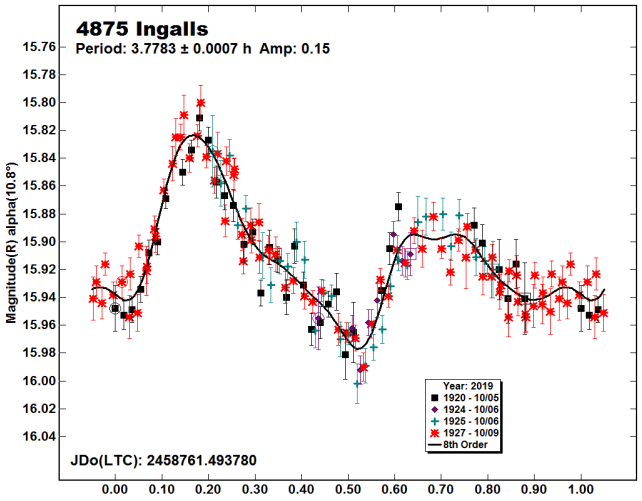


5096 Luzin. The synodic rotation period by Klinglesmith et al. (2013; 3.054 h) was the only one found in the LCDB. Two consecutive nights of observations at SAO in 2019 October resulted in a rather large amplitude (0.39 mag.) bimodal lightcurve with a unique period of $P = 3.051 \pm 0.001$ h.

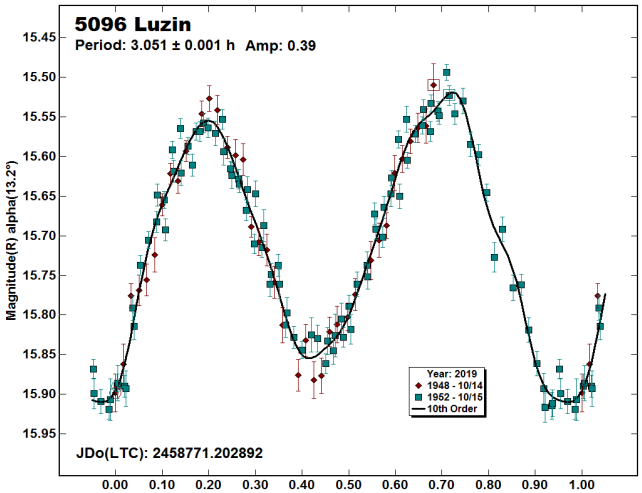


5186 Donalu. Casalnuovo (2016) reported a rotation period of 3.15 h. The period found from the 2019 October SAO data, $P = 3.153 \pm 0.001$ h, is consistent with this Casalnuovo (2016).

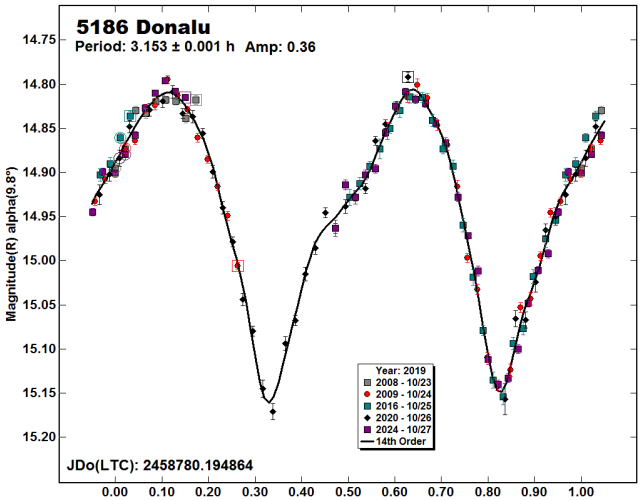


5391 Emmons. Clark and Joyce (2003) found a synodic rotation period of 3.028 h for this inner main-belt asteroid. The 2019 October SAO data obtained on three nights led to an almost identical result of $P = 3.030 \pm 0.001$ h.

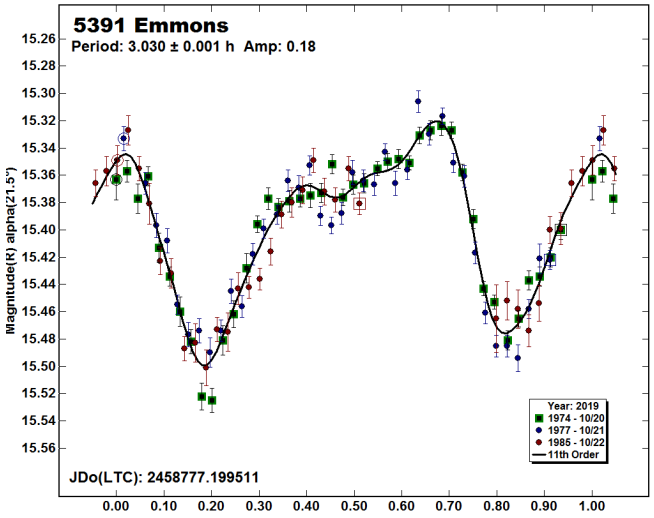


(5512) 1988 VD7. No prior rotation period results on this Flora asteroid exist. Observations were conducted in second half of 2019 December in the course of four nights. Out of the many possible period solutions, the most prominent are the monomodal one at $P = 3.3059 \pm 0.0003$ h and a bimodal lightcurve at the double period of 6.61 h.

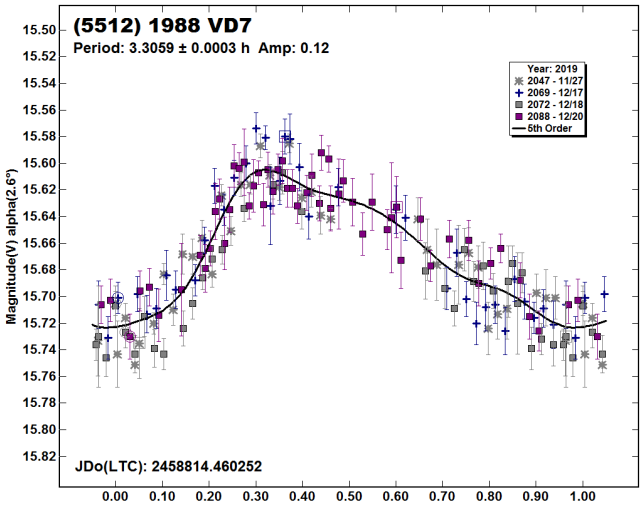


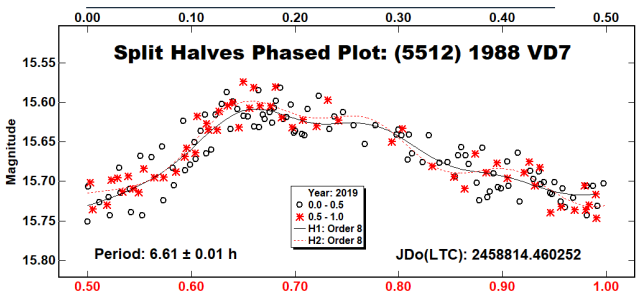

The two halves of the bimodal lightcurve are almost exactly identical, within the boundaries of the data scatter. This fact supports the shorter period as a solution although the possibility of a bimodal period should not be entirely ruled since the minimal differences in the two halves could be concealed in the noise. As in other similar cases, resolving this kind of period ambiguity requires intensive gathering of better-quality data at future apparitions.

5537 Sanya. The only previous rotation period result by Waszczak et al. (2015; 3.427 h) is almost identical to the result derived from the SAO data acquired in 2019 October on three consecutive nights, $P = 3.4254 \pm 0.0009$ h.

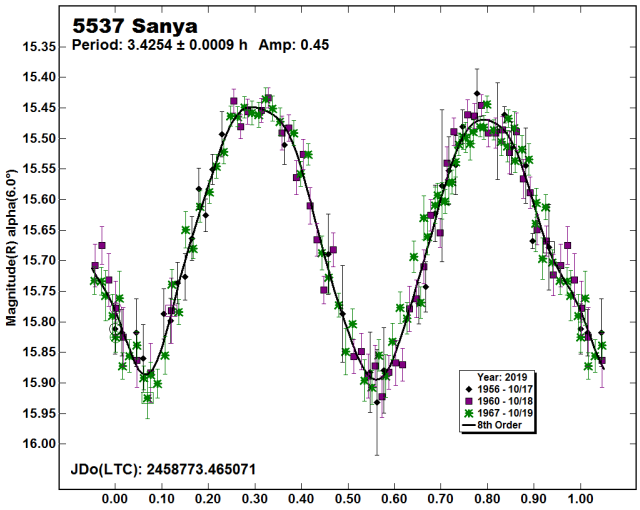


5543 Sharaf. No previous rotation period determinations were found for this Flora family asteroid. Data obtained on two consecutive 2019 December nights reveal an extremely large amplitude (1.21 mag.) bimodal lightcurve phased to a period of $P = 5.972 \pm 0.002$ h, indicating a very elongated shape.

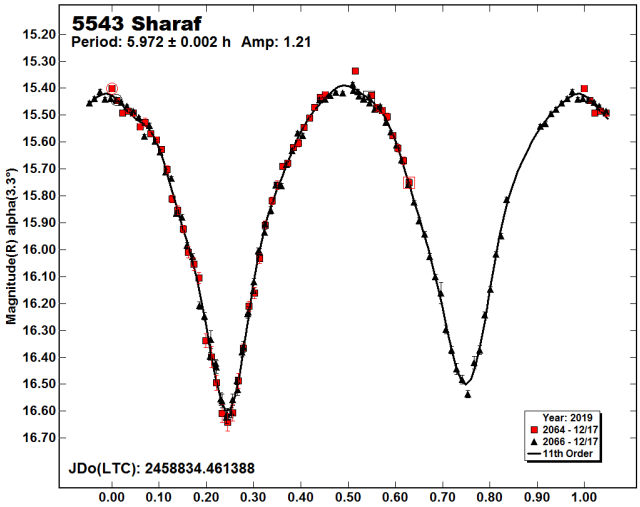


7368 Haldancohn was another BinAstPhot Survey program target observed solely at Sopot Observatory during the 2020 apparition. Data taken on four nights in 2019 February confirm the period result found, also within the BinAstPhot Survey, at the 2017 apparition (Pravec, 2017web; 3.90337 h). The newly established value is $P = 3.9032 \pm 0.0002$ h.

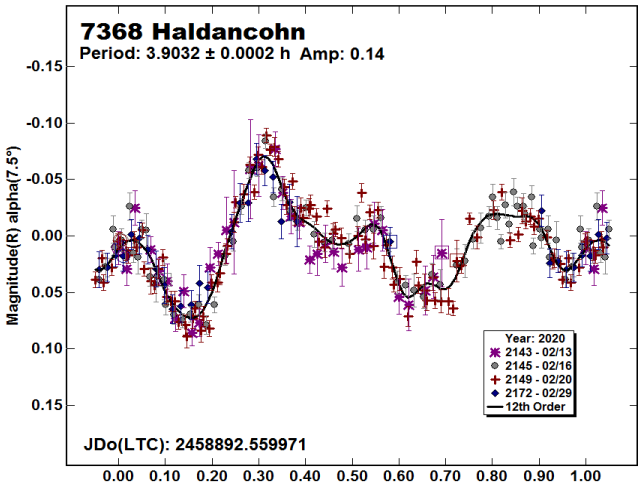


7527 Marples. Behrend (2018web) states 7.85 h for a synodic rotation period. This result is based on a single night data and a provisional lightcurve. The newly established unique bimodal results based on the 2019 October SAO data collected on three consecutive nights are $P = 9.098 \pm 0.004$ h, $A = 0.54$ mag.

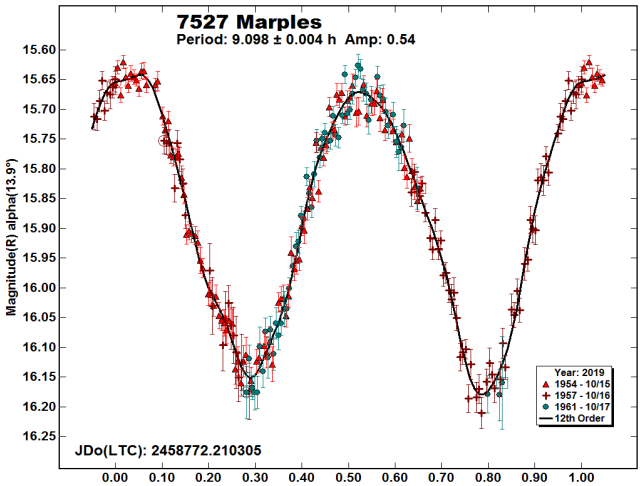


9717 Lyudvasilia. No reports on rotation period determinations were found in the LCDB. The asteroid was observed at Sopot Observatory in the second half of 2019 December over four nights. Period analysis shows a solution of $P = 2.8421 \pm 0.0002$ h.

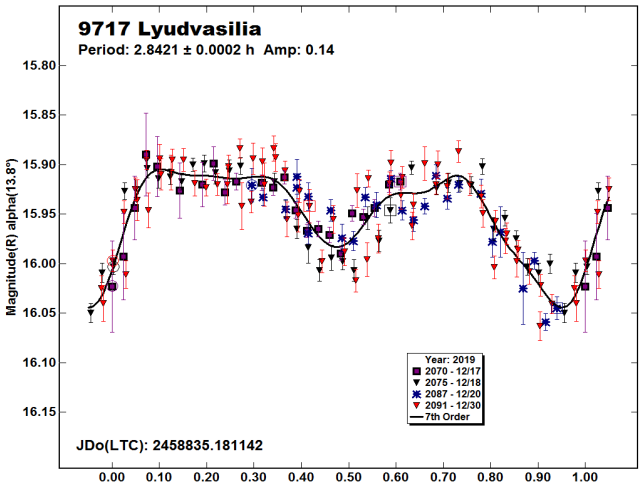

(11230) 1999 JV57, (11420) 1999 KR14 are Flora family members with no previously known rotation periods. The 2019 November-December SAO observations of 1999 JV57 reveal an unequivocal solution of $P$ = 7.0874 ± 0.0003 h and 0.42 mag amplitude. Period analysis of the 2019 October SAO photometric data for 1999 KR14 yields an unambiguous bimodal solution $P$ = 5.975 ± 0.002 h.

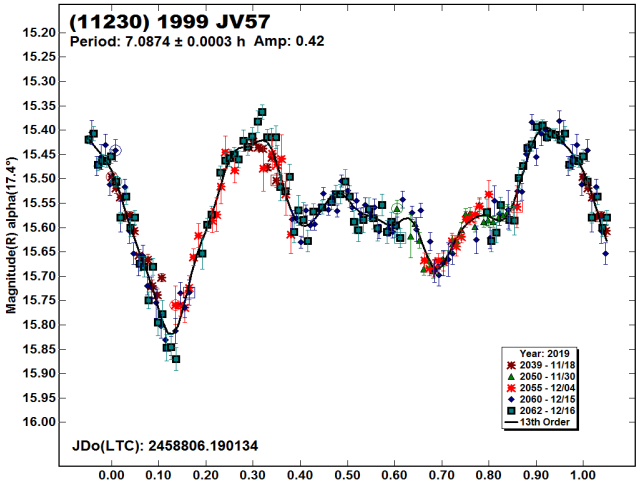


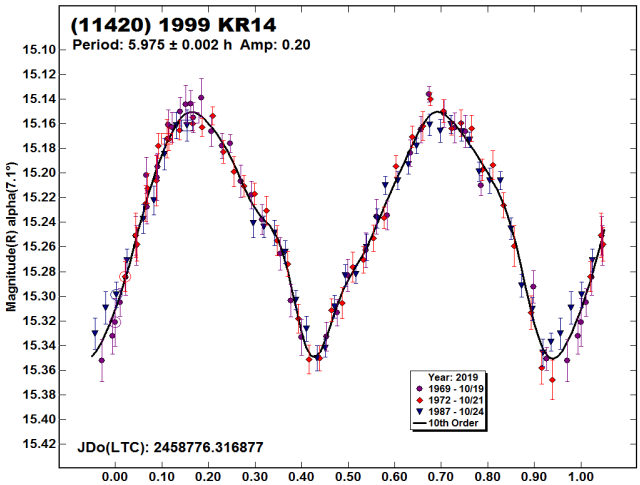


11548 Jerrylewis. The observations conducted solely at SAO for the BinAstPhot Survey show a bimodal lightcurve phased to a period $P$ = 4.5150 ± 0.0003 h as the most favorable solution.

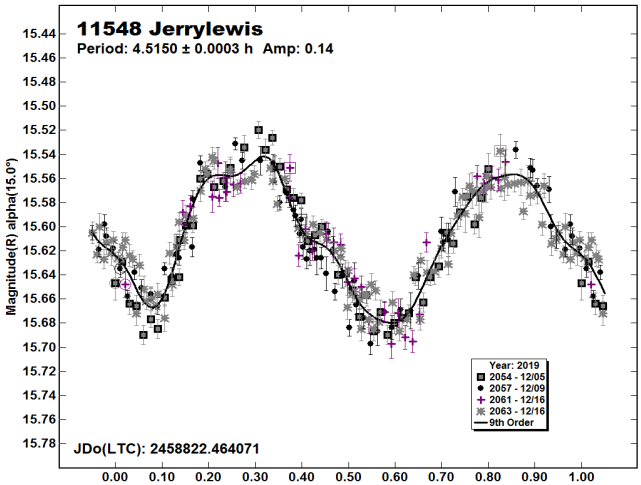


(18172) 2000 QL7 was a BinAstPhot Survey NEA target observed solely at Sopot Observatory from late 2020 January to mid-February, resulting in a total of 8 datasets. An unambiguous rotation period of $P$ = 2.37512 ± 0.00006 h was found by the period analysis.

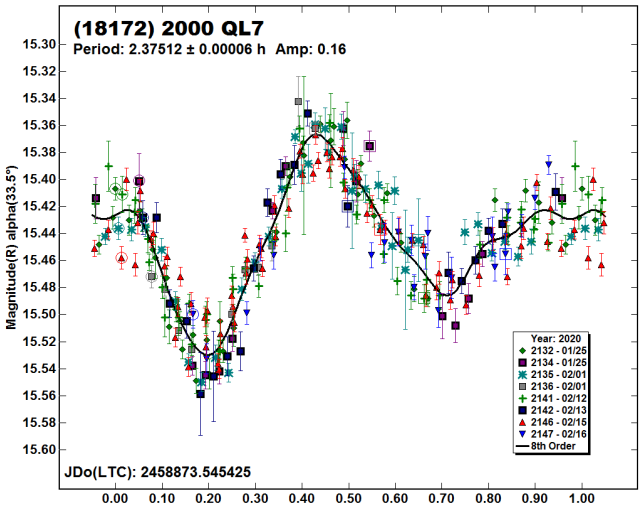


19288 Egami. Warner (2011web; 2.6590 h) is the only previously reported period in the LCDB. Analysis of two consecutive nights of observations in 2020 January confirm that period, $P$ = 2.654 ± 0.002 h.

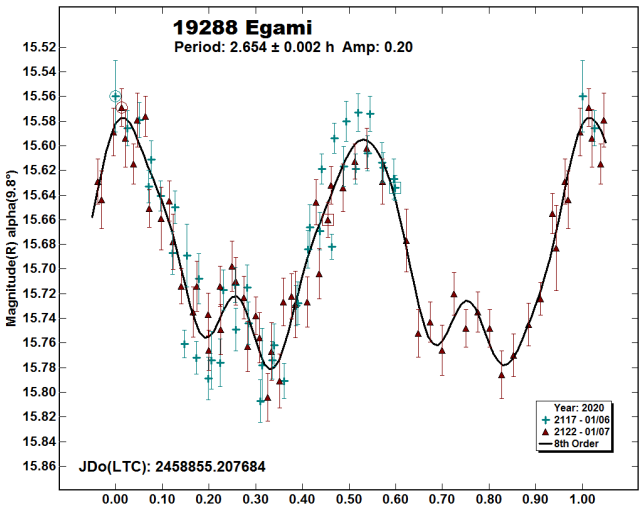


(19492) 1998 JT. The LCDB had no previous period results. Four photometric datasets obtained at SAO in 2019 October show a unique rotation period of $P$ = 2.4088 ± 0.0002 h.

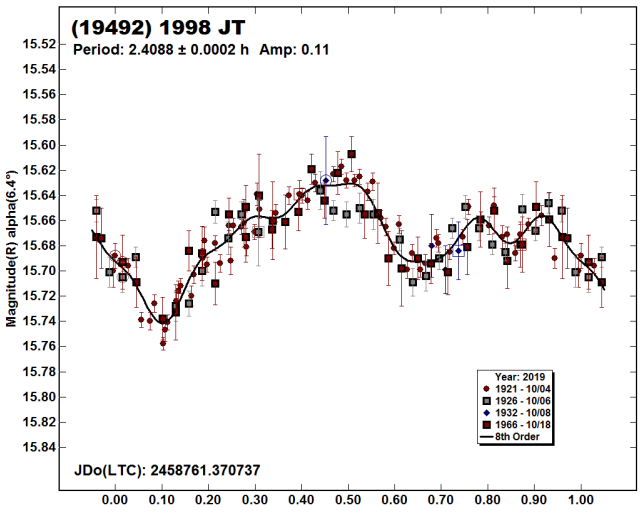


(29032) 2059 T-1. This is a Phocaea family asteroid with no previous rotation period reported. It was observed in late 2019 September and first half of 2019 October, resulting in a total of 6 datasets.

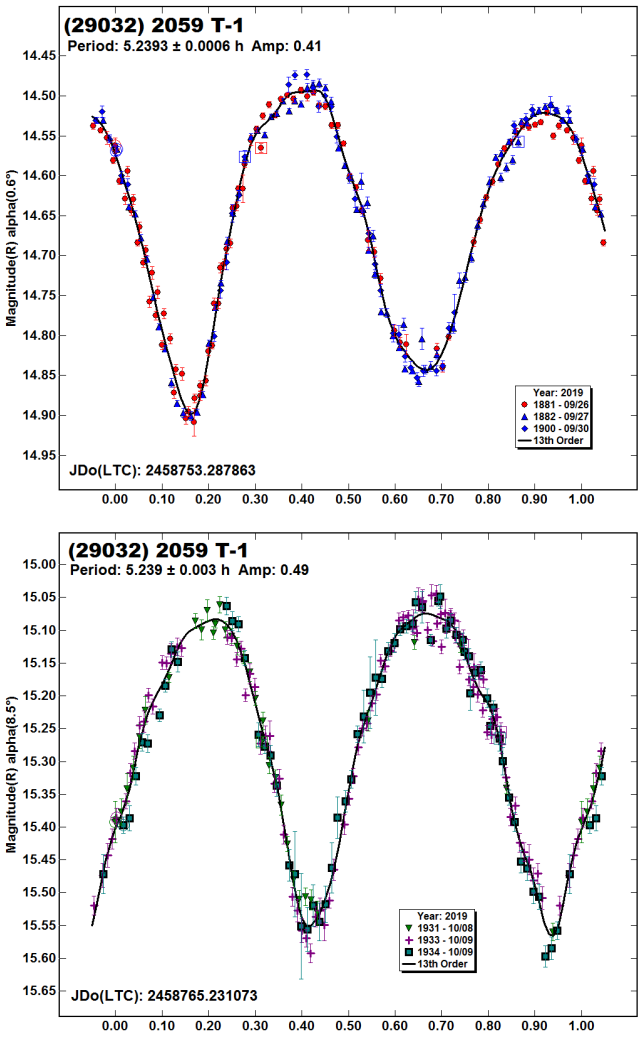


Since the lightcurve shape changed somewhat over the observation period, two separate lightcurves were constructed from well-matched datasets. The first one is formed of 3 datasets obtained in 2019 late September and the second one from the data collected in 2019 October. Both bimodal lightcurves have rather large amplitudes and nearly identical period values of $P = 5.2393 \pm 0.0006$ h and $P = 5.239 \pm 0.003$ h, respectively.

(31560) 1999 EQ14. Waszczak et al. (2015) found a period of 2.950 h. The 2019 October SAO data show a similar value P = 2.9512 ± 0.0003 h.

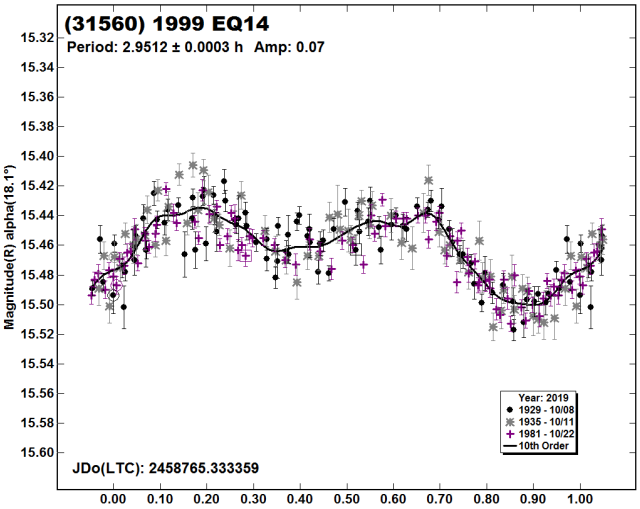


(39197) 2000 XA. Waszczak et al. (2015) found 5.221 h for a rotation period of this Hungaria asteroid. Period analysis conducted on two datasets obtained at SAO in 2019 November at relatively low phase angles indicate a high-amplitude (0.75 mag.) bimodal lightcurve phased to a period of $P = 5.2238 \pm 0.0004$ h as the most plausible solution.

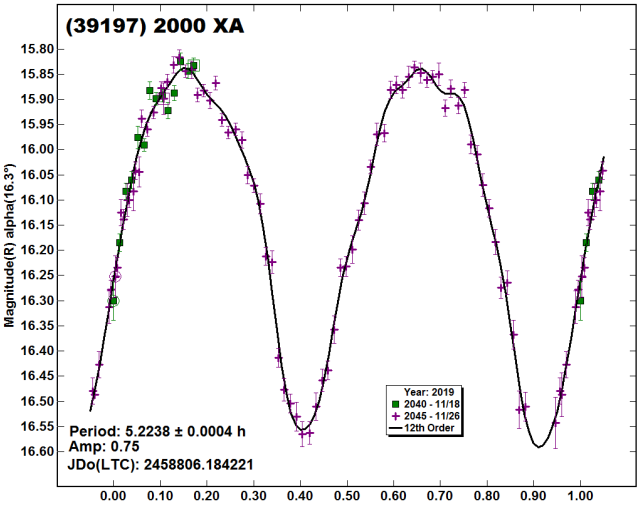


(393493) 2002 QX26. No prior period results were found in the LCDB. Since there were no favorable conditions for multi-night follow-up observing, conclusions on the possible value of rotation period were drawn on the basis of a single night data (2019 October 27-28) with more than one rotational cycle data coverage.

The lightcurve was found to be bimodal and of very large amplitude (1.03 mag.) at a low phase angle. This indicates the unambiguity of the rotation period of $P = 5.90 \pm 0.03$ h (Harris et al., 2014).

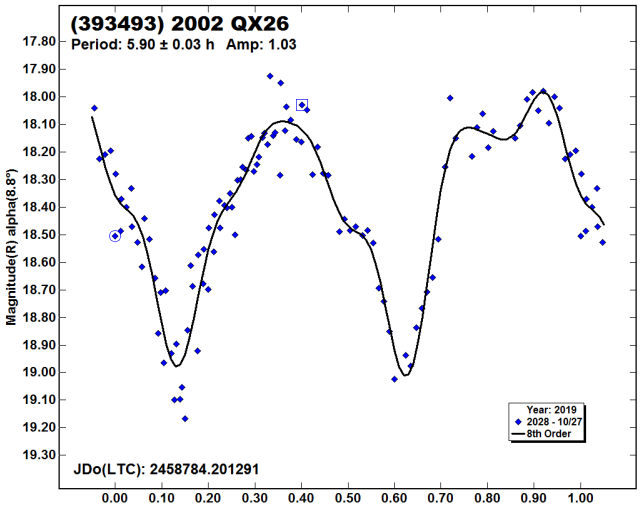


(437316) 2013 OS3. No rotation period has been established for this near-Earth asteroid prior to this determination. An unequivocal synodic rotation period of P = 5.63 ± 0.01 h was found analyzing the 2020 January SAO data taken on four consecutive nights.

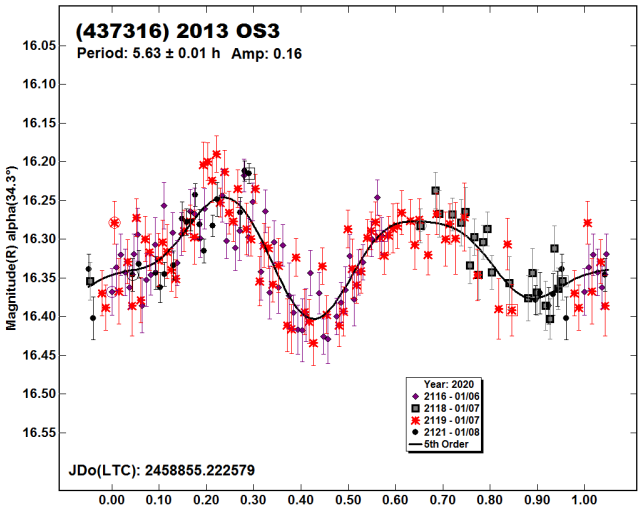


Acknowledgements

Observational work at Sopot Astronomical Observatory is supported by a 2018 Gene Shoemaker NEO Grant from The Planetary Society.

References

Behrend, R. (2005web, 2014web, 2016web, 2018web). CdL Observatoire de Geneve web site. *http://obswww.unige.ch/~behrend/page_cou.html*

Benishek, V. (2019). "Lightcurves and Synodic Rotation Periods for Seven Asteroids: 2019 April-July." *Minor Planet Bull.* **46**, 506-508.

Birlan, M.; Barucci, M.A.; Angeli, C.A.; Doressoundiram, A.; DeSanctis, M.C. (1996). "Rotational Properties of Asteroids: CCD Observations of Nine Small Asteroids." *Planetary and Space Science* **44**, 555-558.

Casalnuovo, G.B. (2016). "Lightcurve Analysis for Nine Main Belt Asteroids." *Minor Planet Bull.* **43**, 112-115.

Clark, M.; Joyce, B. (2003). "Asteroid Lightcurve Photometry from Goodsell Observatory (741)." *Minor Planet Bull.* **30**, 4-7.

Coley, D. (2012). "Asteroid Lightcurve Analysis at the Danhenge Observatory: Apr - Aug 2011." *Minor Planet Bull.* **39**, 23-24.

Dykhuis, M.J.; Molnar, L.A.; Gates, C.J.; Gonzales, J.A.; Huffman, J.J.; Maat, A.R.; Maat, S.L.; Marks, M.I.; Massey-Plantinga, A.R.; McReynolds, M.D.; Schut, J.A.; Stoep, J.P.; Stutzman, A.J. and 4 colleagues. (2016). "Efficient Spin Sense Determination of Flora-region Asteroids via the Epoch Method." *Icarus* **267**, 174-203.

Garceran, A.C.; Aznar, A.; Mansego, E.A.; Rodriguez, P.B.; deHaro, J.L.; Silva, A.F.; Silva, G.F.; Martinez, V.M.; Chiner, O.R. (2016). "Nineteen Asteroids Lightcurves at Asteroids Observers (OBAS) - MPPD: 2015 April - September." *Minor Planet Bull.***43,** 92-97.

Han, X.L.; Li, B.; Zhao, H.; Liu, W.; Sun, L.; Shi, J.; Gao, S.; Wang, S.; Pan, X.; Jiang, P.; Zhou, H. (2013). "Photometric Observations of 782 Montefiore, 3842 Harlansmith, 5542 Moffatt, 6720 Gifu, and (19979) 1989 VJ." *Minor Planet Bull.* **40**, 99-100.

Harris, A.W.; Pravec, P.; Galad, A.; Skiff, B.A.; Warner, B.D.; Vilagi, J.; Gajdos, S.; Carbognani, A.; Hornoch, K.; Kusnirak, P.; Cooney, W.R.; Gross, J.; Terrell, D.; Higgins, D.; Bowell, E.; Koehn, B.W. (2014). "On the maximum amplitude of harmonics on an asteroid lightcurve." *Icarus* **235**, 55-59.

Klinglesmith, D.A.III; Jamieson, Q.; Pilcher, F. (2005). "Lightcurves and Periods for Asteroids 2103 Laverna and 3445 Pinson." *Minor Planet Bull.* **32**, 75-76.

Klinglesmith, D.A.III; Hanowell, J.; Risley, E.; Turk, J.; Vargas, A.; Warren, C.A. (2013). "Asteroid Synodic Periods from Etscorn Campus Observatory." *Minor Planet Bull.***40**, 65-67.

Koff, R.A. (2003). "Lightcurve Photometry of 2890 Vilyujsk, 3106 Morabito, (4288) 1989 TQ1." *Minor Planet Bull.* **30**, 38-39.

Menke, J.; Cooney, W.; Gross, J.; Terrell, D.; Higgins, D. (2008). "Asteroid Lightcurve Analysis at Menke Observatory." *Minor Planet Bull.* **35**, 155-160.

Montgomery, K.A.; Davis, C.; Renshaw, T.; Rolen, J. (2013). "Photometric Study of Four Asteroids at Texas A&M Commerce Observatory." *Minor Planet Bull.* **40**, 212-213.

Oey, J. (2016). "Lightcurve Analysis of Asteroids from Blue Mountains Observatory in 2014." *Minor Planet Bull.* **43**, 45-51.

Pravec, P. (2017web). Photometric Survey for Asynchronous Binary Asteroids web site. *http://www.asu.cas.cz/~ppravec/newres.txt*

Ruthroff, J.C. (2013). "Lightcurve Analysis of Main Belt Asteroids 1115 Sabauda, 1554 Yugoslavia, 1616 Filipoff, 2890 Vilyujsk, (5153) 1940 GO, and (31179) 1997 YR2." *Minor Planet Bull.* **40**, 90-91.

Sheridan, E.E. (2011web). Posting on CALL website. *http://www.MinorPlanet.info/call.html*

| Number | Name | 20yy/mm/dd | Phase | $L_{PAB}$ | $B_{PAB}$ | Period (h) | P.E. | Amp | A.E. | Grp |
|---|---|---|---|---|---|---|---|---|---|---|
| 1274 | Delportia | 20/01/09-20/01/10 | 13.4,13.2 | 133 | 2 | 5.56 | 0.02 | 0.29 | 0.02 | FLOR |
| 1316 | Kasan | 19/10/12-19/10/14 | 28.0,28.4 | 354 | 30 | 5.843 | 0.003 | 0.19 | 0.02 | MC |
| 1706 | Dieckvoss | 20/02/16-20/02/21 | 16.7,14.5 | 176 | -2 | 2.5892 | 0.0004 | 0.16 | 0.02 | MB-I |
| 2075 | Martinez | 19/12/31-20/01/02 | 17.0,15.8 | 123 | 2 | 4.7531 | 0.0007 | 0.27 | 0.02 | PHO |
| 2103 | Laverna | 19/10/24-19/10/28 | 4.1,4.9 | 21 | 9 | 9.240 | 0.005 | 0.15 | 0.03 | MB-O |
| 2227 | Otto Struve | 20/01/05-20/01/08 | 14.2,12.9 | 126 | -6 | 5.397 | 0.002 | 0.15 | 0.02 | FLOR |
| 2432 | Soomana | 19/10/14-19/10/16 | 22.5,22.0 | 64 | 6 | 3.2060 | 0.0006 | 0.42 | 0.02 | V |
| 2566 | Kirghizia | 19/10/18-19/10/19 | 6.4,5.9 | 37 | -2 | 4.448 | 0.002 | 0.70 | 0.02 | V |
| 2871 | Schober | 19/12/17-20/01/04 | 13.9,6.0 | 111 | 8 | 2.85225 | 0.00005 | 0.17 | 0.03 | FLOR |
| 2890 | Vilyujsk | 20/01/02-20/01/24 | 16.8,24.4 | 79 | 9 | 3.4610 | 0.0003 | 0.10 | 0.04 | BAP |
| 2937 | Gibbs | 19/10/11-19/10/13 | 27.4,27.5 | 3 | 34 | 2.9835 | 0.0004 | 0.43 | 0.02 | BAP |
| 3385 | Bronnina | 19/11/20-19/11/21 | 6.7,6.6 | 68 | -7 | 2.974 | 0.009 | 0.23 | 0.02 | FLOR |
| 3385 | Bronnina | 20/01/09-20/01/25 | 18.5,22.5 | 71 | -8 | 2.95911 | 0.00009 | 0.35 | 0.03 | FLOR |
| 3489 | Lottie | 19/10/26-19/11/19 | 14.0,3.5 | 57 | 5 | 2.94832 | 0.00009 | 0.19 | 0.03 | V |
| 3842 | Harlansmith | 19/09/29-19/10/19 | 6.2,15.2 | 355 | 1 | 2.79400 | 0.00005 | 0.30 | 0.03 | MB-I |
| 3904 | Honda | 19/10/13-19/10/20 | 19.0,17.4 | 56 | 19 | 8.464 | 0.003 | 0.30 | 0.03 | EUN |
| 3986 | Rozhkovskij | 19/10/12-19/10/13 | 14.6,14.1 | 41 | 7 | 3.549 | 0.002 | 0.34 | 0.02 | FLOR |
| 4705 | Secchi | 20/03/11-20/03/18 | 11.0,14.3 | 152 | -2 | 2.6566 | 0.0004 | 0.15 | 0.03 | MB-I |
| 4857 | Altgamia | 20/01/02-20/01/24 | 27.5,24.6 | 145 | 33 | 9.0357 | 0.0004 | 0.29 | 0.02 | PHO |
| 4875 | Ingalls | 19/10/05-19/10/09 | 10.9,8.9 | 30 | -7 | 3.7783 | 0.0007 | 0.15 | 0.02 | FLOR |
| 5096 | Luzin | 19/10/14-19/10/15 | 13.2,13.7 | 359 | 7 | 3.051 | 0.001 | 0.39 | 0.02 | V |
| 5186 | Donalu | 19/10/23-19/10/27 | 9.8,11.2 | 17 | 15 | 3.153 | 0.001 | 0.36 | 0.02 | EUN |
| 5391 | Emmons | 19/10/20-19/10/22 | 21.5,22.3 | 356 | 2 | 3.030 | 0.001 | 0.18 | 0.02 | MB-I |
| 5512 | 1988 VD7 | 19/11/26-19/12/20 | *2.7,10.4 | 69 | 0 | 3.3059 | 0.0003 | 0.12 | 0.02 | FLOR |
| 5537 | Sanya | 19/10/16-19/10/19 | 6.0,5.3 | 29 | 7 | 3.4254 | 0.0009 | 0.45 | 0.02 | FLOR |
| 5543 | Sharaf | 19/12/16-19/12/18 | 3.3,2.8 | 89 | -3 | 5.972 | 0.002 | 1.21 | 0.02 | FLOR |
| 7368 | Haldancohn | 20/02/13-20/03/01 | *7,5,4.5 | 155 | 4 | 3.9032 | 0.0002 | 0.14 | 0.02 | FLOR |
| 7527 | Marples | 19/10/15-19/10/17 | 13.9,15.0 | 3 | 6 | 9.098 | 0.004 | 0.54 | 0.02 | FLOR |
| 9717 | Lyudvasilia | 19/12/17-19/12/31 | 13.8,19.4 | 63 | 6 | 2.8421 | 0.0002 | 0.14 | 0.03 | FLOR |
| 11230 | 1999 JV57 | 19/11/18-19/12/16 | 17.4,26.8 | 33 | 2 | 7.0874 | 0.0003 | 0.42 | 0.02 | FLOR |
| 11420 | 1999 KR14 | 19/10/19-19/10/24 | 7.1,5.5 | 33 | -7 | 5.975 | 0.002 | 0.20 | 0.02 | FLOR |
| 11548 | Jerrylewis | 19/12/04-19/12/17 | 15.1,11.4 | 88 | 19 | 4.5150 | 0.0003 | 0.14 | 0.02 | PHO |
| 18172 | 2000 QL7 | 20/01/25-20/02/16 | 33.5,27.9 | 118 | 21 | 2.37512 | 0.00006 | 0.16 | 0.02 | NEA |
| 19288 | Egami | 20/01/06-20/01/07 | 9.9,9.8 | 108 | 20 | 2.654 | 0.002 | 0.20 | 0.03 | EUN |
| 19492 | 1998 JT | 19/10/04-19/10/18 | 6.5,9.8 | 13 | 8 | 2.4088 | 0.0002 | 0.11 | 0.02 | FLOR |
| 29032 | 2059 T-1 | 19/09/26-19/10/01 | 0.5,3.1 | 3 | 1 | 5.2393 | 0.0006 | 0.41 | 0.02 | PHO |
| 29032 | 2059 T-1 | 19/10/08-19/10/10 | 8.4,9.3 | 4 | 4 | 5.239 | 0.003 | 0.49 | 0.02 | PHO |
| 31560 | 1999 EQ14 | 19/10/08-19/10/22 | 18.1,11.9 | 43 | 8 | 2.9512 | 0.0003 | 0.07 | 0.02 | MB-I |
| 39197 | 2000 XA | 19/11/18-19/11/26 | 16.3,20.9 | 34 | 4 | 5.2238 | 0.0004 | 0.75 | 0.02 | H |
| 393493 | 2002 QX26 | 19/10/27-19/10/28 | 8.7,8.8 | 23 | 8 | 5.90 | 0.03 | 1.03 | 0.03 | MB-M |
| 437316 | 2013 OS3 | 20/01/06-20/01/08 | 34.4,33.3 | 105 | 24 | 5.63 | 0.01 | 0.16 | 0.03 | NEA |

Table I. Observing circumstances and results. Phase is the solar phase angle given at the start and end of the date range. If preceded by an asterisk, the phase angle reached an extrema during the period. $L_{PAB}$ and $B_{PAB}$ are the average phase angle bisector longitude and latitude. Grp is the asteroid family/group (Warner *et al.*, 2009): BAP = Baptistina, EUN = Eunomia, FLOR = Flora, H = Hungaria, MB-I/M/O = main-belt inner/middle/outer, MC = Mars Crosser, NEA = near-Earth asteroid, PHO = Phocaea, V = Vestoid.


Stephens, R.D. (2009). "Asteroids Observed from GMARS and Santana Observatories." *Minor Planet Bull.* **36**, 59-62.

Stephens, R.D. (2017). "Asteroids Observed from CS3: 2016 October-December." *Minor Planet Bull.* **44**, 120-122.

VizieR (2019). *http://vizier.u-strasbg.fr/viz-bin/VizieR.*

Waller, E.B. (2013). "Lightcurve Photometry and Rotational Periods of 2890 Vilyujsk and 6223 Dahl." *Minor Planet Bull.* **40**, 109-110.

Warner, B.D. (2005). "Asteroid Lightcurve Analysis at the Palmer Divide Observatory - Fall 2004." *Minor Planet Bull.* **32**, 29-32.

Warner, B.D.; Harris, A.W.; Pravec, P. (2009). "The Asteroid Lightcurve Database." *Icarus* **202**, 134-146. Updated 2019 Jan. *http://www.minorplanet.info/lightcurvedatabase.html*

Warner, B.D. (2010). "Asteroid Lightcurve Analysis at the Palmer Divide Observatory: 2009 December - 2010 March." *Minor Planet Bull.* **37**, 112-118.

Warner, B.D. (2011web). Collaborative Asteroid Lightcurve Link website. *http://www.minorplanet.info/call.html*

Warner, B.D. (2018). *MPO Canopus* software, version 10.7.11.3. *http://www.bdwpublishing.com*

Warner, B.D.; Stephens, R.D. (2019). "Potential Binary and Tumbling Asteroids from the Center for Solar System Studies." *Minor Planet Bull.* **46**. 412-418.

Waszczak, A.; Chang, C.-K.; Ofek, E.O.; Laher, R.; Masci, F.; Levitan, D.; Surace, J.; Cheng, Y.-C.; Ip, W.-H.; Kinoshita, D.; Helou, G.; Prince, T.A.; Kulkarni, S. (2015). "Asteroid Light Curves from the Palomar Transient Factory Survey: Rotation Periods and Phase Functions from Sparse Photometry." *Astron. J.* **150**, A75.

Yankov, A.; Ditteon, R. (2009). "Lightcurves and Periods for Asteroids 1081 Reseda, 2117 Danmark, 2315 Czechoslovakia, 2871 Schober, 6392 Takashimizuno, and (6409) 1992 VC." *Minor Planet Bull.* **36**, 3-4.

# COLLABORATIVE ASTEROID PHOTOMETRY FROM UAI: 2020 JANUARY-MARCH

Lorenzo Franco
Balzaretto Observatory (A81), Rome, ITALY
lor_franco@libero.it

Alessandro Marchini, Leonella-Filippa Saya
Astronomical Observatory, DSFTA - University of Siena (K54)
Via Roma 56, 53100 - Siena, ITALY

Gianni Galli
GiaGa Observatory (203), Pogliano Milanese, ITALY

Giorgio Baj
M57 Observatory (K38), Saltrio, ITALY

Nello Ruocco
Osservatorio Astronomico Nastro Verde (C82), Sorrento, ITALY

Massimiliano Mannucci, Nico Montigiani
Osservatorio Astronomico Margherita Hack (A57)
Florence, ITALY

Luciano Tinelli
GAV (Gruppo Astrofili Villasanta), Villasanta, ITALY

Giulio Scarfì
Iota Scorpii Observatory (K78), La Spezia, ITALY

Pietro Aceti, Massimo Banfi
Seveso Observatory (C24) & Felizzano Observatory
Seveso, ITALY

Paolo Bacci, Martina Maestripieri
GAMP - San Marcello Pistoiese (104), Pistoia, ITALY

Riccardo Papini, Fabio Salvaggio
Wild Boar Remote Observatory (K49)
San Casciano in Val di Pesa (FI), ITALY

Fabio Mortari
Hypatia Observatory, Rimini, ITALY

Mauro Bachini
BSCR Observatory (K47), Santa Maria a Monte (PI), ITALY

Giovanni Battista Casalnuovo, Benedetto Chinaglia
Filzi School Observatory (D12), Laives, ITALY

(Received: 2020 April 12)

Photometric observations of eight main-belt and one near-Earth asteroid were made in order to acquire lightcurves for shape/spin axis models. The synodic period and lightcurve amplitude were found for 78 Diana: 7.2940 ± 0.0006 h, 0.06 mag; 81 Terpsichore: 10.946 ± 0.002 h, 0.14 mag; 118 Peitho: 7.8066 ± 0.0006 h, 0.23 mag; 755 Quintilla: 4.550 ± 0.001 h, 0.04 mag; 782 Montefiore: 4.0726 ± 0.0002 h, 0.51 mag; 1052 Belgica: 2.7094 ± 0.0001 h, 0.08 mag; 3998 Tezuka: 3.08 ± 0.01 h, 0.49 mag; 7132 Casulli: 3.5238 ± 0.0002 h, 0.14 mag; (52768) 1998 OR2: 4.111 ± 0.001 h, 0.30 mag. We also confirmed the binary nature of the asteroid 1052 Belgica and detected the binary nature of the asteroid 7132 Casulli.

Collaborative asteroid photometry was made inside the Italian Amateur Astronomers Union (UAI; 2020) group. The targets were selected mainly in order to acquire lightcurves for shape/spin axis models. The CCD observations were made in 2020 January-March using the instrumentation described in Table I. Lightcurve analysis was performed at the Balzaretto Observatory with *MPO Canopus* (Warner, 2016). All the images were calibrated with dark and flat frames and converted to R magnitudes using solar-colored field stars from the CMC15 catalogue distributed with *MPO Canopus*. Table II shows the observing circumstances and results.

78 Diana is a Ch-type (Bus & Binzel, 2002) middle main-belt asteroid discovered on 1863 March 15 by R. Luther at Dusseldorf. Collaborative observations were made over five nights. DSFTA (2020) on 2020 February 27 acquired images in the V and R bands. This allowed us to determine the color index (V-R) = 0.38 ± 0.03 mag.

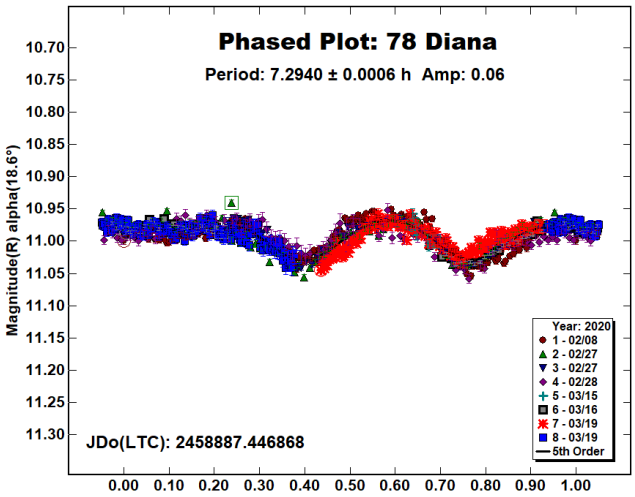


The period analysis shows a synodic period of $P$ = 7.2940 ± 0.0006 h with an amplitude $A$ = 0.06 ± 0.03 mag. The period is close to the previously published results in the asteroid lightcurve database (LCDB; Warner et al., 2009).

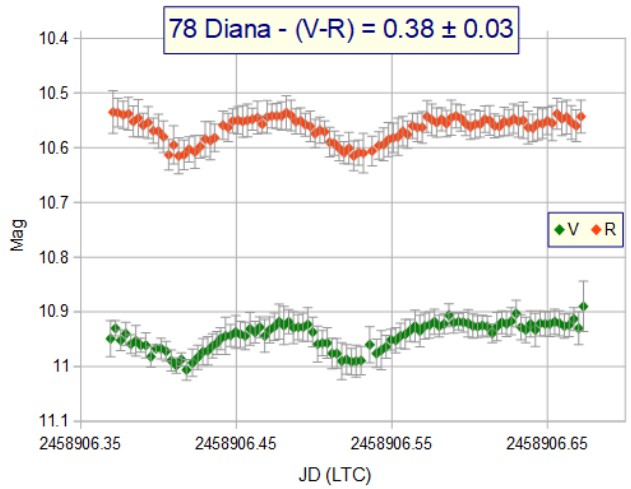


For each lightcurve, we measured the half peak-to-peak R mag and derived the V mag by adding the color index (V-R) = 0.38, previously determined. Using the H-G Calculator function of *MPO Canopus*, we derived $H$ = 8.06 ± 0.05 mag and $G$ = 0.09 ± 0.05. These values are close to results found in the LCDB.

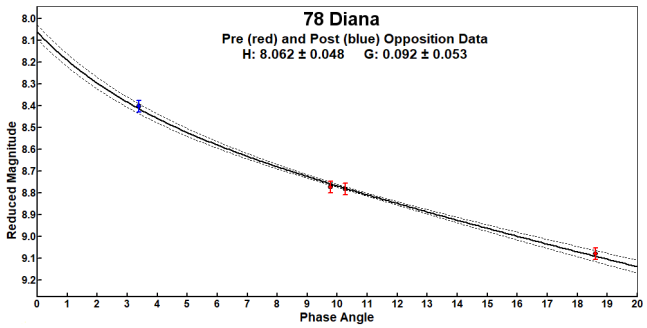


81 Terpsichore is a Cb-type (Bus & Binzel, 2002) outer main-belt asteroid discovered on 1864 September 30 by E. W. Tempel at Marseille. Collaborative observations were made over six nights. We found a synodic period of $P$ = 10.946 ± 0.002 h with an amplitude $A$ = 0.14 ± 0.03 mag. The period is close to the previously published results in the LCDB (Warner et al., 2009).

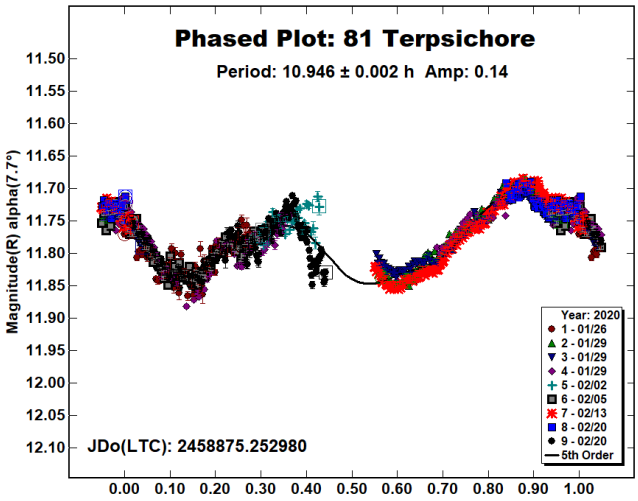


118 Peitho is an S-type (Bus & Binzel, 2002) inner main-belt asteroid discovered on 1872 March 15 by R. Luther at Dusseldorf. Collaborative observations were made over seven nights. We found a synodic period of $P$ = 7.8066 ± 0.0006 h with an amplitude $A$ = 0.23 ± 0.04 mag. The period is close to the previously published results in the asteroid lightcurve database (Warner et al., 2009).

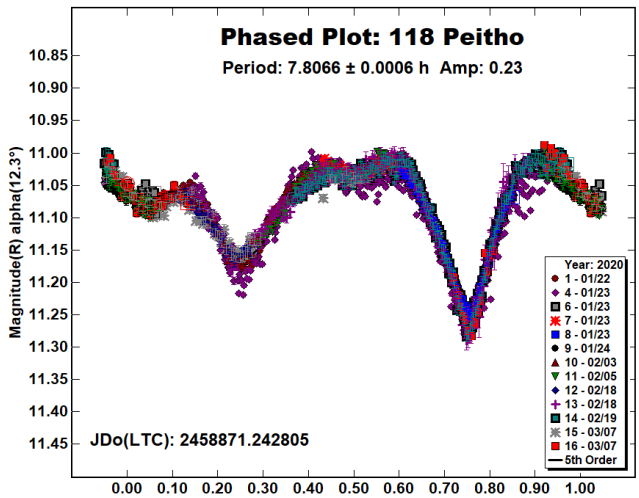


755 Quintilla is an M-type outer main-belt asteroid discovered on 1908 April 6 by J. H. Metcalf at Taunton. Collaborative observations were made over five nights. We found a synodic period of $P$ = 4.550 ± 0.001 h with a low amplitude $A$ = 0.04 ± 0.03 mag. The period is close to the previously published results in the asteroid lightcurve database (LCDB; Warner et al., 2009).

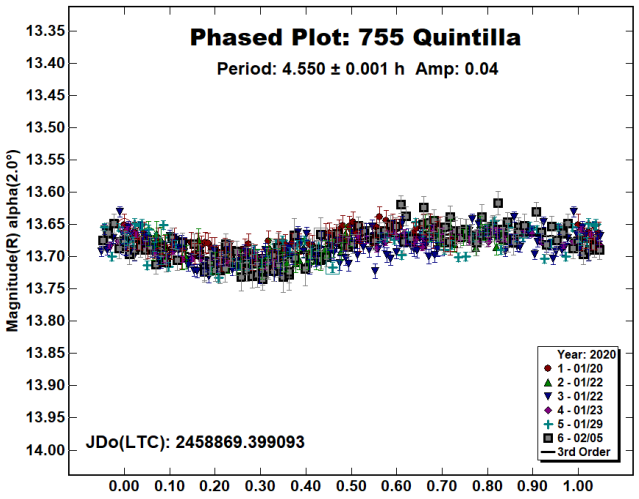


782 Montefiore is a Sl-type (Bus & Binzel, 2002) member of the Flora family; it was discovered on 1914 March 18 by J. Palisa at Vienna. Collaborative observations were made over nine nights. We found a synodic period of $P$ = 4.0726 ± 0.0002 h with an amplitude $A$ = 0.51 ± 0.05 mag. The period is close to the previously published results in the asteroid lightcurve database (LCDB; Warner et al., 2009).

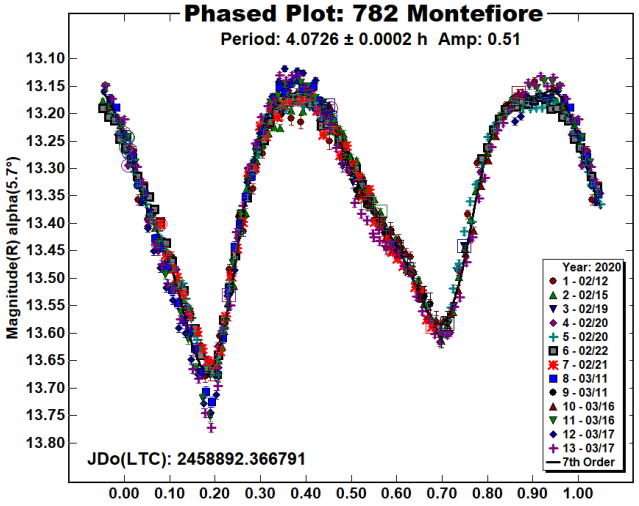


1052 Belgica is an S-type (Bus & Binzel, 2002) member of the Flora family; was discovered on 1925 November 15 by E. Delporte at Uccle. This asteroid is a binary system as reported by Franco et al. (2013). Collaborative observations were made over twelve nights.

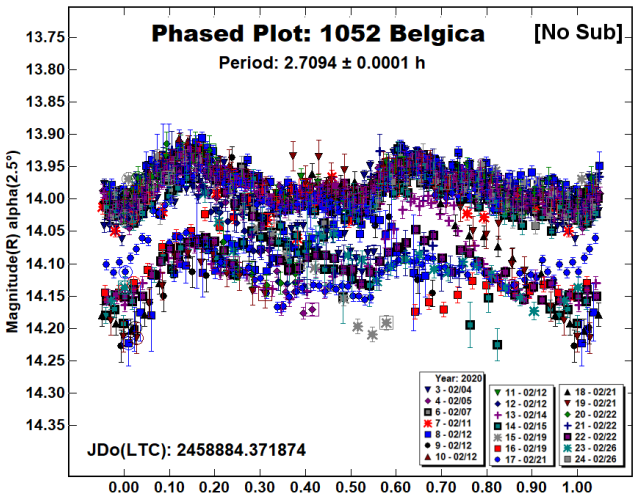


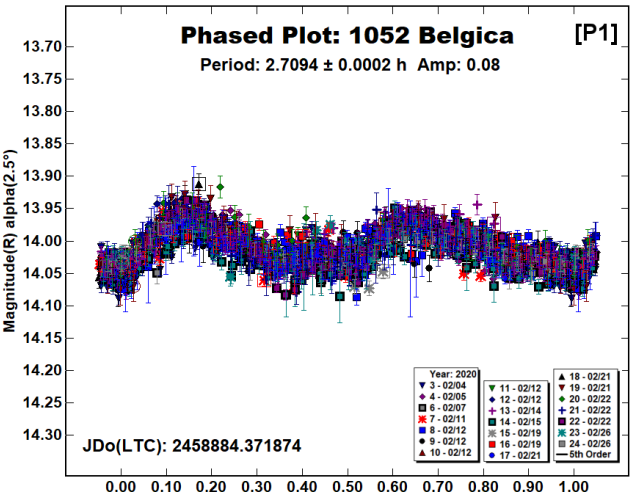


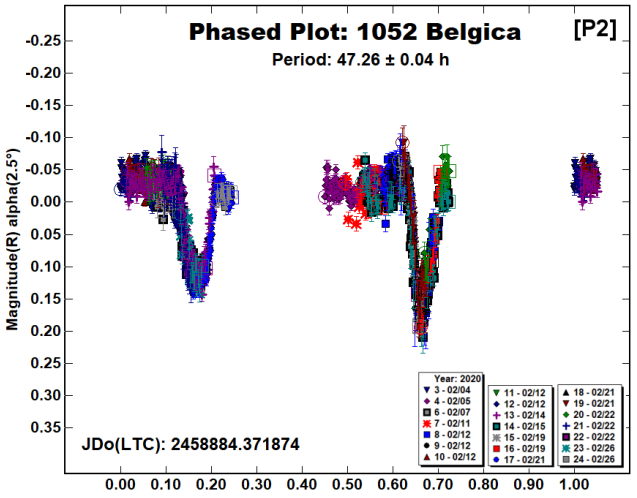


We found a primary synodic rotational period of *P1* = 2.7094 ± 0.0001 h with an amplitude *A1* = 0.08 ± 0.04 mag and orbital period $P_{ORB}$ = 47.26 ± 0.04 h. Mutual eclipse/occultation events that are 0.16 to 0.28 mag deep gives a lower limit to the secondary-to-primary mean-diameter ratio of *Ds/Dp* ≥ 0.34 ± 0.04. All these results are consistent with those previously published by Franco et. al. (2013).

3998 Tezuka is a medium albedo inner main-belt asteroid discovered on 1989 January 1 by T. Kojima at Chiyoda. This asteroid was observed at DSFTA (2020) on 2020 January 22 in the same field of the asteroid 118 Peitho.

We found a synodic period of *P* = 3.08 ± 0.01 h with an amplitude *A* = 0.49 ± 0.04 mag. The period is close to the previously published result by Omae et al. (2016).

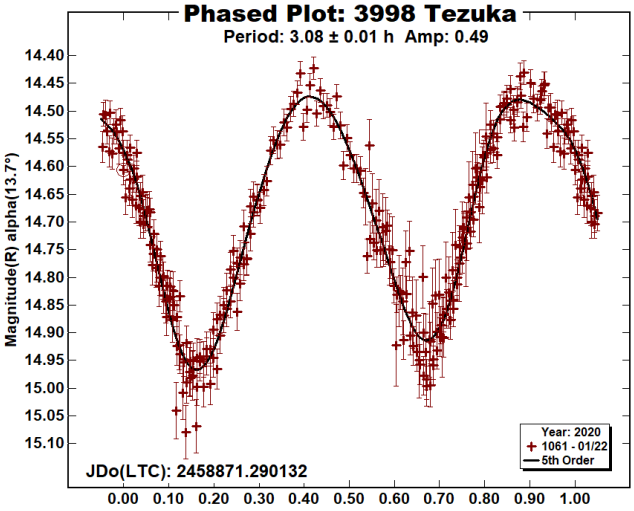


7132 Casulli is a low albedo inner main-belt asteroid discovered on 1993 September 17 by A. Vagnozzi at Stroncone. Collaborative observations were made over twelve nights. Some attenuation events made us hypothesize it was a binary system, as suspected by Behrend (2013), intensifying our observing sessions in order to fix the orbital period of the satellite.

We found a primary synodic rotational period of $P_1$ = 3.5238 ± 0.0002 h with an amplitude *A1* = 0.14 ± 0.04 mag and orbital period $P_{ORB}$ = 36.54 ± 0.02 h. Mutual eclipse/occultation events that are 0.11 to 0.16 mag deep gives a lower limit to the secondary-to-primary mean-diameter ratio of *Ds/Dp* ≥ 0.21 ± 0.04. The new binary system was announced through the ATel 13590 (Franco et. al., 2020).

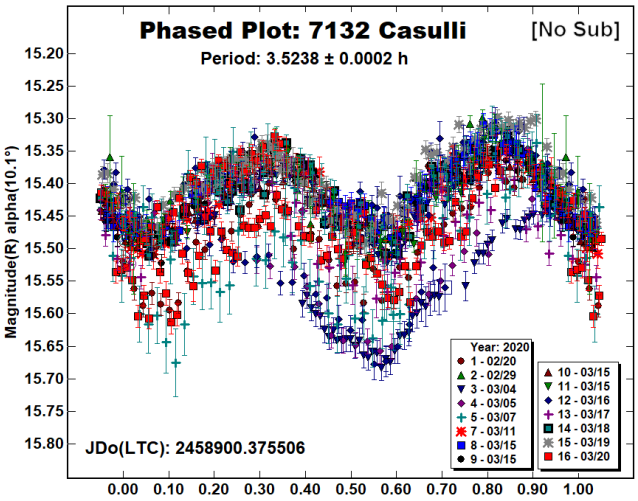

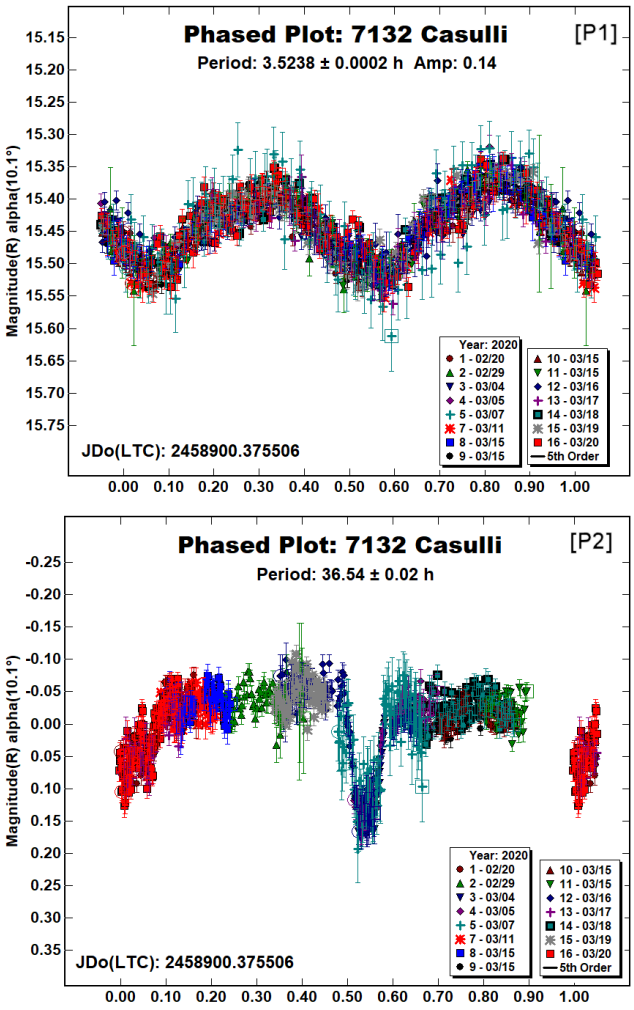


(52768) 1998 OR2 is an Amor near-Earth asteroid classified as Potentially Hazardous Asteroid (PHA); it was discovered on 1998 July 24 by NEAT at Haleakala. Collaborative observations were made over five nights during the approach phase to Earth. We found a synodic period of $P$ = 4.111 ± 0.001 h with an amplitude $A$ = 0.30 ± 0.05 mag. The period is close to the previously published result by Koehn et al. (2014).

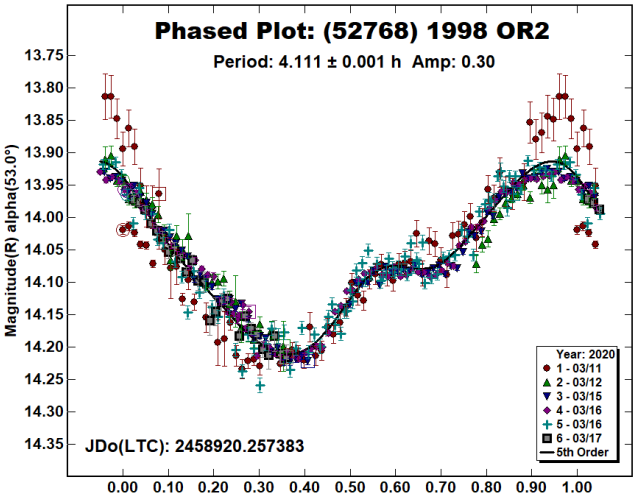


References

Behrend, R. (2013). Observatoire de Geneve web site. *http://obswww.unige.ch/~behrend/page_cou.html*

Bus, S.J.; Binzel R.P. (2002). "Phase II of the Small Main-Belt Asteroid Spectroscopic Survey - A Feature-Based Taxonomy." *Icarus* **158**, 146-177.

DSFTA (2020). Dipartimento di Scienze Fisiche, della Terra e dell'Ambiente – Astronomical Observatory, University of Siena. *https://www.dsfta.unisi.it/en/research/labs-eng/astronomicalobservatory*

Franco, L.; Pravec, P.; Ferrero, A.; Martinez, L. (2013). "(1052) Belgica." *CBET* **3372**.

Franco, L.; Marchini, A.; Bonnoli, G.; Papini, R.; Bacci, P.; Maestripieri, M.; Ruocco, N.; Montigiani, N.; Mannucci, M.; Scarfi, G. (2020). "The asteroid (7132) Casulli is a binary system." *Astronomer's Telegram* **13590**.

Harris, A.W.; Young, J.W.; Scaltriti, F.; Zappala, V. (1984). "Lightcurves and phase relations of the asteroids 82 Alkmene and 444 Gyptis." *Icarus* **57**, 251-258.

Koehn, B.W.; Bowell, E.G.; Skiff, B.A.; Sanborn, J.J.; McLelland, K.P.; Pravec, P.; Warner, B.D. (2014). "Lowell Observatory Near-Earth Asteroid Photometric Survey (NEAPS) - 2009 January through 2009 June." *Minor Planet Bulletin* **41**, 286-300.

Omae, Y.; Ebisu, D.; Kawano, M.; Kanda, T.; Takano, T.; Tanaka, A.; Nakata, A.; Hirono, K.; Moriuchi, S.; Nakamura, S.; Mizoguchi, T.; Tanigawa, T. (2016). "Lightcurves for Asteroids 3998 Tezuka and 10399 Nishiharima." *Minor Planet Bulletin* **43**, 272-274.

UAI (2020). "Unione Astrofili Italiani" web site. *https://www.uai.it*

Warner, B.D.; Harris, A.W.; Pravec, P. (2009) "The asteroid lightcurve database." *Icarus* **202**, 134-146. Updated 2020 March 25. *http://www.minorplanet.info/lightcurvedatabase.html*

Warner, B.D. (2016). MPO Software, *MPO Canopus* v10.8.1.1. Bdw Publishing. *http://minorplanetobserver.com*

| Observatory (MPC code) | Telescope | CCD | Filter | Observed Asteroids (#Sessions) |
|---|---|---|---|---|
| Astronomical Observatory of the University of Siena (K54) | 0.30-m MCT *f/5.6* | SBIG STL-6303e(bin 2x2) | Rc, C | 118 (4), 78 (4), 782 (2), 3998 (1), 7132 (6) |
| GiaGa Observatory (203) | 0.36-m SCT *f/5.8* | Moravian G2-3200 | Rc | 782 (3), 118 (3), 1052 (8) |
| M57 (K38) | *0.30-m* RCT *f/5.5* | SBIG STT-1603 | C | 81 (2), 118 (4), 782 (1), 1052 (1), 52768 (1) |
| Osservatorio Astronomico Nastro Verde (C82) | *0.35-m* SCT *f/6.3* | SBIG ST10XME (bin 2x2) | C | 1052 (1), 7132 (2), 52768 (5) |
| Osservatorio Astronomico Margherita Hack (A57) | *0.35-m* SCT *f/8.3* | SBIG ST10XME (bin 2x2) | Rc | 78 (1), 782 (1), 1052 (4), 7132 (1) |
| GAV | 0.20-m SCT *f/6.3* | SXV-H9 | Rc | 81 (4), 118 (1), 1052 (1) |
| Iota Scorpii(K78) | 0.40-m RCT *f/8.0* | SBIG STXL-6303e(bin 2x2) | Rc | 81 (1), 755 (1), 782 (1), 1052 (2), 7132 (1) |
| Seveso Observatory (C24) | *0.30-m* SCT *f/6.3* | SBIG ST8-XME (bin 2x2) | Rc | 81 (1), 782 (1) |
| Felizzano Observatory | *0.20-m* SCT *f/6.3* | Moravian KAF8300 | Rc | 78 (1), 1052 (1) |
| GAMP (104) | 0.60-m NRT *f/4.0* | Apogee Alta | C | 1052 (2), 7132 (2) |
| WBRO (K49) | 0.235-m SCT *f/10* | SBIG ST8-XME | C | 755 (1), 7132 (2) |
| Hypatia Observatory (L62) | *0.*25-m NRT *f/4.9* | SBIG ST8-XE | C | 755 (2), 1052 (1) |
| BSCR Observatory (K47) | *0.25-m* SCT *f/5.1* | DTA DISCOVERY PLUS 1600 | C | 118 (1) |
| Filzi School Observatory (D12) | 0.35-m RCT *f/8.0* | QHY9 (KAF8300) | C | 755 (1) |

Table I. Observing Instrumentations. MCT: Maksutov-Cassegrain, NRT: Newtonian Reflector, RCT: Ritchey-Chretien, SCT: Schmidt-Cassegrain.

| Number | Name | 2020 mm/dd | Phase | $L_{PAB}$ | $B_{PAB}$ | Period(h) | P.E. | Amp | A.E. | Grp |
|---|---|---|---|---|---|---|---|---|---|---|
| 78 | Diana | 02/08-03/19 | *18.2,3.4 | 175 | -4 | 7.2940 | 0.0006 | 0.06 | 0.03 | MB-M |
| 81 | Terpsichore | 01/26-02/20 | 7.6,16.1 | 114 | 9 | 10.946 | 0.002 | 0.14 | 0.03 | MB-O |
| 118 | Peitho | 01/22-03/07 | 12.3,25.9 | 107 | 10 | 7.8066 | 0.0006 | 0.23 | 0.04 | MB-I |
| 755 | Quintilla | 01/20-02/05 | 2.0,7.4 | 116 | -3 | 4.550 | 0.001 | 0.04 | 0.03 | MB-O |
| 782 | Montefiore | 02/12-03/17 | *5.7,15.7 | 150 | 7 | 4.0726 | 0.0002 | 0.51 | 0.05 | FLOR |
| 1052 | Belgica | 02/04-02/26 | 2.5,12.9 | 133 | 4 | 2.7094 | 0.0001 | 0.08 | 0.04 | FLOR |
| | | | | | | 47.26 | 0.04 | 0.28 | 0.02 | |
| 3998 | Tezuka | 01/22 | 13.6 | 105 | 9 | 3.08 | 0.01 | 0.49 | 0.04 | MB-I |
| 7132 | Casulli | 02/20-03/20 | *10.1,8.9 | 167 | -4 | 3.5238 | 0.0002 | 0.14 | 0.04 | MB-I |
| | | | | | | 36.54 | 0.02 | 0.16 | 0.02 | |
| 52768 | 1998 OR2 | 03/11-03/17 | 53.1,59.0 | 139 | 14 | 4.111 | 0.001 | 0.30 | 0.05 | NEA |

Table II. Observing circumstances and results. The first line gives the results for the primary of a binary system. The second line gives the orbital period of the satellite and the maximum attenuation. The phase angle is given for the first and last date. If preceded by an asterisk, the phase angle reached an extrema during the period. $L_{PAB}$ and $B_{PAB}$ are the approximate phase angle bisector longitude/latitude at mid-date range (see Harris et al., 1984). Grp is the asteroid family/group (Warner et al., 2009).

# A PHOTOMETRIC STUDY OF 470 KILIA

Frederick Pilcher
Organ Mesa Observatory
4438 Organ Mesa Loop
Las Cruces, NM 88011 USA
fpilcher35@gmail.com

Tom Polakis
Command Module Observatory
121 W. Alameda Dr.
Tempe, AZ 85282 USA

(Received: 2020 April 10)

Based on more than five months of observations, we find for 470 Kilia a synodic rotation period of 296.2 ± 2 hours, maximum amplitude 0.30 ± 0.05 magnitudes, color index V-R=0.51. We calculate H=10.25 ± 0.05 and G=0.23 ± 0.05 at mid-light in the V photometric system. Tumbling is confirmed, but the second tumbling period could not be found due to commensurability with the principal period.

Two previously published rotation periods for minor planet 470 Kilia are by Stephens (2009), 290 h with possible tumbling; and Behrend (2010), 26.4 h. Pilcher at Organ Mesa Observatory and Polakis at Command Module Observatory collaborated in a more extensive campaign. Pilcher used a 0.35-m f/10 Meade LX200 GPS Schmidt-Cassegrain (SCT) telescope, SBIG STL-1001E CCD, and a clear filter to obtain 73 sessions. Polakis used a 0.32-m f/6.7 Dall-Kirkham telescope, SBIG STXL-6303 CCD, clear filter to obtain 21 sessions.

Solar colored stars were selected for magnitude calibration for all sessions. Pilcher used stars with r' magnitudes from the Carlsberg Meridian Circle 15 (CMC15) catalog (Muiñoz et al. 2014), and adjusted to the Johnson R magnitude system, according to the formula by Dymock and Miles (2009), R = r'-0.22. This catalog is internally consistent usually within 0.05 magnitudes but occasionally somewhat larger inconsistencies are found. Polakis also used solar colored stars whose magnitudes were obtained from the ATLAS catalog (Tonry et al. 2018), which is incorporated directly into MPO Canopus. The ATLAS catalog derives Sloan griz magnitudes using a number of available catalogs. All r' magnitudes from Polakis's data were adjusted upward by 0.22 magnitudes to conform with the Cousins R magnitude system used by Pilcher. The fit by this simple technique was in most cases 0.02 magnitudes or better.

MPO Canopus software plots multi-session lightcurves by correcting night-to-night magnitude variations caused by changes in Earth and Sun distances and phase angle. Magnitude variations arising from the changing position of the target in the sky relative to Earth are removed with this correction as explained below, and changes that remain are due only to rotational behavior of the target. Corrections for Earth and Sun distances depend upon inverse square brightness laws, and are precise and reliable. The surface properties of the asteroid determine how rapidly the magnitude changes with phase angle and are quantitatively defined by the phase slope parameter, G.

For all asteroids, MPO Canopus utilizes the value of G listed in the MPC orbital database. For 470 Kilia the listed value is the default G=0.150. We obtained data needed to improve the resultant lightcurve with improved values of H and G. To achieve this improvement, 20 data points were obtained alternately in R and V filters on 2020 Mar. 16 by author Pilcher. The same calibration stars were used for both the R and V filter sessions. Dymock and Miles (2009) provide formulas for converting r', J, and Ks in the CMC14 catalog (and also for the expanded CMC15 catalog) to Cousins R and Johnson V magnitudes.

R=r'-0.22  V=0.6278*(J-Ks)+0.9947*r'

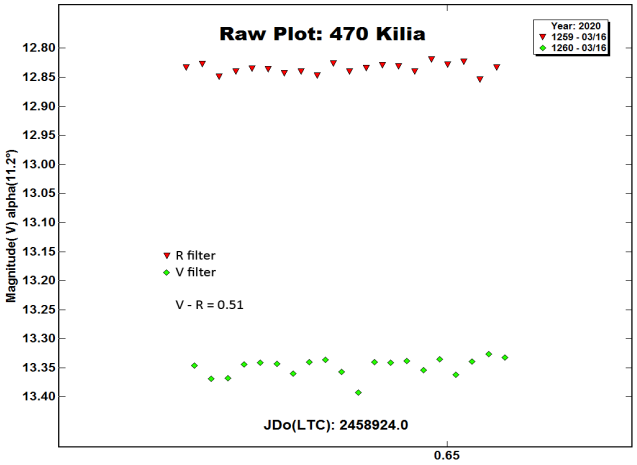


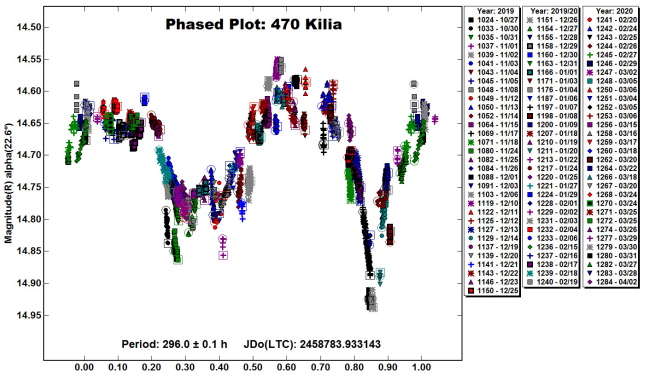


R magnitudes derived from CMC15 r' magnitudes were used for the R filter session. V magnitudes derived from CMC15 r', J, and Ks magnitudes were used for the V filter session. We present the raw lightcurve of all data points from both sessions. Adjusting the R magnitudes downward by 0.51 produces a best fit with minimum rms error. Hence we find V-R=0.51.

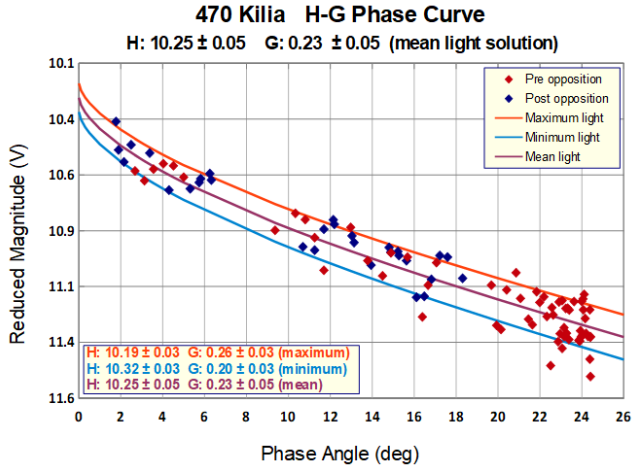

| Number | Name | yyyy/mm/dd | Phase | LPAB | BPAB | Period(h) | P.E | Amp | A.E. |
|---|---|---|---|---|---|---|---|---|---|
| 470 | Kilia | 2019/10/27-2020/04/02 | * 22.6, 18.3 | 152 | -5 | 296.2 | 2.0 | 0.30 | 0.05 |

Table I. Observing circumstances and results. Pts is the number of data points. The phase angle is given for the first and last date, unless a minimum (second value) was reached. LPAB and BPAB are the approximate phase angle bisector longitude and latitude at mid-date range (see Harris et al., 1984).

The authors thank Lorenzo Franco for constructing an H-G plot for maximum, mean, and minimum light. The R magnitudes in the data were converted to the V magnitude system by the aforementioned V-R=0.51. The H-G plotting subroutine of MPO Canopus was used to find separate plots at maximum light, mean light, and minimum light. These plots were combined on a spreadsheet showing, at mean light H=10.25±0.05, G=0.23±0.05; at maximum light H=10.19±0.03, G=0.26±0.03; at minimum light H=10.32±0.03, G=0.20±0.03.

MPO Canopus V.10.7 (Warner, 2016) contains a subroutine by which the default G=0.150 can be changed for all sessions. The value of G is changed to 0.23 to produce the phased lightcurve for all 94 sessions that is included in this paper. This lightcuve has best fit to a period 296.0 ± 0.1 hours and amplitude 0.30 ± 0.05 magnitudes. Most of the scatter in the lightcurve is due to tumbling, as explained in the next paragraph.

Petr Pravec (personal communication) used simultaneous dual-period software to search for evidence of tumbling. The main period is well established: 296.2 h (realistic error 2 h). The MPO Canopus result, shown in the lightcurve, is 296.0 ± 0.1 hours. The 0.1-hour formal error is unrealistically small. For this paper we adopt the value of 296.2 ± 2 hours. Tumbling was confirmed, but as for the second period, unfortunately it appears commensurate with the main period, so its solution is not unique. One candidate period is 119.3 h (which is near 2/5 commensurate with the main period). But the fit is not robust, as no higher than the 2nd order Fourier series can be meaningfully fitted to the data because of the period commensurability.

We conclude that the synodic rotation period of 470 Kilia is 296.2 ± 2 hours, an amplitude of 0.30 ± 0.05 magnitudes, with confirmed evidence of tumbling. We also find the photometric color index V-R=0.51, and in the V photometric system H=10.32 ± 0.05 and G=0.23 ± 0.05 at mid-light.

References

Behrend, R. (2010). Observatoire de Geneve web site. *http://obswww.unige.ch/~behrend/page_cou.html*

Dymock, R.; Miles, R. (2009). "A method for determining the V magnitudes of asteroids from CCD images." *J. Br. Astron. Assoc.* **119**, **3**, 149-156.

Harris, A.W.; Young, J.W.; Scaltriti, F.; Zappala, V. (1984). "Lightcurves and phase relations of the asteroids 82 Alkmene and 444 Gyptis." *Icarus* **57**, 251-258.

Muiñoz, J.L.; Evans, D.W. (2014). "The CMC15, the last issue of the series Carlsberg Meridian Catalogue, La Palma." *Astron. Nach.* **335**, 367.

Stephens, R.D. (2009). "Asteroids observed from GMARS and Santana Observatories – April to May 2009." *Minor Planet Bull.* **36**, 157-158.

Tonry, J.L.; Denneau, L.; Flewelling, H.; Heinze, A.N.; and five additional co-authors (2018). "The ATLAS all-sky stellar reference catalog." *Astrophys. J.* **867**, 105.

Warner, B.D. (2016). MPO Canopus software. *http://bdwpublishing.com*

# ROTATION PERIOD DETERMINATION FOR ASTEROIDS 4194 SWEITZER, 4421 KAYOR, 4705 SECCHI, (9219) 1995 WO8 AND (11493) 1988 VN5

Alessandro Marchini, Eleonora Bernardi, Leonella-Filippa Saya
Astronomical Observatory, DSFTA - University of Siena (K54)
Via Roma 56, 53100 - Siena, ITALY
marchini@unisi.it

Riccardo Papini, Fabio Salvaggio
Wild Boar Remote Observatory (K49)
San Casciano in Val di Pesa (FI), ITALY

(Received: 2020 April 15)

Photometric observations of five main-belt asteroids were conducted from the Astronomical Observatory of the University of Siena and the Wild Boar Remote Observatory, both located in Italy, in order to determine their synodic rotation periods. For 4194 Sweitzer we found: $P$ = 18.757 ± 0.012 h, $A$ = 0.45 ± 0.02 mag; for 4421 Kayor: $P$ = 91.02 ± 0.03 h, $A$ = 0.54 ± 0.03 mag; for 4705 Secchi: $P$ = 2.657 ± 0.001 h, $A$ = 0.12 ± 0.03 mag; for (9219) 1995 WO8: $P$ = 9.453 ± 0.008 h, $A$ = 0.57 ± 0.01 mag; for (11493) 1988 VN5: $P$ = 7.669 ± 0.005 h, $A$ = 0.48 ± 0.06 mag.

CCD photometric observations of five main-belt asteroids were carried out in 2019 December – 2020 March at the Astronomical Observatory of the University of Siena (K54), a facility inside the Department of Physical Sciences, Earth and Environment (DSFTA, 2020), and at the Wild Boar Remote Observatory (K49) in San Casciano in Val di Pesa (Florence). At the Astronomical Observatory, data were obtained with a 0.30-m *f*/5.6 Maksutov-Cassegrain telescope, SBIG STL-6303E NABG CCD camera, and clear filter; the pixel scale was 2.30 arcsec when binned at 2×2 pixels. At the Wild Boar Remote Observatory, data were obtained with a 0.235-m *f*/10 (SCT) telescope, SBIG ST8-XME NABG CCD camera, and no filter; the pixel scale was 1.6 arcsec in binning 2×2. All exposures were 300 seconds.

Data processing and analysis were done with *MPO Canopus* (Warner, 2018). All images were calibrated with dark and flat-field frames and the instrumental magnitudes converted to R magnitudes using solar-colored field stars from a version of the CMC-15 catalogue distributed with *MPO Canopus*. Table I shows the observing circumstances and results.

4194 Sweitzer (1982 RE) was discovered on 1982 September 15 by E. Bowell at the Anderson Mesa Station of the Lowell Observatory and named in honor of Paul A. Sweitzer (b. 1936), a reporter of the Arizona Daily Sun during 1958-1994 who made a special effort to report on events and astronomical discoveries at the Lowell Observatory (Minor Planet Circ. 28089). It is a main-belt asteroid with a semi-major axis of 2.698 AU, eccentricity 0.044, inclination 7.530 deg, and an orbital period of 4.43 years. Its absolute magnitude is $H$ = 12.1 (JPL, 2020) while its spectral class is Cb (Bus and Binzel, 2002; Xu et al., 1995). The WISE/NEOWISE satellite infrared radiometry survey (Masiero et al., 2012) found a diameter $D$ = 17.0 ± 0.3 km using an absolute magnitude $H$ = 12.0.

Observations were conducted over four nights and collected 255 data points. The period analysis shows a bimodal solution for the rotational period of $P$ = 18.757 ± 0.012 h with an amplitude $A$ = 0.45 ± 0.02 mag.

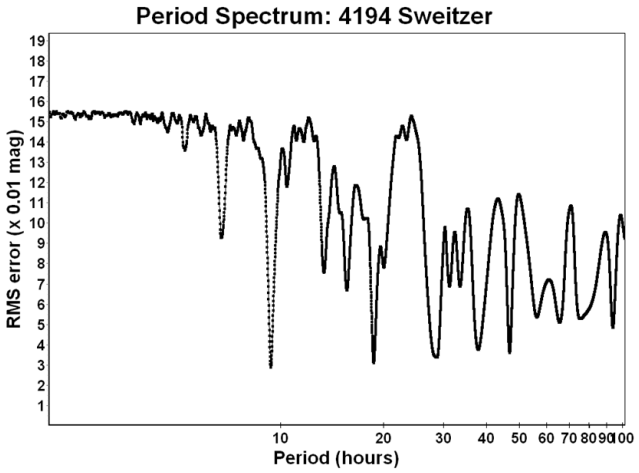


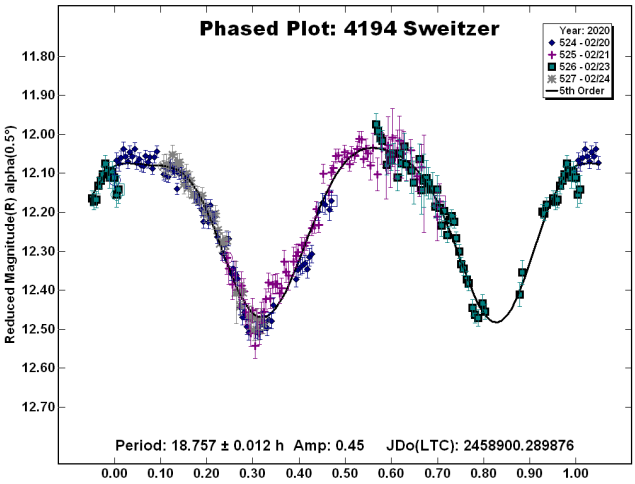


4421 Kayor (1942 UC) was discovered on 1942 January 14 at Heidelberg by K. Reinmuth and named after G. V. Williams in honor of his parents, Kay and Roy, for their support over the years (Minor Planet Circ. 21131). It is a main-belt asteroid with a semi-major axis of 2.661 AU, eccentricity 0.195, inclination 16.241 deg, and an orbital period of 4.34 years. Its absolute magnitude is $H$ = 12.3 (JPL, 2020). The WISE/NEOWISE satellite infrared radiometry survey (Masiero et al., 2012) found a diameter $D$ = 9.2 ± 0.1 km using an absolute magnitude $H$ = 12.19.

Observations over eleven nights collected 572 data points. The asteroid turned out to be a very slow rotator; despite the large amount of data collected in almost two months, we were not able to cover all the period due to bad weather and gaps from phase 0.40 to 0.50 and from 0.75 to 0.90 still remain. Our analysis led us to a solution of $P$ = 91.02 ± 0.03 h with an amplitude $A$ = 0.54 ± 0.03 mag as the most likely rotational period for this asteroid. Further observations will permit to reduce the uncertainty of this solution.

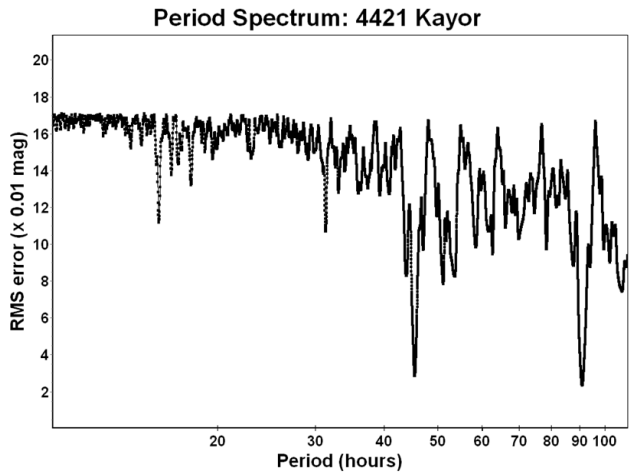


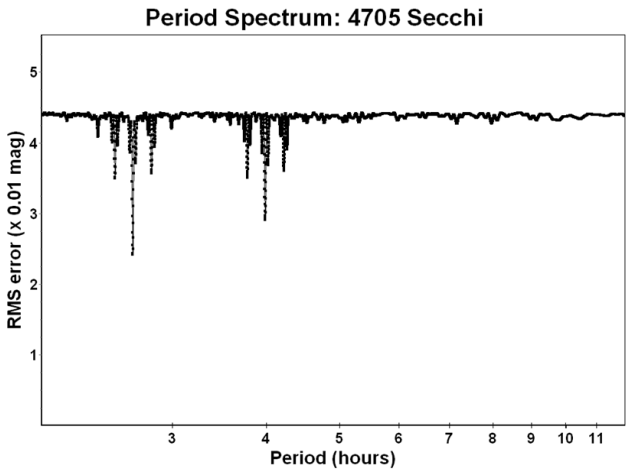


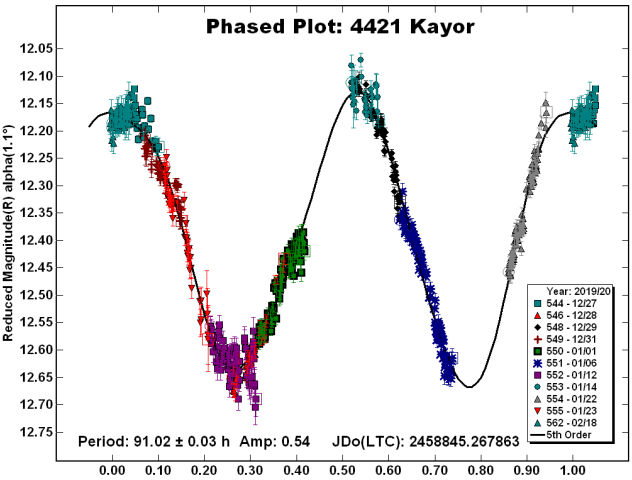


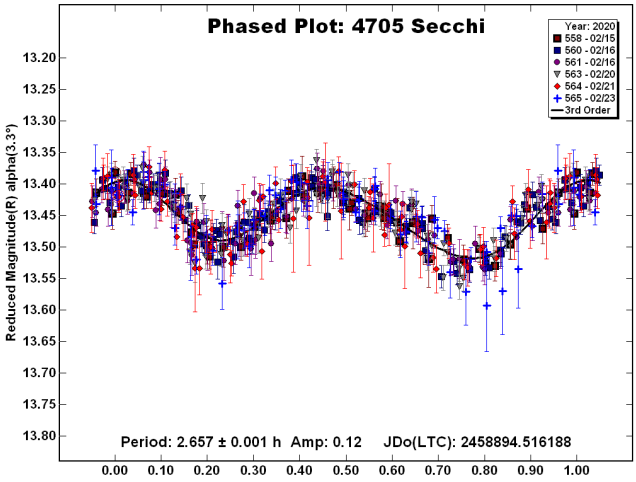


4705 Secchi (1988 CK) was discovered on 1988 February 13 at San Vittore Observatory in Bologna and named after Angelo Secchi (1818-1878), an Italian astronomer, director of the observatory of the Collegio Romano in Rome from 1848 to 1878, famous for his work on stellar spectroscopy (Minor Planet Circ. 20160). 4705 Secchi is a main-belt asteroid with a semi-major axis of 2.330 AU, eccentricity 0.128, inclination 8.638 deg, and an orbital period of 3.56 years. Its absolute magnitude is $H$ = 13.2 (JPL, 2020) while its diameter is $D$ = 5.6 ± 0.3 km (Masiero et al., 2011).

Observations were conducted over six nights and collected 439 data points. The period analysis shows a clear bimodal solution for the rotational period of $P$ = 2.657 ± 0.001 h with an amplitude $A$ = 0.12 ± 0.03 mag.

(9219) 1995 WO8 was discovered on 1995 November 18 at Nachi-Katsuura by Y. Shimizu and T. Urata. It is a main-belt asteroid with a semi-major axis of 3.196 AU, eccentricity 0.221, inclination 14.171 deg, and an orbital period of 5.71 years. Its absolute magnitude is $H$ = 12.0 (JPL, 2020) while its diameter is $D$ = 19.0 ± 0.2 km (Masiero et al., 2011).

Observations were conducted over three nights and collected 213 data points. The period analysis shows a bimodal solution for the rotational period of $P$ = 9.453 ± 0.008 h with an amplitude $A$ = 0.57 ± 0.01 mag.

| Number | Name | yyyy/mm/dd | Phase | $L_{PAB}$ | $B_{PAB}$ | Period(h) | P.E. | Amp | A.E. | Grp |
|---|---|---|---|---|---|---|---|---|---|---|
| 4194 | Sweitzer | 2020/02/20-2020/02/24 | *0.4,2.1 | 151 | -1 | 18.757 | 0.012 | 0.45 | 0.02 | MB |
| 4421 | Kayor | 2019/12/27-2020/02/19 | *1.2,23.0 | 100 | 4 | 91.02 | 0.03 | 0.54 | 0.03 | MB |
| 4705 | Secchi | 2020/02/15-2020/02/23 | *3.4,1.4 | 151 | 0 | 2.657 | 0.001 | 0.12 | 0.03 | MB |
| 9219 | 1995 WO8 | 2020/03/16-2020/03/18 | 8.2,7.9 | 188 | 13 | 9.453 | 0.008 | 0.57 | 0.01 | MB |
| 11493 | 1988 VN5 | 2020/02/20-2020/02/24 | 0.3,2.4 | 151 | -1 | 7.669 | 0.005 | 0.48 | 0.06 | MB |

Table I. Observing circumstances and results. The first line gives the results for the primary of a binary system. The second line gives the orbital period of the satellite and the maximum attenuation. The phase angle is given for the first and last date. If preceded by an asterisk, the phase angle reached an extrema during the period. $L_{PAB}$ and $B_{PAB}$ are the approximate phase angle bisector longitude/latitude at mid-date range (see Harris *et al.*, 1984). Grp is the asteroid family/group (Warner *et al.*, 2009).

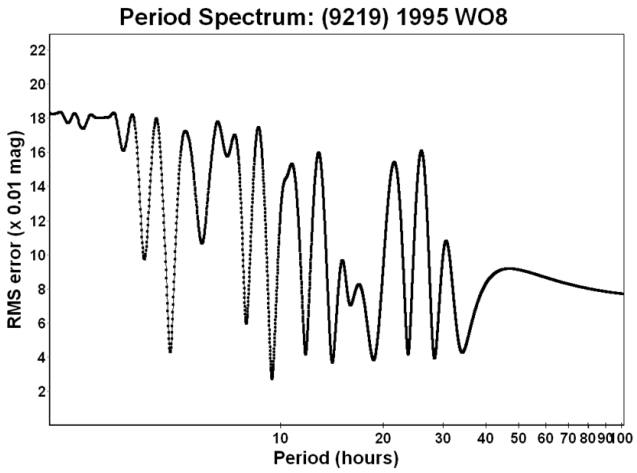


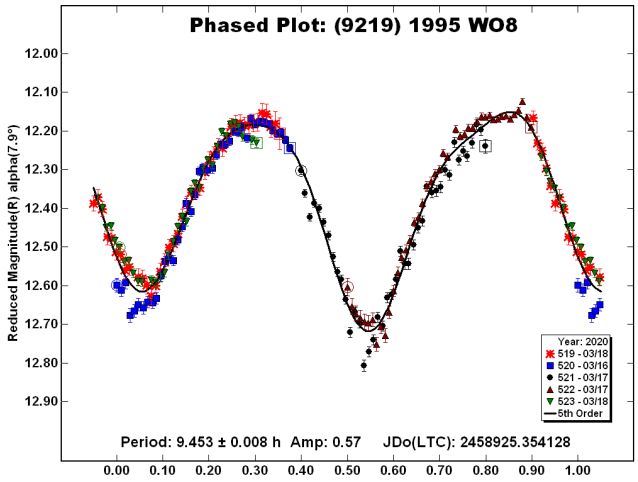


(11493) 1988 VN5 was discovered on 1988 November 4 at Klet by A. Mrkos. It's a main-belt asteroid with a semi-major axis of 2.436 AU, eccentricity 0.167, inclination 2.549 deg, and an orbital period of 3.80 years. Its absolute magnitude is $H$ = 14.5 (JPL, 2020).

Observations were conducted over four nights and collected 257 data points. The period analysis shows a bimodal solution for the rotational period of $P$ = 7.669 ± 0.005 h with an amplitude $A$ = 0.48 ± 0.06 mag.

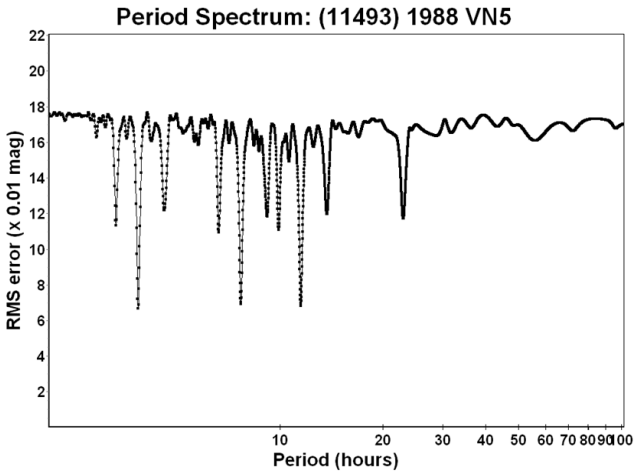


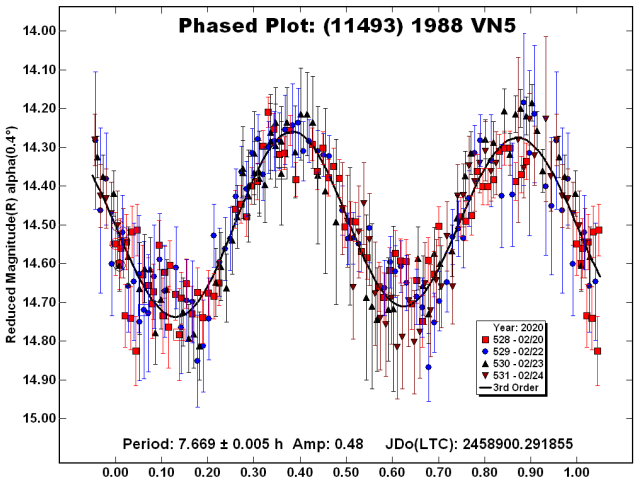


Acknowledgements

Eleonora Bernardi and Leonella-Filippa Saya, students of the course in Physics and Advanced Technologies at the Department of Physical Sciences, Earth and Environment, looked after the observations of some asteroids presented in this article during their internship activities at the Astronomical Observatory of the University of Siena, and appear deservedly as authors. Minor Planet Circulars (MPCs) are published by the International Astronomical Union's Minor Planet Center.
*https://www.minorplanetcenter.net/iau/ECS/MPCArchive/MPCArchive_TBL.html*

References

Bus, S.J.; Binzel, R.P. (2002). "Phase II of the small main-belt asteroid spectroscopic survey: A feature-based taxonomy." *Icarus* **158**, 146-177.

DSFTA (2020). Dipartimento di Scienze Fisiche, della Terra e dell'Ambiente – Astronomical Observatory.
*https://www.dsfta.unisi.it/en/research/labs-eng/astronomicalobservatory*

Harris, A.W.; Young, J.W.; Scaltriti, F.; Zappala, V. (1984). "Lightcurves and phase relations of the asteroids 82 Alkmene and 444 Gyptis." *Icarus* **57**, 251-258.

JPL (2020). Small-Body Database Browser.
*http://ssd.jpl.nasa.gov/sbdb.cgi#top*

Masiero, J.R.; Mainzer, A.K.; Grav, T.; Bauer, J.M.; Cutri, R.M.; Dailey, J.; Eisenhardt, P.R.M.; McMillan, R.S.; Spahr, T.B.; Skrutskie, M.F.; Tholen, D.; Walker, R.G.; Wright, E.L.; DeBaun, E.; Elsbury, D.; Gautier IV, T.; Gomillion, S.; Wilkins, A. (2011). "Main Belt Asteroids with WISE/NEOWISE. I. Preliminary Albedos and Diameters." *Astrophys. J.* **741**, A68.

Masiero, J.R.; Mainzer, A.K.; Grav, T.; Bauer, J.M.; Cutri, R.M.; Nugent, C.; Cabrera, M.S. (2012). "Preliminary Analysis of WISE/NEOWISE 3-Band Cryogenic and Post-cryogenic Observations of Main Belt Asteroids." *Astrophys. J. Letters* **759**, L8.

Warner, B.D. (2018). MPO Software, MPO Canopus v10.7.7.0. Bdw Publishing. *http://minorplanetobserver.com*

Warner, B.D.; Harris, A.W.; Pravec, P. (2009). "The Asteroid Lightcurve Database." *Icarus* **202**, 134-146. Updated 2019 Aug. *http://www.minorplanet.info/lightcurvedatabase.html*

Xu, S.; Binzel, R.P.; Burbine, T.H.; Bus, S.J. (1995). "Small main-belt asteroid spectroscopic survey: Initial Results." *Icarus* **115**, 1-35.

## LIGHTCURVE ANALYSIS OF ASTEROID 4700 CARUSI

Caroline E. Odden, Julia Zhu, Ihor Barakaiev, Mykhailo Bilokur, Zora A. Colleye, Maximilian P. de Saint-Exupery, Yeheun Lee, Ishaan R. Mundra, Hanna A. Nazzaro, Irura N. Nyiha, Alejandro Pedroza, Prem S. Prabhakar, Anntonia C. Taylor, Yuxin Xie, Charles S. Yoon, Sakiya M. Yusuf, Estelle C. Zhu, Sebastain Zhu
Phillips Academy Observatory (MPC I12)
180 Main Street
Andover, MA 01810 USA
ceodden@andover.edu

Jonathan Kemp
Middlebury College
Mittelman Observatory
Middlebury, VT 05753 USA

Aaron Sliski
Mittelman Observatories
Mayhill, NM 86339 USA

(Received: 2020 April 15)

Photometric observations of asteroid 4700 Carusi were made from the Phillips Academy Observatory and the Mittelman Observatories at New Mexico Skies from 2019 December 18 to 2020 February 07. The rotational period of the asteroid is determined to be 11.656 ± 0.001 h, with an amplitude of 0.49 ± 0.05 mag.

Photometric observations of asteroid 4700 Carusi were made between 2019 December and 2020 January from the Phillips Academy Observatory (PAO) and the Mittelman Observatories at New Mexico Skies in Mayhill, New Mexico. This work was undertaken as part of an astronomy research course taught at Phillips Academy, a high school in Andover, Massachusetts. Students used the CALL website to identify asteroids with previously unmeasured periods and favored candidates with high declinations, apparent visual magnitudes between 15 and 17, and appealing names. These students were responsible for acquiring all images from Phillips Academy Observatory. Coauthor Jonathan Kemp collaborated on the project, supplying six data sets from a remotely operated 0.50-m telescope at New Mexico Skies. In addition, coauthor Aaron Sliski contributed a data set on 2020 February 07, using a 0.95-m Boller and Chivens telescope. This telescope was previously located at the Fitz Randolph Observatory of Princeton University and has since been moved to New Mexico Skies.

Observations were acquired from Phillips Academy using an 0.50-m *f*/6.8 Corrected Dall-Kirkham (CDK) Astrograph telescope manufactured by PlaneWave Instruments. Images were captured with an Andor Tech iKon DW436 camera with a 2048×2048 array of 13.5-micron pixels. The resulting image scale was 0.81 arcseconds per pixel. Images were 300 seconds in length and were obtained over four nights from 2019 December 16 to 2019 December 21. Observations at the Mittelman Observatories at New Mexico Skies were also made using an 0.51-m *f*/6.8 Corrected Dall-Kirkham (CDK) Astrograph telescope

| Number | Name | 2019/2020 mm/dd | Phase | LPAB | BPAB | Period(h) | P.E. | Amp | A.E. | Grp |
|---|---|---|---|---|---|---|---|---|---|---|
| 4700 | Carusi | 12/16-02/07 | 3.0,22.8 | 90.1 | 2.6 | 11.656 | 0.001 | 0.49 | 0.05 | MB |

Table I. Observing circumstances and results. The phase angle is given for the first and last date. If preceded by an asterisk, the phase angle reached an extrema during the period. $L_{PAB}$ and $B_{PAB}$ are the approximate phase angle bisector longitude/latitude at mid-date range (see Harris et al., 1984). Grp is the asteroid family/group (Warner et al., 2009).

manufactured by PlaneWave Instruments. Images were taken with an SBIG STX (KAF-16803) camera with a 4096×4096 array of 9-micron pixels. The resulting image scale was 0.54 arcsecs per pixel. Image integrations were 240 seconds in length and were obtained over six nights from 2019 December 19 to 2020 January 04. Observations on 2020 February 07 were made with a 0.95-m *f*/3.8 telescope by Boller and Chivens. The Newtonian telescope has been substantially redesigned from the original Cassegrain configuration. Images were taken with an Apogee Aspen CG16M camera with a 4096×4096 array of 9-micron pixels. The resulting image scale was 0.49 arcsecs per pixel. Images were 120 seconds in length and were averaged in pairs before photometry was performed. All images were unbinned and unguided, and *AstroImageJ* software (Collins et. al., 2018) was used to calibrate all images with appropriate dark, flat, and bias frames.

*MPO Canopus* (Warner, 2018) was utilized for lightcurve analysis of 4700 Carusi. Comparison stars were chosen from the MPOSC3 catalog, supplied with *MPO Canopus*, to have near solar color, a B-V value close to 0.8, and a V-R value close to 0.45 (Warner, 2012). The composite lightcurve for 4700 Carusi utilized the Fourier Analysis for Lightcurves (FALC) algorithm developed by Alan Harris (Harris et al., 1989) and modified by Petr Pravec (Warner, 2012).

4700 Carusi. Discovered on 1986 September 06 by E. Bowell at the Anderson Mesa station of the Lowell Observatory, this main-belt asteroid was named in honor of Andrea Carusi, a pioneer in the fields of cometary orbits and asteroid families (MPC, 2019). Analysis of 577 data points yielded a rotational period of 11.656 ± 0.001 h with amplitude 0.49 ± 0.05 mag. The Asteroid Lightcurve Database (LCDB) did not reveal any previous rotational period results for 4700 Carusi (Warner et al., 2009). The resulting lightcurve is well covered, and the bimodal solution is strongly favored by the period spectrum (included).

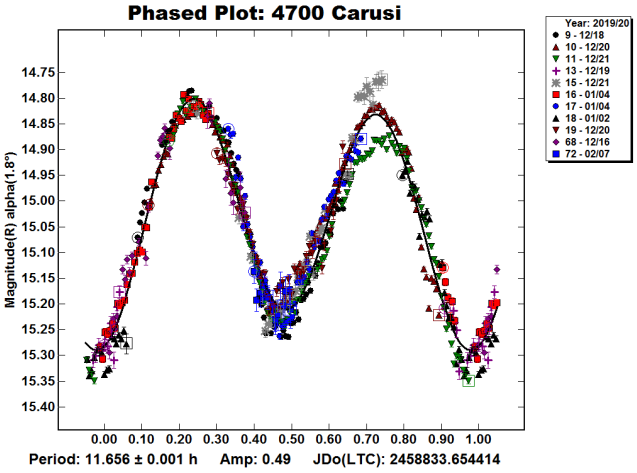


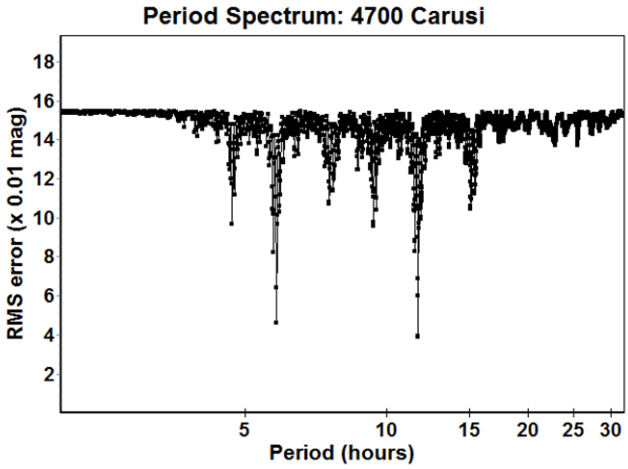


Acknowledgements

Research at the Phillips Academy Observatory is supported by the Israel Family Foundation. Funding for the Andor Tech camera and PlaneWave telescope at Phillips Academy was provided by the Abbot Academy Association, the Donald T. Ganem Fund, and the Taylor Family. This work includes observations obtained with the Mittelman Observatories 0.5-m and 0.95-m telescopes at New Mexico Skies in Mayhill, New Mexico.

References

CALL: Potential Lightcurve Targets (with LCDB data) Query. *http://www.minorplanet.info/PHP/call_OppLCDBQuery.php*

Collins et al., 2018, *AstroImageJ*, v. 3.2.21. *http://www.astro.louisville.edu/software/astroimagej/*

MPC (2019). Discovery Circumstances: Numbered Minor Planets (1)-(5000). *https://www.minorplanetcenter.net/iau/lists/NumberedMPs000001.html*

Harris, A.W.; Young, J.W.; Scaltriti, F.; Zappala, V. (1984). "Lightcurves and phase relations of the asteroids 82 Alkmene and 444 Gyptis." *Icarus* **57**, 251-258.

Harris, A.W.; Young, J.W.; Bowell, E.; Martin, L.J.; Millis, R.L.; Poutanen, M.; Scaltriti, F.; Zappala, V.; Schober, H.J.; Debehogne, H.; Zeigler, K. (1989). "Photoelectric Observations of Asteroids 3, 24, 60, 261, and 863." *Icarus* **77**, 171-186.

JPL (2019). Small Body Database Browser. *http://ssd.jpl.nasa.gov/sbdb.cgi*

Warner, B.D. (2012). *The MPO Users Guide: A Companion Guide to the MPO Canopus/PhotoRed Reference Manuals.* BDW Publishing, Colorado Springs, CO.

Warner, B.D. (2018). MPO Software, *MPO Canopus* v10.7.12.2. Bdw Publishing. *http://bdwpublishing.com*

Warner, B.D.; Harris, A.W.; Pravec, P. (2009). "The Asteroid Lightcurve Database." *Icarus* **202**, 134-146. Updated 2020 March 25. *http://www.minorplanet.info/lightcurvedatabase.html*

# ROTATIONAL PERIODS AND LIGHTCURVES OF 4421 KAYOR, 7118 KUKLOV AND (12853) 1998 FZ97

Alfonso Noschese
AstroCampania Associazione
and
Osservatorio Elianto (K68)
via V. Emanuele III, 95, 84098
Pontecagnano (SA) Italy
a.noschese@astrocampania.it

Maurizio Mollica
AstroCampania Associazione, Naples, Italy

Antonio Vecchione
AstroCampania Associazione, Naples, Italy

(Received: 2020 April 13)

Lightcurves for main-belt asteroids 4421 Kayor, 7118 Kuklov and (12853) 1998 FZ97 were obtained with three different telescopes from 2019 June to 2020 February, and are analyzed for rotation period and peak-to-peak amplitude.

The aim of this research was to find the rotational periods and lightcurves of 4421 Kayor, 7118 Kuklov and (12853) 1998 FZ97, since there were no entries in the LCDB for these asteroids at the time of the observations.

CCD photometric observations of 7118 Kuklov were carried out by means of Elianto observatory located in the south of Italy (Pontecagnano) using a 0.3-m Newton telescope operating at f/4 equipped with a Moravian KAF1603 ME CCD camera (1536×1024 array of 9-micron pixels), clear filter. Measurements of (12853) 1998 FZ97 were carried out at 'Salvatore Di Giacomo' observatory (L07) located at Agerola (Naples), Italy by means of a 0.50-m Ritchen-Chretien telescope operating at f/8 using a FLI-PL4240 CCD camera (2048×2048 array of 13.5-micron pixels), clear filter. The observations of 4421 Kayor were performed using a 0.25-m Ritchey-Chretien telescope operating at f/8 located in the south of Italy (Pontecagnano) equipped with a SBIG STT Kodak KAF-8300 CCD camera (3326×2504 array of 5.4-micron pixels), clear filter. All images were astrometrically aligned, dark and flat-field corrected using *Maxim DL* software. *MPO Canopus* (Warner, 2017) was used to measure the magnitude, perform Fourier analysis, and produce the final lightcurves. In particular, data were reduced in *MPO Canopus* using differential photometry. Night-to-night zero-point calibration was accomplished by selecting up to five comparison stars with near-solar colors using the "comp star selector" feature. To analyze the data points of 7118 Kuklov and (12853) 1998 FZ97, the CMC15 star catalog (Warner, 2007) was used for determining the comparison star magnitudes while APASS catalogue was used for reducing data related to 4421 Kayor. The "StarBGone" routine within *MPO Canopus* was used to subtract stars that occasionally merged with the asteroid during the observations. *MPO Canopus* was also used for rotation period analysis. The software employs a FALC Fourier analysis algorithm developed by Harris et al. (1989).

4421 Kayor was discovered on 1942 January 14 by Reinmuth, K. at Heidelberg. It is a main-belt asteroid with a semi-major axis of 2.662 AU, orbital period of 4.3 years, eccentricity of 0.195 and inclination of 16.241 deg. This nine-kilometer-asteroid has an absolute magnitude of 12.3 and a geometric albedo of 0.244 (JPL, 2020). CCD photometric observations were performed between 2020 January 1 and 23. Ten observation sessions were produced for lightcurve analysis to collect data points and adopting an exposure time ranging between 180 s and 240 s. Our data analysis gave a rotational period for this object of 91.03 ± 0.03 h with an amplitude of 0.45 mag.

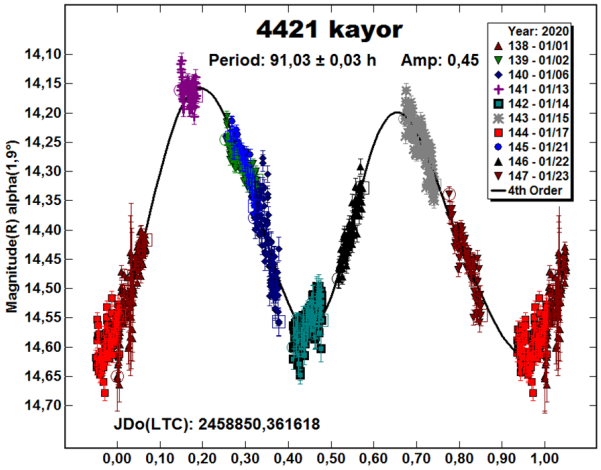


7118 Kuklov was discovered on 1988 November 4 by A. Mrkos at Klet. It is a main-belt asteroid with a semi-major axis of 2.655 AU, orbital period of 4.3 years, eccentricity of 0.128 and inclination of 12.527 deg. This ten-kilometer-asteroid has an absolute magnitude of 12.5 and a geometric albedo of 0.186 (JPL, 2020). CCD photometric observations were performed between 2020 January 22 and February 15. Six observation sessions were produced for lightcurve analysis to collect the data points and adopting an exposure time ranging between 360 s and 420 s. Our data analysis gave a rotational period for this object of 21.724 ± 0.011 h with an amplitude of 0.69 mag.

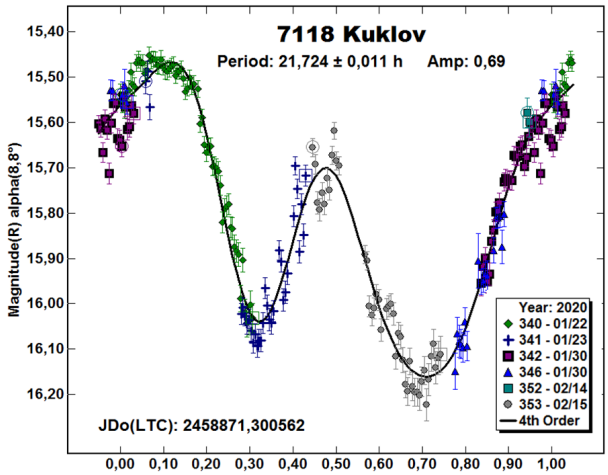

| Number | Name | 20yy mm/dd | Pts | Phase | $L_{PAB}$ | $B_{PAB}$ | Period(h) | P.E. | Amp | A.E. | Grp |
|---|---|---|---|---|---|---|---|---|---|---|---|
| 4421 | Kayor | 20/01/01-20/01/23 | 949 | 1.95-13.77 | 98.1 | 2.5 | 91.03 | 0.03 | 0.45 | 0.01 | MB |
| 7118 | Kuklov | 20/01/22-20/02/15 | 207 | 8.84-14.68 | 120.6 | -16.2 | 21.724 | 0.011 | 0.69 | 0.01 | MB |
| 12853 | 1998 FZ97 | 19/06/08-19/06/12 | 420 | 2.45-16.41 | 253.2 | 3.5 | 17.482 | 0.022 | 0.26 | 0.01 | MB |

Table I. Observing circumstances and results. The phase angle is given for the first and last date. $L_{PAB}$ and $B_{PAB}$ are the approximate phase angle bisector longitude and latitude at mid-date range (Harris *et al.*, 1984). Grp is the asteroid family/group (Warner et al., 2009).

(12853) 1998 FZ97 was discovered on 1998 March 31 by LINEAR at Socorro. This is a main-belt asteroid with a semi-major axis of 2.555 AU, orbital period of 4.08 years, eccentricity of 0.228 and inclination of 6.047 deg. Its diameter is 5.2 km, the absolute magnitude is 13.5 and the geometric albedo results 0.34 (JPL, 2020). A total of 420 lightcurve data points was collected from 2019 June 8 to 12 in six observing sessions by using an exposure time of 180 s. It was found a period of 17.482 ± 0.022 hours which was strongly suggested by the period spectrum analysis. The fit gave a lightcurve with an amplitude of 0.26 mag.

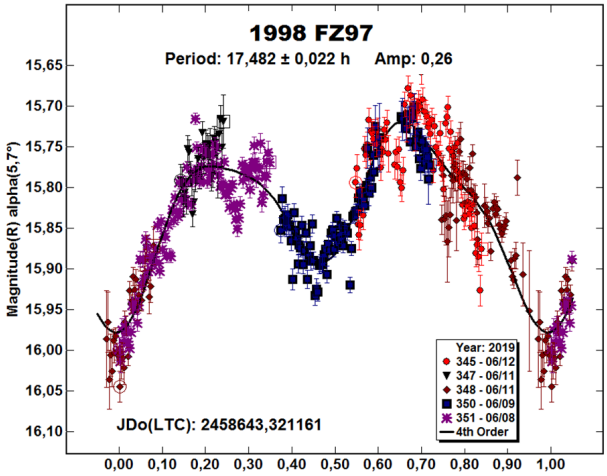


Table I gives the observing circumstances and results for the analyzed asteroids.

References

Harris, A.W.; Young, J.W.; Scaltriti, F.; Zappala, V. (1984). "Lightcurves and phase relations of the asteroids 82 Alkmene and 444 Gyptis." *Icarus* **57**, 251-258.

Harris, A.W.; Young, J.W.; Bowell, E.; Martin, L.J.; Millis, R.L.; Poutanen, M.; Scaltriti, F.; Zappala, V.; Schober, H.J.; Debehogne, H.; Zeigler, K.W. (1989). "Photoelectric Observations of Asteroids" 3, 24, 60, 261, and 863." *Icarus* **77**, 171-186.

JPL (2020). Small-Body Database Browser. *https://ssd.jpl.nasa.gov/sbdb.cgi*

Warner, B.D. (2007). "Initial Results of a Dedicated H-G Program." *Minor Planet Bull*. **34**, 113-119.

Warner, B.D.; Harris, A.W.; Pravec, P. (2009). "The Asteroid Lightcurve Database." *Icarus* **202**, 134-146. *http://www.minorplanet.info/lightcurvedatabase.html*

Warner, B.D. (2017). MPO Software, MPO Canopus version 10.7.11.1. Bdw Publishing. *http://minorplanetobserver.com*

## LIGHTCURVE PHOTOMETRY OPPORTUNITIES: 2020 JULY-SEPTEMBER

Brian D. Warner
Center for Solar System Studies / MoreData!
446 Sycamore Ave.
Eaton, CO 80615 USA
brian@MinorPlanetObserver.com

Alan W. Harris
MoreData!
La Cañada, CA 91011-3364 USA

Josef Ďurech
Astronomical Institute
Charles University
18000 Prague, CZECH REPUBLIC
durech@sirrah.troja.mff.cuni.cz

Lance A.M. Benner
Jet Propulsion Laboratory
Pasadena, CA 91109-8099 USA
lance.benner@jpl.nasa.gov

(Received: 2020 April 15 Revised: 2020 April 24)

We present lists of asteroid photometry opportunities for objects reaching a favorable apparition and have no or poorly-defined lightcurve parameters. Additional data on these objects will help with shape and spin axis modeling using lightcurve inversion. We also include lists of objects that will or might be radar targets. Lightcurves for these objects can help constrain pole solutions and/or remove rotation period ambiguities that might come from using radar data alone.

We present several lists of asteroids that are prime targets for photometry during the period 2020 July-September.

In the first three sets of tables, "Dec" is the declination and "U" is the quality code of the lightcurve. See the latest asteroid lightcurve data base (LCDB; Warner et al., 2009a) documentation for an explanation of the U code:

*http://www.minorplanet.info/lightcurvedatabase.html*

The ephemeris generator on the CALL web site allows you to create custom lists for objects reaching V ≤ 18.0 during any month in the current year and up to five years in the future, e.g., limiting the results by magnitude and declination, family, and more.

*http://www.minorplanet.info/PHP/call_OppLCDBQuery.php*

We refer you to past articles, e.g., Warner et al. (2009b) for more detailed discussions about the individual lists and points of advice regarding observations for objects in each list.

Once you've obtained and analyzed your data, it's important to publish your results. Papers appearing in the *Minor Planet Bulletin* are indexed in the Astrophysical Data System (ADS) and so can be referenced by others in subsequent papers. It's also important to make the data available to others. We urge you to consider submitting your raw data to the ALCDEF database. This can be accessed for uploading and downloading data at

*http://www.alcdef.org*

Containing almost 3.7 million observations for 14,962 objects (2020 April 24), this makes the site one of the larger publicly available sources for raw asteroid time-series lightcurve data.

Now that many backyard astronomers and small colleges have access to larger telescopes, we have expanded the photometry opportunities and spin axis lists to include asteroids reaching V = 15.5 and brighter (sometimes 15.0 when the list has too many potential targets).

Lightcurve/Photometry Opportunities

Objects with U = 3– or 3 are excluded from this list since they will likely appear in the list for shape and spin axis modeling. Those asteroids rated U = 1 should be given higher priority over those rated U = 2 or 2+, but not necessarily over those with no period. On the other hand, d*o not overlook asteroids with* U = 2/2+ *on the assumption that the period is sufficiently established.* Regardless, do not let the existing period influence your analysis since even highly-rated results have been proven wrong at times. Note that the lightcurve amplitude in the tables could be more or less than what's given. Use the listing only as a guide.

An entry in bold italics is a near-Earth asteroid (NEA).

| Number | Name | Brightest Date | Mag | Dec | LCDB Data Period | Amp | U |
|---|---|---|---|---|---|---|---|
| 9013 | Sansaturio | 07 01.0 | 15.5 | -2 | | | |
| 9130 | Galois | 07 01.6 | 15.2 | -20 | | | |
| 6663 | Tatebayashi | 07 02.0 | 15.4 | -11 | 4.8 | 0.35 | 2 |
| 19197 | Akasaki | 07 02.7 | 15.3 | -48 | | | |
| 9607 | 1992 DS6 | 07 03.1 | 15.2 | -39 | | | |
| 2604 | Marshak | 07 03.5 | 14.7 | -11 | > 30. | 0.17 | 2 |
| 8931 | Hirokimatsuo | 07 04.6 | 15.0 | -27 | | | |
| 2896 | Preiss | 07 06.1 | 14.0 | -10 | 24. | 0.3 | 2 |
| 11141 | Jindrawalter | 07 06.5 | 15.5 | -18 | 5.89 | 0.65 | 2 |
| 16123 | Jessiecheng | 07 07.8 | 15.5 | -21 | 3.98 | 0.11-0.18 | 2+ |
| 2682 | Soromundi | 07 08.1 | 14.7 | -18 | 9.385 | 0.30 | 2 |
| 2994 | Flynn | 07 08.4 | 15.3 | -27 | 9.747 | 0.14 | 2 |
| 2442 | Corbett | 07 08.6 | 14.9 | -13 | > 10. | 0.12-0.19 | 2 |
| 48898 | 1998 MO5 | 07 09.1 | 15.3 | -16 | | 0.42 | |
| 14564 | Heasley | 07 09.8 | 15.5 | -21 | 10.091 | 0.63 | 2 |
| 2120 | Tyumenia | 07 11.1 | 14.8 | +4 | 2.769 | 0.33-0.39 | 2 |
| 14220 | Alexgibbs | 07 11.9 | 14.9 | -27 | | | |
| 24276 | 1999 XO169 | 07 14.0 | 15.5 | -23 | | | |
| 10672 | Kostyukova | 07 14.3 | 15.3 | -18 | 78.468 | 0.08 | 1 |
| ***6569*** | ***Ondaatje*** | ***07 15.1*** | ***14.6*** | ***-26*** | ***5.959*** | ***0.70-0.98*** | ***2*** |
| 3876 | Quaide | 07 15.4 | 15.2 | -25 | | | |
| 34391 | 2000 RX67 | 07 16.6 | 15.4 | -23 | | | |
| 3313 | Mendel | 07 16.7 | 14.9 | -13 | | | |
| 36327 | 2000 LV33 | 07 17.8 | 15.2 | -21 | | | |
| 3393 | Stur | 07 18.0 | 15.4 | -10 | | | |
| 17296 | 3541 P-L | 07 18.2 | 15.4 | -24 | 6.205 | 0.71 | 2 |
| 18323 | 1983 RZ2 | 07 18.2 | 15.3 | -22 | 3.29 | 0.55-0.64 | 2 |
| 6831 | 1991 UM1 | 07 19.4 | 14.9 | -28 | | | |
| 1588 | Descamisada | 07 20.5 | 15.1 | -26 | | | |
| 37187 | 2000 WP60 | 07 20.9 | 14.7 | -24 | | | |
| 19959 | 1985 UJ3 | 07 22.8 | 15.3 | -21 | | | |
| 3519 | Ambiorix | 07 24.9 | 13.9 | -21 | 5.78 | 0.19 | 2 |
| 2863 | Ben Mayer | 07 25.0 | 15.5 | -20 | | 0.87 | |
| 21033 | 1989 UM | 07 25.5 | 15.5 | -19 | | | |
| 10798 | 1992 LK | 07 26.0 | 15.5 | -30 | | | |
| 1180 | Rita | 07 26.6 | 13.9 | -25 | 13.09 | 0.05-0.30 | 2 |
| 8984 | Derevyanko | 07 27.2 | 15.5 | -38 | | | |
| 33881 | 2000 JK66 | 07 28.2 | 14.5 | -20 | | | |
| 13111 | Papacosmas | 07 28.5 | 15.2 | -15 | | 0.61 | |
| 9545 | Petrovedomosti | 07 28.8 | 15.2 | -12 | | | |
| 63254 | 2001 BW54 | 07 29.2 | 15.5 | -19 | | | |
| 2747 | Cesky Krumlov | 07 29.5 | 15.4 | -24 | 438.71 | 0.63 | 2 |
| 2125 | Karl-Ontjes | 07 30.1 | 14.8 | -19 | | | |
| 5656 | Oldfield | 07 30.3 | 15.4 | -11 | 5.3 | 0.20 | 2 |
| 9308 | Randyrose | 07 30.3 | 15.4 | -14 | | | |
| 3096 | Bezruc | 07 30.8 | 15.2 | -4 | | | |
| 6049 | Toda | 08 02.6 | 15.5 | -14 | | | |
| 7014 | Nietzsche | 08 02.7 | 15.0 | -12 | | | |
| 3783 | Morris | 08 03.0 | 14.7 | -29 | 6.816 | 0.15 | 2 |
| 34058 | 2000 OT44 | 08 03.0 | 15.5 | -21 | | | |
| 11401 | Pierralba | 08 03.5 | 15.0 | -25 | | | |
| 3869 | Norton | 08 03.8 | 14.9 | -10 | | | |
| 4208 | Kiselev | 08 06.1 | 15.5 | -11 | | | |
| 16004 | 1999 BZ3 | 08 06.4 | 15.4 | -15 | | | |
| 2168 | Swope | 08 06.8 | 14.4 | -16 | | | |
| 6434 | Jewitt | 08 08.0 | 14.6 | -14 | 3.237 | 0.28 | 2 |

| Number | Name | Brightest Date | Mag | Dec | LCDB Data Period | Amp | U |
|---|---|---|---|---|---|---|---|
| 17770 | Baume | 08 08.4 | 14.9 | -17 | 3.263 | 0.20-0.35 | 2 |
| 4331 | Hubbard | 08 08.6 | 14.6 | -26 | | | |
| 2160 | Spitzer | 08 08.8 | 15.3 | -16 | 5.9 | | 2- |
| 3303 | Merta | 08 08.8 | 15.5 | -20 | | | |
| 1978 | Patrice | 08 09.9 | 13.8 | -25 | 5.881 | 0.13 | 2+ |
| 6266 | Letzel | 08 11.0 | 14.9 | -10 | | | |
| 9246 | Niemeyer | 08 11.5 | 15.2 | -16 | | 0.64 | |
| 2740 | Tsoj | 08 11.7 | 15.3 | -3 | 22.042 | 0.89 | 2 |
| 183230 | 2002 TC58 | 08 12.4 | 14.8 | -24 | | | |
| 7106 | Kondakov | 08 12.6 | 15.2 | -13 | 7.596 | | 2 |
| 4117 | Wilke | 08 12.7 | 15.3 | -4 | | | |
| 6196 | Bernardbowen | 08 13.4 | 15.5 | -18 | | | |
| 28565 | 2000 EO58 | 08 14.1 | 15.1 | -5 | 3.83 | 0.04 | 1 |
| 9034 | Oleyuria | 08 16.4 | 15.5 | -8 | | | |
| 17544 | Kojiroishikawa | 08 16.7 | 15.4 | -19 | | | |
| 6043 | Aurochs | 08 17.0 | 15.0 | -13 | | 0.45 | |
| 8812 | Kravtsov | 08 18.7 | 15.3 | -25 | | | |
| 11003 | Andronov | 08 19.2 | 15.5 | -20 | 4.522 | 0.19 | 2+ |
| 4714 | Toyohiro | 08 19.8 | 14.9 | -15 | 14.706 | 0.07 | 2 |
| 2532 | Sutton | 08 20.6 | 14.5 | -15 | 51.362 | 0.02 | 1 |
| 10036 | McGaha | 08 22.2 | 15.2 | -8 | | | |
| 11840 | 1986 QR2 | 08 22.6 | 15.1 | -14 | | | |
| 66284 | 1999 JU15 | 08 23.0 | 15.4 | -24 | | | |
| 4073 | Ruianzhongxue | 08 23.2 | 15.3 | -12 | | 0.32 | |
| 2238 | Steshenko | 08 23.5 | 15.4 | -13 | | 0.81 | |
| 68130 | 2001 AO17 | 08 24.9 | 15.1 | -5 | | | |
| 14643 | Morata | 08 25.0 | 14.9 | -12 | > 24. | 0.1 | 1 |
| 22276 | Belkin | 08 25.4 | 15.5 | -22 | | | |
| 6536 | Vysochinska | 08 25.9 | 15.2 | -15 | 6.109 | 0.53 | 2+ |
| 1877 | Marsden | 08 26.5 | 15.5 | -18 | 14.4 | 0.22 | 2 |
| 3889 | Menshikov | 08 27.1 | 15.2 | -14 | | | |
| 14767 | 1137 T-1 | 08 27.3 | 15.4 | -5 | | | |
| 8003 | Kelvin | 08 27.5 | 15.5 | -15 | | | |
| 4553 | Doncampbell | 08 28.0 | 15.1 | -5 | 13.021 | 0.29 | 2 |
| 12832 | 1997 CE1 | 08 29.0 | 15.2 | -19 | | | |
| 24801 | 1994 PQ15 | 08 29.8 | 15.5 | -6 | | | |
| 34373 | 2000 RT44 | 08 29.9 | 15.5 | -10 | | | |
| 2344 | Xizang | 08 31.5 | 14.1 | -14 | 13. | 0.39 | 2 |
| 2236 | Austrasia | 08 31.7 | 13.8 | -18 | | | |
| 8530 | Korbokkur | 09 01.7 | 15.1 | -18 | | | |
| 4800 | Veveri | 09 01.8 | 15.4 | -3 | 6.215 | | |
| 1298 | Nocturna | 09 02.0 | 14.5 | -3 | 34.8 | 0.11 | 2 |
| 6386 | Keithnoll | 09 02.2 | 13.7 | -21 | 3.138 | 0.08 | 2+ |
| 56086 | 1999 AA21 | 09 02.7 | 15.0 | -1 | | | |
| 5996 | Julioangel | 09 02.8 | 15.3 | +6 | | | |
| 2680 | Mateo | 09 03.1 | 14.3 | -9 | | | |
| 16470 | 1990 OM2 | 09 04.9 | 15.4 | -9 | | | |
| 2622 | Bolzano | 09 05.5 | 15.4 | -14 | 3.057 | 0.34 | 2 |
| 11528 | Mie | 09 06.7 | 15.0 | -18 | 7.202 | 0.38 | 2 |
| 13819 | 1999 SX5 | 09 07.4 | 15.3 | -29 | | 0.27 | |
| 8246 | Kotov | 09 08.2 | 15.4 | -5 | | | |
| 58143 | 1983 VD7 | 09 08.4 | 14.5 | -26 | | | |
| 4964 | Kourovka | 09 08.8 | 15.2 | -5 | | | |
| 10829 | Matsuobasho | 09 09.6 | 15.5 | -21 | | | |
| 10731 | 1988 BL3 | 09 10.0 | 14.8 | +8 | 28.02 | 0.23-0.41 | 2 |
| 19336 | 1997 AF | 09 10.1 | 15.5 | -20 | | | |
| 11574 | d'Alviella | 09 10.5 | 15.4 | -17 | 12.549 | 0.15 | 2 |
| 4053 | Cherkasov | 09 11.9 | 15.5 | -2 | | | |
| 4620 | Bickley | 09 12.0 | 15.2 | -13 | | | |
| 114534 | 2003 BT19 | 09 12.1 | 14.9 | -40 | | | |
| 2488 | Bryan | 09 12.5 | 15.1 | -18 | | | |
| 13920 | Montecorvino | 09 12.6 | 15.4 | +1 | | | |
| 19352 | 1997 EL | 09 14.6 | 15.4 | -10 | | | |
| 16447 | Vauban | 09 16.2 | 15.4 | +8 | | | |
| 5521 | Morpurgo | 09 16.3 | 14.9 | -22 | 6.191 | 0.89 | 2 |
| 3612 | Peale | 09 16.5 | 15.5 | -9 | | | |
| 11220 | 1999 JM25 | 09 16.5 | 15.2 | +10 | 11.28 | 0.61 | 2 |
| 16694 | 1995 AJ | 09 16.9 | 15.4 | +11 | | 0.15 | |
| 936 | Kunigunde | 09 18.5 | 13.8 | -5 | 8.8 | 0.25 | 2 |
| 13008 | 1984 SE6 | 09 18.8 | 15.2 | -3 | | | |
| 1537 | Transylvania | 09 19.3 | 14.7 | +4 | > 12. | 0.15 | 1 |
| 5542 | Moffatt | 09 19.6 | 15.2 | -24 | 5.187 | 0.12 | 2+ |
| 23983 | 1999 NS11 | 09 19.6 | 15.5 | -10 | | | |
| 7094 | Godaisan | 09 20.0 | 15.5 | -4 | | | |
| 35371 | 1997 UZ21 | 09 21.9 | 15.1 | -2 | | | |
| 23648 | Kolar | 09 23.2 | 15.1 | -9 | | | |
| 4843 | Megantic | 09 23.3 | 15.5 | -5 | | | |
| 6594 | Tasman | 09 23.9 | 15.5 | +4 | | | |
| 6792 | Akiyamatakashi | 09 24.0 | 14.2 | -7 | | | |
| 9401 | 1994 TS3 | 09 24.4 | 15.5 | -13 | 3.693 | 0.29 | 2 |
| 2514 | Taiyuan | 09 25.4 | 15.5 | +1 | | | |
| ***887*** | ***Alinda*** | ***09 26.6*** | ***15.5*** | ***-19*** | ***73.97*** | ***0.35*** | ***2*** |
| 2434 | Bateson | 09 28.1 | 15.2 | -7 | | | |
| 5169 | Duffell | 09 28.1 | 15.5 | +4 | 8.711 | 0.25 | 2 |
| 9011 | 1984 SU | 09 29.0 | 15.3 | +6 | | | |
| 2299 | Hanko | 09 29.1 | 14.3 | +0 | | | |
| 51442 | 2001 FZ25 | 09 29.2 | 15.2 | +9 | | | |
| 3970 | Herran | 09 30.2 | 14.9 | -4 | 8.09 | 0.36-0.36 | 2+ |

Low Phase Angle Opportunities

The Low Phase Angle list includes asteroids that reach very low phase angles. The "α" column is the minimum solar phase angle for the asteroid. Getting accurate, calibrated measurements (usually V band) at or very near the day of opposition can provide important information for those studying the "opposition effect." Use the on-line query form for the LCDB to get more details about a specific asteroid.

*http://www.minorplanet.info/PHP/call_OppLCDBQuery.php*

You will have the best chance of success working objects with low amplitude and periods that allow covering at least half a cycle every night. Objects with large amplitudes and/or long periods are much more difficult for phase angle studies since, for proper analysis, the data must be reduced to the average magnitude of the asteroid for each night. This reduction requires that you determine the period and the amplitude of the lightcurve; for long period objects that can be difficult. Refer to Harris et al. (1989) for the details of the analysis procedure.

As an aside, some use the maximum light to find the phase slope parameter (*G*). However, this can produce significantly different values for both *H* and *G* versus when using average light, which is the method used for values listed by the Minor Planet Center.

The International Astronomical Union (IAU) has adopted a new system, H-$G_{12}$, introduced by Muinonen et al. (2010). It will be some years before H-$G_{12}$ becomes widely used. Furthermore, it still needs refinement. That can be done mostly by having data for more asteroids, but only if at very low and moderate phase angles. We strongly encourage obtaining data every degree between 0° to 7°, the non-linear part of the curve that is due to the opposition effect. At angles α > 7°, well-calibrated data every 2° or so out to about 25-30°, if possible, should be sufficient. Coverage beyond about 50° is not generally helpful since the H-G system is best defined with data from 0-30°.

| Num | Name | Date | α | V | Dec | Period | Amp | U |
|---|---|---|---|---|---|---|---|---|
| 981 | Martina | 07 01.2 | 0.99 | 14.1 | -26 | 11.267 | 0.15-0.24 | 2 |
| 1336 | Zeelandia | 07 04.3 | 0.21 | 14.0 | -23 | 15.602 | 0.50-0.61 | 3 |
| 2854 | Rawson | 07 05.2 | 0.87 | 14.7 | -25 | 4.775 | 0.61-0.63 | 3 |
| 1350 | Rosselia | 07 05.8 | 0.95 | 14.5 | -20 | 8.140 | 0.3 -0.54 | 3 |
| 777 | Gutemberga | 07 07.7 | 0.27 | 14.2 | -22 | 12.88 | 0.15-0.25 | 2 |
| 551 | Ortrud | 07 12.2 | 0.19 | 13.9 | -22 | 17.416 | 0.14-0.19 | 3 |
| 3266 | Bernardus | 07 13.2 | 0.38 | 13.8 | -22 | 10.757 | 0.27-1.14 | 3 |
| 1837 | Osita | 07 14.2 | 0.70 | 14.8 | -20 | 3.819 | 0.48-0.59 | 3 |
| 763 | Cupido | 07 15.0 | 0.19 | 14.6 | -21 | 151.5 | 0.24-0.45 | 3- |
| 554 | Peraga | 07 15.7 | 0.17 | 12.3 | -22 | 13.713 | 0.11-0.28 | 3 |
| 2195 | Tengstrom | 07 15.7 | 0.82 | 14.8 | -23 | 2.821 | 0.17-0.45 | 3 |
| 846 | Lipperta | 07 18.0 | 0.07 | 14.3 | -21 | 1641. | 0.30 | 2 |
| 3519 | Ambiorix | 07 24.9 | 0.72 | 14.0 | -21 | 5.78 | 0.19 | 2 |
| 24827 | Maryphil | 07 24.9 | 0.46 | 14.7 | -21 | 11.653 | 0.44 | 3- |
| 9068 | 1993 OD | 07 26.6 | 0.94 | 14.7 | -18 | 3.407 | 0.19-0.20 | 3 |
| 33881 | 2000 JK66 | 07 28.0 | 0.71 | 14.5 | -20 | | | |
| 530 | Turandot | 07 28.8 | 0.34 | 12.3 | -18 | 19.960 | 0.10-0.16 | 3- |
| 360 | Carlova | 07 31.0 | 0.43 | 12.7 | -17 | 6.183 | 0.30-0.49 | 3 |
| 885 | Ulrike | 08 01.2 | 0.70 | 14.0 | -16 | 4.90 | 0.55-0.72 | 3 |
| 577 | Rhea | 08 03.3 | 1.00 | 12.7 | -20 | 12.249 | 0.21-0.24 | 3- |
| 44 | Nysa | 08 05.8 | 0.14 | 10.5 | -17 | 6.422 | 0.24-0.52 | 3 |
| 2168 | Swope | 08 06.8 | 0.16 | 14.4 | -16 | | | |
| 221 | Eos | 08 08.1 | 0.70 | 11.1 | -14 | 10.443 | 0.05-0.12 | 3 |
| 17770 | Baume | 08 08.3 | 0.44 | 14.9 | -17 | 3.263 | 0.20-0.35 | 2 |
| 223 | Rosa | 08 10.9 | 0.81 | 14.4 | -18 | 20.283 | 0.06-0.13 | 3 |
| 1514 | Ricouxa | 08 15.3 | 0.37 | 13.5 | -13 | 10.438 | 0.62 | 3 |
| 2324 | Janice | 08 16.8 | 0.12 | 15.0 | -13 | 23.2 | 0.19 | 2- |
| 6043 | Aurochs | 08 17.0 | 0.20 | 15.0 | -13 | | 0.45 | |
| 661 | Cloelia | 08 17.5 | 0.84 | 13.8 | -16 | 5.536 | 0.26 | 3 |
| 1748 | Mauderli | 08 17.7 | 0.54 | 14.8 | -15 | 5.552 | 0.1 -0.25 | 3 |
| 291 | Alice | 08 19.2 | 0.36 | 14.2 | -12 | 4.313 | 0.15-0.55 | 3 |
| 8563 | 1995 US | 08 19.4 | 0.30 | 14.9 | -13 | 3.197 | 0.56 | 3 |
| 7593 | 1992 WP4 | 08 19.6 | 0.57 | 15.0 | -11 | 2.557 | 0.14-0.17 | 3 |
| 4714 | Toyohiro | 08 19.7 | 0.95 | 15.0 | -15 | 14.706 | 0.07 | 2 |
| 1528 | Conrada | 08 19.9 | 0.74 | 14.9 | -14 | 6.321 | 0.41-0.49 | 3 |
| 1289 | Kutaissi | 08 20.3 | 0.70 | 14.1 | -11 | 3.60 | 0.20-0.42 | 3 |
| 114 | Kassandra | 08 22.1 | 0.63 | 12.3 | -10 | 10.743 | 0.23-0.25 | 3 |

| Num | Name | Date | α | V | Dec | Period | Amp | U |
|---|---|---|---|---|---|---|---|---|
| 851 | Zeissia | 08 22.1 | 0.25 | 14.4 | -12 | 9.34 | 0.38-0.53 | 3 |
| 3738 | Ots | 08 26.0 | 0.51 | 14.6 | -11 | 4.170 | 0.74 | 3 |
| 20 | Massalia | 08 28.9 | 0.35 | 9.6 | -09 | 8.098 | 0.17-0.27 | 3 |
| 279 | Thule | 08 30.6 | 0.70 | 14.5 | -12 | 23.896 | 0.02-0.10 | 3 |
| 212 | Medea | 08 30.8 | 0.89 | 12.4 | -06 | 10.283 | 0.04-0.16 | 3 |
| 467 | Laura | 08 31.0 | 0.96 | 14.5 | -06 | 70.63 | 0.15 | 3 |
| 3280 | Gretry | 09 04.6 | 0.84 | 14.5 | -05 | 10.56 | 0.35-0.51 | 3- |
| 573 | Recha | 09 06.3 | 0.18 | 12.8 | -06 | 7.166 | 0.20-0.34 | 3 |
| 805 | Hormuthia | 09 06.7 | 0.37 | 13.3 | -05 | 9.510 | 0.05 | 3- |
| 1143 | Odysseus | 09 08.3 | 0.59 | 14.9 | -03 | 10.114 | 0.15-0.22 | 3 |
| 147 | Protogeneia | 09 10.9 | 0.93 | 12.8 | -02 | 7.853 | 0.25-0.28 | 3 |
| 2088 | Sahlia | 09 12.7 | 0.78 | 14.7 | -06 | 10.37 | 0.12 | 2 |
| 586 | Thekla | 09 14.1 | 0.64 | 13.5 | -02 | 13.670 | 0.24-0.30 | 3 |
| 399 | Persephone | 09 17.6 | 0.90 | 13.5 | +01 | 9.136 | 0.40 | 3 |
| 434 | Hungaria | 09 19.1 | 0.56 | 12.3 | -02 | 26.521 | 0.51-0.75 | 3 |
| 1162 | Larissa | 09 19.2 | 0.43 | 15.0 | -03 | 6.516 | 0.12-0.20 | 3 |
| 2719 | Suzhou | 09 22.1 | 0.45 | 15.0 | -01 | | | |
| 1679 | Nevanlinna | 09 24.2 | 0.64 | 14.7 | -01 | 17.92 | 0.16 | 3- |
| 616 | Elly | 09 24.3 | 0.95 | 13.9 | +03 | 5.297 | 0.34-0.44 | 3 |
| 91 | Aegina | 09 24.6 | 0.26 | 11.8 | +00 | 6.025 | 0.12-0.27 | 3 |
| 1692 | Subbotina | 09 25.2 | 0.48 | 14.3 | +02 | 9.246 | 0.30 | 3 |
| 681 | Gorgo | 09 27.9 | 0.81 | 14.7 | +00 | 6.461 | 0.42 | 3 |
| 1576 | Fabiola | 09 27.9 | 0.17 | 14.5 | +02 | 6.889 | 0.2 -0.26 | 3- |

Shape/Spin Modeling Opportunities

Those doing work for modeling should contact Josef Ďurech at the email address above. If looking to add lightcurves for objects with existing models, visit the Database of Asteroid Models from Inversion Techniques (DAMIT) web site

*https://astro.troja.mff.cuni.cz/projects/damit/*

Additional lightcurves could lead to the asteroid being added to or improving one in DAMIT, thus increasing the total number of asteroids with spin axis and shape models.

Included in the list below are objects that:

1. Are rated U = 3– or 3 in the LCDB
2. Do not have reported pole in the LCDB Summary table
3. Have at least three entries in the Details table of the LCDB where the lightcurve is rated U ≥ 2.

The caveat for condition #3 is that no check was made to see if the lightcurves are from the same apparition or if the phase angle bisector longitudes differ significantly from the upcoming apparition. The last check is often not possible because the LCDB does not list the approximate date of observations for all details records. Including that information is an on-going project.

Favorable apparitions are in bold text. NEAs are in italics.

| | | Brightest | | | LCDB Data | | |
|---|---|---|---|---|---|---|---|
| Num | Name | Date | Mag | Dec | Period | Amp | U |
| 1562 | Gondolatsch | 07 04.7 | 14.1 | -19 | 8.78 | 0.30- 0.4 | 3- |
| 111 | Ate | 07 05.4 | 11.8 | -26 | 22.072 | 0.08-0.18 | 3 |
| 793 | Arizona | 07 06.6 | 14.0 | -46 | 7.399 | 0.22-0.25 | 3 |
| 551 | Ortrud | 07 12.2 | 13.9 | -22 | 17.416 | 0.14-0.19 | 3 |
| 772 | Tanete | 07 12.6 | 13.0 | -54 | 17.258 | 0.07-0.18 | 3 |
| 1346 | Gotha | 07 13.2 | 15.4 | -4 | 2.6407 | 0.10-0.16 | 3- |
| **1084** | **Tamariwa** | **07 13.6** | **13.5** | **-15** | **6.1961** | **0.25-0.42** | **3** |
| **197** | **Arete** | **07 15.2** | **12.0** | **-29** | **6.6084** | **0.10-0.16** | **3** |
| 554 | Peraga | 07 15.8 | 12.3 | -22 | 13.7128 | 0.11-0.28 | 3 |
| 2195 | Tengstrom | 07 15.8 | 14.7 | -23 | 2.8211 | 0.17-0.45 | 3 |
| 454 | Mathesis | 07 16.5 | 12.6 | -31 | 8.378 | 0.20-0.37 | 3 |
| 151 | Abundantia | 07 19.4 | 12.6 | -31 | 9.864 | 0.15-0.20 | 3 |
| 2951 | Perepadin | 07 19.8 | 15.2 | -41 | 4.781 | 0.54-0.76 | 3 |
| 303 | Josephina | 07 20.8 | 13.3 | -28 | 12.497 | 0.12-0.15 | 3 |
| 444 | Gyptis | 07 23.3 | 11.0 | -4 | 6.214 | 0.10-0.18 | 3 |
| 126 | Velleda | 07 24.4 | 11.8 | -25 | 5.3672 | 0.07-0.22 | 3 |
| 4183 | Cuno | 07 25.3 | 15.5 | +19 | 3.5595 | 0.47-0.84 | 3 |
| **9068** | **1993 OD** | **07 26.8** | **14.9** | **-18** | **3.4073** | **0.19-0.20** | **3** |
| 535 | Montague | 07 26.9 | 12.7 | -26 | 10.2482 | 0.18-0.25 | 3 |
| 806 | Gyldenia | 07 27.2 | 15.1 | -38 | 16.852 | 0.10-0.27 | 3 |
| **530** | **Turandot** | **07 28.9** | **12.3** | **-18** | **19.96** | **0.10-0.16** | **3-** |
| 2647 | Sova | 07 29.0 | 15.2 | -17 | 9.366 | 0.23-0.35 | 3 |
| 5806 | Archieroy | 08 03.2 | 14.6 | -9 | 12.163 | 0.34-0.47 | 3 |
| 1146 | Biarmia | 08 06.8 | 13.2 | +12 | 5.47 | 0.20-0.32 | 3 |
| 5431 | Maxinehelin | 08 07.4 | 15.1 | +4 | 5.1951 | 0.18-0.25 | 3 |
| 788 | Hohensteina | 08 09.1 | 13.0 | -2 | 37.137 | 0.10-0.18 | 3 |
| 461 | Saskia | 08 11.5 | 15.2 | -15 | 7.348 | 0.25-0.36 | 3 |
| 145 | Adeona | 08 13.4 | 12.5 | -30 | 15.071 | 0.04-0.15 | 3 |
| **14211** | **1999 NT1** | **08 18.0** | **15.4** | **+20** | **3.5856** | **0.12-0.17** | **3** |
| 1656 | Suomi | 08 21.7 | 15.3 | +10 | 2.583 | 0.11-0.20 | 3 |
| ***85275*** | ***1994 LY*** | ***08 21.8*** | ***13.7*** | ***-31*** | ***2.6962*** | ***0.07-0.16*** | ***3*** |
| 851 | Zeissia | 08 22.1 | 14.4 | -12 | 9.34 | 0.38-0.53 | 3 |
| 308 | Polyxo | 08 24.5 | 11.6 | -8 | 12.029 | 0.08-0.15 | 3- |
| 905 | Universitas | 08 27.7 | 13.4 | -19 | 14.238 | 0.22-0.33 | 3 |
| 3951 | Zichichi | 09 01.2 | 15.4 | +0 | 3.3942 | 0.25-0.35 | 3 |
| 517 | Edith | 09 04.2 | 13.3 | -3 | 9.2747 | 0.08-0.18 | 3 |
| 514 | Armida | 09 05.6 | 13.1 | -1 | 21.851 | 0.16-0.27 | 3 |
| 1143 | Odysseus | 09 08.4 | 14.9 | -3 | 10.114 | 0.15-0.22 | 3 |
| **375** | **Ursula** | **09 12.3** | **11.3** | **+2** | **16.899** | **0.04-0.17** | **3** |
| 586 | Thekla | 09 14.1 | 13.5 | -2 | 13.67 | 0.24-0.30 | 3 |
| 1626 | Sadeya | 09 16.9 | 14.1 | +33 | 3.42 | 0.07-0.22 | 3 |
| 1044 | Teutonia | 09 17.2 | 13.7 | -8 | 3.153 | 0.20-0.32 | 3 |
| **737** | **Arequipa** | **09 18.7** | **10.6** | **+2** | **7.0259** | **0.10-0.27** | **3** |
| 1817 | Katanga | 09 19.7 | 15.1 | -35 | 8.481 | 0.22-0.42 | 3 |
| 288 | Glauke | 09 20.8 | 14.4 | -6 | 1170. | 0.36- 0.9 | 3 |
| **1406** | **Komppa** | **09 22.1** | **14.7** | **+8** | **3.508** | **0.14-0.20** | **3** |
| 4063 | Euforbo | 09 22.9 | 15.4 | -20 | 8.846 | 0.15-0.24 | 3 |
| 91 | Aegina | 09 24.6 | 11.8 | +0 | 6.025 | 0.12-0.27 | 3 |
| 911 | Agamemnon | 09 24.6 | 14.7 | +11 | 6.592 | 0.04-0.29 | 3 |
| 301 | Bavaria | 09 26.8 | 13.9 | -3 | 12.253 | 0.25-0.31 | 3 |
| 14465 | 1993 NB | 09 28.0 | 15.0 | -18 | 4.9703 | 0.49-0.69 | 3 |
| 659 | Nestor | 09 28.7 | 15.2 | +4 | 15.98 | 0.22-0.31 | 3 |
| 1314 | Paula | 09 30.4 | 14.5 | +12 | 5.9498 | 0.81-1.24 | 3 |

Of particular note is 288 Glauke. This is a known tumbler so lightcurve analysis will be complicated but not impossible. For tumblers, data at viewing aspects similar to past observations have more value than would be for single axis rotators, when re-observing would be mostly redundant, unless at significantly different phase angles.

Radar-Optical Opportunities

Past radar targets:
*http://echo.jpl.nasa.gov/~lance/radar.nea.periods.html*

Arecibo targets:
*http://www.naic.edu/~pradar*
*http://www.naic.edu/~pradar/ephemfuture.txt*

Goldstone targets:
*http://echo.jpl.nasa.gov/asteroids/goldstone_asteroid_schedule.html*

These are based on *known* targets at the time the list was prepared. It is very common for newly discovered objects to move up the list and become radar targets on short notice. We recommend that you keep up with the latest discoveries the Minor Planet Center observing tools.

In particular, monitor NEAs and be flexible with your observing program. In some cases, you may have only 1-3 days when the asteroid is within reach of your equipment. Be sure to keep in touch with the radar team (through Benner's email or their Facebook or Twitter accounts) if you get data. The team may not always be observing the target but your initial results may change their plans. In all cases, your efforts are greatly appreciated.

Use the ephemerides below as a guide to your best chances for observing, but remember that photometry may be possible before and/or after the ephemerides given below. Note that *geocentric* positions are given. Use these web sites to generate updated and *topocentric* positions:

MPC: *http://www.minorplanetcenter.net/iau/MPEph/MPEph.html*
JPL: *http://ssd.jpl.nasa.gov/?horizons*

In the ephemerides below, ED and SD are, respectively, the Earth and Sun distances (AU), V is the estimated Johnson V magnitude, and α is the phase angle. SE and ME are the great circle distances (in degrees) of the Sun and Moon from the asteroid. MP is the lunar phase and GB is the galactic latitude. "PHA" indicates that the object is a "potentially hazardous asteroid", meaning that at some (long distant) time, its orbit might take it very close to Earth.

About YORP Acceleration

Many, if not all, of the targets in this section are near-Earth asteroids. These objects are particularly sensitive to YORP acceleration. YORP (Yarkovsky–O'Keefe–Radzievskii–Paddack) is the asymmetric thermal re-radiation of sunlight that can cause an asteroid's rotation period to increase or decrease. High precision lightcurves at multiple apparitions can be used to model the asteroid's *sidereal* rotation period and see if it's changing.

It usually takes four apparitions to have sufficient data to determine if the asteroid rotation rate is changing under the influence of YORP. This is why observing an asteroid that already has a well-known period remains a valuable use of telescope time. It is even more so when considering the BYORP (binary-YORP) effect among binary asteroids that has stabilized the spin so that acceleration of the primary body is not the same as if it would be if there were no satellite.

To help focus efforts in YORP detection, Table I gives a quick summary of this quarter's radar-optical targets. The family or group for the asteroid is given under the number name. Also, under the name will be additional flags such as "PHA" for Potentially Hazardous Asteroid, NPAR for a tumbler, and/or "BIN" to indicate the asteroid is a binary (or multiple) system. "BIN?" means that the asteroid is a suspected but not confirmed binary. The period is in hours and, in the case of binary, for the primary. The Amp column gives the known range of lightcurve amplitudes. The App columns gives the number of different apparitions at which a lightcurve period was reported while the Last column gives the year for the last reported period. The R SNR column indicates the estimated radar SNR using the tool at

*http://www.naic.edu/~eriverav/scripts/index.php*

The SNRs were calculated using the current MPCORB absolute magnitude (H), a period of 4 hours (2 hours if $D \leq 200$ m) if it's not known, and the approximate minimum Earth distance during the current quarter. These are estimates only and assume that the radars are fully functional.

If the SNR value is in bold text, the object was found on the radar planning pages listed above. Otherwise, the planning tool at

*http://www.minorplanet.info/PHP/call_OppLCDBQuery.php*

was used to find known NEAs that were V < 18.0 during the quarter. An object is usually placed on the list only if the estimated Arecibo SNR > 10 when using the SNR calculator mentioned above.

It's rarely the case, especially when shape/spin axis modeling, that there are too many observations. Remember that the best set for modeling includes data not just from multiple apparitions but from as wide a range of phase angles during each apparition as well.

The "A" is for Arecibo; "G" is for Goldstone.

| Asteroid | Period | Amp | App | Last | R SNR |
|---|---|---|---|---|---|
| **(441987) 2010 NY65 NEA** | **4.973** | **0.21 0.24** | **4** | **2019** | **A: 310 G: 100** |
| (242450) 2004 QY2 NEA | - | - | - | - | A: 60 G: 20 |
| **(8014) 1990 MF NEA** | **-** | **-** | **-** | **-** | **A: 280 G: 95** |
| **2006 NL NEA** | **-** | **-** | **-** | **-** | **A: 110 G: 35** |
| (85989) 2003 QH5 NEA PHA | 7.6638 | 0.5 1.3 | 10 | 2019 | A: 40 G: 15 |
| (480936) 2003 QH5 NEA | **-** | **-** | **-** | **-** | **A: 15** |
| 9162 Kwiila NEA | - | - | - | - | A: 15 |
| (85275) 1994 LY NEA BIN? | 2.6962 | 0.07 0.16 | 1 | 2007 | A: 110 G: 35 |
| (411165) 2010 DF1 NEA | - | - | - | - | A: 10 |
| **2011 ES4 NEA** | **-** | **-** | **-** | **-** | ***A: 725*** **G: 240** |
| **(465824) 2010 FR NEA PHA** | **-** | **-** | **-** | **-** | **A: 55 G: 20** |
| **2013 TD NEA** | **-** | **-** | **-** | **-** | ***A: 225*** **G: 75** |

Table I. Summary of radar-optical opportunities for the current quarter. Period and amplitude data are from the asteroid lightcurve database (LCDB; Warner et al., 2009a). SNR values are *estimates* that are affected by radar power output along with rotation period, size, and distance. They are given for relative comparisons among the objects in the list. An Arecibo SNR in italics indicates that the SNR is from the calculator while the radar web site gives a different (usually lower) value.

**(441987) 2010 NY65 (H = 21.3)**

The rotation period of this 160-m NEA is either 4.97 h (Warner and Stephens, 2020) or 5.55 h (Warner and Stephens, 2019a), give or take. The difference is one-half rotation over 24 hours. If the curve is highly symmetrical, it will be easy to encounter *rotational aliasing*, which is caused by not knowing the true number of rotations over the span of a data set. Put another way, the wrong solution matches data from a given night to the wrong half of the lightcurve.

Because of the short summer evenings for Northern observers, getting a complete rotation every time may not be possible. A well-coordinated campaign involving well-separated observers would be highly beneficial.

| DATE | RA | Dec | ED | SD | V | α | SE | ME | MP | GB |
|---|---|---|---|---|---|---|---|---|---|---|
| 07/01 | 16 03.3 | +20 23 | 0.06 | 1.05 | 17.1 | 55.4 | 122 | 37 | +0.79 | +46 |
| 07/02 | 16 13.6 | +18 25 | 0.06 | 1.05 | 17.3 | 52.7 | 125 | 36 | +0.88 | +43 |
| 07/03 | 16 21.8 | +16 48 | 0.07 | 1.06 | 17.5 | 50.6 | 126 | 38 | +0.94 | +40 |
| 07/04 | 16 28.4 | +15 27 | 0.08 | 1.07 | 17.7 | 48.9 | 128 | 43 | +0.98 | +38 |
| 07/05 | 16 33.9 | +14 18 | 0.08 | 1.07 | 17.8 | 47.6 | 129 | 50 | +1.00 | +37 |
| 07/06 | 16 38.6 | +13 19 | 0.09 | 1.08 | 18.0 | 46.5 | 130 | 59 | -0.99 | +35 |
| 07/07 | 16 42.6 | +12 27 | 0.10 | 1.08 | 18.2 | 45.6 | 131 | 68 | -0.96 | +34 |
| 07/08 | 16 46.1 | +11 42 | 0.10 | 1.09 | 18.3 | 44.8 | 131 | 78 | -0.91 | +33 |
| 07/09 | 16 49.2 | +11 01 | 0.11 | 1.09 | 18.4 | 44.2 | 131 | 87 | -0.85 | +32 |
| 07/10 | 16 51.9 | +10 24 | 0.12 | 1.10 | 18.6 | 43.7 | 132 | 97 | -0.77 | +31 |

**(242450) 2004 QY2 (H = 14.7)**

The observing window for this 3.4 km NEA is very short; it starts just about the time this issue is released and ends only a few days into July.

| DATE | RA | Dec | ED | SD | V | α | SE | ME | MP | GB |
|---|---|---|---|---|---|---|---|---|---|---|
| 06/20 | 00 23.3 | -35 32 | 0.32 | 1.11 | 14.8 | 65.4 | 98 | 85 | -0.02 | -80 |
| 06/22 | 00 32.8 | -33 06 | 0.29 | 1.09 | 14.6 | 67.6 | 97 | 105 | +0.01 | -83 |
| 06/24 | 00 43.1 | -30 13 | 0.27 | 1.08 | 14.5 | 70.2 | 95 | 125 | +0.09 | -86 |
| 06/26 | 00 54.5 | -26 44 | 0.25 | 1.06 | 14.4 | 73.3 | 93 | 144 | +0.25 | -89 |
| 06/28 | 01 07.1 | -22 31 | 0.23 | 1.04 | 14.3 | 77.0 | 90 | 158 | +0.46 | -84 |
| 06/30 | 01 21.1 | -17 24 | 0.21 | 1.03 | 14.2 | 81.3 | 87 | 153 | +0.69 | -78 |
| 07/02 | 01 36.8 | -11 14 | 0.19 | 1.01 | 14.2 | 86.5 | 83 | 136 | +0.88 | -71 |
| 07/04 | 01 54.4 | -03 55 | 0.18 | 0.99 | 14.2 | 92.5 | 78 | 117 | +0.98 | -62 |
| 07/06 | 02 14.3 | +04 26 | 0.17 | 0.98 | 14.4 | 99.1 | 71 | 98 | -0.99 | -53 |
| 07/08 | 02 36.5 | +13 27 | 0.16 | 0.96 | 14.6 | 106.0 | 65 | 80 | -0.91 | -42 |

**(8014) 1990 MF (H = 18.7)**

There is no period given in the LCDB for 1990 MF, which has an estimated diameter of 540 meters. This is large enough that the period should be $P \geq 2$ hours. There are two opportunities in 2020 to observe the asteroid. The first is a two-week window at the start of July. The second is in the last quarter of the year, mostly in November. That ephemeris is included here for planning purposes.

| DATE | RA | Dec | ED | SD | V | α | SE | ME | MP | GB |
|---|---|---|---|---|---|---|---|---|---|---|
| 07/01 | 14 41.0 | +01 36 | 0.11 | 1.07 | 16.2 | 58.0 | 117 | 15 | +0.79 | +53 |
| 07/03 | 14 34.5 | +03 29 | 0.10 | 1.06 | 16.1 | 62.2 | 113 | 41 | +0.94 | +56 |
| 07/05 | 14 27.3 | +05 36 | 0.10 | 1.05 | 16.1 | 66.7 | 108 | 70 | +1.00 | +59 |
| 07/07 | 14 19.2 | +08 00 | 0.09 | 1.04 | 16.1 | 71.5 | 104 | 98 | -0.96 | +62 |
| 07/09 | 14 10.0 | +10 44 | 0.08 | 1.03 | 16.1 | 76.7 | 99 | 126 | -0.85 | +65 |
| 07/11 | 13 59.1 | +13 52 | 0.08 | 1.02 | 16.1 | 82.4 | 93 | 149 | -0.68 | +69 |
| 07/13 | 13 46.2 | +17 28 | 0.07 | 1.02 | 16.2 | 88.7 | 87 | 158 | -0.50 | +74 |
| 07/15 | 13 30.4 | +21 35 | 0.07 | 1.01 | 16.3 | 95.6 | 81 | 140 | -0.31 | +80 |
| | | | | | | | | | | |
| 11/01 | 04 34.3 | +19 56 | 0.35 | 1.30 | 18.1 | 23.3 | 149 | 27 | -1.00 | -18 |
| 11/04 | 04 27.5 | +19 30 | 0.36 | 1.32 | 18.1 | 19.6 | 153 | 11 | -0.90 | -20 |
| 11/07 | 04 20.8 | +19 03 | 0.37 | 1.34 | 18.1 | 16.1 | 158 | 50 | -0.66 | -21 |
| 11/10 | 04 14.1 | +18 38 | 0.38 | 1.36 | 18.0 | 12.6 | 163 | 91 | -0.35 | -23 |
| 11/13 | 04 07.7 | +18 13 | 0.40 | 1.38 | 18.0 | 9.2 | 167 | 136 | -0.07 | -24 |
| 11/16 | 04 01.5 | +17 49 | 0.42 | 1.40 | 18.0 | 6.0 | 171 | 176 | +0.01 | -26 |
| 11/19 | 03 55.7 | +17 27 | 0.43 | 1.42 | 18.0 | 3.2 | 175 | 132 | +0.19 | -27 |
| 11/22 | 03 50.4 | +17 06 | 0.45 | 1.44 | 18.0 | 2.1 | 177 | 91 | +0.48 | -28 |
| 11/25 | 03 45.6 | +16 48 | 0.48 | 1.46 | 18.3 | 3.9 | 174 | 53 | +0.76 | -29 |
| 11/28 | 03 41.2 | +16 32 | 0.50 | 1.48 | 18.5 | 6.3 | 170 | 17 | +0.95 | -30 |

**2006 NL (H = 20.0)**

The 300-m 2006 NL was listed only on the Goldstone planning page even though it does reach declinations within Arecibo's observing range. Fortunately, the moon shouldn't be too much a problem during the first few weeks of July. There is no period in the LCDB. The estimated diameter is 300 meters.

| DATE | RA | Dec | ED | SD | V | α | SE | ME | MP | GB |
|---|---|---|---|---|---|---|---|---|---|---|
| 07/05 | 22 20.3 | +71 41 | 0.07 | 1.01 | 17.8 | 96.5 | 79 | 102 | +1.00 | +12 |
| 07/07 | 20 14.2 | +62 33 | 0.06 | 1.02 | 16.9 | 82.7 | 94 | 84 | -0.96 | +15 |
| 07/09 | 19 03.3 | +45 50 | 0.06 | 1.04 | 16.2 | 65.3 | 112 | 76 | -0.85 | +17 |
| 07/11 | 18 25.1 | +26 30 | 0.06 | 1.06 | 15.8 | 48.0 | 130 | 87 | -0.68 | +17 |
| 07/13 | 18 02.5 | +09 55 | 0.07 | 1.07 | 15.8 | 36.1 | 142 | 110 | -0.50 | +15 |
| 07/15 | 17 48.0 | -02 08 | 0.08 | 1.09 | 16.0 | 30.7 | 147 | 136 | -0.31 | +13 |
| 07/17 | 17 38.1 | -10 31 | 0.10 | 1.10 | 16.4 | 29.8 | 148 | 162 | -0.15 | +11 |
| 07/19 | 17 31.1 | -16 24 | 0.12 | 1.11 | 16.9 | 30.8 | 146 | 166 | -0.03 | +9 |
| 07/21 | 17 26.1 | -20 39 | 0.13 | 1.13 | 17.3 | 32.4 | 144 | 140 | +0.00 | +8 |
| 07/23 | 17 22.5 | -23 50 | 0.15 | 1.14 | 17.6 | 34.0 | 141 | 111 | +0.07 | +7 |

**(85989) 1999 JD6 (H = 17.1, PHA)**

Here is another radar target that has limited visual opportunities. In this case, the 1.1 km NEA is reasonably placed for just the first part of July. The period is about 7.67 h (Polishook and Brosch, 2008; Warner and Stephens, 2019b). The amplitude has ranged from 1.0-1.5 mag (LCDB; Warner et al., 2009a).

| DATE | RA | Dec | ED | SD | V | α | SE | ME | MP | GB |
|---|---|---|---|---|---|---|---|---|---|---|
| 07/01 | 22 49.9 | +15 49 | 0.29 | 1.14 | 16.8 | 58.2 | 108 | 121 | +0.79 | -38 |
| 07/02 | 22 54.8 | +16 27 | 0.28 | 1.13 | 16.7 | 59.1 | 107 | 110 | +0.88 | -38 |
| 07/03 | 23 00.1 | +17 08 | 0.27 | 1.12 | 16.6 | 60.1 | 107 | 99 | +0.94 | -38 |
| 07/04 | 23 06.0 | +17 51 | 0.26 | 1.12 | 16.6 | 61.2 | 106 | 88 | +0.98 | -38 |
| 07/05 | 23 12.3 | +18 38 | 0.25 | 1.11 | 16.5 | 62.4 | 105 | 77 | +1.00 | -38 |
| 07/06 | 23 19.2 | +19 27 | 0.23 | 1.10 | 16.4 | 63.8 | 104 | 67 | -0.99 | -38 |
| 07/07 | 23 26.9 | +20 19 | 0.22 | 1.09 | 16.3 | 65.3 | 103 | 58 | -0.96 | -38 |
| 07/08 | 23 35.4 | +21 15 | 0.21 | 1.08 | 16.3 | 67.0 | 102 | 49 | -0.91 | -38 |
| 07/09 | 23 44.8 | +22 14 | 0.20 | 1.07 | 16.2 | 68.9 | 100 | 42 | -0.85 | -38 |
| 07/10 | 23 55.3 | +23 17 | 0.19 | 1.06 | 16.1 | 71.1 | 99 | 35 | -0.77 | -38 |

**(480936) 2003 QH5 (H = 20.1)**

The estimated diameter of this NEA is about 280 meters, large enough that the period should be more than about 2 hours.

| DATE | RA | Dec | ED | SD | V | α | SE | ME | MP | GB |
|---|---|---|---|---|---|---|---|---|---|---|
| 07/10 | 02 10.5 | -12 52 | 0.09 | 1.01 | 18.2 | 91.9 | 83 | 43 | -0.77 | -67 |
| 07/13 | 01 49.4 | -03 23 | 0.09 | 1.02 | 17.9 | 88.3 | 87 | 9 | -0.50 | -63 |
| 07/16 | 01 28.1 | +06 26 | 0.09 | 1.02 | 17.8 | 84.2 | 91 | 34 | -0.22 | -55 |
| 07/19 | 01 06.6 | +15 52 | 0.09 | 1.03 | 17.7 | 79.9 | 95 | 74 | -0.03 | -47 |
| 07/22 | 00 45.0 | +24 16 | 0.10 | 1.04 | 17.7 | 75.9 | 99 | 113 | +0.02 | -39 |
| 07/25 | 00 23.7 | +31 20 | 0.10 | 1.04 | 17.8 | 72.2 | 102 | 143 | +0.23 | -31 |
| 07/28 | 00 02.7 | +37 02 | 0.11 | 1.05 | 17.9 | 69.1 | 105 | 136 | +0.56 | -25 |
| 07/31 | 23 42.3 | +41 30 | 0.13 | 1.06 | 18.1 | 66.4 | 107 | 107 | +0.86 | -20 |
| 08/03 | 23 22.7 | +44 56 | 0.14 | 1.07 | 18.2 | 64.1 | 109 | 79 | +0.99 | -15 |
| 08/06 | 23 04.2 | +47 30 | 0.15 | 1.08 | 18.3 | 62.1 | 110 | 59 | -0.94 | -12 |

**9162 Kwiila (H = 17.8)**

At 820 meters, this is among the larger NEAs listed here. There is no period given in the LCDB. As with many others in the list, the first month or so of the quarter will be the only chance to observe the asteroid for the rest of 2020.

| DATE | RA | Dec | ED | SD | V | α | SE | ME | MP | GB |
|---|---|---|---|---|---|---|---|---|---|---|
| 07/01 | 22 01.9 | +10 40 | 0.52 | 1.36 | 18.6 | 40.3 | 120 | 109 | +0.79 | -34 |
| 07/05 | 22 10.7 | +12 56 | 0.47 | 1.32 | 18.4 | 41.4 | 121 | 62 | +1.00 | -34 |
| 07/09 | 22 20.8 | +15 33 | 0.42 | 1.28 | 18.1 | 43.0 | 121 | 30 | -0.85 | -34 |
| 07/13 | 22 32.9 | +18 37 | 0.38 | 1.25 | 17.9 | 45.1 | 120 | 45 | -0.50 | -33 |
| 07/17 | 22 48.0 | +22 16 | 0.33 | 1.21 | 17.6 | 48.1 | 118 | 79 | -0.15 | -32 |
| 07/21 | 23 07.6 | +26 41 | 0.29 | 1.17 | 17.4 | 52.2 | 115 | 116 | +0.00 | -31 |
| 07/25 | 23 34.8 | +31 59 | 0.25 | 1.13 | 17.1 | 57.8 | 110 | 142 | +0.23 | -28 |
| 07/29 | 00 14.3 | +38 11 | 0.22 | 1.09 | 17.0 | 65.5 | 103 | 131 | +0.67 | -24 |
| 08/02 | 01 13.9 | +44 32 | 0.20 | 1.05 | 17.0 | 75.7 | 93 | 104 | +0.97 | -18 |
| 08/06 | 02 39.6 | +48 59 | 0.18 | 1.00 | 17.2 | 88.1 | 81 | 78 | -0.94 | -10 |

**(85275) 1994 LY (H = 16.1, BIN?)**

Pravec et al. (2007) reported this 1.8-km asteroid as a suspected binary with a satellite orbital period of about 48 h. This is commensurate with an Earth day, which calls for a coordinated observing campaign involving a number of observers, individually or in groups, at significantly different longitudes. The primary lightcurve has a period of 2.6962 h and, as is often expected of the primary of a binary asteroid, a relatively low amplitude (0.07-0.16 mag).

The ephemeris covers the second half of 2020 since the asteroid is reasonably placed for that period. Note, however, that it remains near the galactic equator until mid-September.

| DATE | RA | Dec | ED | SD | V | α | SE | ME | MP | GB |
|---|---|---|---|---|---|---|---|---|---|---|
| 07/01 | 18 17.6 | +24 16 | 0.37 | 1.29 | 16.0 | 35.5 | 132 | 62 | +0.79 | +18 |
| 07/21 | 18 00.0 | +20 03 | 0.25 | 1.19 | 15.1 | 41.1 | 130 | 125 | +0.00 | +20 |
| 08/10 | 17 50.1 | -01 16 | 0.15 | 1.11 | 14.0 | 47.5 | 126 | 121 | -0.66 | +13 |
| 08/30 | 18 24.0 | -55 35 | 0.12 | 1.06 | 13.8 | 61.3 | 113 | 38 | +0.90 | -18 |
| 09/19 | 01 24.6 | -78 35 | 0.19 | 1.06 | 15.0 | 68.0 | 102 | 98 | +0.04 | -38 |
| 10/09 | 03 19.0 | -64 47 | 0.28 | 1.10 | 15.8 | 61.2 | 104 | 96 | -0.60 | -46 |
| 10/29 | 03 20.3 | -53 23 | 0.37 | 1.18 | 16.2 | 51.2 | 112 | 62 | +0.94 | -52 |
| 11/18 | 03 12.7 | -41 16 | 0.47 | 1.29 | 16.7 | 42.0 | 119 | 101 | +0.11 | -58 |
| 12/08 | 03 12.4 | -28 14 | 0.60 | 1.41 | 17.2 | 36.0 | 123 | 122 | -0.50 | -59 |
| 12/28 | 03 22.4 | -16 01 | 0.78 | 1.53 | 17.9 | 33.9 | 120 | 43 | +0.96 | -53 |

**(411165) 2010 DF1 (H = 21.8)**

The estimated diameter of 2010 DF1 is only 130 meters. This makes it a potential super-fast rotator, i.e., $P < 2$ h. In order to avoid *rotational smearing* (Pravec et al., 2000), exposure times should be kept to a minimum until a preliminary period can be determined. Otherwise, the rotation information may be lost entirely or, at the least, the amplitude significantly underestimated.

| DATE | RA | Dec | ED | SD | V | α | SE | ME | MP | GB |
|---|---|---|---|---|---|---|---|---|---|---|
| 08/20 | 23 58.7 | +51 16 | 0.05 | 1.03 | 17.9 | 66.1 | 111 | 115 | +0.01 | -11 |
| 08/21 | 23 52.8 | +41 13 | 0.05 | 1.04 | 17.6 | 56.7 | 121 | 132 | +0.05 | -20 |
| 08/22 | 23 48.4 | +31 14 | 0.05 | 1.05 | 17.4 | 47.4 | 130 | 145 | +0.12 | -30 |
| 08/23 | 23 45.1 | +21 54 | 0.06 | 1.06 | 17.3 | 38.8 | 139 | 149 | +0.21 | -38 |
| 08/24 | 23 42.4 | +13 35 | 0.06 | 1.06 | 17.2 | 31.5 | 147 | 139 | +0.31 | -46 |
| 08/25 | 23 40.2 | +06 25 | 0.07 | 1.07 | 17.2 | 25.5 | 153 | 125 | +0.42 | -52 |
| 08/26 | 23 38.4 | +00 22 | 0.07 | 1.08 | 17.3 | 20.9 | 158 | 109 | +0.53 | -57 |
| 08/27 | 23 36.8 | -04 41 | 0.08 | 1.09 | 17.4 | 17.6 | 161 | 93 | +0.64 | -61 |
| 08/28 | 23 35.5 | -08 55 | 0.09 | 1.09 | 17.6 | 15.6 | 163 | 77 | +0.74 | -64 |
| 08/29 | 23 34.2 | -12 28 | 0.10 | 1.10 | 17.7 | 14.6 | 164 | 62 | +0.83 | -67 |
| 08/30 | 23 33.1 | -15 28 | 0.10 | 1.11 | 17.9 | 14.3 | 164 | 48 | +0.90 | -68 |
| 08/31 | 23 32.2 | -18 00 | 0.11 | 1.12 | 18.1 | 14.6 | 164 | 35 | +0.95 | -70 |

**2011 ES4 (H = 25.7)**

The observing window in early September is short. The estimated diameter is only 20 meters. This presents many possibilities: super-fast rotator and/or tumbling. Here is another case where exposures should be kept as short as possible for the initial observations. Given the large sky motion and V > 18, the circumstances favor those with larger instruments.

| DATE | RA | Dec | ED | SD | V | α | SE | ME | MP | GB |
|---|---|---|---|---|---|---|---|---|---|---|
| 09/01 | 04 38.0 | +18 40 | 0.01 | 1.01 | 18.9 | 91.0 | 88 | 105 | +0.98 | -19 |
| 09/02 | 02 59.4 | +19 20 | 0.01 | 1.01 | 18.3 | 67.5 | 112 | 71 | +1.00 | -34 |
| 09/03 | 01 46.4 | +17 41 | 0.01 | 1.02 | 18.2 | 49.9 | 130 | 43 | -0.99 | -43 |
| 09/04 | 00 59.1 | +15 40 | 0.02 | 1.02 | 18.4 | 38.2 | 141 | 22 | -0.97 | -47 |
| 09/05 | 00 28.4 | +13 59 | 0.02 | 1.03 | 18.6 | 30.4 | 149 | 15 | -0.93 | -49 |
| 09/06 | 00 07.6 | +12 41 | 0.02 | 1.03 | 18.8 | 24.9 | 154 | 24 | -0.87 | -49 |
| 09/07 | 23 52.7 | +11 40 | 0.03 | 1.03 | 19.0 | 21.0 | 158 | 38 | -0.80 | -49 |
| 09/08 | 23 41.6 | +10 52 | 0.03 | 1.04 | 19.2 | 18.1 | 161 | 51 | -0.72 | -48 |
| 09/09 | 23 33.0 | +10 14 | 0.04 | 1.04 | 19.4 | 16.0 | 163 | 64 | -0.63 | -48 |
| 09/10 | 23 26.3 | +09 42 | 0.04 | 1.05 | 19.6 | 14.4 | 165 | 78 | -0.54 | -48 |

**(465824) 2010 FR (H = 21.6, PHA)**

The estimated diameter is 140 meters. There is no period given in the LCDB. However, the size is about at the "line" where super-fast rotation, $P < 2$ h, has a higher probability. The moon doesn't cooperate this time around: it's nearly full when the asteroid is brightest.

| DATE | RA | Dec | ED | SD | V | α | SE | ME | MP | GB |
|---|---|---|---|---|---|---|---|---|---|---|
| 08/25 | 00 26.6 | +34 43 | 0.11 | 1.08 | 18.9 | 50.1 | 125 | 136 | +0.42 | -28 |
| 08/26 | 00 36.3 | +35 16 | 0.10 | 1.07 | 18.7 | 51.3 | 124 | 129 | +0.53 | -28 |
| 08/27 | 00 47.5 | +35 50 | 0.10 | 1.07 | 18.6 | 52.7 | 123 | 121 | +0.64 | -27 |
| 08/28 | 01 00.5 | +36 23 | 0.09 | 1.06 | 18.5 | 54.4 | 121 | 113 | +0.74 | -26 |
| 08/29 | 01 15.8 | +36 54 | 0.08 | 1.05 | 18.4 | 56.4 | 120 | 105 | +0.83 | -26 |
| 08/30 | 01 33.8 | +37 20 | 0.08 | 1.05 | 18.3 | 58.8 | 117 | 97 | +0.90 | -25 |
| 08/31 | 01 55.1 | +37 37 | 0.07 | 1.04 | 18.2 | 61.7 | 115 | 90 | +0.95 | -24 |
| 09/01 | 02 20.1 | +37 37 | 0.07 | 1.04 | 18.1 | 65.2 | 111 | 83 | +0.98 | -22 |
| 09/02 | 02 49.2 | +37 12 | 0.06 | 1.03 | 18.0 | 69.4 | 107 | 77 | +1.00 | -20 |
| 09/03 | 03 22.5 | +36 10 | 0.06 | 1.02 | 18.0 | 74.4 | 103 | 71 | -0.99 | -17 |
| 09/04 | 03 59.1 | +34 17 | 0.05 | 1.02 | 18.1 | 80.2 | 97 | 65 | -0.97 | -14 |
| 09/05 | 04 37.7 | +31 26 | 0.05 | 1.01 | 18.2 | 86.8 | 90 | 60 | -0.93 | -10 |

**2013 TD (H = 26.6)**

This 10-m NEA is included only to call it to the attention of anyone with a very large scope (1-m at least). Even that may not be enough since the moon is nearly full and the asteroid keeps close to the galactic equator. If nothing else, astrometry prior to and after any radar observations may prove useful.

| DATE | RA | Dec | ED | SD | V | α | SE | ME | MP | GB |
|---|---|---|---|---|---|---|---|---|---|---|
| 09/28 | 19 25.8 | +09 56 | 0.01 | 1.01 | 19.8 | 72.2 | 107 | 44 | +0.86 | -3 |
| 09/29 | 20 25.0 | +21 09 | 0.01 | 1.01 | 19.0 | 59.8 | 120 | 47 | +0.92 | -10 |
| 09/30 | 21 57.6 | +33 30 | 0.01 | 1.01 | 18.5 | 45.6 | 134 | 47 | +0.97 | -17 |
| 10/01 | 23 49.6 | +40 20 | 0.01 | 1.01 | 18.5 | 37.7 | 142 | 45 | +0.99 | -21 |
| 10/02 | 01 19.4 | +40 32 | 0.01 | 1.01 | 18.9 | 37.8 | 142 | 41 | -1.00 | -22 |

References


Harris, A.W.; Young, J.W.; Contreiras, L.; Dockweiler, T.; Belkora, L.; Salo, H.; Harris, W.D.; Bowell, E.; Poutanen, M.; Binzel, R.P.; Tholen, D.J.; Wang, S. (1989). "Phase relations of high albedo asteroids: The unusual opposition brightening of 44 Nysa and 64 Angelina." *Icarus* **81**, 365-374.

Muinonen, K.; Belskaya, I.N.; Cellino, A.; Delbò, M.; Levasseur-Regourd, A.-Ch.; Penttilä, A.; Tedesco, E.F. (2010). "A three-parameter magnitude phase function for asteroids." *Icarus* **209**, 542-555.

Polishook, D.; Brosch, N. (2008). "Photometry of Aten asteroids – More than a handful of binaries." *Icarus* **194**, 111-124.

Pravec, P.; Hergenrother, C.; Whiteley, R.; Sarounova, L.; Kusnirak, P. (2000). "Fast Rotating Asteroids 1999 TY2, 1999 SF10, and 1998 WB2." *Icarus* **147**, 477-486.

Pravec, P.; Wolf, M.; Sarounova, L. (2007). *http://www.asu.cas.cz/~ppravec/neo.htm*

Warner, B.D.; Harris, A.W.; Pravec, P. (2009a). "The asteroid lightcurve database." *Icarus* **202**, 134-146.

Warner, B.D.; Harris, A.W.; Pravec, P.; Durech, J.; Benner, L.A.M. (2009b). "Lightcurve Photometry Opportunities: 2009 October-December." *Minor Planet Bulletin* **36**, 188-190.

Warner, B.D.; Stephens, R.D. (2019a). "Near-Earth Asteroid Lightcurve Analysis at the Center for Solar System Studies: 2018 July-September." *Minor Planet Bull*. **46**, 27-40.

Warner, B.D.; Stephens, R.D. (2019b). "Near-Earth Asteroid Lightcurve Analysis at the Center for Solar System Studies." *Minor Planet Bull*. **46**, 423-438.

Warner, B.D.; Stephens, R.D. (2020). "Near-Earth Asteroid Lightcurve Analysis at the Center for Solar System Studies: 2019 July-September." *Minor Planet Bull*. **47**, 23-34.

(This page deliberately left blank.)

## IN THIS ISSUE

This list gives those asteroids in this issue for which physical observations (excluding astrometric only) were made. This includes lightcurves, color index, and H-G determinations, etc. In some cases, no specific results are reported due to a lack of or poor quality data. The page number is for the first page of the paper mentioning the asteroid. EP is the "go to page" value in the electronic version.

***THE MINOR PLANET BULLETIN*** (ISSN 1052-8091) is the quarterly journal of the Minor Planets Section of the Association of Lunar and Planetary Observers (ALPO, http://www.alpo-astronomy.org). Current and most recent issues of the *MPB* are available on line, free of charge from:
*http://www.minorplanet.info/MPB*
The Minor Planets Section is directed by its Coordinator, Prof. Frederick Pilcher, 4438 Organ Mesa Loop, Las Cruces, NM 88011 USA (fpilcher35@gmail.com) Dr. Alan W. Harris (MoreData! Inc.; harrisaw@colorado.edu), and Dr. Petr Pravec (Ondrejov Observatory; ppravec@asu.cas.cz) serve as Scientific Advisors. The Asteroid Photometry Coordinator is Brian D. Warner (Center for Solar System Studies), Palmer Divide Observatory, 447 Sycamore Ave., Eaton, CO 80615 USA (brian@MinorPlanetObserver.com).

*The Minor Planet Bulletin* is edited by Professor Richard P. Binzel, MIT 54-410, 77 Massachusetts Ave, Cambridge, MA 02139 USA (rpb@mit.edu). Brian D. Warner (address above) is Associate Editor, and Dr. David Polishook, Department of Earth and Planetary Sciences, Weizmann Institute of Science (david.polishook@weizmann.ac.il) is Assistant Editor. The *MPB* is produced by Dr. Robert A. Werner (rawerner@polygrav.org). The Associate Producer is Dr. Pedro A. Valdés Sada (psada2@ix.netcom.com). The MPB is distributed by Dr. Melissa Hayes-Gehrke. Direct all subscriptions, contributions, address changes, etc. to:

Dr. Melissa Hayes-Gehrke
UMD Astronomy Department
1113 PSC Bldg 415
College Park, MD 20742 USA
(mhaysege@umd.edu)

Effective with Volume 38, the *Minor Planet Bulletin* is a limited print journal, where print subscriptions are available only to libraries and major institutions for long-term archival purposes. In addition to the free electronic download of the *MPB* noted above, electronic retrieval of all *Minor Planet Bulletin* articles (back to Volume 1, Issue Number 1) is available through the Astrophysical Data System
*http://www.adsabs.harvard.edu/*.

Authors should submit their manuscripts by electronic mail (rpb@mit.edu). Author instructions and a Microsoft Word template document are available at the web page given above. All materials must arrive by the deadline for each issue. Visual photometry observations, positional observations, any type of observation not covered above, and general information requests should be sent to the Coordinator.

* * * * *

The deadline for the next issue (47-4) is July 15, 2020. The deadline for issue 48-1 is October 15, 2020.